The role of macropore flow from PLOT to catchment scale

Nederlandse Geografische Studies / Netherlands Geographical Studies

Redactie / Editorial Board
Drs. J.G. Borchert (Editor in Chief)
Prof. Dr. J.M.M. van Amersfoort
Dr. P.C.J. Druijven
Prof. Dr. A.O. Kouwenhoven
Prof. Dr. H. Scholten

Plaatselijke Redacteuren / Local Editors
Dr. R. van Melik,
Faculteit Geowetenschappen Universiteit Utrecht
Dr. D.H. Drenth,
Faculteit der Managementwetenschappen Radboud Universiteit Nijmegen
Dr. P.C.J. Druijven,
Faculteit der Ruimtelijke Wetenschappen Rijksuniversiteit Groningen
Drs. F.J.P.M. Kwaad,
Fysich-Geografisch en Bodemkundig Laboratorium Universiteit van Amsterdam
Dr. L. van der Laan,
Economisch-Geografisch Instituut Erasmus Universiteit Rotterdam
Dr. J.A. van der Schee,
Centrum voor Educatieve Geografie Vrije Universiteit Amsterdam
Dr. F. Thissen,
Afdeling Geografie, Planologie en Internationale Ontwikkelingsstudies Universiteit van Amsterdam

Redactie-Adviseurs / Editorial Advisory Board
Prof. Dr. G.J. Ashworth, Prof. Dr. P.G.E.F. Augustinus, Prof. Dr. G.J. Borger,
Prof. Dr. K. Bouwer, Prof. Dr. J. Buursink, Prof. Dr. G.A. Hoekveld,
Dr. A.C. Imeson, Prof. Dr. J.M.G. Kleinpenning, Dr. W.J. Meester,
Prof. Dr. F.J. Ormeling, Prof. Dr. H.F.L. Ottens, Dr. J. Sevink, Dr. W.F. Sleegers,
T.Z. Smit, Drs. P.J.M. van Steen, Dr. J.J. Sterkenburg, Drs. H.A.W. van Vianen,
Prof. Dr. J. van Weesep

ISSN 0169-4839

Netherlands Geographical Studies 390

The role of macropore flow from PLOT to catchment scale

A study in a semi-arid area

Loes van Schaik

Utrecht 2010

Koninklijk Nederlands Aardrijkskundig Genootschap
Faculteit Geowetenschappen Universiteit Utrecht

ISBN 978-90-6809-433-6

Graphic design, cartography and figures:
GeoMedia (Faculty of Geosciences, Utrecht University) [7457]

Copyright © Loes van Schaik

Niets uit deze uitgave mag worden vermenigvuldigd en/of openbaar gemaakt door middel van druk, fotokopie of op welke andere wijze dan ook zonder voorafgaande schriftelijke toestemming van de uitgevers.

All rights reserved. No part of this publication may be reproduced in any form, by print or photo print, microfilm or any other means, without written permission by the publishers.

Printed in the Netherlands by A-D Druk b.v. – Zeist

Contents

Figures

Tables

Acknowledgements

In the summer of 2002 shortly after my graduation from university, a visit to Coen Ritsema at Alterra (Wageningen) resulted in a short, interesting brainstorm session and a topic for a PhD study. Coen then managed to get together all the necessary support and financing, and in June 2003 I could start on this PhD-project. Though at times I was juggling to bring up the energy and concentration for the work, my motivation never failed: I spent the following years with great pleasure working on this research, the result of which lies here before you. Of course, without the wonderful support of many people around me, this would not have been possible and here I would like to thank all of you who helped out.

It is customary to end with last but not least and then mention one's partner. I would like to mention my partner Jerie in the first place as his consent and his support were the main conditions for me to start off on a PhD, and to continue (and enjoy) my work so much in the past years. My children, Eva, Iris and Oscar, in the next place, were sure to provide the necessary diversion and pleasure and helped to keep things in perspective. Occasionally flexibility was asked from their side and grandparents, family or friends were involved in the caretaking, to whom we are all very thankful.

As mentioned before Coen Ritsema was at the basis of this project and with his enthusiasm and energy managed to create the PhD position. Furthermore, I will always be very grateful to Steven de Jong, my promotor, for his never-ending support and confidence in the project throughout the years. He also proved to be a very fine and rapid reviewer time and again. Victor Jetten, always extremely enthusiastic and full of ideas, was a very motivating supervisor and finally, yet importantly, Jos van Dam completed the group of supervisors wonderfully with his quiet, meditated comments. Mainly during the last phases of modeling I strongly appreciated his help.

The fieldwork, the fundament of all that I have done, would have been impossible without the students: Telma, Sanne, Koen and Joachim, thanks a lot! Additionally, the support from the technical laboratory was great: Bas, Henk, Marcel, Chris, Hassan and Theo. And of course in the fieldwork area, the staff of the University of Extremadura, el Departamento de Geografía, in particular Susanne Schnabel, Marco Maneta, Alvaro, David and Manuel: muchissimas gracias por su apoyo en Parapuños de Doña Maria. Además agradacemos a la gente de Monroy, donde hemos pasado un muy buen tiempo y disfrutado a menudo los menus del dia en La Bodega del Herrador!

A special word of thanks furthermore goes to Rob Hendriks, Edzer Pebesma, Elisabeth Addink, Ger de Rooij and Theo van Asch who during different stages of the work helped out with theoretical or practical advice or some interesting discussions.

Of course all colleagues from Utrecht and Wageningen, where I was quietly (read unofficially) allowed to join the group: I enjoyed the pleasant working atmosphere, the coffee breaks and all. Here of course I want to mention my roommates: to start with Gilles and Roy, but also those of the first days in Utrecht: Marc Gouw and Leonie and not to forget the "roommates"in Wageningen: Tessa, Ype and Anton, thanks for frequently allowing me to occupy a desk in your room. In the past years I have gratefully made use of the available supporting services in Utrecht: Geomedia (Margot, Rien, Ton, Margriet), secretaresses (Juul, Annina en Irene), personeelsdienst (in het bijzonder Carla Schoof) en NGS (Rianne), allemaal hartelijk dank.

Finally, my parents, family and friends, only shortly mentioned before, but they were, are and always will be very important to me/us. Thank you all for being there. Thanks for all the nice times we spent and hopefully will spend together. Even though we are now slightly farther away, our door is always open for all of you: karibu sana, welcome!

1 Introduction

1.1 Introduction

Worldwide many arid and semi-arid regions are facing the risk of landscape degradation or even desertification due to water scarcity and mal management. Climate change is expected to increase water scarcity in the future. Regional climate change predictions are often ambiguous, but all IPCC scenarios (IPCC, 2007) predict an increase in temperatures for arid and semi-arid regions of at least 1.5 °C by the end of the 21st century. Projections of mean annual precipitation differ: for some areas an increase in total precipitation is expected and for other areas a decrease. However the inter annual and intra-annual variability is likely to increase, regardless of the total precipitation. This means less events with more extreme rainfall intensities will take place, which will lead to higher runoff percentages. These changes in temperature and precipitation will probably decrease soil moisture availability and thereby influence the vegetation cover. A vegetation cover on one hand can increase infiltration due to stemflow and the creation of macropores around the root network and on the other hand slows down the runoff, through the higher surface roughness, and thereby decreases erosivity of rainfall and decreases peakflow. A decrease in vegetation cover therefore will have a negative feedback on the soil moisture content and runoff production. Additionally in some areas change in vegetation cover may even further increase the maximum temperatures over and above what the carbon dioxide will do on its own according to Diffenbaugh (2005). In order to assess the impact of climate change on water availability and vegetation it is essential to fully understand the hydrological processes which influence infiltration and soil moisture distribution.

Traditionally flow in the unsaturated zone is treated as a uniform front in a soil column for which a representative elementary volume can be defined with representative soil physical characteristics. In practice there is always some small scale spatial variability in infiltration fronts and in water flow through soils. Part of this variability is the result of small scale heterogeneity in a soil profile, which at a larger scale can become negligible through lateral mixing within the profile. However, in case the variability in fluxes in the flow direction is large and lateral exchange between flow paths is limited; this will result in significant variability in travel times within a soil even at a larger scale. A high variability of fluxes in the flow direction can result in rapid flow of water and solutes along certain pathways by-passing (a large) part of the porous media, which is called preferential flow. Many field studies have shown preferential flow to be a wide spread phenomenon.

One of the most important characteristics of preferential flow is the fact that it is non-equilibrium flow: this means that for various reasons fast infiltrating water in the preferential flow paths does not have sufficient time to equilibrate with slowly moving resident water in the bulk of the soil matrix (Fluhler et al., 1996; Jarvis, 1998). Also the assumption that pores fill

and start to participate in water flow depending on their size (all small pores to be filled before larger pores can participate in flow) is found in many cases not to apply. Accordingly the use of a homogeneously applied Richards-based flow equation is not adequate for the modeling of the soil-water balance.

Beven (2001) stated that only a correct simulation and prediction of flow pathways leads to a correct description of the internal hydrological behaviour in a catchment. Water flow in the vadose zone determines the partitioning of rainfall to runoff or infiltration. Furthermore flow variability in the vadose zone influences the availability of water for evapotranspiration in different soil layers and percolation to groundwater. It is therefore important to correctly describe the nature of flow in the vadose zone. Preferential flow may also strongly influence the flow paths and travel time of solutes through a soil, and it is generally recognized as one of the most important processes which affect solute transport and contamination (Edwards et al, 1993).

In short preferential flow may strongly influence soil water availability, solute transport, groundwater level fluctuations and catchment scale erosion and discharge generation. As preferential flow has been found to be a widespread phenomenon, a lot of research is performed in this field recently, resulting in various reviews and special issues of journals on preferential flow (e.g. Beven and Germann, 1982; DeBano, 2000; Doerr et al, 2000; de Rooij, 2000; Simunek et al., 2003; Special issues: Steenhuis et al., 1996; Ritsema and Dekker, 2000; Roulier and Schulin, 2008). The following is a summary of relevant literature which serves as a background to this thesis, resulting in the objectives of this thesis and subsequently the outline of the thesis.

1.2 Literature background

There are different types of preferential flow: macropore flow (Beven and Germann, 1982; Edwards et al., 1993), fingered flow (Raats, 1973; Hillel and Baker, 1988; Bauters et al., 1998; de Rooij, 2000) and funnel flow (Ju and Kung, 1997a, b). The subdivision into different types is based on difference in flow processes:

- Macropore flow is flow through pores which are much larger than the average soil matrix pores;
- Fingered flow is the formation of an unstable flow pattern in an otherwise macroscopically homogeneous soil profile. This is the result of resistance to flow at a certain depth in the soil, and subsequently a limited amount of breakthrough points along the infiltration front where flow fingers grow;
- Funnelled flow is flow which is redirected in the soil by large impeding structures such as clay lenses or large stones.

The different preferential flow types also have various possible origins. Macropore flow may result from either bio-pores, cracks in clayey soils or soil aggregates. Fingered flow or unstable wetting fronts can originate due to e.g. water repellency, soil layering or air entrapment. And finally funnelling is redirection of the main flow due to large clay lenses or stones. This results in differences in spatial and temporal variability of the preferential flow, depending on the flow type as well as on the origin of preferential flow. For example the volume of soil cracks will be largest

under dry circumstances, so a high intensity rainfall event in dry circumstances will generate the largest preferential flow due to cracks. While flow into bio-pores is probably larger under wet circumstances as the matrix infiltration capacity is then exceeded more rapidly, meaning more water will flow to the macropores. Regardless of the origin, preferential flow and it's hydrological influence is a transient, threshold dependent process. The complexity of the processes and the high spatial and temporal variability make it very difficult to build process models, to measure the processes in the field and to upscale this information to catchment scale.

1.2.1 Types of preferential flow

Macropore flow

Preferential flow through macropores is considered as a phenomenon that occurs in many soils, having a strong influence on the total infiltration flux (Booltink et al., 1993; Léonard et al., 2001). Macropore flow often occurs through mainly vertical, interconnected macropores. Macropores and sometimes also mesopores are defined as pores that drain mainly by gravitational forces. Different boundary values for the pore radius are used to define minimum macropore size; many authors mention values ranging between 30-3000 μm (Beven and Germann, 1982). Soil pipes are large continuous macropores which are subject to erosion processes. The influence of soil pipes in hillslope hydrology has been studied in detail by Kitahara et al. (1988), Jones (1997), Jones and Connelly (2002).

Macropores and sub-surface channels result from either biological activity (eg., root channels, worm holes, etc), geological forces (eg., subsurface erosion, desiccation and synaerisis cracks and fractures) or agro technical practices (e.g., ploughing, bores and wells) (Figure 1.1). Surface cracks and channels that bypass the root zone are also responsible for rapid transport of moisture and chemicals through the unsaturated zone. Macropores may also lead to soil piping and subsurface erosion. This however is not within the scope of this thesis.

Temporal and spatial variability

Hydrologically effective macropores, resulting from plant roots, soil fauna or piping, can be produced in 1 or 2 years time and in undisturbed circumstances can last for considerable time periods. Cracks in fine-textured soils, formed by dessication, depend on the soil moisture content and are thus subject to seasonal variation. The cracks do tend to reoccur repeatedly at the same places. Saturation of the soil inhibits the activity of animals and roots and will lead to a breakdown of soil structure. Therefore the role of macropores is largely limited to depths where saturation is an ephemeral phenomenon.

The influence of soil tillage on macroporosity is mainly destructive. Though ploughing creates cracks in the topsoil, it cuts natural macropores and decreases the amount of earthworms. Also the use of heavy machinery compacts the soils and thus destroys part of the macroporosity (Beven and Germann, 1982).

Hydrological impacts

Macropore flow results in a large spatial variability of infiltration and hydraulic conductivity within a soil profile (Zehe and Fluhler, 2001). Enhanced lateral throughflow and rapid by-pass flow towards the groundwater are characteristic for macropore flow. Macropores are also known

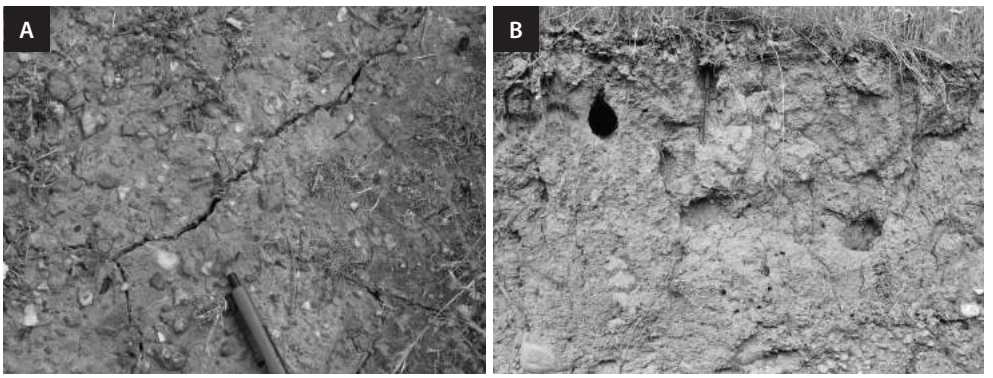

Figure 1.1: Examples of macropores, a) a crack in a dried out fine textured soil, b) root holes and an animal burrow in a gully side-wall in the Parapuños catchment, Extremadura, Spain.

to provide important preferential flow paths for the generation of subsurface stormflow in hillslopes (Sidle et al., 2001). The higher the rainfall intensity, the larger the infiltration excess, which can flow straight into the macropores and thus enhance macropore flow, even though the soil matrix may still be far from saturated. In reality macropores are often found to transmit water while the surrounding soil matrix is not saturated, indicating hydraulic discontinuities (Cammeraat, 1992).

Beven and Germann (1982) distinguished two types of large voids in soils: those which are hydrologically effective and those which aren't. Preferential flow requires a certain length and continuity. Different numbers and sizes of pores may be hydrologically effective under different conditions. Weiler (2001) demonstrated that the high macropore flow rate usually does not limit the process of infiltration. The flow of water through macropores is therefore determined by the factors that control infiltration to macropores. These factors are: rainfall volume and intensity (Trojan and Linden, 1992), initial soil water content, position of the macropore opening with reference to the microrelief (Trojan and Linden, 1992), the area draining to the macropore (Trojan and Linden, 1992; Weiler and Naef, 2003), slope of the soil surface (Weiler and Naef, 2003b) and the number of macropores per unit area (Léonard et al., 1999; Weiler and Naef, 2003b). These factors can be subdivided into two kinds of factors: event-related factors (rainfall intensity and antecedent moisture content) and site-related factors (density and distribution of macropores, surface roughness and slope).

Macropores become effective on large scales mainly when size and connectivity of the pores increase and the effects of capillary tension decrease, but Perret et al. (1999) showed that the tortuosity and topology are as important as length, hydraulic radius and density of macropores. It is very difficult to estimate the effectivity of macropores, as generally only a part of the macropores in a soil participate in the flow. Furthermore macropore connectivity may vary with soil moisture content (Tsuboyama et al., 1994). Although individual macropores are generally short, they are connected through nodes of loose soil or buried organic matter. The conductivity of these nodes depends on local soil water conditions and thereby, with wetting of the soil the macropore connectivity increases. Based on this idea Sidle et al. (2001) proposed the idea of

Figure 1.2: An example of coated macropores from the Parapuños experimental catchment in the Extremadura, Spain (note the coin at the bottom as an indication of scale)

self-organizing macropore networks, which consist of many short segments of macropores and can become large preferential flow systems as the soil gets wet. In undulating areas, macropores may prevent long term saturation of the soils, through their contribution to rapid drainage (Sidle et al., 2001), thereby decreasing the landslide initiation potential (Fannin et al, 2000). Uchida (2004) however found that once the capacity of the preferential features is exceeded, this may lead to high pore water pressures in the surrounding soils and thereby increase landslide initial potential.

Water and chemicals that travel in macroporous soils often bypass the bulk of the soil matrix, resulting in a loss of nutrients for plants and crops. For example, a single, continuous 0.3 mm diameter macropore can conduct more water than surrounding soil of 100 mm diameter. As the water entry value for pores is larger with larger pore sizes, initiation of macropore flow will mainly occur after the infiltration capacity of the soil matrix is exceeded. Rainfall intensities of 1 to 10 mm/h may be sufficient to initiate macropore flow, depending on antecedent precipitation (Beven and Germann, 1982). In soils with a low hydraulic conductivity, even a small amount of macroporosity can increase the flux density of the saturated soil by more than 1 order of magnitude.

Cammeraat (1992) found that at ponding or saturated conditions flow in horizontal worm channels is evident. Flow in macropores and channels can occur with little or no interaction with the surrounding soil-matrix. The infiltration of water from the macropores into the soil matrix can be hampered by smearing of earthworm excrements (Figure 1.2) or by cigar-like rolled litter at the channel wall (Cammeraat, 1992). Also the infiltration of water into the soil-matrix can be strongly limited by possible water repellency of the matrix. The importance of horizontal infiltration from macropores into the soil matrix is dependent on the storage time of water in the macropores. Factors which influence this storage time are the total storage capacity, vertical and lateral losses from the macropores and the rate of replenishment, either through a permeable topsoil or directly by runoff into the network (Van Beek and Van Asch, 1999).

Fingered flow

Fingered flow is the result of wetting front instability (Figure 1.3). Possible causes for wetting front instability are (De Rooij, 2000) water repellency, an increase of the soil hydraulic conductivity with depth, redistribution of infiltration after the end of a rain shower or irrigation and air entrapment.

In this paragraph fingered flow due to water repellency is focused on. Profile heterogeneities or lenses in the soil profile are usually caused by textural differences and other factors at scales significantly larger than the pore/pedon-scale. And the redistribution of water, air entrapment and non-ponding rainfall are dependent rather on meteorological conditions than on the soil properties

Origin and occurrence

Doerr et al. (2000) have composed an elaborate summary on the causes, characteristics and hydro-geomorphological significance of water repellency. They described the different origins of the coatings responsible for water repellency (biological, i.e. plant organic compounds, fungi or micro-organisms, and non-biological, i.e. soil temperature or fire and soil texture).

Soil water repellency seems to be more of a rule than an exception. According to (Dekker and Ritsema, 1994) 75% of the cropland and grassland topsoils in the Netherlands are slightly to extremely water-repellent, and more than 95% of the topsoils in nature reserves are strongly to extremely water-repellent. A considerable amount of studies in different regions of the world suggest that water repellency can be found in many parts of the world and in all sorts of climates (Doerr et al., 2000; Jaramillo et al., 2000).

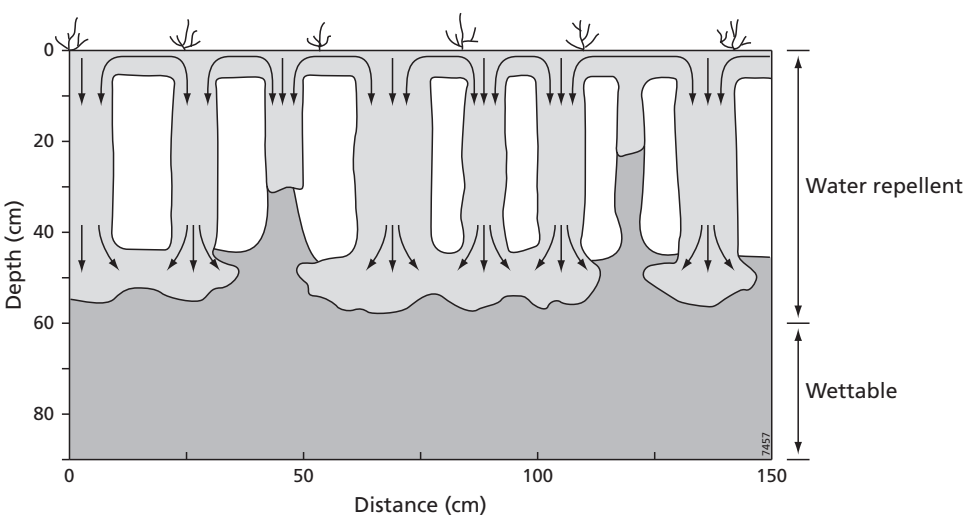

Figure 1.3: Fingered flow patterns in a soil: at the soil surface lateral flow to the fingers takes place and in the fingers flow is vertical down to the wettable subsoil, where the fingers spread again.

Water repellency is found under different vegetation types including forests, brushwood, grassland, and agricultural land and golf courses (DeBano, 2000). The degree of water repellency may depend on land-use history, a natural vegetation in some cases being more water-repellent than cultivated land (Sonneveld et al., 2003). Nevertheless it does not seem possible to use soil or vegetation characteristics to predict accurately the occurrence or the degree of water repellency that can be expected in a soil (Doerr et al., 2000).

Bauters et al. (2000) tried to derive a soil specific wetting curve from the contact-angle of water and soil particles, depending on the water repellency of soils, with which the infiltration into the soil can be characterized.

Temporal and spatial variability
Soil water repellency is largely regarded as a seasonal phenomenon, being usually low or completely absent under prolonged wet conditions and most severe during extended dry periods (e.g. Ritsema and Dekker, 1994). It is generally assumed that water repellency becomes readily re-established and that the fingers re-occur at exactly the same places upon drying (e.g. Doerr et al., 2000; Ritsema et al., 1998).

Dekker and Ritsema (1994) made a distinction between actual and potential water repellency and a critical soil water content above which the soil is wettable and below which the soil is water-repellent. A prolonged contact with water leads to a loss of water repellency, and positive water pressures, occurring through ponding or perched water tables for example, can overcome the water repellency.

Water repellency has often been reported to be spatially discontinuous within the soil both horizontally and vertically. For *Eucalyptus* however, with an abundant production of hydrophobic compounds and/or a thick litter layer a spatially homogeneous water repellency is found in catchments in Portugal (Doerr, 1998). Doerr et al. (1996) also found that water repellency was common from the mineral surface down to near the bedrock for both burnt and unburnt forest soils in Portugal, and attributed this to a high release of hydrophobic substances into the relatively shallow soils.

Hydrological impacts
In the case of wetting front instability the topsoil usually functions as a distribution zone. In the distribution zone horizontal flow takes place towards the fingers. In the fingers the water flows vertically to the wettable subsoil, where dispersion of the flow takes place. Fingers may merge or split on their way down to the wettable zone. Under sufficiently high rainfall rates the soil water contents within the preferential flow paths are near saturation. Lateral expansion of fingers will depend on the water supply and the origin of fingering. In general fingers are quite persistent and as long as the flow capacity of the fingers is not exceeded, they will hardly grow. Depending on the degree of water repellency, diffusion from fingers into the matrix can be neglected.

Summarised the hydrological process of fingered flow reported in the literature can be described as follows:
- an initial resistance to flow;

- water pressure builds up;
- resistance to flow is locally overcome;
- spatially localized infiltration and/or percolation, with fingered flow development;
- effects on the three-dimensional distribution and dynamics of soil moisture;
- enhanced streamflow responses to rainstorms;
- enhanced total streamflow.

Water repellency and resulting preferential flow has been found to depend on the antecedent soil moisture content and critical water content, the amount and intensity of rainfall and the storage capacity of the distribution zone.

It is also normally argued that because of enhanced overland flow on and increased erodibility of water-repellent soil, slopewash, and sometimes the formation of rills and gullies, may be promoted (Doerr et al., 2000).

Fingered flow is predominantly vertical flow. The influence of fingered flow on the large scale will therefore strongly depend on the connection to groundwater or drains, which may continue rapid transport in lateral direction.

Funneled flow

Funneled flow is redirection of flow over sloping layers or lenses in a soil. In sedimentary soils often sloping layers exist of inclined very coarse sand or clay and silt lenses in a sandy vadose zone. These layers can funnel the vertical uniform unsaturated matrix flow into congregated by-pass or preferential flow paths. In the case of large clay and silt lenses or stones, redirection of a large part of the water flow along the slope of the impeding layer may take place, as the water supply through the sandy matrix is much higher than the impeding layer can conduct.

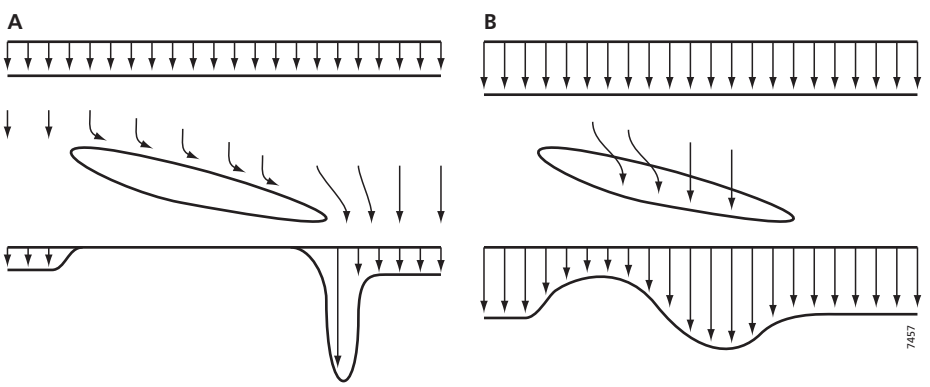

Figure 1.4: The funnel effect in sandy soil. With a relatively low flow rate a fast-moving spout forms beneath the lower end of an inclined layer (a). At higher flow rates, the coarse layers begin to leak, and the funnel effect become less significant (b).

In the case of a coarse sand layer, the funneling is the result of a capillary boundary between the fine topsoil and the coarse subsoil. This is in origin similar to the origin of fingering in the case of fine-soil, coarse soil layering. Kung (1993) demonstrated that funneled flow only occurs when the water-entry potential of the lower, coarser soil is less negative than the air-entry potential of the upper, finer soil (a so-called Haines' jump) and at the same time infiltration rates are smaller than a certain critical rate. Whether fingering or funneling will take place depends mainly on the slope of the soil layers, the moisture content of the soil profile, the infiltration rate, the conductivity of the overlaying soil and the magnitude of the Haines' jump (Kung, 1990). Fingering will only take place under dry conditions of the subsoil, while funneling kan even occur when the moisture content of the whole soil profile is at its field capacity.

Walter et al. (2000) also found that in case of funnelling due to capillary barriers (Haines' jumps) between a fine and a coarse layer, the slope of the layer and the infiltration rate will largely determine the effectiveness of the capillary barriers. Ju and Kung (1997a) showed that contaminant breakthrough time in simulations accounting for funneled flow was only 25% of that in one-dimensional homogeneous profiles. They also showed that the ratio of the total mass leached from the funneled flow simulation compared to the homogeneous flow, increased exponentially with decreasing water application rate. The impact of funneled flow is largest when the application rate is low.

1.2.2 Measurement techniques

A major difficulty in modeling the impact of preferential flow is the measurement of quantitative indicators for preferential flow. Many methods for measuring preferential flow are labour-intensive and destructive. Measurements are also often limited in the spatial and or temporal resolution, which in view of the large spatial and temporal variability of this phenomenon is a serious disadvantage. Therefore a consistent measurement method is not yet acchieved (Droogers et al., 1998; Perret et al., 1999). As the main issue is to capture the variability of fluxes, it is important to be aware of the value of the measurement results for indicating preferential flow. The following is a short summary and evaluation of the main measurement methods which are currently applied to measure preferential flow.

Classical methods for measuring the persistence and the degree of water repellency are the water drop penetration time (Letey, 1969) or the molarity with an ethanol droplet test (Watson and Letey, 1970). These methods can only classify the degree in groups from wettable to extremely water-repellent and though the tests are easily performed in a laboratory, intensive sampling of the soil profile is needed to be able to detect the horizontal and vertical variation of water repellency. In addition the actual water repellency is dependent on soil moisture content. Ritsema and Dekker (1996) studied the effect of sampling strategy on the detection of preferential flow paths in a water-repellent sandy soil. A sample spacing of up to 22 cm over a distance of several meters is just sufficient to collect information about preferential flow paths. Using larger sample spacings, the water content distributions apparently became more horizontally stratified. Increasing the sample size by pooling pairs of adjacent 100 cm^3 soil samples over a distance of several meters, still allowed the detection of preferential flow paths. Preferential flow paths were no longer observed for larger sample sizes. Enlarging the sample size reduces the calculated standard deviation and coefficient of variation. As preferential flow paths may vary in space and

Figure 1.5: Example of a dye-infiltration profile from the Parapuños catchment, Extremadura, Spain.

time, however, the optimal number of samples to detect these paths may vary, indicating that sampling strategies need to be flexible in design.

Methods which can be applied in the laboratory (and sometimes also in the field) to assess the density and spatial distribution of macropores are the use of dye-tracing, resin impregnation (Ringrose-Voase, 1996), macropore tracing on clear plastic sheets, X-ray computed tomography (CT-scan) (Perret et al., 1999), MRI-scans (Amin et al., 1997) and in-situ photography or estimation of the macroporosity of a soil-profile. As only part of a macropore network will conduct water and the effectivity of a macropore network is dependent on soil moisture content, the value of mapping the full macroporosity of a soil is disputable.

Dye infiltration profiles (Figure 1.5) are often used to describe and quantify preferential flow patterns (Ghodrati and Jury, 1990; Flury et al., 1994; Zehe and Flühler, 2001; Ohrstrom et al. 2002). The infiltration profiles show the spatial variability in infiltration, but it is important to realize that stained area is not equal to soil moisture content and it is very difficult to obtain information on distribution of tracer concentrations from the stained profiles (Forrer et al., 2000). Furthermore the infiltration experiments and the subsequent profile excavations are very labour intensive and give only single event infiltration patterns, so the temporal variability remains unknown. Also the infiltration depth of the tracer is strongly dependent on the experimental conditions, such as rainfall intensity, rainfall duration and antecedent moisture content. Infiltration profiles have been used to deduce areas with different flow types in a soil (Weiler, 2001).

The inverse augerhole method has occasionally been used to find infiltration and saturated hydraulic conductivity rates. This was thought to be a sound way to measure the influence of the continuity of macropores and take into account lateral flow of infiltrating water. Cameira et al. (2000) evaluated a two-domain model of infiltration using the conventionally measured soil hydraulic properties considered as soil matrix properties, supplemented by macropore flow capacity measured with a tension infiltrometer. The results indicate that there is the need to develop a new technique to determine appropriate soil matrix and macropore properties in

macroporous field soils. The hydraulic properties determined by conventional methods are apparently the properties of soil matrix, but seem to miss the effect of larger pores that are above the 1.0 mm diameter assumed to be the lower limit for macropores. The macropore properties determined with a tension infiltrometer apparently do not distinguish between continuous and dead-end macropores, and do not give any indication of the continuity of macropores with depth. The Tension Disc Infiltrometer (Angulo-Jaramillo et al., 1996) is a widely used apparatus for measuring the permeability of soils at different soil suctions (Figure 1.6). It is even used to determine mean pore radius of the conducting pores and to determine the mobile/immobile fractions of a soil or to deduce matrix and macropore properties (Logsdon, 2002) in other words preferential flow paths.

When using point samples for the estimation of preferential flow, there is always the possibility that the by-pass flow is missed, regardless of the sampling strategy. Therefore methods for continuous sampling of water and solute drainage on a larger scale might be useful. These methods involve the collection of soil water drained by either the force of gravity (e.g., gravity pan samplers, agricultural tile lines, and shallow wells) or by applying a "capillary"suction (e.g., porous cup samplers, wick lysimeters) (Boll et al., 1992). The multi-sampler Wick lysimeter (Figure 1.7) for example is placed below a soil column of 30 by 30 cm and collects the drainage of multiple compartments, which can be monitored according to the necessity. De Rooij and Stagnitti (2002) developed a method to describe the full spatio-temporal behaviour of solute leaching from multi compartment samplers. Lately multi compartment samplers are being built to measure spatial variability of fluxes using variable suction plates and drop counting techniques (Bloem, 2008; Mertens et al., 2008). Multi compartment samplers are under continuous development, but they are still labour intensive and costly and the value of the results may depend largely on whether a good contact can be assured between the soil and the wick-lysimeter. Also these samplers have to be installed at a chosen depth in the soil, while the variability of fluxes might be dependent on the depth at which the measurement is done. And the question remains whether a surface area of 30 by 30 cm is sufficient to capture the local spatial variability in fluxes or how many samplers are needed to give some idea of field scale variability of preferential flow.

The above measurement techniques are mainly focussed on the small scale influence of preferential flow on the infiltration and percolation of water in shallow soil profiles. To

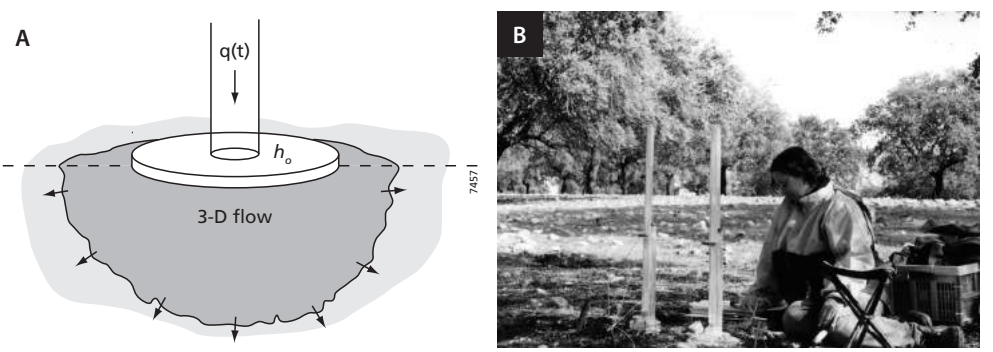

Figure 1.6: a) Schematic representation of a tension disk infiltrometer, b) field measurement with tension disk infiltrometer.

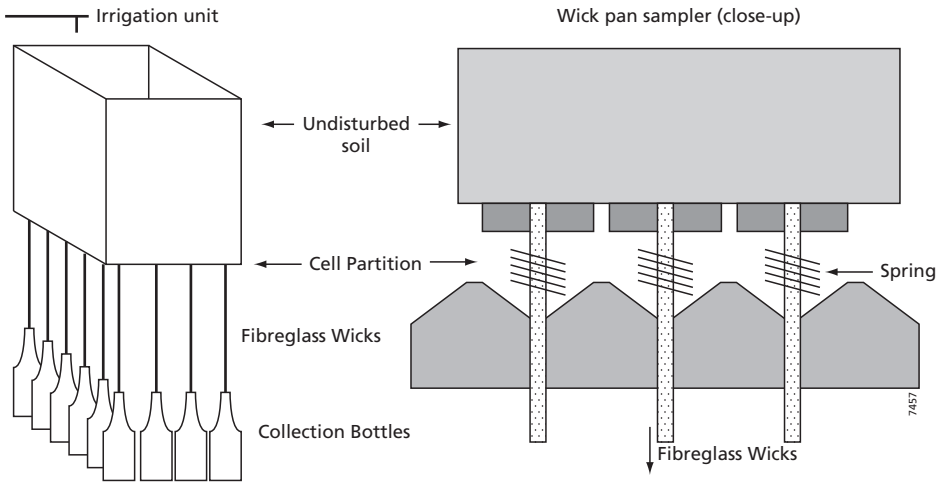

Figure 1.7: Example of the Multi-sampler Wick Lysimeter.

understand the influence of preferential flow at catchment scale it is important to measure the preferential flow at that scale too. For hillslope or catchment scale variability of preferential flow, multiple small scale measurements are sometimes performed in a study area. Whether this is enough to capture the influence of preferential flow at catchment scale is doubtful. Also the influence of preferential flow at larger scales is often inferred from drainage rates and concentrations of geochemical and isotopic tracer in discharge water. Hydrograph separations (Buttle, 1994) are often used to infer the contribution of "old water"and "new water"or event water and pre-event water to the area discharge. Due to mixing, diffusion and dispersion along the flowpaths both in the soil (Kirchner, 2003; Bishop et al., 2004) as well as at soil surface (Jones et al., 2008), the chemical signature of the discharge can be difficult to interpret.

For some hillslopes the subsurface stormflow produced by the macropores or soil pipes has been intercepted and measured with tipping buckets (Uchida et al., 2005). This may be a very accurate method to study the influence of rainfall amount and intensity and antecedent soil moisture content on the flow in single macropores. However it is questionable whether monitoring the outflow of a (limited) number of macropores is enough to quantify the influence of macropore flow on subsurface stormflow for a whole hillslope.

Finally some geophysical measurement techniques such as ground penetrating radar (GPR) and electrical resistivity imaging (ERI) are under constant improvement and have been signaled as promising for preferential flow monitoring (Overmeeren et al., 1997; Robinson et al., 2008). Though the understanding of the reflection patterns can be subjective, automatic interepretation of the measurements is becoming more powerful. Important aspects of GPR are penetration depth and resolution, these are dependent on the period of the emitted pulse. The use of GPR in silty sands and clays or in very stony soils is still problematic (Huisman et al., 2003a,b). The measurement equipment is expensive, but once available, large areas can be rapidly measured. A large advantage of these techniques is that the soil remains undisturbed and large scale

measurements can be done relatively easily. The measurements provide resident soil moisture contents, but a sequence of measurements of one profile can result in information on flow patterns.

1.2.3 Preferential flow modelling

Model concepts

Macropore flow has been found to depend on the amount and intensity of rainfall, the value of the saturated hydraulic conductivity at the soil surface, the absorption of water by the soil-matrix, and the geometry of the macropore system (Ludwig et al., 1999). This results in the following model components necessary in the modeling of macropore flow, as they have been summarized by Beven and Germann (1982):

- the spatial and temporal characteristics of the macropore flow domain;
- initiation of flows in macropores;
- the nature of flows in the matrix domain;
- the nature of flows in the macropore domain;
- interaction between the domains.

The model approaches for simulating preferential flow in soils can be divided into Physically based or statistic and stochastic models. The first model type is often based on the Richards

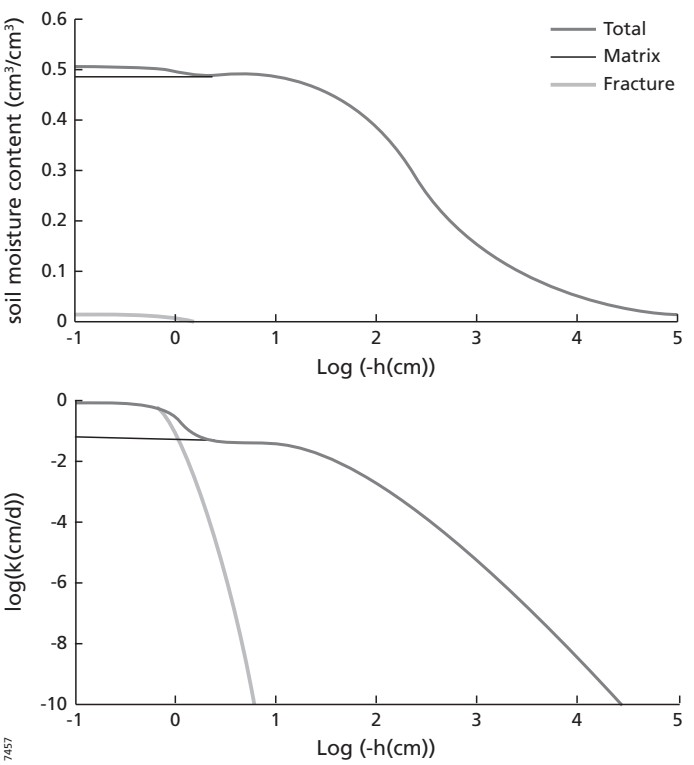

Figure 1.8: Water retention and conductivity curves for dual porous media.

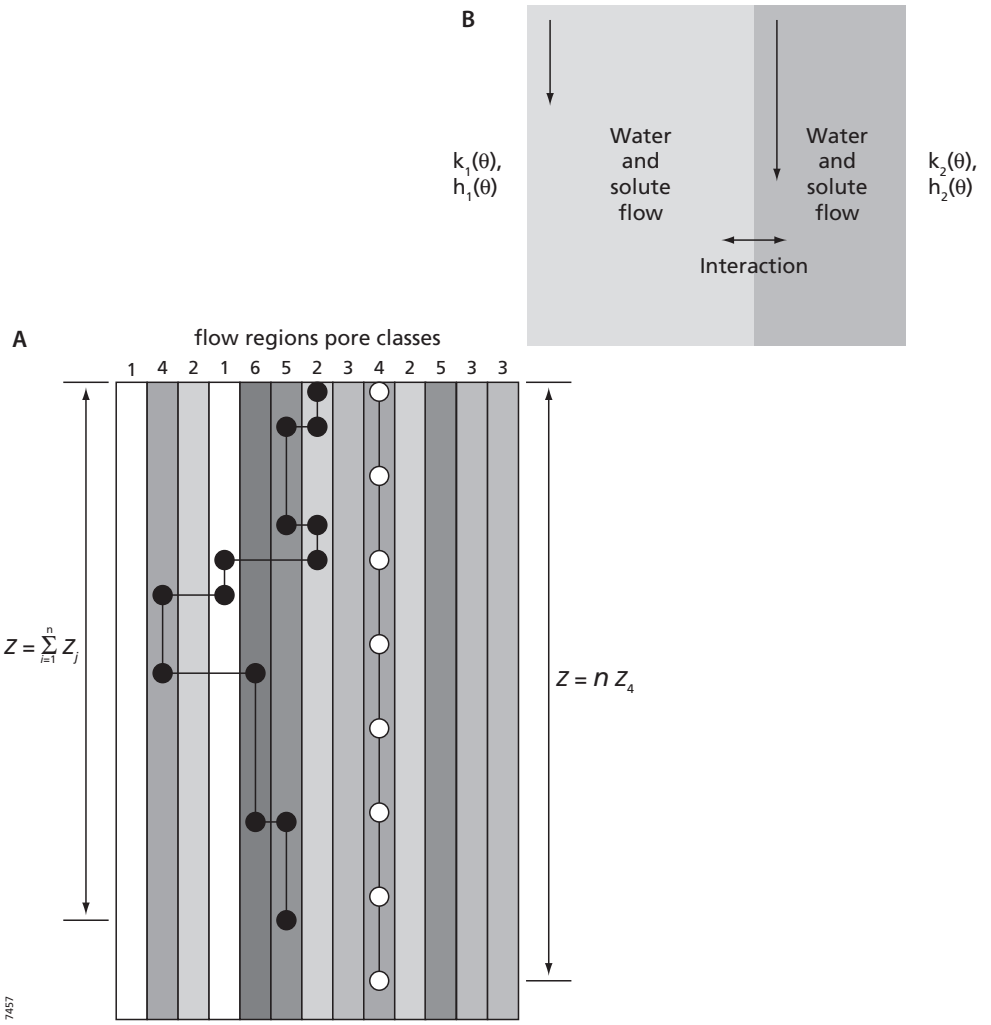

Figure 1.9: Schematic representation of a) a capillary bundle model (Flühler et al., 1996), b) a dual domain model.

flow equations, Darcy equations, and the assumption of uniform flow within a flow domain. The second consists of probability density functions (Kung et al., 2005), multi-component end member mixing analysis (Elsenbeer et al., 1995), fractal analysis (Molz et al., 2004) or time series analysis.

In the following the physically based model concepts are further discussed. Most of the physically based models dealing with preferential flow can be classed in the following model concepts (Ma and Selim, 1997; Simunek et al., 2003):

- dual-porosity or multi-porosity models use the Richards equation, with composite equations for the soil hydraulic properties (Figure 1.8). The water retention curve is formed by the linear supposition of weighted subcurves, resulting in humped water retention and hydraulic conductivity curves. This model type does result in a significant increase in hydraulic conductivity near saturation, but when used in a single domain model, will still lead to a uniform wetting front, as all the small pores have to be filled before the larger ones partake in the flow. An important drawback in the dual porosity models is therefore that they cannot model the occurrence of large by-pass flow at low saturation levels, which may occur in case of infiltration excess.
- mobile-immobile two-region models are based on the Richards equation, extended with a concept of mobile and immobile fractions of soil water. A major difficulty in applying the mobile-immobile concept is the definition of the fractions of mobile and immobile water. There is no convective transport between the two regions.
- capillary bundle models, which assume transport to occur through capillary channels of different sizes without interaction (Figure 1.9a). The CDE is applied to each bundle independently. The complexity of pore geometry, connectivity between pore sizes and interaction between the pore-channels, undermine the utility of the capillary bundle models.
- two-flow or multiple flow domain models (also called dual-permeability), where the flow is assumed to occur through two or more domains with different pore sizes and distinct velocities (Figure 1.9b). The interaction between the two domains is usually treated as a first-order linear function of pressure or concentration gradients. Also infiltration models and other approaches have been used. The flow domains and their flow velocities cannot be experimentally differentiated. When minimizing the interaction between the domains, the model approaches the capillary bundle models. And when the flow velocity in one domain approaches zero, the concept becomes similar to the mobile-immobile concept. Dual permeability or multi permeability models are an elaborated version of multi domain models. In this case the water flow can be treated differently for the different domains: using Poiseuille's law, the Richards flow equation, kinematic wave equations, Green and Ampt or Philip infiltration models, unit hydraulic gradient assumption or as tube flow (under ponded conditions turbulent flow in macropores has been proved experimentally by Logsdon (1995)).

These model concepts have been implemented in various models that are discussed in the next paragraph.

Examples of preferential flow models

As in any other field of hydrological science an abundance of models have been developed to simulate preferential flow. Many of these models are based on one of the above described model concepts. In the following a small number of these models is briefly discussed and used as examples of some very different preferential flow models: for different types of preferential flow, physically based to lumped or empirical models and from small scale to catchment scale.

Small scale modelling of fingered flow

De Rooij (1996) developed a theory of three region flow for water-repellent soils. The topsoil was considered a distribution zone, then comes a water-repellent zone where flow takes place

through fingers and under the fingers a moist subsoil where finger dissipation takes place, according to flow from a disc source. With this model De Rooij (1996) found that a thick wettable subsoil can possibly undo part of the acceleration of solute leaching caused by the fingers. Many expressions for the finger size have been found, based on laboratory experiments. The finger size is found to depend mainly on hydraulic conductivity, precipitation and initial water content, but the predictions remain fairly poor and finger dimensions change during the year and during rain showers (De Rooij, 2000).

Steenhuis et al. (1994) assumed that fingered flow commences after the distribution zone has become saturated and modeled water flow in the finger based on saturated unit gradient flow. The fraction of soil participating in fingered flow was made dependent on the precipitation, so the flow velocity remained constant, but with higher precipitation the mobile fraction grew.

Nguyen et al. (1999), Nieber (1996), Nieber et al. (2000) and Ritsema et al. (1998) used comparable models for unstable flow resulting from water repellency. Nieber (1996) found that in case the water entry capillary pressure on the main wetting curve is less than the air-entry capillary pressure on the main drainage curve, an initial perturbation of the wetting front will grow and persist after sequential drying and wetting. The models consist of numerical solutions of two-dimensional Richards equations or mass balance equations, a wetting and a drying curve based on the water retention and hydraulic conductivity curves of van Genuchten and Mualem's hysteresis theory (Mualem, 1974). The initial conditions include a perturbed front at the top, which corresponds to the destabilization process.

Selker et al. (1996) presented a simple model for fingered flow as the combined effect of wetting front instability, soil characteristics, finger persistence and merger, and climate. He used an estimation of finger spacing and moisture content and a solution of Richards equation for the finger growth. The maximum pore water velocity is calculated with the ratio of the saturated hydraulic conductivity over the saturated water content.

In the SWAP (Soil Water Atmosphere Plant) model Van Dam (2000) used a mobile-immobile concept for the simulation of water-repellent flow. They assumed that the water retention curve as measured in the laboratory applies for the fingers. The Richards equation is used for the flow in the fingers. The effective water retention function and hydraulic conductivity are obtained by multiplying the lab-measured values with the fraction of mobile region (F). And as F varies in time with the moisture content, this is included with a linear relationship between F and log (h). Van Dam et al. (2004) also incorporated a more advanced model concept in SWAP based on the work of Ritsema et al. (1993) and Selker et al. (1996). The soil is divided in three layers: the distribution zone, the finger zone and the redistribution zone. As long as the water content in the finger zone is above the critical measure, the flow is modeled with the Richards equation, for the whole profile. In case the water content in the finger zone drops beneath the critical level, a zero flux condition is set at the bottom of the distribution zone. Flow in the fingers is described with the Richards equation with a flux condition at the top and a head condition at the bottom. Change in the cross section and length of fingers is possible.

Zurmuhl and Durner (1996) tested the use of a dual porosity model versus a single porosity model. They combined three different mobile-immobile approaches to simulate the influence of transient conditions on preferential flow and solute transport. In the first approach they defined a constant immobile water content. The second approach is based on a constant ratio of θ_m/θ, the immobile water content is thus always proportional to the total water content. In their third approach the immobile water content is determined such that at any water content the immobile region provides 0.0005 of the actual conductivity. They found that only for the third case where θ_m changes with the water content, depending on the hydraulic conductivity function, enhanced preferential transport was simulated at high infiltration rates. In the other cases different hydraulic regimes only caused minor differences in solute transport.

Small scale modeling of macropore flow

MACRO is a physically-based, one-dimensional, numerical model of water flow and solute movement in macroporous soil (Larsbo and Jarvis, 2003). It is a dual domain model with Richards' equation and the convection-dispersion equation to model soil water flow and solute transport in the matrix, while a simplified capacitance type-approach is used for the macropores. Exchange between the flow domains is calculated using physically based, first order expressions depending on an effective aggregate half-width. Flow to field drains and groundwater flow are also included in the model.

In the SWAP model Kroes et al. (2008) included a model concept for water and solute movement in cracked clay soils or macropores. The shrinkage characteristic of a clay soil is used to describe the swelling and shrinking, including the crack volume and depth. The infiltration excess flows as runoff to the cracks. The water collected in the cracks will either infiltrate laterally into the soil matrix (according to a first order linear function of pressure gradient) or flow rapidly to nearby drains or ditches. In SWAP there is also the possibility to choose for an advanced macropore flow description. In that case the flow through macropores is based on the macropore geometry. The macropore geometry is given with a depth dependent function of the macropore volume. From this function the fraction of macropores ending within a soil layer is calculated and water entering these macropores infiltrates in that soil layer. This infiltration takes place according to either the soil sorptivity in a dry situation or pressure gradient in a wet soil situation, depending on which flux is larger.

Field scale or catchment scale models

At field scale or catchment scale the influence of preferential flow will mainly depend on the connection of vertical preferential flow to rapid lateral flow paths. In case of fingered flow the influence at larger scales will therefore strongly depend on water table or drain depth. In case of macropores or cracks in clayey soils many studies have shown lateral subsurface flow to be an important component of the soil water balance, mainly in forested hilly areas (Jones, 1997; Uchida et al., 2005; Tromp-van Meerveld and McDonnell, 2006; Negishi et al., 2008).

Field scale applications of preferential flow models have to include spatial variability of the soil hydraulic properties and boundary conditions on the water regime. Field applications of preferential flow models use either deterministic or stochastic methods, of which deterministic models have been more widely tested for water and solute transport, due to their ease in

accommodating chemical non-equilibrium retention reactions (Ma and Selim, 1997). A few of the existing models for macropore flow are summarized in the following.

Some models of preferential flow used at hillslope or catchment scale do not actually include lateral preferential flow, but are large scale models with mainly vertical preferential flow connected to shallow groundwater flow or rapid lateral flow on the bedrock surface(e.g. Zehe et al. 2001; Christiansen et al., 2004; Beckers and Alila, 2004).

Hillflow 3D (Bronstert and Plate, 1997) is an example of a comprehensive hillslope model, which simulates a series of hydrological processes such as interception, evapotranspiration, infiltration into the soil-matrix and macro-pores, lateral and vertical subsurface soil water flow in the matrix and preferential flow paths, surface runoff and channel discharge.

Herbst and Diekkruger (2003) modeled the spatial variability of soil moisture in a micro-scale catchment, in a 3-D variably saturated flow model based on finite elements, including the process of macropore flow and surface runoff in their model using a simplified concept: they appointed part of the matrix infiltration-excess to the macropores and the rest to surface runoff. In their model there is no interaction of water between the soil-matrix and the macropores. The macropore and surface runoff are delayed by the surface resistance and the length of the flow path to the channel. Judging on the measured and predicted hydrograph their model performs reasonably well, though the groundwater flow seems to be underestimated.

Brooks (2003) found that the bulk lateral hydraulic conductivity of a soil greatly depends on the depth of saturation. He mentions an exponential decrease of conductivity in the topsoil in case of macropores. He suggests using a double exponential relationship between saturated hydraulic conductivity and depth. This method is similar to the dual porosity approach in that the lateral saturated conductivity is raised exponentially when the top soil becomes saturated. The drawback is here again that the rapid lateral flow can only take place when the soil becomes saturated, there is no rapid subsurface flow in unsaturated conditions.

Jones and Connelly (2002) produced a semi-distributed physically based pipe flow model. Both ephemeral and permanent flow in pipes is simulated, and also the complexity of a branching network is taken into account. The flow of water in the pipes is calculated as a function of wetted perimeter of the soil pipe, length of the pipe and velocity at which the water enters the pipe.

In their model Hill–vi Weiler and McDonnell (2007) allow for lateral preferential flow only under saturated conditions, using a parabolic decrease in saturated conductivity with depth. Additionally they define a depth dependent drainable porosity for the soil. Pipe flow was included in this model, by randomly distributing short lengths of pipes over the grid cells. The height of these pipes above bedrock is randomly set (based on the defined normal distribution). These pipes can rapidly transport water and solutes from one cell to it´s neighbour.

Zhang et al. (2006) also introduced a macropore domain to the REW model approach, which accounts for preferential flow of water in both the vertical as well as the lateral direction. In their

model flow is driven by gravity, there is no exchange between macropores and matrix and the lateral macropores are parallel to soil surface.

For many of the above mentioned models the inclusion of preferential flow showed clearly better results than the models without preferential flow. Also according to the models a large part of the hydrograph is possibly caused by preferential flow. Nevertheless the models made upto now are largely simplified models and mainly aim to better predict the streamflow; whether the flow processes in the unsaturated zone are well represented cannot be proved with only outflow data, but require detailed within catchment observations and model evaluations.

1.3 Objectives

The literature summary and the concusions which can be drawn from this summary form the basis on which the following PhD research was performed. The physical processes underlying preferential flow (such as macro-pore flow, cracks in clay soils, water repellency and soil heterogeneity) have been the subject of many studies over the years. Also the measurement techniques and parameterisation of the soil moisture distribution and water flow caused by preferential flow at small scale have been intensively studied. Various modelling attempts, based on physical processes, multi porosity and multi domain simplifications for vertical unsaturated flow on a spatially small scale are continuously studied and improved.

It is known that preferential flow paths may enhance a large spatial variability in infiltration and percolation and runoff or lateral through flow and thus create a fast reaction of the groundwater levels and significant subsurface flow after a rainfall event. Still, it remains difficult to simulate preferential flow and its transient properties to full satisfaction, due to the complexity of spatial and temporal variability. Many areas in the world face problems of drought, erosion, occasional floods and pollution, which may even be enhanced by the occurrence of preferential flow. It is important to correctly describe the flow processes in the vadose zone, not only for a correct simulation of the present-day situation, but mainly also for a correct prediction of how future scenario's may influence the hydrology.

The main research goals or challenges in the field of preferential flow are:

- finding an adequate solution for measuring and modelling the transient characteristics of preferential flow, thresholds for the initiation and degree of preferential flow;
- solving the problem of measuring and parameterizing preferential flow at different scales. A major difficulty in modeling the impact of preferential flow is the measurement of quantitative indicators for preferential flow and/or conversion of measurements to parameters for hydrological models (VanClooster et al, 2000; Herbst et al., 2005; Larsbo and Jarvis, 2005). In most modeling attempts fractions are used. As long as the parameters used in modeling are determined by optimization techniques, an effective fraction might be sought. However the geometry and the density of preferential flow channels is important for their impact on the water flow and these features may be transient, as the spatial extension of preferential flow paths often depends on soil moisture content;
- characterizing the interaction between the preferential flow path and the soil matrix;

- developing combined models which deal with the existence of different types of preferential flow simultaneously. Different types of preferential flow may occur in one area. The influence of preferential flow on the hydrology of that area can therefore be highly complex. This is the case in the north of Portugal, for example, where the water repellency clearly enhances high runoff on plot scale, but there are apparently sufficient sinks, possibly macropores, which prevent the produced runoff from actually reaching the stream (Doerr et al., 2003; Ferreira et al., 2000). Also Burch et al. (1989) found on Australian highly water-repellent soils that relatively few macropores could be able to infiltrate the maximum rainfall intensities experienced at this location, even when highly hydrophobic surface conditions exist.

The main objective of this PhD research is to assess the influence of preferential flow on the water balance from plot scale to catchment scale, by the combined use of field and lab measurements and physically based models. In order to achieve this objective the following steps can be distinguished:

- analysis of preferential flow measurements at different spatial scales to gain understanding on the preferential flow processes from plot scale to catchment scale;
- analysis of the spatial distribution of preferential flow;
- plot scale and catchment scale modelling of preferential flow using a combination of field data and physically based preferential flow models.

The main focus in the hydrological modelling is on the separation of matrix and preferential flow, as this is an important issue for the correct simulation of the threshold for initiation of preferential flow and therefore for the transient characteristics of the preferential flow. For this research the physically based hydrological models SWAP (for plot scale) and Hillflow 3D (for catchment scale) were chosen (based on the hydrological functioning of the catchment as explained in Chapter 4). These models allow for preferential flow to occur regardless of the matrix soil moisture contents and interaction between macropores and matrix dependent on the matrix conditions.

As the combination of measurements and physically based models is an important part of this research, the choice of a study catchment is of great interest. A semi-arid catchment in the Extremadura, Spain, was chosen, the argumentation for which is given in Chapter 2. The main origin of preferential flow in the area is macroporosity. This narrows the research objective to preferential flow due to macroporosity in a semi-arid catchment, where the main hydrological problems are soil moisture availability and erosion, thus soil moisture distribution and runoff production are important here.

1.4 Thesis outline

Following this introduction, in Chapter 2, the study area used for this research is described including a summary of hydrological functioning of the area based on previous literature and existing measurements. As a large amount of field data was gathered for this study, and used for the interpretation of preferential flow at different scales, a complete overview of these measurements and methods is given in Chapter 3, with a description of basic data analysis and results of the field study. The first step into quantification of the influence of preferential flow

is made in Chapter 4, where the basic analysis of the field data leads to an indication of the influence of preferential flow from plot scale to catchment scale on the hydrology: soil moisture contents, water level fluctuations in the profiles and subsurface stormflow. In Chapter 5 the spatial variability of preferential flow influence on plot scale infiltration patterns is studied, and this variability is related to site specific characteristics. In Chapter 6 the plot scale infiltration patterns are used in combination with the physically based macropore flow model SWAP (Kroes et al., 2008) to determine macropore parameters. This is followed by the simulation of catchment scale influence of preferential flow using an adapted version of the Hillflow model (Bronstert, 1995) in Chapter 7. The main conclusions and suggestions for future research are given in the concluding synthesis, Chapter 8.

2 Description of the research area

2.1 Selection of the fieldwork area

The modeling of preferential flow and validation with field data involves gathering a large amount of field data, the choice of a suitable fieldwork area was important and restricted to area's with:

- expected presence of preferential flow;
- relatively uniform soil and land use;
- possibility to measure different components of the soil water balance (infiltration, percolation, groundwater level, soil moisture storage, lateral flow in unsaturated zone, runoff and catchment discharge);
- availability of geophysical and hydrological data on the catchment;
- a catchment with clear boundaries in three dimensions (clear watershed boundaries and closed bottom);
- logistics: - availability of water, electricity, etc,
  - accessibility of the area.

Based on these criteria the Parapuños catchment in the Spanish Extremadura was chosen. The Parapuños catchment (see Figure 2.1), is located near the city of Cáceres, Extremadura, approximately halfway between Madrid and Lissabon in a rather homogeneous landscape, a large peneplain with a typical agro-silvo-pastoral land use called Dehesa. Dehesa is the dominating landscape of the south-western Iberian Peninsula. The Dehesas face problems of landscape

Figure 2.1 Location of the study area, near the city of Caceres in Extremadura, Spain (from Ceballos and Schnabel, 1998), the hatched area shows the extension of the Spanish Dehesa landscape.

degradation: lack of tree regrowth, soil erosion, soil degradation and increased runoff, due to changes in management (Schnabel and Ferreira, 2004). Future climate change, bringing higher average temperatures and more extreme precititation, with longer droughts will further enhance the landscape degradation. This study area has been an experimental catchment of the University of Extremadura since the year 2000. An overview of existing hydrological measurements and findings based on these measurements is given in this Chapter. The additional measurements performed for this PhD research, including basic analysis and results of these measurements are summarised in Chapter 3.

The catchment is part of a private farm, of about 900 ha in an open shrubland area with scattered oak trees as shown in Figure 2.6. Land use is extensive livestock farming with sheep, cattle and Iberian pigs. It is a first order basin, with average slopes of 8%. The catchment aspect faces SSW. The catchment is about 1 km^2 in size and lies at an altitude of ±350-435 m asl.

The main advantages of Parapuños are that it is a small catchment with a relatively homogeneous vegetation- and soil type. Thanks to the pronounced relief and the shallow soils, the spatial boundaries of the catchment can be estimated reasonably well based on the topography. Also the bottom boundary of the catchment is an almost impervious material: greywackes and schists (of Precambrian to Upper Carboniferous origin). Seepage of water into weathered cracks or root holes (which have been found to penetrate partly into the bedrock) is assumed to be very little and to be mainly a temporary sink, as this can be withdrawn by trees for evapotranspiration during the dry summer. The catchment dries out completely during the summer, which means a full years water balance can be made up easily as total precipitation must be equal to the yearly total discharge and evapotranspiration (Ceballos and Schnabel, 1998). Also, there is already a

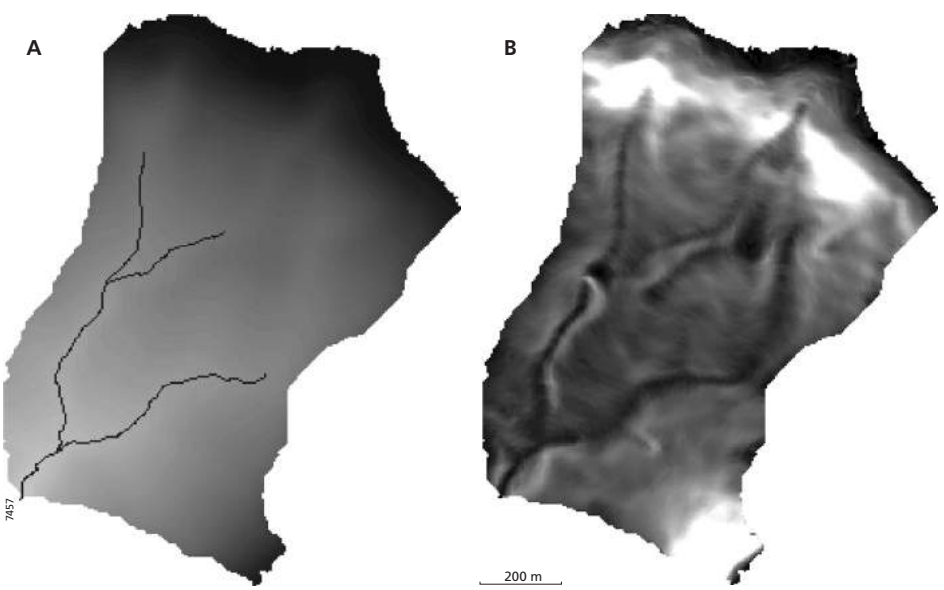

Figure 2.2: DEM, including the ephemeral gully system, and slope map of the study area.

large existing dataset and an ongoing measurement campaign (see paragraph 2.6). Furthermore the area is easily accessible.

2.2 Geology and soils

The following paragraph is a summary of geological information taken from Devesa Alcaraz (1995), García Navarro and López Piñeiro (2002) and IGME (1987). Geologically the study area is part of the great central-extremenian anticline. The oldest material that is found in the Extremadura dates back to the Precambrium. From the precambrium to the Upper Carboniferous period sediments were deposited under marine circumstances. There was slight uplift of the area and a sequence of regressions and transgressions caused periods of erosion and sedimentation in the area. After the sedimentation a period of deformation started. During the hercynic orogenesis, when Laurasia and Gondwana were pushed together to form the supercontinent Pangea, the Tethys sea was closed and uplifted. It was during the hercynic orogenesis that the most drastic physiographical changes took place in the region: marine circumstances were changed into a mountain range. Hereby the schists, greywackes and quartzites, sediments from the Precambrian to the upper carboniferous period, were uplifted and faulted. Ever since the Perm, when the mountains reached their highest altitude, a continuous slow process of erosion and denudation started. During the Alpine Orogenesis reactivation of the hercynic faults gave a rejuvenation of the relief. During the Paleocene and the Miocene there was a lowering of the river grabens of the Tagus and the Guadiana, with a simultaneous uplift of the mountain ridges. Sediment was deposited in the lower areas. During the Pliocene – Pleistocene the area was affected by intensive fluvial erosion (due to arid conditions with occasionally very intense rainfall), which caused the deposition of a very badly sorted sediment. This sediment is typical for the area, and is named Raña: a pediment formed of rounded quartzites in a clayey matrix. This resulted in the present landscape of mountain ridges (the synclines, composed partly of quartzites) and peneplain (the anticlines consisting of schists and greywacke).

The Parapuños is a small headwater catchment, which belongs to the basin of the Almonte river, a tributary to the Tagus river. The hilltops in the catchment are covered with the previously mentioned badly-sorted Raña deposit. These soils are extremely stony, have a reddish sandy loam or loamy sand matrix and reach depths of 80-90 cm. Along the hill slopes the soils are very shallow (20-40 cm) with occasional stone/pebble layers. The soil type along the hilltop to valley bottom varies from sandy loam, through loam to silty loam, with a (silty) clay loam layer at larger depth. The valley bottoms are covered with a fresh deposit of eroded material from the hilltops/slopes. In the valley bottom the soil depth varies strongly in relation with the irregular surface of the underlying schists, with a maximum depth of about 90 cm and frequent vertically oriented schist rock outcrops (Figure 2.3). The texture of soils developed on the schists in the valley bottom is mainly silty loam, with frequently large stones and occasional pebble layers in the subsoil. Organic matter content in the soils is generally between 2 to 4 % in the upper layer. The soils are acid (with pH values between 4.1 and 6.9) and are poor in nutrients, mainly Phosphorous (personal comment, Prof. S. Schnabel, University of Extremadura).

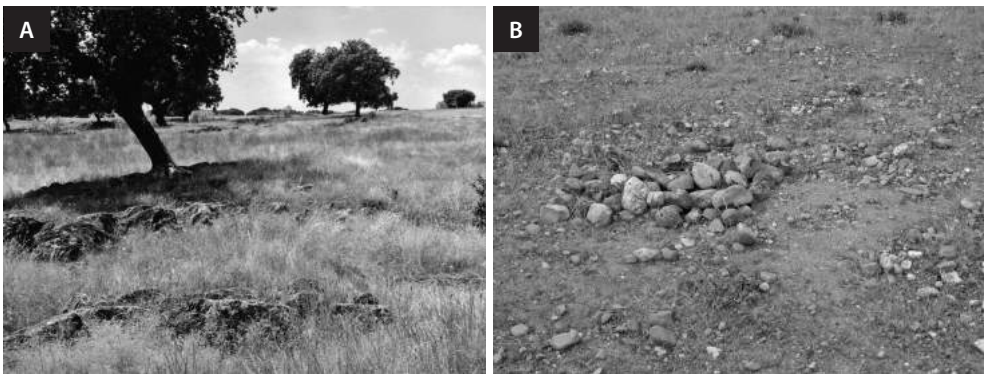

Figure 2.3: Examples of rock outcrops and stoniness.

2.3 Climate

The climate in this region is Mediterranean with Atlantic and continental influences. This results in moderate winters (with average January temperatures of 8.1 °C) and hot and dry summers (June to September, with an average temperature of 25.6 °C in July and August and regular maximum temperatures above 40°C). The average annual precipitation is 514 mm, distributed over an average of 85 rain days. There is a dry period from June to September and a wet season from October to April (Meteorological station, Cáceres). When using the Unesco aridity index, the climate can be classified as semiarid. The high temperatures, large amount of sunlight hours (estimated at 3000 hours a year) and high global radiation (as can be seen from Figure 2.4 for a large part of the year evapotranspiration is strongly water limited). There are no evapotranspiration measurements for the area, but the annual rainfall-runoff coefficient was found to be on average 6.9%. The other 93.1% of the precipitation, being approximately 479 mm is probably a reasonable estimate of average annual actual evapotranspiration, but alike the precipitation this will also be highly variable, mainly depending on the water availability.

A thorough rainfall analysis by Schnabel (1998) shows that there is a high annual and interannual variability of rainfall (standard deviation of annual rainfall is 155 mm), which leads to frequent droughts with a duration of more than two years. Most of the rain falls in high magnitude rainfall events (69.1 % of rainfall in 25% of the events). Most of the events have intensities under 10 mm/h. Rainfall intensities higher than 20 mm/h occur on average 6.7 times a year and very high intensity rainfall, in excess of 50 mm/h on average almost once a year (f=0.93) (Schnabel, 1997).

2.4 Vegetation and land use

The Dehesa land-use is a semi-natural land-use, which is typical for a large part of the south western Iberian Peninsula (approximately 4 million hectares). Historical research (Martín Vicente and Fernández Alés, 2006) shows that in the 18-th century oak shrub lands were

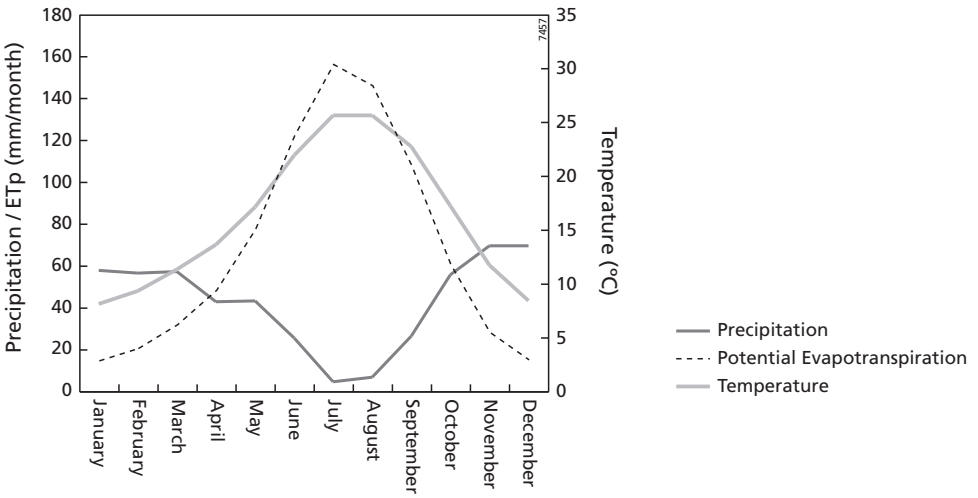

Figure 2.4: Monthly distribution of precipitation, temperature and potential evapotranspiration for the Cáceres meteorological station (Maneta, 2006), 30 year average (1961-1990).

common in the area. Only after large parts of the land were privatised the open oak parklands developed, due to the changes in management practices favourable to grazing. Originally the term Dehesa comes from the Latin 'defesa' meaning protected. This term was used for private rangelands or hunting and fishing reserves and by now encompasses the land use system, from geographical and ecological to even socio-economical meaning. Dehesas are openly spaced woodlands (tree densities vary between 5-40 trees per ha.), with agro-silvo-pastoral landuse, a Mediterranean, semi-arid climate and poor soils (shallow, acid, low organic matter content) (Schnabel and Ferreira, 2004). The limiting natural conditions (water scarcity, hard climate conditions and poor soils) result in this typical landscape. Similar land use systems are found in other Mediterranean countries (Cerdá et al., 1998).

The Holm Oaks (*Quercus ilex*) are the only trees present in the area. The tree density varies from0 to 139 trees ha^{-1} (Figure 2.5), but has an average value of 20 trees per hectare (Maneta, 2006). The Oak trees are valuable as their acorn production is used to raise Iberian pigs. During winter time, to maximize their production, the trees are regularly pruned. Furthermore the trees produce shade in summertime. The understory of grass and shrubs is generally dominated by winter annuals and to a lesser extent by tree regrowth, and small evergreen shrubs (such as *Retama sphaerocarpa*, *Cytisus multiflora* and *Lavandula stoechas*). The herbaceous understory (with a very high biodiversity of 135 species reported in Dehesas (Marañon (1985) in Martín Vicente and Fernández Alés, 2006)), serves as fodder for the extensive grazing of sheep. During the summer months the herbaceous layer dries out completely. Within four to six weeks after rainfall starts in autumn, the area has a full green cover of grass once again.

Part of the Dehesas are used for cereal cultivation. In the past this area has varied, depending on the economical situation, and occasionally every patch of land which was barely workable, was used for cultivation. Scars of the ploughing in the past are still visible in parts of the Parapuños

Figure 2.5: Aerial photograph of the catchment, clearly showing the variation in tree density in the area.

catchment. Also some parts of the catchment have a very high density of sheep trails. And in the centre of the catchment there is still a fenced part where cereal is sown to attract birds (pigeons and partridges) for prey in the hunting season. Though relatively homogeneous in vegetation, the tree and shrub density is very variable (a dense shrub layer mainly along the hillslopes and the herbaceous layer mainly dominant in the valley bottom). The herbaceous layer is only present in the wet season. Part of the surface soil is also sealed with lichen or crusting, mainly along the hillslope, near the rim.

While in many areas modern agriculture is held responsible for the extinction of plant, insect or bird species, the Dehesa's have a high bio-diversity both on a within-habitat and between habitat scale (Plieninger and Wilbrand, 2001). Due to the combination of exploitation and habitat conservation, the Dehesa's are considered a model for sustainable agriculture (Martín Vicente and Fernández Alés, 2006). Nevertheless the Dehesa landscapes are threatened by erosion, soil degradation and lack of tree regrowth: in some cases caused by overgrazing and in others by land abandonment (Schnabel and Ferreira, 2004). As vegetation plays an important role in the hydrological processes, landscape degradation and erosion, it is an important factor in the understanding of the hydrological functioning of the area and changes in land-use may also have a strong impact on the hydrology of the area.

2.5 Hydrology

Hydrological research in the Dehesa's in the past has focused mainly on rainfall-runoff relations (Ceballos and Schnabel, 1998; Ceballos et al., 1998) and erosion (Schnabel, 1997; Schnabel

Figure 2.6: Examples of vegetation in a relatively bare soil site and a site with a denser shrub layer.

et al., 1998). When analyzing the rainfall-runoff, Ceballos and Schnabel (1998) found a strong relationship between the precipitation and evapotranspiration as well as between the precipitation and area discharge. Depending on the moisture conditions of the catchment, overland flow can be either hortonian or saturated overland flow. The form of a hydrograph of a typical first order catchment indicates rapid surface runoff. Annual runoff coefficients are generally low (on average 6.9 %) and comparable to those of other semi-arid watersheds. Their variability depends strongly on the distribution of precipitation throughout the year and also on the annual rainfall totals (Ceballos and Schnabel, 1998).

Thanks to the pronounced relief and the shallow soils, the spatial boundaries of the catchment can be estimated reasonably well based on the topography. Also the bottom boundary of the catchment is an almost impervious material: greywackes and schists (of Precambrian to Upper Carboniferous origin). Seepage of water into weathered cracks or root holes (which have been found to penetrate partly into the bedrock) is assumed to be little and to be used as a source for tree evapotranspiration in summer, so it is only a temporary storage. Furthermore the catchment dries out completely during the summer, which means a full years water balance can be made up easily as total precipitation must be equal to the yearly total discharge plus evapotranspiration (Ceballos and Schnabel, 1998).

Mateos and Schnabel (2002) found that the interceptionof Holm Oaks (*Quercus rotundifolia*) mounted up to 26.8 % and stemflow was 0.3% of rainfall, respectively. The spatial variation of throughfall is very high and the total amount was mainly controlled by the amount of precipitation, and to a lesser degree by rainfall intensity, temperature and air humidity. Nevertheless, due to the low tree density, the total interception in case of a tree density of 15 per hectare is estimated to be only 4%, this is a lower density than the average 20 trees per hectare as estimated for the study area by Maneta (2006). Interception by shrubs ranged from 21.0% (*Retama sphaerocarpa*) to 31.6% (*Thymus vulgaris*) for the most common shrubs in the area (Llorens and Domingo, 2007). Mateos and Schnabel (2002) determined a storage capacity of 1.1 mm for Holm Oaks in a nearby area. Corbett and Crouse (1968) determined values of grass interception and canopy storage in a Mediterranean climate, in California to be 8% interception.

The effect of vegetation on soil water dynamics was studied as well (Cammeraat and Imeson, 1999; Cammeraat, 2004; Cubera et al., 2004; Joffre and Rambal, 1993; Montero et al., 2004; Moreno et al., 2005). Cammeraat and Imeson (1999) concluded that vegetation patterns of stipa grass (*Stipa tenacissima*) intercept eroded material and increase infiltration. Cammeraat (2004) found that runoff and sediment yield depend largely on the vegetation structure at different scales in a semi-arid catchment in Spain. Soils developing under a tree canopy are richer in nutrients and organic matter and have a greater water-holding capacity and a macroporosity favorable to infiltration and redistribution of water (Joffre and Rambal 1988). Tree roots extend far beyond the tree canopy, which suggests they can draw water from far beyond their canopy deck (Moreno et al., 2005). In a detailed study of fine root distribution in Dehesas of central western Spain, Moreno et al. (2005) found that the root length density of herbaceous plant roots decreases exponentially with depth and their roots are mainly located in the upper 30 cm of the soil profiles. Holm-oak root length density was found to be almost uniform with depth and distance to the tree, with 33 m maximum horizontal extension of tree roots. The root length density of trees is much smaller than that of herbaceous plants in the upper 10 cm, 2.4 km m^{-3} versus 23.7 km m^{-3}. Soil water depletion by trees in the deeper layers continues even in summer, when herbaceous plants are dried up and soil evaporation is negligible, thus the competition for water between trees and herbaceous vegetation is limited (Cubera et al., 2004; Joffre and Rambal, 1993; Montero et al., 2004; Moreno et al., 2005). Tree roots occasionally extend down into the bedrock, where they can draw some extra water from the temporary water storage in cracks or weathered bedrock, as mentioned above.

Joffre and Rambal (1993) estimated the mean annual evapotranspiration to be on average 591 mm under tree cover and 400 mm outside tree cover in a Dehesa area slightly south from the

Figure 2.7: Meteorological station in the valley bottom of the catchment.

study area, with annual rainfall between 600 and 800 mm. They found daily transpiration values between 1.65 and 2.04 mm for *Quercus ilex*, with monthly values of 50 – 60 mm in July and August. For open grass they found daily values of 0.6-1.0 mm in autumn and up to 2.3 to 2.9 mm in spring, which is the period of maximum growth. The growing season for the grass layer starts shortly after the first autumn rains, within 6 weeks there is a full soil cover. The grass dries out completely by the end of May. Whether a strict distribution of evapotranspiration below and outside the canopy is possible in an open vegetation structure as exists in the Dehesas may

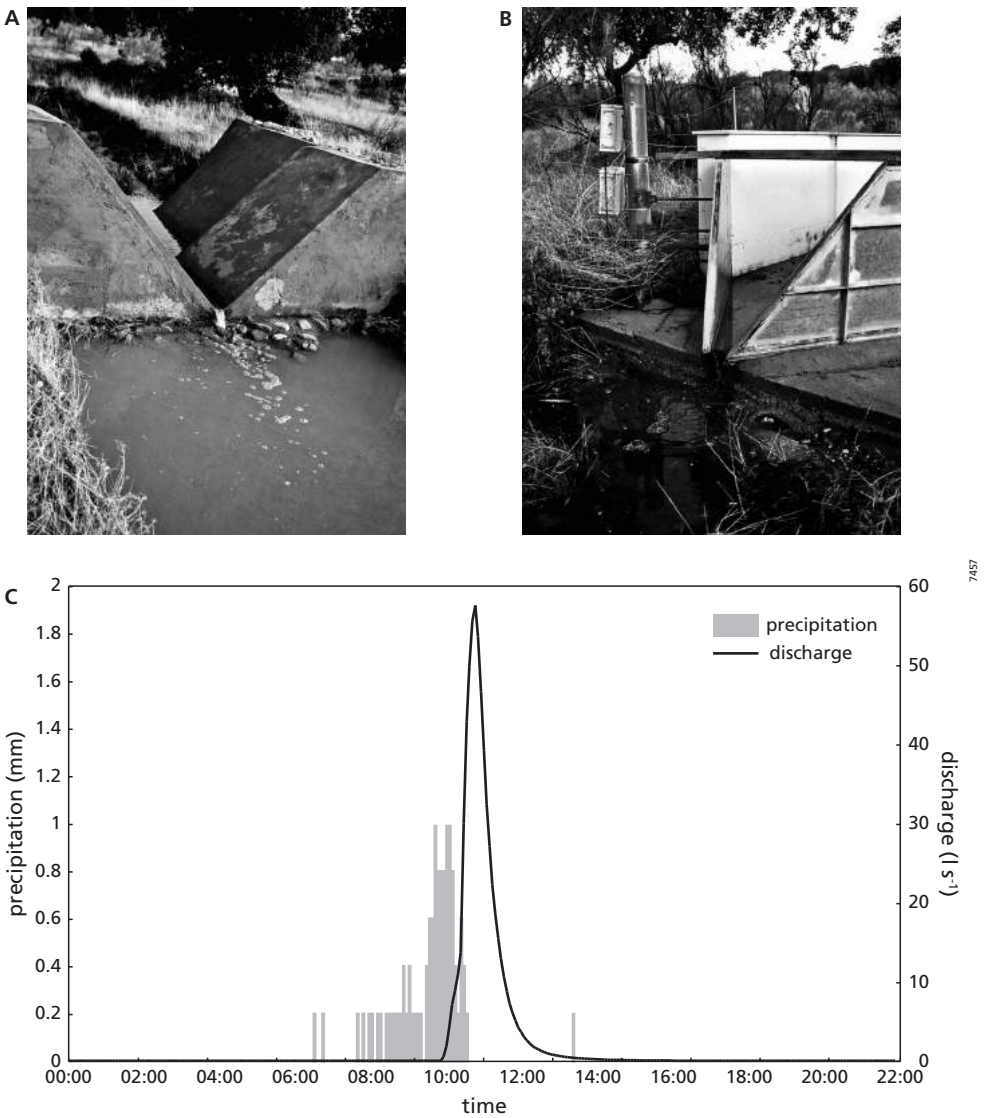

Figure 2.8: a) Discharge measurement gauges for the entire catchment (a) and the hillslope subcatchment (b) and c) a typical discharge hydrograph

Table 2.1: Summary of measurements done by the University of Extremadura in the Parapunos catchment, measurement apparatus, and resolution.

Measurement type	Measurement apparatus	Interval
Precipitation	1 Omnidata ARG 100 2 ONSET automatic tipping buckets	5-min resolution
Temperature	Campbell 50Y sensor	5-min resolution
Global radiation, Net radiation	SKYE SKL2650 Campbell NR Lite sensors resp.	5-min resolution
Wind speed	YOUNG Gill12002/12005 sensor	5-min resolution
Air humidity	Campbell 50 Y sensor	5-min resolution
Catchment discharge	Water level recorder	5 min resolution
Soil moisture content	8 echo sensors, in 2 profiles at four 16 TDRs in 2 profiles, at four different depths	Manual read out, every two weeks

be questionable according to Moreno et al. (2005) as the tree roots extend far beyond the tree canopy.

There are two main gullies which drain the study area, but which are dry for a large part of the year. Discharge occurs only during or shortly after rainfall events, with a maximum duration of 4 or 5 days after rainfall stops, under very wet catchment conditions (only a couple of hours in dry catchment conditions). Remarkably the gullies show discontinuities at the surface in width and depth. It is not clear what produces these discontinuities, possibly some layers of very high conductivity, such as the pebble layers found in the gully sidewall. Another possibility is that the opposite occurs: the gully may not be able to work it's way through some very hard rock outcrops surfacing along it's pathway.

2.6 Existing measurements

The existing ongoing measurements (Table 2.1) include: meteorological data (temperature, humidity, net radiance, global radiance, wind speed and – direction (Figure 2.7)), rainfall measurements at three locations (from spring 2006 onwards this was extended to six measurement locations), soil moisture content in two profiles (a total of 16 probes) and catchment discharge (Figure 2.8) (all at a 5 min resolution, except for the soil moisture, which is read out manually approximately once every two weeks). All measurement locations are given in Figure 3.1.

Rainfall
The spatial variation in the rainfall measured with the three gauges (Figure 3.1) was studied and appears to be minimal. The standard deviation in measured rainfall between the different gauges amounted to 7% of the total average annual rainfall, mainly caused by the higher rainfall measurements in the meteorological station (Figure 2.9a). Though the gauges were all calibrated before placement in the field, the difference in measurements between the Meteorology station

and the other two gauges could be partly caused by measurement errors, as this gauge is of a different type than the other two. Starting from Februari 2005 a number of new gauges were placed in the area and the gauge from the meteorology station was removed due to failure. The first results of the measurements of the total of six gauges in the catchment for the period of February 2005 to August 2006 show that the standard deviation between this larger set of gauges is 5% of the total average rainfall. As the rainfall amounts of the individual gauges

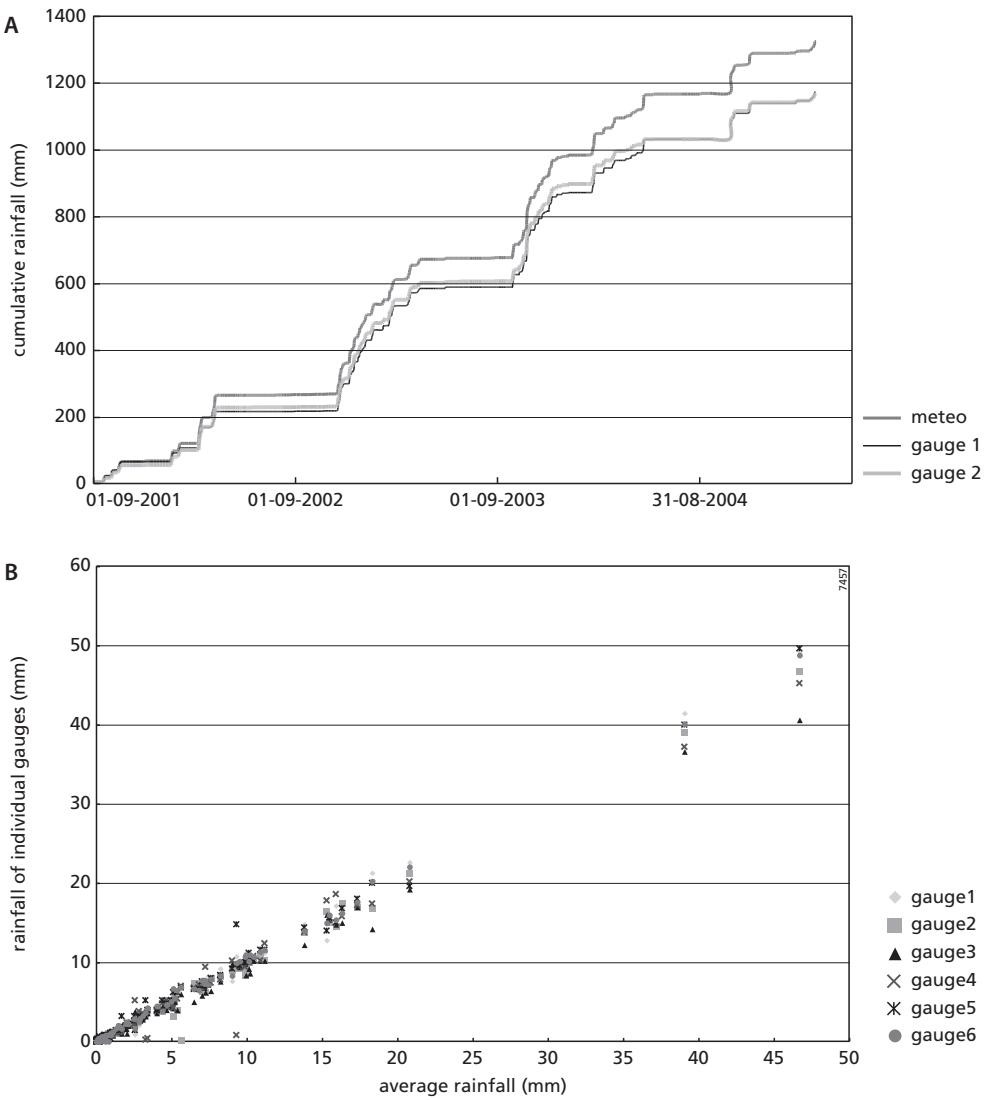

Figure 2.9: Cumulative rainfall a) for the three different rain gauges from March 2001 to March 2005 and b) comparison of rainfall measurements for six new rainfall gauges spread through the area with the average rainfall, from Februari 2005 to August 2006.

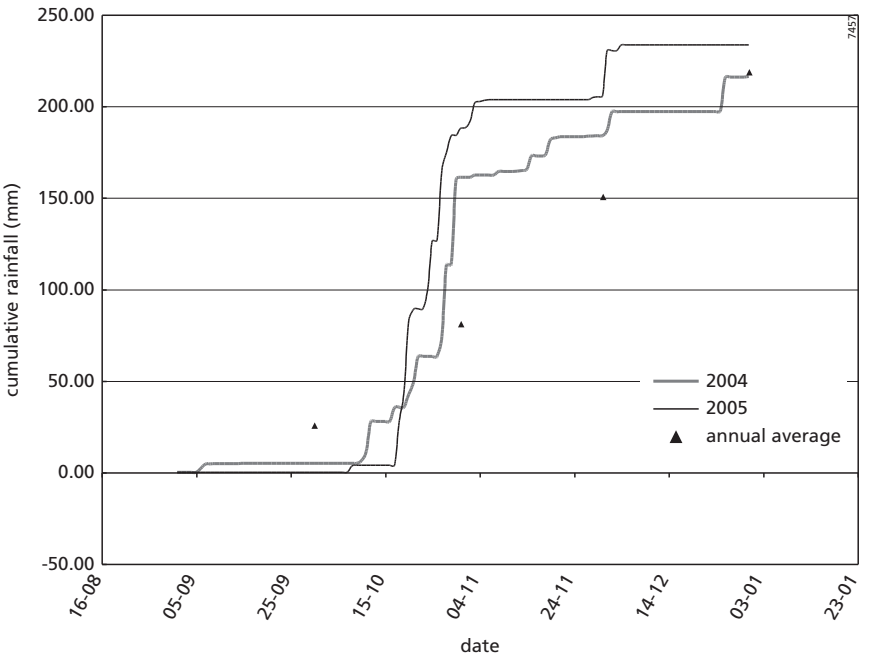

Figure 2.10: Cumulative rainfall for the fall of 2004 and 2005, compared to long term annual average data.

compared to the average measured rainfall (Figure 2.9b) shows very little deviation, for the modeling exercises in this thesis the average rainfall of the different measurements is used.

The main measurement campaigns for this research took place in the fall of 2004 and the fall of 2005. Therefore the periods used for the analysis and modelling exercises were the hydrological years of '04-'05 and '05-'06. The rainfall for these specific years was lower (336.3 and 368.6 mm) than long term annual average (514 mm) and a large amount fell during a couple of high intensity rainstorms in the October months (Figure 2.10). For the fall of 2004 (1st of September to the 3rd of December) the discharge amounts to 11.2% of the 234 mm of precipitation. For the same period in 2005 this was 8.6% of 196.8 mm of precipitation. The discharge percentage for the full hydrological years amounted to 7.9% for '04-'05 and 7.6% for '05-'06 (excluding some short periods where the discharge measurements were hampered).

Soil moisture content

The first series of soil moisture measurements were performed with Echo sensors (soil moisture sensors based on capacitance measurements (Bell et al., 1987)) showed a clear indication of preferential flow (Figure 2.11). Two series of sensors were placed at four depths in the soil. The reactions in moisture contents in one of the profiles during and shortly after rainfall were rapid and in a different order than to be expected. The sensors at 20 cm depth hardly reacted, while the deeper sensors showed rapid increase and even some rapid decrease after rainfall. This

indicates there must be some rapid pathway to conduct water down to the depth of 70 or even 90 cm within hours from the start of rainfall in a relatively dry soil and there must be some dryer surrounding soil to redistribute the water to after the supply ceases. In the other soil profile there were hardly any reactions, but a gradual, steady increase in water content in the sensors at 20 and

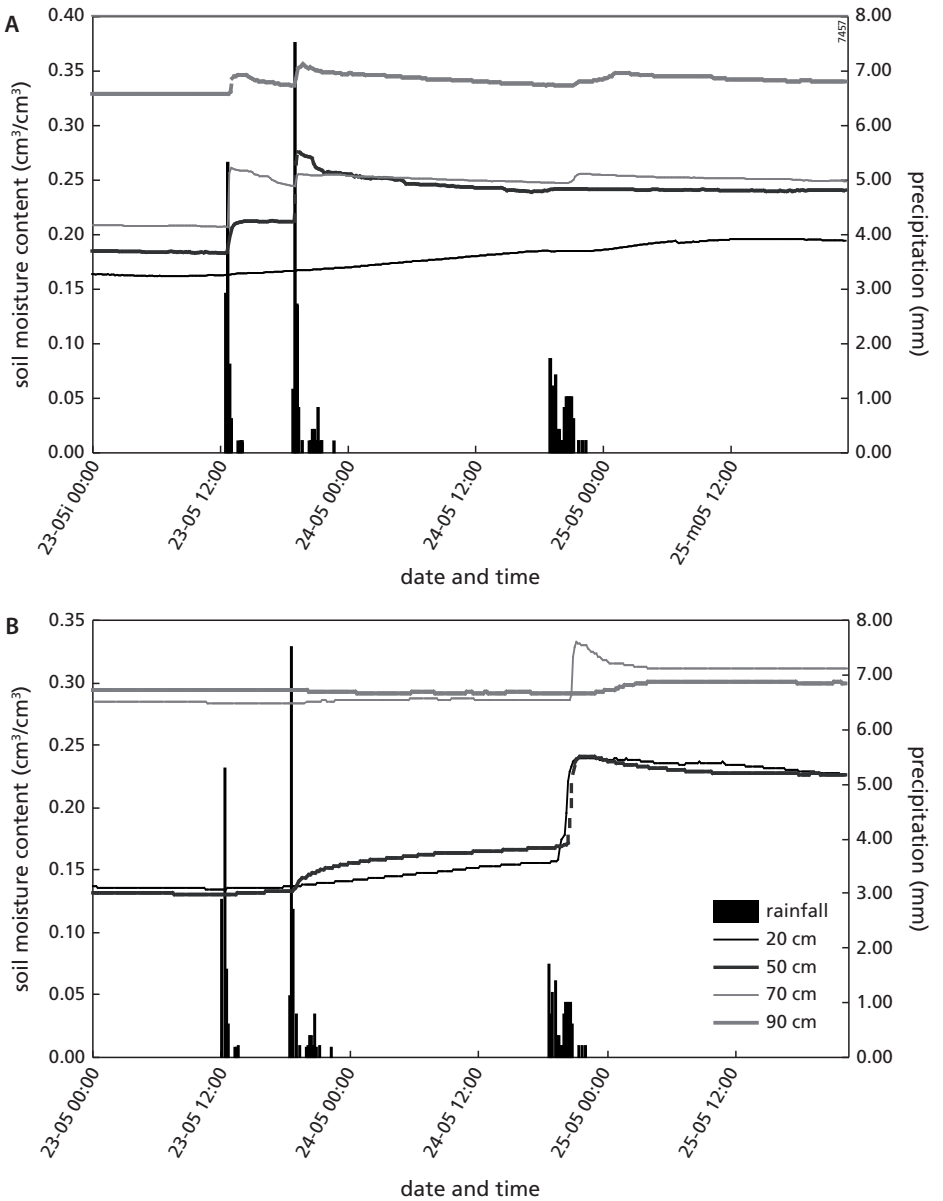

Figure 2.11: Soil moisture content reactions to rainfall in two pits (a and b) with Echo- sensors at four different depths.

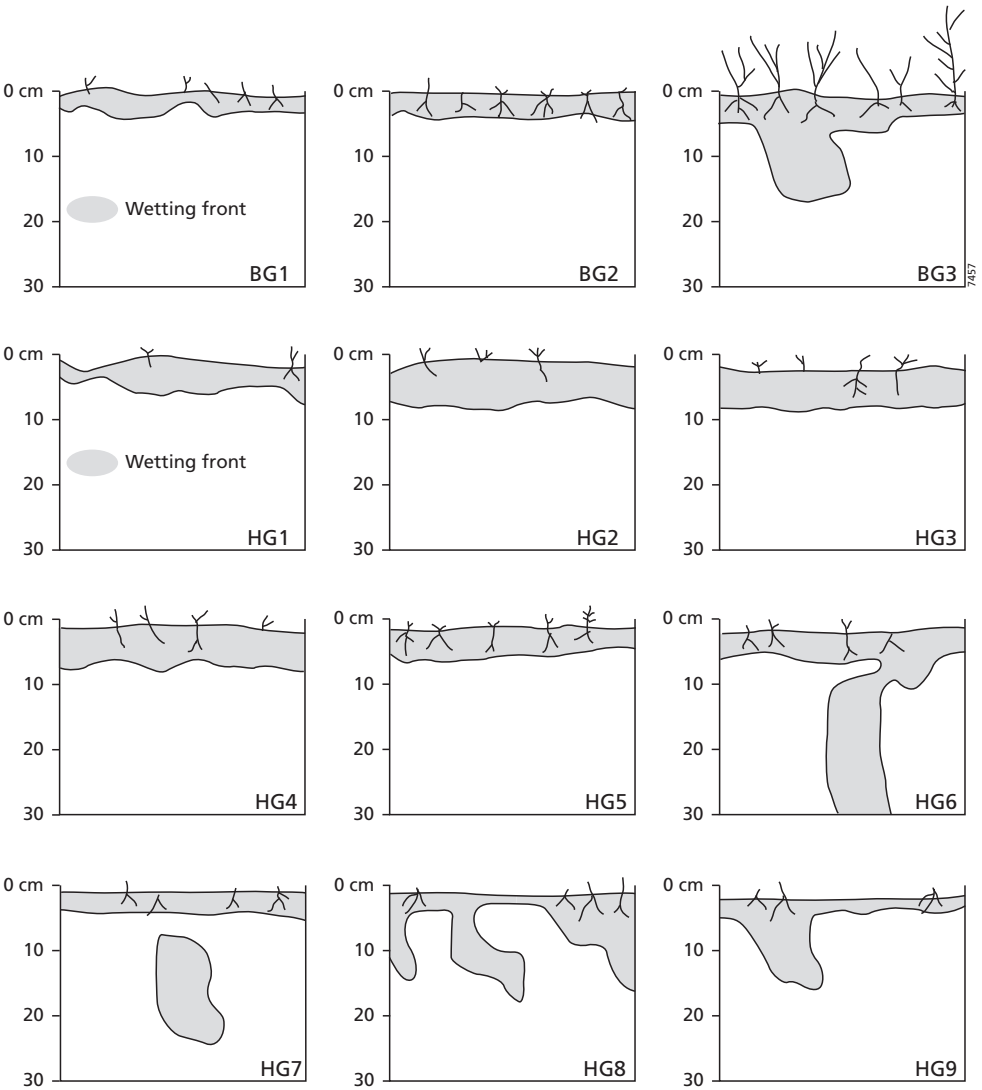

Figure 2.12: Examples of infiltration patterns as found by Cerdá et al. (1998) in a rainfall-runoff study in the Dehesas.

50 cm depths, which could be a sign of a uniform infiltration front, slowly moving down. Then after the longer duration rainfall with lower intensities the moisture contents in the first profile were hardly influenced, while the second profile showed some jumps in moisture content, the impact decreasing with depth in the soil.

2.7 Preferential flow

Cerdá et al. (1998) found non-uniform infiltration patterns due to macroporosity and water repellency in rainfall- runoff studies in the Dehesa's (Figure 2.12). Joffre and Rambal (1993) also concluded that infiltration under the trees was influenced by macroporosity. Different origins of macroporosity were observed in this study area: old root channels, ant burrows, worm burrows and even large burrows of mice were seen to cause underground rapid flow of water. Locally cracks were visible at the soil surface in the dry period (these cracks however had limited width of maximally a few millimetres. Also the large soil heterogeneity along the upper rim, the high amount of (large) stones in the soils and the occurrence of pebble layers in the valley bottom may cause preferential flow.

In the valley bottom an interesting soil profile is ready to the eye: the gully edge (Figure 2.13). This profile shows many macropores, of different sizes, ranging from small to large more or less tubular holes and thin cracks, some of which have a clear coating along the sides. There are also some pebble layers visible in the finer matrix.

2.8 Conclusions

The Parapuños catchment was chosen as research area for this PhD research based on the clear hydrological boundaries of the catchment, relative homogeneity of vegetation, accessibility of the area and availability of basic hydrological and meteorological data. Literature and visible evidence of macropores in the area, indicate that preferential flow occurs in this catchment, which makes it suitable as a study area. Soil moisture content measurements in the study area indicate preferential infiltration of water to deep soil layers under high intensity rainfall. A lot of research has been done on the hydrology of Dehesa's, and many hydrological and meteorological measurements are already performed in the study area, but the influence of preferential

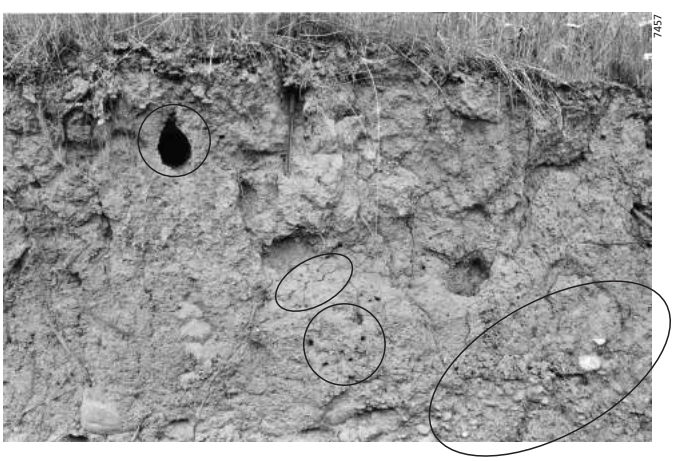

Figure 2.13: Visible macropores, some with coating, along the gully side profile.

flow on the hydrology from small scale to catchment scale is still unknown. Therefore this research concentrates on additional measurements in the study area, to investigate the degree of preferential flow and to use in combination with hydrological models for quantification of preferential flow. Though at a catchment scale the yearly water balance can be calculated fairly well, the spatial and temporal distribution of evapotranspiration is likely to remain difficult to quantify.

3 Measurements and methods

3.1 Introduction

As discussed in chapter one a major difficulty in modelling the impact of preferential flow is determining quantitative indicators for preferential flow. As the main goal of this PhD research is to quantify the influence of preferential flow from plot scale to catchment scale using field data and physically based models, the gathering of field data on preferential flow at different scales is very important.

For the preferential flow modelling first of all the basic hydrological and meteorological data for catchment scale hydrological modelling are necessary. Most of these data, such as rainfall, meteorology data and discharge are available with a 5-min resolution (see Chapter 2). Furthermore the soil moisture content was measured with a total of 16 TDR probes at four different depths, divided over two profiles in the valley bottom. Initially Echo sensors were used, but these began to fail after some time and were then replaced by TDR probes.

Preferential flow is a transient process, which occurs mainly under high intensity rainstorms. Preferential flow furthermore occurs at different scales. At the small scale it results in a variation in infiltration and soil moisture distribution. At hillslope scale it may produce rapid lateral flow over large distances, finally resulting in subsurface stormflow at the catchment scale. In order to model preferential flow at catchment scale it is important to understand the role of preferential flow at these different scales. Therefore preferential flow should be measured at varying spatial and temporal resolutions. An overview of all the additional measurements performed for this research is given in Table 3.1. The measurement locations are all shown in Figure 3.1.

Small scale preferential infiltration
During a field campaign in the fall of 2004 plot scale measurements were performed to measure infiltration patterns and their spatial distribution throughout the catchment. Therefore rainfall simulations were performed at 18 plots with a Brilliant Blue tracer (CI 42090). In order to study the influence of site specific variables and soil physical parameters on the spatial distribution of preferential flow, additional site variables and soil physical measurements were collected. The locations of these measurements were distributed throughout the catchment and in different soil and vegetation units (Table 3.2), based on the units described in previous research in the Dehesa's (Ceballos and Schnabel, 1998; Cerdá et al., 1998).

Hillslope and catchment scale preferential flow
To study the soil moisture content profiles from dry to wet catchment conditions under natural circumstances, including hillslope processes, a total of 67 TDR probes were placed in six profiles along two hillslopes in the area. The TDR probes were manually read out twice a day

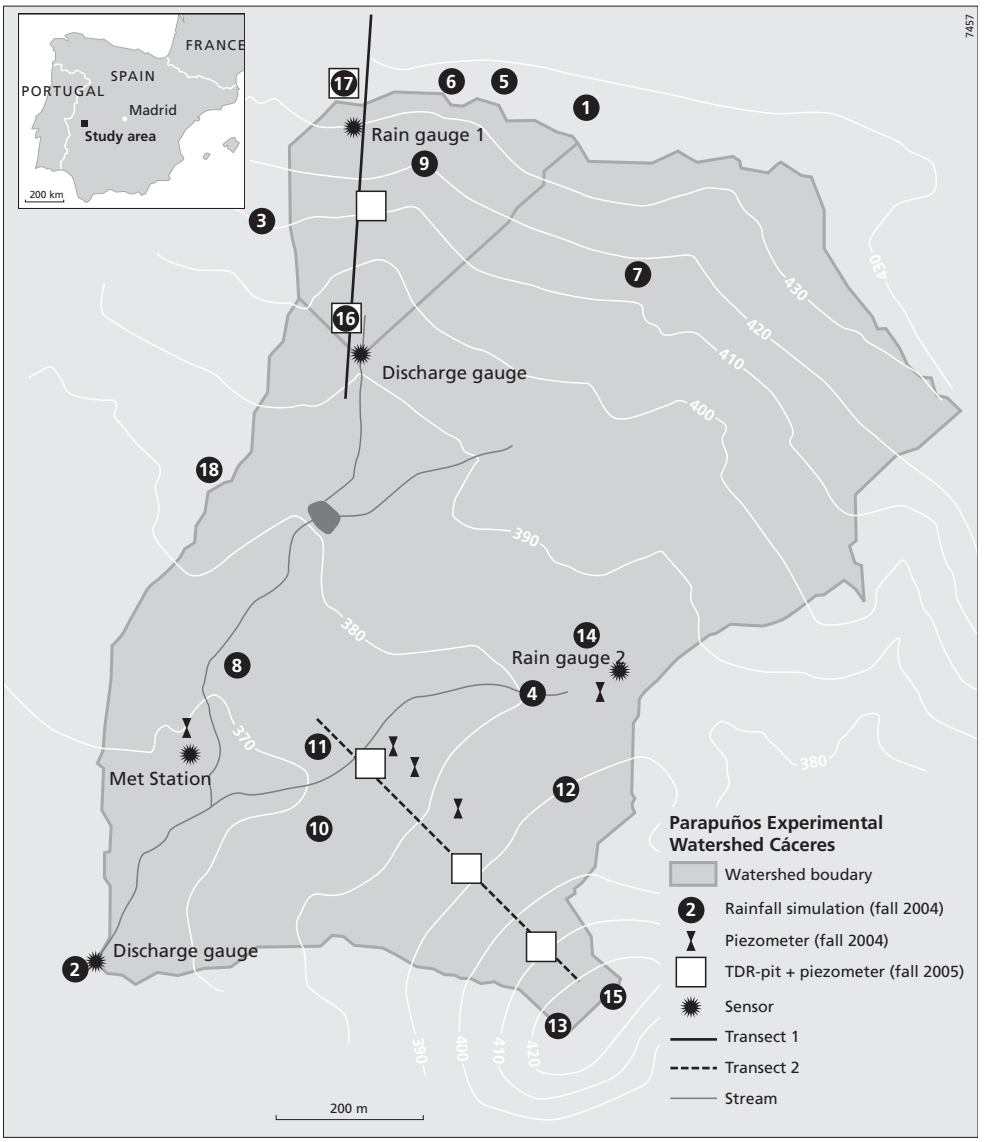

Figure 3.1: The Parapuños experimental catchment, including locations of field measurements.

from October to November 2005. Soil profile descriptions for the TDR pits are given in Table 3.3 (these profiles are considered to be representative for the hillslopes: from hilltop to valley bottom). From the 1st of September 2004 to the 5th of January 2005 the groundwater level was monitored continuously at five locations (at a 10 min resolution). From the 23rd of September to the 18th of May the groundwater monitoring was continued in two of the old groundwater pipes and at six new locations, next to the TDR-pits in the two hillslopes. These data added to the catchment rainfall and discharge give insight in flow processes at hillslope and catchment

Table 3.1: Summary of additional measurements performed for this research, interval and number of measurements

Data	Measurement method	Interval	Number of measurements
Vegetation cover	Ground survey	– – -	18
Soil depth	Excavation/soil profile description	– – -	18
Soil (Physical) data			
Soil type	Soil survey	– – -	18 plots
Stone coverage fraction	Soil survey	– – -	18 plots
Texture, OM content	Laser Difraction, glowing (soil samples from 100 cm^3 cilinders)	– – -	18 plots, 2-4 layers
Porosity, bulk density, initial moisture content, saturated conductivity	Soil samples (100 cm^3 cilinders)	– – -	18 plots, 2-4 layers (2 samples per layer)
Water retention characteristics, hydraulic conductivity curves	Multi step outflow experiments	– – -	18 plots, 2-4 layers
Waterbalance components			
Groundwater level	8 Keller pressure transducers with automatic recording	10 min resolution	11
Soil moisture contents	Profiles with 6 to 12 TDR sensors	Twice per day	6 profiles
Through flow component	Three gutters to collect throughflow from different soil layers	10 minute interval (during 1 hour) for a chosen rainfall event	1profile
Preferential flow parameters			
Preferential infiltration parameters	Dye-tracer infiltration patterns		18
Degree of water repellency	Water drop penetration time		18

scale and therefore indirect information on the influence of preferential flow at catchment scale. Also for one event lateral throughflow in the valley bottom was measured in a soil profile (29th of October 2004)

3.2 Small scale measurements

3.2.1 Dye-tracer rainfall simulations

Introduction

As described in Chapter 1 a consistent measurement method, description, parameterisation and verification of the macropore geometry and interaction process is not yet achieved. Lately dye tracers were successfully used in field experiments to visualize the continuity and hydrological effectiveness of preferential flow paths in soils (Weiler, 2001). The main aim of the tracer experiments for this research was to quantify the presence of preferential flow paths. An

Table 3.2: Combination location – vegetation coverage in Parapuños catchment. For locations of the measurements see Figure 3.1.

	Tree cover	Open space	Shrub	Sheep trail	Total
Rim	5, 15	1, 13	*	6, 17	6
Hillslope	9, 18	7	3, 16	12	6
Valley	8	2	10, 14	4, 11	6
total	5	4	4	5	

**) As there is hardly any shrub-layer present on the rim, this combination is not measured.*

Table 3.3: Soil profile descriptions (with Munsell colour codes), for six TDR-pits along two transects in the catchment. For locations of theTDR- pits see Figure 3.1.

Hillslope 1			**Hillslope 2**		
Hill top	Hillslope	Valley Bottom	Hill top	Hillslope	Valley Bottom
0 – 55 cm dull orange (7.5YR 6/4) sandy loam very stony	0 – 30 cm yellowish brown (10YR6/6) loamy layer with many stones	0 – 30 cm reddish brown (5YR4/8) silt loam 30 – 55 cm reddish clay	0-35 cm dull brown (7.5YR5/3) loamy matrix, many stones, some roots	0- 45 cm Brownish (10YR4/4) loamy matrix, many stones	0-90 cm yellow brown (10YR6/6) silt loam, some stones, some roots and some macropores
at 30 cm layer with very high stone content	30 – 35 cm clayey layer with some stones	55 cm – bedrock (schist)	35-70 cm bright reddish brown (5YR5/6) clay, occasional roots	45 cm – bedrock (schist)	fine pebble layer on top of the schist
55 – 65 cm bright reddish brown (5YR5/8) clayey matrix, large stones	35 cm – bedrock		70 cm – deeper yellow scaly material, probably weathered schist		90 cm – bedrock (schist)
65 cm – bedrock					

additional aim for this investigation was to deduct parameters for the simulation of preferential flow in a hydrological model. Therefore the geometry/continuity of the preferential flow paths and the interaction between the preferential flow paths and soil matrix was needed.

The dye-tracer Brilliant Blue FCF was used (CI 42090). The tracer is ordered from the DYNEMIC PRODUCTS LTD, Ahmedabad, India, with min. 85 dry mass % pure dye. Brilliant Blue FCF is the best tracer available for vadose zone hydrological studies (e.g. Ghodrati and Jury, 1990; Flury et al. 1994; Flury and Fluhler, 1995; Perillo et al., 1998; Ketelsen and Meyer-Windel, 1999; German-Heins and Flury, 2000) due to:

- good visibility: good colour contrast with the soil and a self- sharpened tracer front caused by the non-linear sorption isotherm;
- low toxicity (food colorant);
- weak adsorption in soils (only a slight retardation of the dye front compared to the water front).

As to the last point Andreini and Steenhuis (1990) and Perillo et al. (1998, 1999) showed that the extent of retardation of the Brilliant Blue front compared to the water front is related to the water velocity: the larger the water velocity, the smaller the retardation factor. Furthermore sorption of Brilliant Blue FCF was found to be positively correlated with clay content and negatively correlated with organic matter content (Ketelsen and Meyer-Windel, 1999). A high clay content and low organic matter content may lead to a high adsorption of the dye, which reduces the use of Brilliant Blue as a tracer for water flow paths. Iron and aluminium (hydr) oxides and the pH do not appear to have any influence on the adsorption of Brilliant Blue (Ketelsen and Meyer-Windel, 1999).

Different opinions exist as to the influence of initial moisture content on the initiation of macropore flow. Flury et al. (1994) concluded that initial moisture content had little or no influence on the type of flow. But others (e.g. Bouma, 1991; Feyen, 1998; Trojan and Linden, 1992; van Stiphout et al., 1987; Vilholth et al, 1998; Weiler, 2001; and Zehe and Flühler, 2001) do find an influence of initial soil moisture content on macropore flow initiation, as the initial water content influences the infiltration capacity of the soil matrix. The tracer experiments were performed as much as possible during dry soil conditions, so that the results are comparable among the different locations.

The experiments were conducted under high intensity rainfall (44mm/h), to ensure that maximum infiltration to both matrix as well as macropores occurs at all the locations. As these measurements are done at a plot scale under simulated rainfall, the influence of hillslope

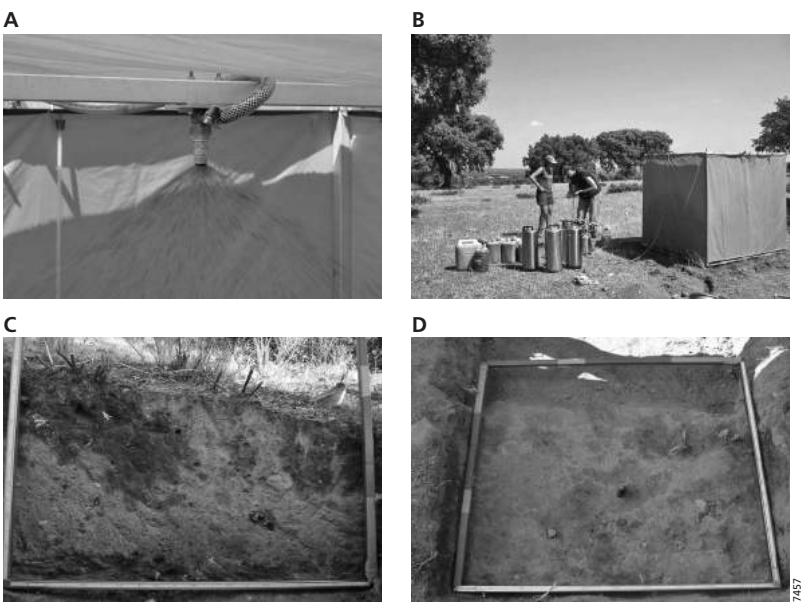

Figure 3.2: Experimetal setup for rainfall simulations: a) spraying nozzle, b) spraying tent, water reservoirs and pressure tank, c) vertical soil profile with dye-infiltration pattern, d) horizontal soil profile with dye infiltration pattern.

hydrological processes such as rainfall variation, runoff/runon and lateral groundwater flow do not occur. The rainfall simulations are performed only once per location, thereby ignoring the transient characteristics of preferential flow.

Calibration of rainfall simulator

The distribution of rainfall on the soil surface is important as a large variability therein might produce preferential flow as an experimental artefact. For the rainfall simulations the distribution under three different spraying nozzles were tested and calibrated (5-75 in Fulljet 7 SS, 1/4 HH SS 10 14W, 1/4 HH SS 8W). The measurements were done in a spraying tent (Figure 3.2), where the nozzle was fixed to the centre of the top of a cuboid frame, consisting of 1.5 m long aluminium bars. An additional frame can be used to increase the frame and spraying height to 2.5 m. Water was supplied to the nozzle under an approximately constant pressure using a pump, pressure tanks and water reservoirs. The rainfall is protected from wind influence by a tent. And the cuboid frame is levelled to a horizontal position.

To measure the rainfall distribution a set of 24 measurement cups, with a diameter of 6.5 cm and a height of approximately 10 cm, were placed on the soil surface. The three spraying nozzles were tested by imposing different pressures on the water tanks and calculating the average and standard deviation of the rainfall for the whole 2.25 m^2 and for the inner 1m^2 separately, as this is the area which was used for the excavation of infiltration profiles, after the rainfall simulations. After considering the average intensity and distribution of rainfall and the loss of water to the sides of the plot, the nozzle 1/4 HH SS 8W was chosen for the simulations. Using this nozzle at 1.5 m height from soil surface and a pressure of 1 bar applied at the height of the pressure tank, resulted in an average rainfall intensity of 44.0 mm/h and a standard deviation of 2.8 mm/h for the inner 1 m^2. This intensity is comparable with a 10 minute maximum rainfall intensity with a 2 year return period (Schnabel et al., 1998). As the aim of the experiment is to visualise

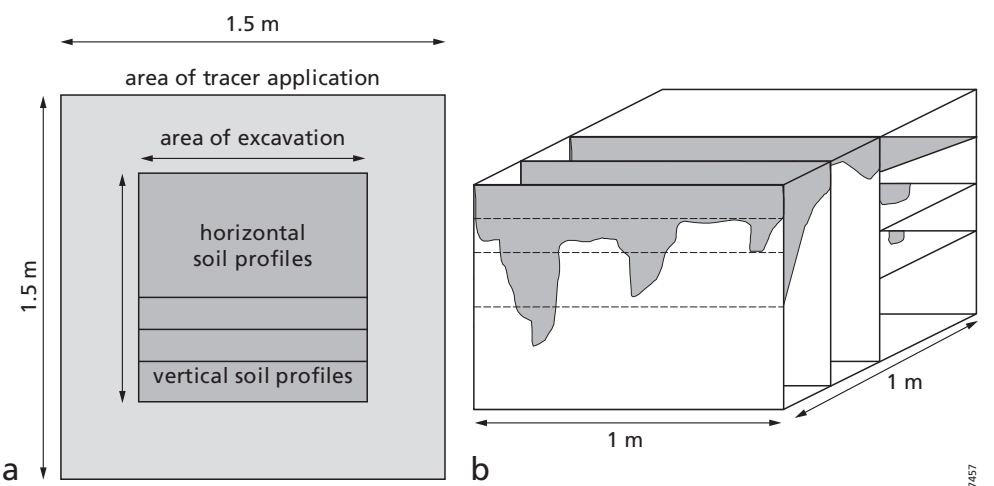

Figure 3.3: Position of the vertical and horizontal soil profiles a) within the tracer applied plot, b) relative to each other in the 3D excavated pit.

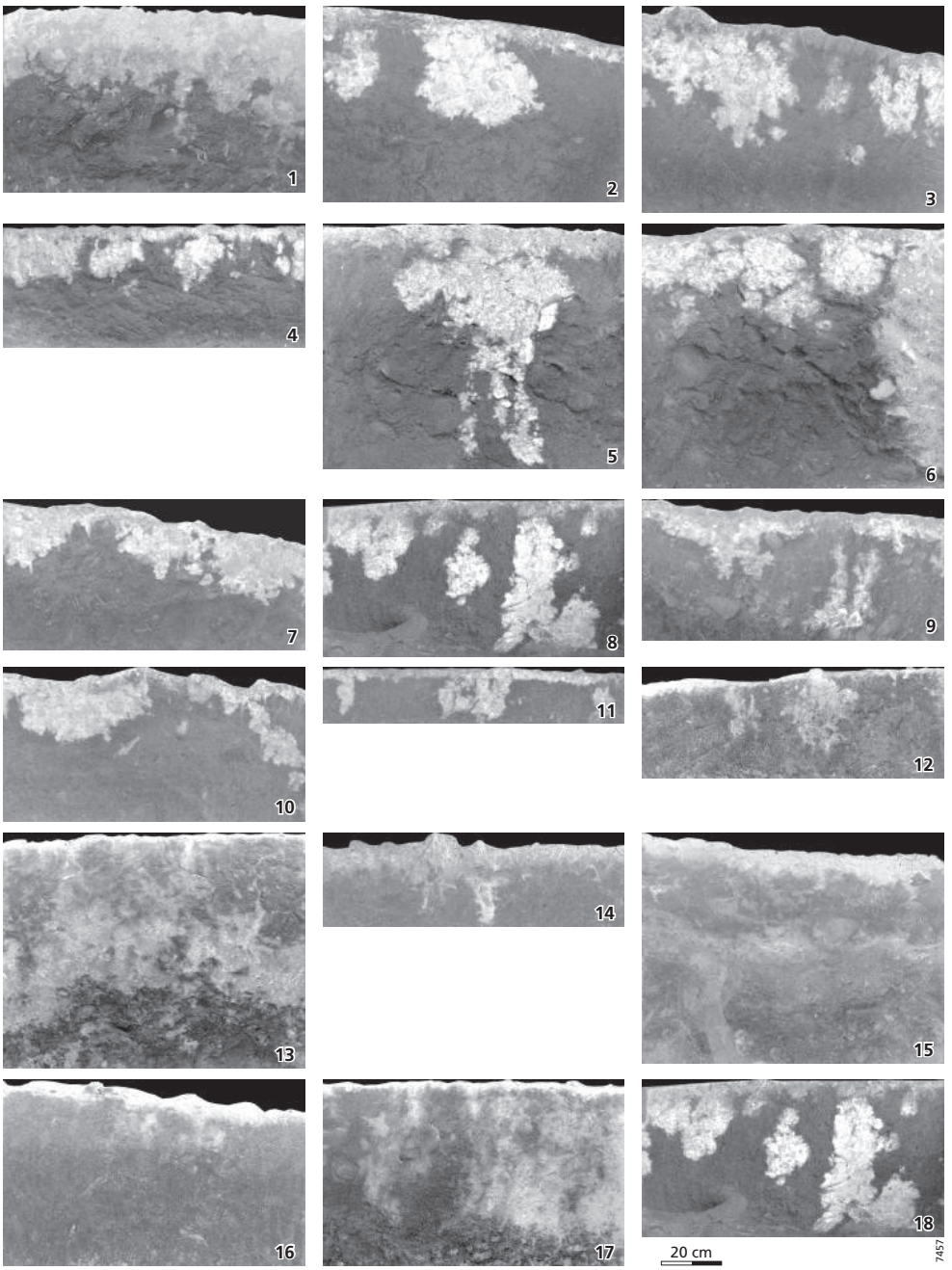

Figure 3.4: Examples of dye-stained infiltration patterns: one profile per location.

the geometry of the preferential pore network, for reaching a good depth of infiltration and in view of the retardation factor of Brilliant Blue, this high intensity is chosen. This high rainfall intensity is also used in earlier rainfall simulations in the area (Ceballos et al., 1998).

Excavation of soil profiles

One day after the tracer application, excavation of the inner 1 m^2 of the sprinkled area began. To start with three vertical soil profiles were dug. The next day three to five horizontal profiles were prepared at different depths in the profile, depending on the layering in the soil. The ensemble of the soil profiles yielding an approximation of a 3D infiltration view (Figure 3.3). Of the 2.25 m^2 sprayed surface only the inner 1 m^2 was used for the preparation of the infiltration profiles, to avoid boundary effects.

The actual channels of preferential flow in the case of macropore flow, which is assumed to be the main cause in this area, have a very limited diameter (generally up to 1 cm width, for worm and ant burrows and various sized decayed root channels). The dye-stained flow paths found in previous research have a width of 5 to 15 cm (e.g. 10-15 cm Ohrstrom et al. (2002),

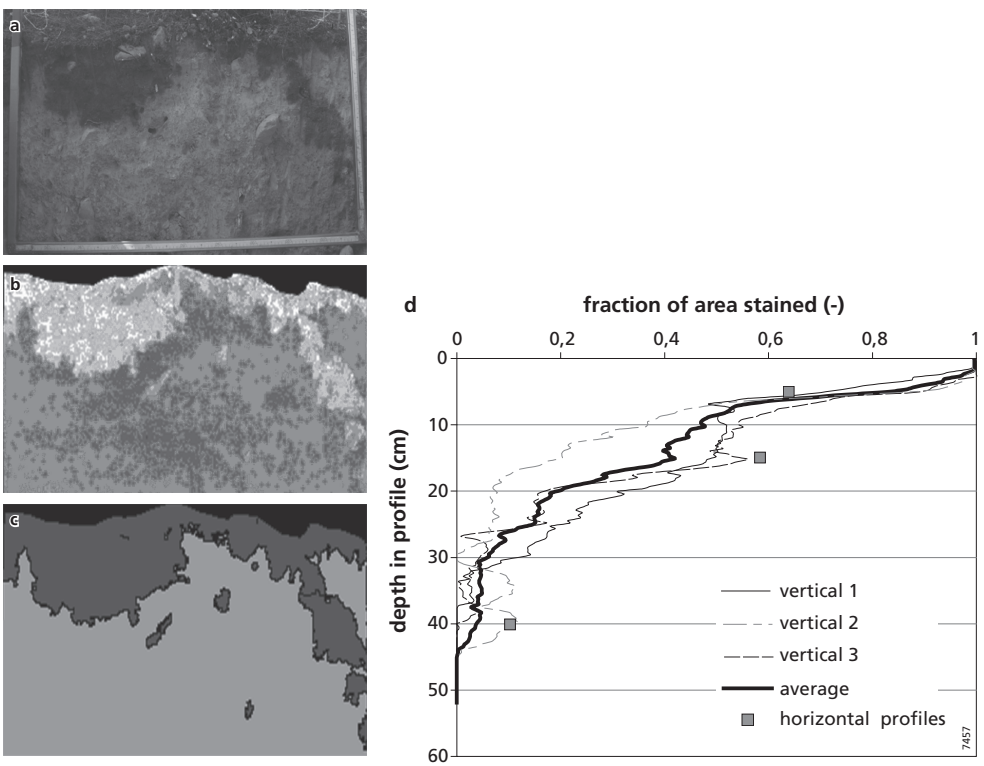

Figure 3.5: Different stages in the picture processing: a) the raw picture, b) the geometrically corrected picture, with a color filter, c) the classified picture, illustrating the wetted surface in the soil profile, d) stained area versus depth for the three vertical and three horizontal profiles and average stained area versus depth for location 10.

5-10 cm Ghodrati and Jury (1990), 9.4 cm Booltink and Bouma (1991), 5-10 cm Perillo et al. (1999), 0-20 cm Weiler (2001)). These stained paths are the result of flow through the actual preferential flow path and interaction with the surrounding matrix.

Picture processing and preferential flow parameters
Each of the soil profiles was photographed using a digital camera with a picture resolution of 2200*1700 (Figure 3.4). The profile pictures were used to derive information on the flow through the preferential flow paths and the matrix. Therefore the pictures were first processed to obtain a classification of dye-stained area as opposed to dry soil. In the field a frame of 1 m^2 (with a centimetre scale along two adjacent sides) was placed against the soil profiles as a reference for the geometrical correction of the photographs (done in Erdas Imagine 8.7). Then the stained areas were enhanced in the images by applying a colour filter (in Erdas Imagine 8.7) and classified (using both eCognition (2002) and Arcview) (Figure 3.5). The three vertical infiltration profiles per location were used to calculate the stained area versus depth, an example is shown in Figure 3.5. There is in general some difference between the profiles of a location, as in one profile there may be only one preferential flow path, while the next may have hit on two preferential flow paths. Therefore the average stained area profiles of the three vertical profiles was used to calculate the preferential flow parameters per location. The preferential flow parameters were calculated using the stained depth in relation to the soil surface per picture column. This is considered to be representative for the infiltration under $1m^2$ surface area.

3.2.2 Landscape characteristics and soil physical parameters

At the 18 locations of the rainfall simulations (Figure 3.1) additional soil physical and landscape characteristics were measured (Table 3.4):

- bulk density, porosity and saturated conductivity (on kopecki ring samples 100 cm3), two samples per soil layer at every profile. Part of these ring samples were subsequently used for Multi Step Outflow experiments;
- the slope was estimated using the average angle of the sprinkling tent with the underneath surface, after the tent was levelled for sprinkling;
- surface stoniness was estimated as a fraction of soil surface coverage, using the stone counts from the soil survey (where stones were divided into different size-classes) and calculating an average surface area for the stones in each class;
- the initial moisture conditions of the plots were measured, at different depths, just before each rainfall simulation;
- texture measurements were done and vegetation and soil profiles were described;
- water drop penetration time measurements (Letey, 1969) were done on the soil surface, by dropping two drops of water on the surface and measuring the infiltration time, to rule out water repellency.

Catchment scale distribution of vegetation and texture
Based on the intensive field campaigns maps of spatial distribution of vegetation and texture have been made. The catchment scale maps made for the estimation of spatial distribution of preferential flow have a resolution of 5 by 5 m (Chapter 5 in this thesis) for the catchment scale modelling a resolution was used of 15 by 15 m (Chapter 7 in this thesis). For the map of spatial distribution of the vegetation cover the catchment was divided into a total of eleven mapping

Table 3.4: Characteristics of the measurement locations in the field, ordered by location on the slope. For the soil physical measurements the average values of two Kopecki ring samples (100 cm^3) from the surface layer (0-10 cm) are shown here.

Location (sprinkling date)	Texture	Vegetation	Initial Moisture/ cm3/cm3	Bulk density/g/ cm3	Porosity /m3/m3	Surface Stoniness fraction/-	Slope /%
Hilltop							
1 (10 Sept)	loam	open space	0.02	1.56	0.33	0.04	1
5 (24 Sept)	sandy loam	tree cover	0.03	1.27	0.50	0.28	2
6 (27 Sept)	sandy loam	sheep trails	0.02	1.58	0.37	0.18	2
13 (22 Oct)	loamy sand	open space	0.25	1.31	0.48	0.41	1
15 (29 Oct)	loamy sand	tree cover	0.35	– [a]	– [a]	0.77	1
17 (5 Nov)	sandy loam	sheep trails	0.35	1.58	0.32	0.37	1
Hillslope							
3 (16 Sept)	sandy loam	shrub cover	0.05	1.49	0.40	0.03	4
7 (1 Oct)	loam	open space	0.02	1.53	0.37	0.27	7
9 (8 Oct)	loam	tree cover	0.03	1.41	0.46	0.09	8
12 (19 Oct)	silt loam	sheep trails	0.17	1.47	0.45	0.07	7
16 (1 Nov)	silt loam	shrub cover	0.36	1.63	0.40	0.02	5
18 (8 Nov)	silt loam	tree cover	0.21	1.02	0.56	0.00	2
Valley Bottom							
2 (13 Sept)	silt loam	open space	0.03	1.57	0.39	0.02	5
4 (20 Sept)	silt loam	sheep trails	0.05	1.41	0.47	0.04	1
8 (4 Oct)	silt loam	tree cover	0.05	1.06	0.59	0.01	1
10 (11 Oct)	silt loam	shrub cover	0.06	1.29	0.50	0.04	2
11 (14 Oct)	silt loam	sheep trails	0.03	1.43	0.49	0.01	1
14 (25 Oct)	silt loam	shrub cover	0.40	1.63	0.40	0.04	1

a It was not possible to take a representative sample of the topsoil for location 15, as the soil was extremely loose and kept falling apart while taking the samples.

units with relatively homogeneous vegetation patterns. To start with the tree cover was derived from the aereal photograph (see Figure 2.5), which clearly shows the location of trees. The tree cover map was processed into a percentage of trees per pixel based on greyscale (Figure 3.6a), black being full tree cover. Furthermore the fractions of grass, shrubs and sheep trails were estimated for the eleven mapping units with clearly different understory (Figure 3.6b, Table 3.5). This resulted in the fraction of each pixel which was resp. tree cover, grass, shrubs and sheep trail. These fractions were multiplied by the nominal values assigned to the different vegetation types to obtain a value for the vegetation cover of the pixels Figure 3.7a. The texture map (Figure 3.7b) was based on the textural analysis of a large number of soil samples and knowledge on the distribution of soil types gained during intensive field campaigns, such as visible changes of soil types at the soil surface.

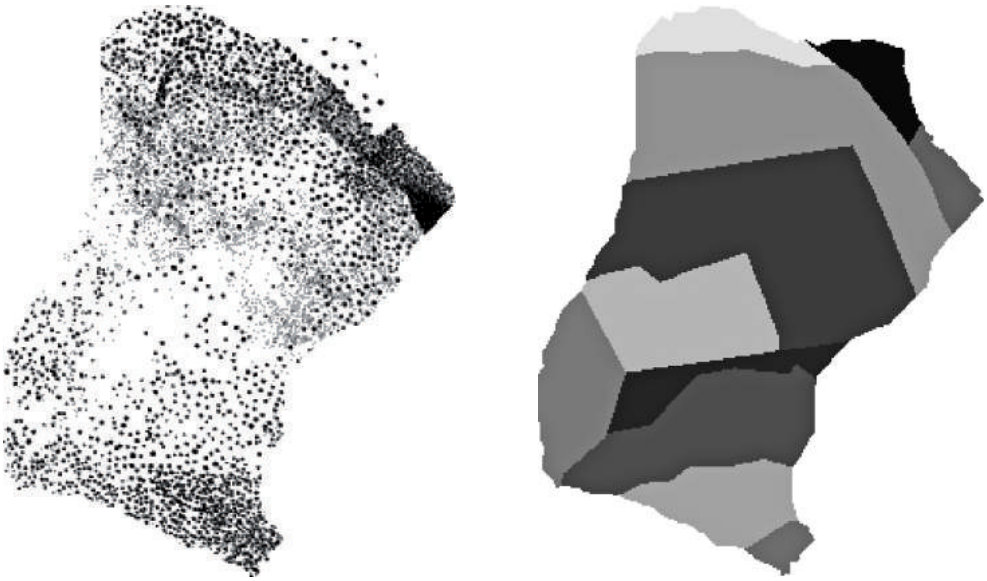

Figure 3.6: a) Tree cover per pixel, based on grey scale, black being full tree cover, b) map of different units in the catchment with relatively homogeneous understory, consisting of different cover fractions of shrubs, grass and sheep trails (see Table 3.5). The straight lines in the unit boundaries are the result of fences, dividing the catchment into areas with different management practices.

Table 3.5: Fractions of different vegetation cover (shrubs, grass and sheep trails) for the different vegetation units in the catchment.

Vegetation unit	**Fractions of vegetation cover in the understory**		
	Shrubs	Grass	Sheep trails
1	0.0	0.8	0.2
2	0.0	1.0	0.0
3	0.2	0.8	0.0
4	0.45	0.35	0.2
5	0.2	0.7	0.1
6	0.0	0.8	0.2
7	0.3	0.5	0.2
8	0.0	0.5	0.5
9	0.1	0.5	0.4
10	0.4	0.4	0.2
11	0.1	0.9	0.0

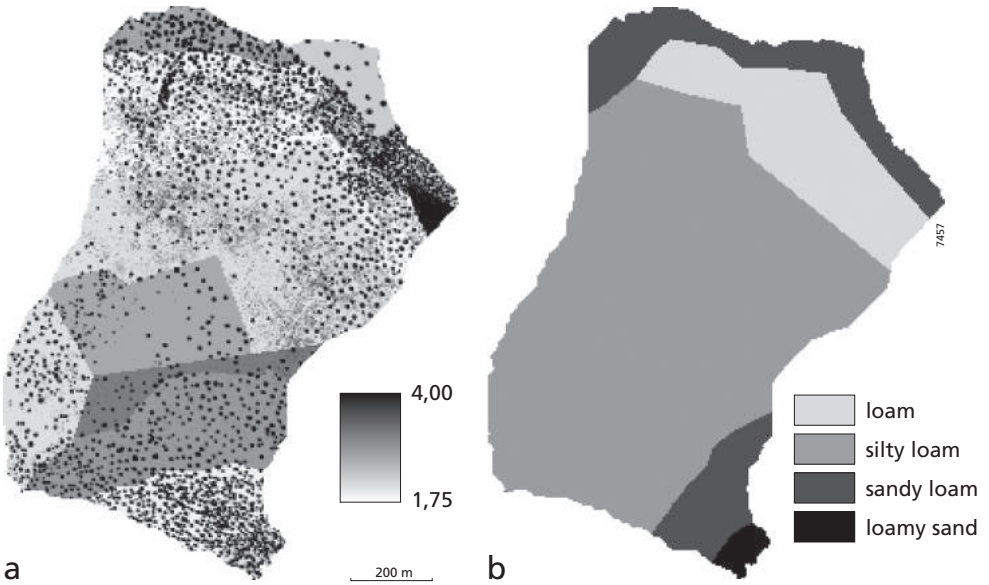

Figure 3.7: a) Map of spatial distribution of vegetation cover in the catchment and b) spatial distribution of texture, as used for the modelling exercises in this thesis.

3.2.3 Multi Step Outflow experiments

Introduction

Multi Step Outflow or MSO (van Dam et al., 1994) is an indirect method to measure soil hydraulic properties (Figure 3.8). The Mualem van Genuchten (MvG) parameters (Van Genuchten, 1980) for the water retention and conductivity curve are optimised using inverse modelling and measurements of moisture content and outflow under application of pressure increments. A selection of 42 of the kopecki ring samples were used for Multi Step Outflow experiments to determine the water retention curve and the hydraulic conductivity curves for the different soil types. The soil samples were saturated and installed in the outflow apparatus. A pressure of 30 cm was applied to start with. After stabilization of the water content in the samples, five different pressures were applied in steps (going from 30 to 60, 140, 250, 500 and 1000 cm). After each pressure step, for a period of 24 hours, the outflow was monitored, with increasing time intervals starting directly after the pressure application, until the outflow was negligible.

Mualem van Genuchten fit on outflow data

The Mualem van Genuchten parameters were obtained by fitting the outflow data (an example is given in Figure 3.9). As the results of the Multi Step Outflow are to be used for the behaviour of the fine matrix, the saturated moisture content and conductivity were set free in the optimisation, resulting in a much lower optimised value for both than the actual measurements of saturated moisture content and conductivity under ponded conditions showed (Table 3.6). This is consistent with the idea that the Multi Step Outflow experiments measure the true matrix/small pore system characteristics, while the samples may have a small number of larger pores in them resulting in much higher saturated conductivity and water content values.

At the opposite range of the soil moisture contents (near residual moisture content) there is also a discrepancy between the fitted Mualem van Genuchten curve and initial soil moisture contents measured in the field. In the field the initial soil moisture contents, measured gravimetrically on the 100 cm^3 kopecki ring samples in the beginning of September, down to even 50-60 cm of soil depth were approximately 0.05 cm^3/cm^3 (between 0.03 to 0.07 cm^3/cm^3). The use of the fitted Mualem van Genuchten curve implicates that the modelled soil moisture content will hardly drop beneath a soil moisture content of approximately 0.12 cm^3/cm^3, as the water reduction by plants is then minimal (pF=4.2 is the absolute wilting point used in many (agro)hydrological models) and the soil evaporation at depths of 50 cm is negligible.

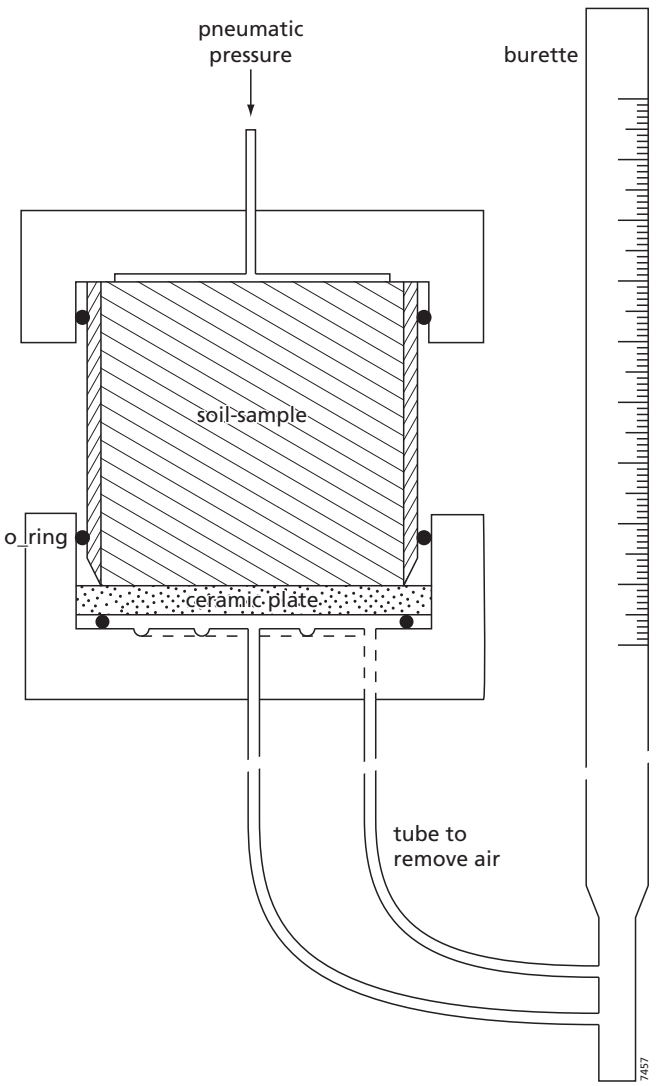

Figure 3.8: Multi Step outflow experimental setup.

The Multi Step Outflow data are only measured over a limited range of imposed pressure, the maximum being 1000 cm. The fitted Mualem van Genuchten curve therefore is based on a limited range and is extrapolated to the extremes. The influence of adjusting the Mualem van Genuchten fit, by introducing an extra moisture content point into the pF curve was studied. The optimisation was then performed using both the outflow measurements and an added

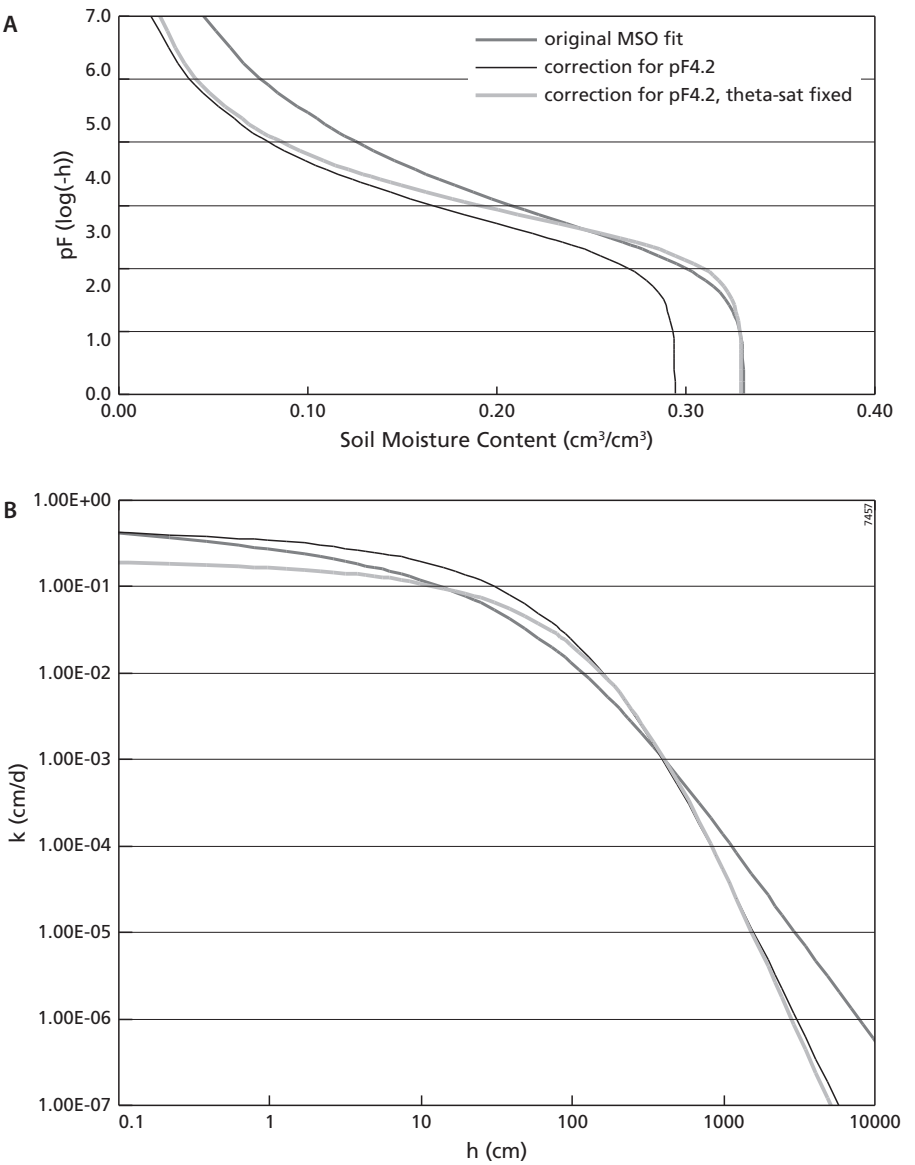

Figure 3.9: Mualem van Genuchten parameter fitting on the Multi Step Outflow data a) example of pF fits, b) example of k(h) fits.

moisture content of 0.05 at a pF of 4.2. In this case the pF curve mainly shifted to the left and the conductivity remained near saturated for a long time (Figure 3.9). Though the theta-sat point was fitted in the original MSO fits, it is much more likely than the lower theta-sat from the adjusted curves. Therefore fitting with the theta-sat fixed was also investigated. This resulted in a steeper pF curve, which did reach the low water contents measured at pF 4.2, but the saturated conductivity decreased too much.

The Mualem van Genuchten curve is a theoretically explained but empirical fit to the water retention data, which however is often found to deviate from the actual data at the extremes (very dry, very wet). There are three explanations which may partly cover the difference between the fits and the measured low moisture contents. First of all the MSO-measurements cover a very limited range of soil moisture contents and this fitted curve is extrapolated to the extremes, while the Mualem van Genuchten curves are known often not to fit the full range from saturated to residual moisture context. Also the transpiration for semi-arid vegetation may continue till higher soil suctions, up to a matric potential of 2.5 MPa or even 3.5 MPa (≈ pF 4.5)(e.g. Richards et al., 1983; Cameron, 2001; Sofo et al. 2008), so the soils may dry out further than pF 4.2 in summertime. Using the original MSO fits, however, the pF curve is almost vertical near the low end so little would be gained with this explanation. Another explanation may be that the evaporation in a soil with macropores may have some influence even to larger soil depths, as there is a direct connection between the deeper soil and the air and the temperatures are extremely high and air is dry. In the end the choice was made to stick to the original Mualem van Genuchten fits, as they represent both the retention data and the outflow data for the range of moisture contents measured with the MSO best. The deviations from the Mualem van Genuchten curve for the wet end will be treated with the separation of matrix and macropore characteristics and the dry end deviations are treated by adapting the Water retention curve at the dry end with using the available field data. In order to allow the soils to dry out further in summer months the original MvG curve is linearly adapted at the dry end, starting from pF =

Table 3.6: Mualem van Genuchten parameters as fitted on the Multi Step Outflow measurements (for some soils only one or two samples were used in the MSO experiments) and measured saturated moisture content and conductivity.

	Average parameters from multi step outflow experiments						**Average soil sample measurement**	
Soil Layer	θ_r (cm^3/cm^3)	$\theta_{s,mso}$* (cm^3/cm^3)	α (1/cm)	N (-)	$k_{s,mso}$* (cm/d)	λ (-)	$\theta_{s,meas}$* (cm^3/cm^3)	$k_{s,meas}$* (cm/d)
loamy sand (top)	0.03	0.50	0.0387	1.1915	1.41	2.0	0.54	222.0
sandy loam (top)	0.03	0.30	0.0380	1.251	12.5	-0.880	0.35	240.0
sandy loam (sub)	0.01	0.35	0.0068	1.134	0.5	1.785	0.36	143.0
loam (top)	0.03	0.39	0.0144	1.117	0.7	2.0	0.44	42.0
loam (sub)	0.03	0.42	0.0068	1.134	0.3	1.56	0.45	56.0
silty loam (top)	0.03	0.35	0.0072	1.254	0.70	0.731	0.41	77.0
silty loam (sub1)	0.03	0.38	0.0086	1.205	0.30	-0.630	0.43	33.0
silty loam (sub2)	0.03	0.40	0.0172	1.130	1.1	0.75	0.41	1.1

* The difference between the fitted saturated moisture content and saturated conductivity with the measured values is interpreted as an indication of macropore volume and macropore flow.

3.0 until the measured value of approx 0.05 cm^3/cm^3 near the wilting point for semi-arid plants as reported in literature (≈ pF 4.5, e.g. Richards et al., 1983; Cameron, 2001; Sofo et al., 2008).

Mualem van Genuchten parameters for different soil types and depths

The 42 ring samples used in the Multi Step Outflow experiments came from different locations and different soil layers. As there is some variability within the hydraulic characteristics of the samples representing one soil type/layer, the curve with the most average behaviour was taken to be representative (Figure 3.10). The most extreme curves are also shown, which are the curves with the highest and lowest slope (which is an indication of water availability). For the

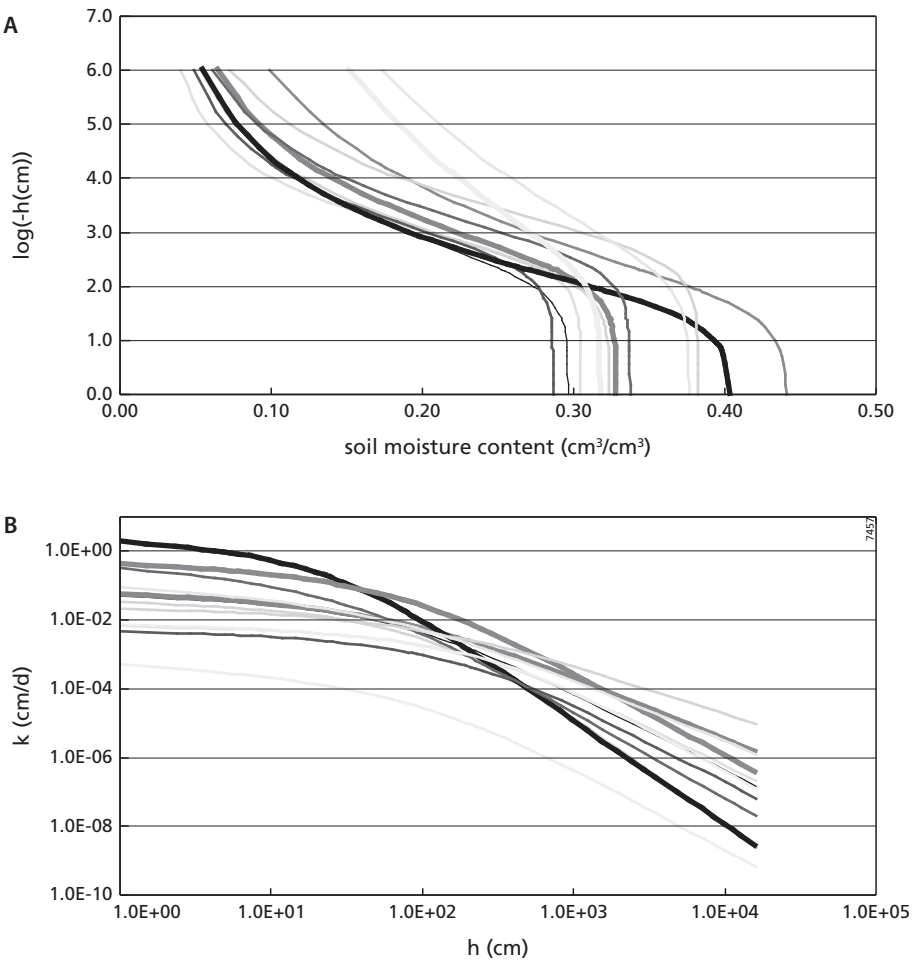

Figure 3.10: Example of optimized Mualem van Genuchten curves for all the soil samples of the silty loam sub soil, with the curve with average behavior (bold black) and the extremes (bold grey). The most average curve is eventually used for the soil hydraulic characteristics of the matrix in the modeling exercises.

modelling exercises in this thesis the curves with the most average behaviour are selected per soil type and layer. The resulting Mualem van Genuchten parameters of the average curves and the extreme curves per soil type and layer are found in Table 3.6, together with the measured saturated water content and conductivity.

3.3 Hillslope scale measurements

3.3.1 Soil moisture content

Introduction

To assess the spatial and temporal distribution of soil-moisture 67 TDR-probes (Topp et al., 1980; Robinson et al., 2003) were used to monitor soil content (SMC) in six soil profiles, located along two hill slopes. The TDR-probes were hand-made following a design of the staff of the University of Extremadura (personal communication with prof. Schnabel and A. Gómez Guttiérez) (see Figure 3.11): two metal rods were fixed to coaxial cable and then enveloped with a small cup full of resin around the connection, resulting in parallel rods with a length of approximately 8.8 cm and a diameter of 4 mm, at a distance of 2.9 cm from each other. The measurements were done manually, from the 5th of October to the 6th of November 2005, using a Tektronix Cable Tester, 1502C.

Sensor calibration

A couple of probes were calibrated in the laboratory and the sensor specific calibration showed that the sensor specific measurement error is on average 1.2%. Also a soil specific calibration was performed. The Topp equation is often used to calculate the soil moisture content from the dielectric permittivity measured with the TDR probes. The use of this equation for different soils is however frequently disputed (Jones et al., 2002, Kelleners et al., 2005). The equation is mainly not applicable in soils with high organic matter or clay content, but has been found to deviate from true moisture contents for many different soils. Therefore a soil-specific calibration should also be performed. At the six different TDR pits, soil was collected and a soil-specific calibration was performed in the laboratory. The soil samples were saturated and the TDR probes were inserted. Then the samples were slowly drained, while measuring the weight and dielectric permittivity with intervals. A few methods were evaluated to find an appropriate curve for this relationship, nevertheless none of the curves was found to perform best, as they all showed deviations in part of the range of SMC (Figure 3.12). The curves which were used for fitting the laboratory measurements were:

- the Topp equation: $\theta = -5.3*10^{-2} + 2.92*10^{-2}\varepsilon - 5.5*10^{-4}\varepsilon^2 + 4.3*10^{-6}\varepsilon^3$
- the adapted Topp equation, where the first coefficient in the equation was optimised;
- the completely adapted Topp equation, where all the coefficients in the Topp equation were optimised;
- a curve related to the square root of permittivity (as proposed by Roth et al. (1992) and Malicki et al. (1996)): $\theta = a*\varepsilon^{0.5} + b$;
- an adapted root function where the exponent of the permittivity is adapted.

The curve with the best fit to the gravimetrically measured SMC was generally the adapted Topp equation, where all the coefficients of the Topp equation were optimised. The resulting

RMSE for these curves is between 1-2 vol % SMC from dry to wet condition, for the different field locations. The error however is generally higher for low moisture contents.

Field measurements
The TDR probes were installed in horizontal layers in the pits, approximately 20 cm apart (their exact locations depending on stones in the soil profile). The measurement volume of the TDR-probes is approximately 1 dm^3. The fraction of matrix versus preferential flow path encompassed in the measurement volume is unknown. The measured difference in water content is therefore not a direct difference between the flow regimes, but a high variability of water content within a soil layer is an indicator of preferential flow.

The soil moisture content measurements were gathered under natural conditions, during the transition from dry to wet conditions. The rainfall from October to November of 2005 is given in Figure 3.13, together with an example of the average soil moisture content and its standard deviation of one layer of TDR-probes. This example is a horizontal layer of 5 TDR-probes in the soil profile of the valley bottom of transect 1 (for the location within the catchment see Figure 3.1).

The TDR-measurements show that the soil matrix slowly becomes wetter from the beginning of October to the 28th of October. Then the matrix becomes suddenly saturated and remains near saturated thereafter. There is a large variation in soil moisture content within the soil layer in the beginning of the wetting season: up to almost 8 vol %. The standard deviation increases during or after rainfall when the preferential flow paths are most active and then decrease slightly, while the soil moisture is redistributed in the profile. On the 28th of October this soil layer becomes almost saturated and the standard deviation in water content decreases to approximately 2 vol %.

Due to the poor resolution of measurements, both spatial and temporal, it is difficult to draw conclusions about preferential flow from the data. Preferential flow and variation in soil moisture content is largest during and shortly after a rainstorm. As the measurements were done only twice a day at most, the moment of measurements may influence strongly the measured variation

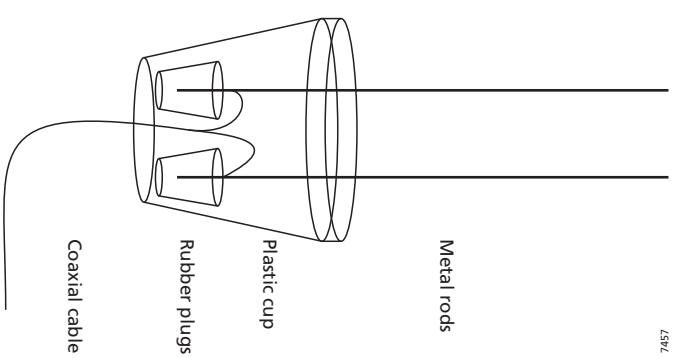

Figure 3.11: Handmade TDR-sensor. The distance between rods is 2.9 cm and the length of rods is 8.8cm. The plastic cup is filled with resin.

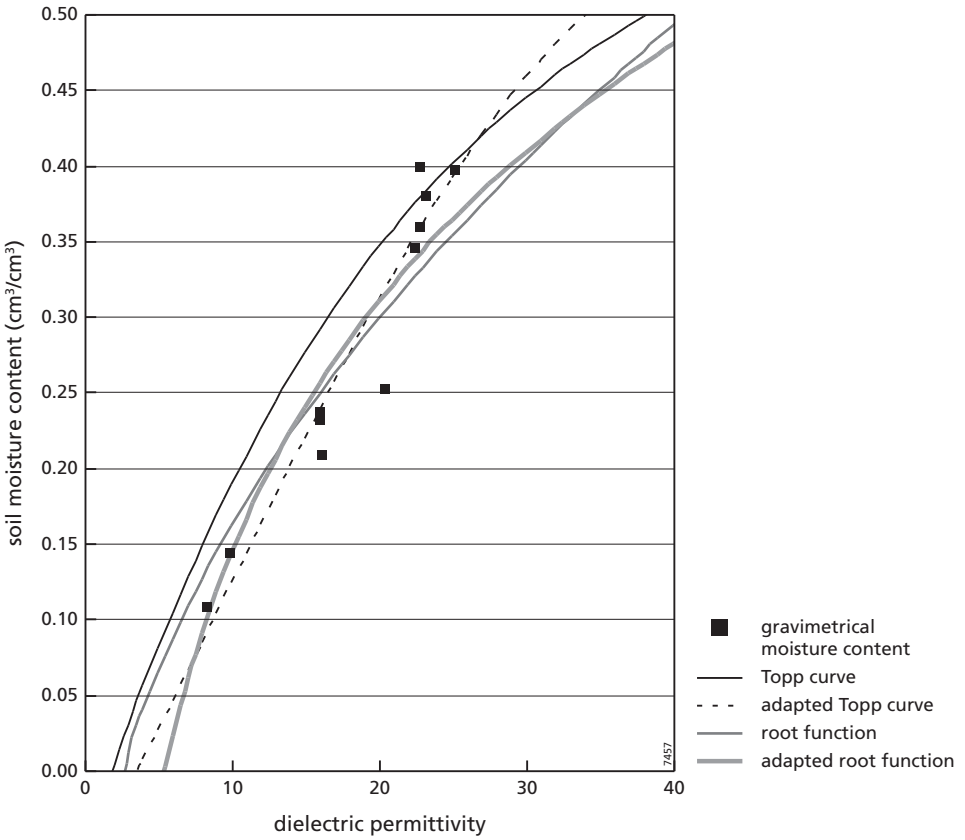

Figure 3.12: An example of the fitted curves for the optimisation of the relationship between the dielectric permittivity and the soil moisture content.

in soil moisture content. The direct use of the soil moisture content measurements to characterise preferential flow may be disputable, they can indirectly be used to support the interpretation of groundwater reactions and for the calibration of a preferential flow model.

3.3.2 Water level measurements

A total of 11 piezometer pipes were installed in the Parapuños area. From the 1st of September 2004 to the 5th of January 2005 the water level was monitored continuously at 5 locations (at a 10 min resolution) using Keller pressure transducers, which contain automatic dataloggers. The pressure transducers were each calibrated in the laboratory before they were installed in the field and as regularly a possible drift was checked. The depth of the piezometer pipes reached down to bedrock. The depth of bedrock was confirmed when excavating the soil profiles for the sprinkling experiments. The piezometer measurements were corrected for atmospheric pressure with a barometric measurement in the meteorology station in the catchment. Water levels were all expressed as water column height above bedrock.

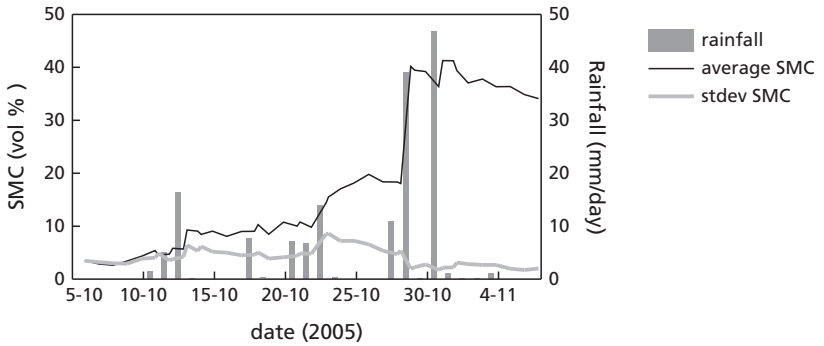

Figure 3.13: Rainfall and soil moisture content (measured twice a day) along transect 1 at the beginning of the rainy season, at 20-25 cm depth at the bottom of the slope (5 probes). Presented are average and standard deviations of SMC at each site.

It is clear that for a rapidly reacting system like the hillslopes in our catchment (see example in Figure 3.14) it is essential to have a high resolution measurement scheme. Figure 3.14 shows that a 10-min resolution gives unnecessary information, while the hourly or two-hourly resolutions show clear loss of information on temporal variability of the waterlevel. From the 23rd of September 2005 to the 18th of May 2006 the piezometer measurements were continued in two of the old piezometer pipes and at six new locations (with a short interruption of measurements at the beginning of November) using a 30 min resolution.

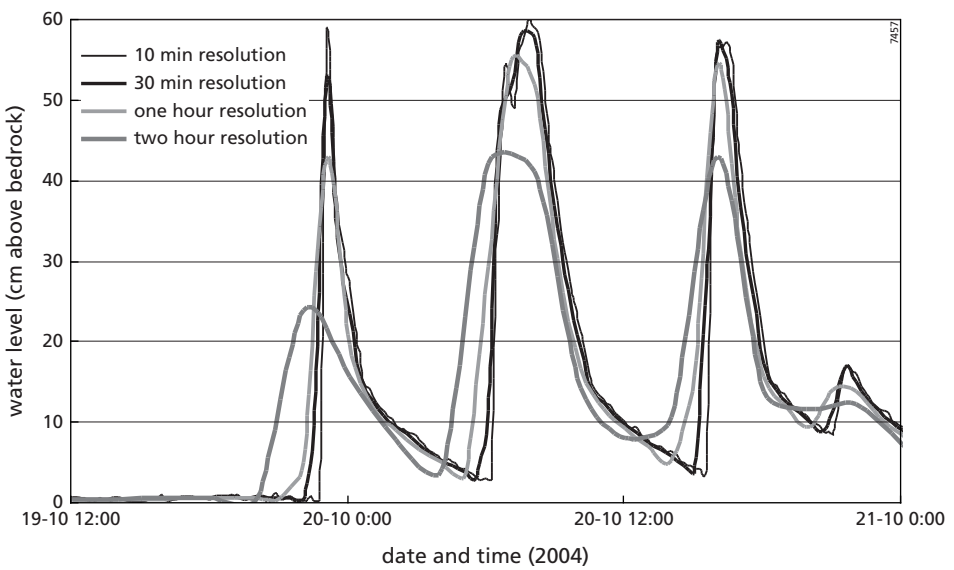

Figure 3.14: Influence of temporal measurement resolution on piezometer data fluctuations.

Figure 3.15:Trench with gutters to measure lateral throughflow.

3.3.3 Lateral throughflow

One of the excavated soil pits in the valley bottom (location 10) was subsequently used for measurement of lateral throughflow. The sidewall facing upslope, was extended to form a two meter wide trench, with a smooth vertical profile. In this profile three gutters were placed at different depths (the bottom of the gutters was approximately 15 cm, 30 cm and 50 cm under soil surface) to measure the lateral throughflow of different soil layers (Figure 3.15). The gutters were 50 cm wide and 15 cm high. They were inserted into the soil using three 50 cm long steel pins. Fine sand was used to fill up the gap between the soil profile and the gutter and the bottom of the gutter was connected to some bottles to collect the throughflow. The runoff coming from upslope was redirected to the sides of the trench, using a metal sheet, slightly inserted into the soil and some lateral gutters. The trench was covered with a large thick plastic sheet. The water flow in the different layers was found to be so fast that the bottles were not enough to collect the water over longer time intervals. The water level in the bottom of the pit rose rapidly, mainly through fast flow in the pebble layer at the bottom of the profile, which was covered by the lower gutter. During one rainfall event the volume of water flowing out of the gutter at the bottom was measured for 1 minute intervals during half an hour. The average outflow from this gutter was 40 ml/min, which corresponds to a conductivity of 1.9 m/d for the pebble layer.

3.4 Conclusions

The measurement campaigns were designed to understand the hydrological system of the catchment and to obtain information on preferential flow from plot scale (small scale variability

in infiltration) to catchment scale (subsurface rapid flow). Although field measurements are always limited in scale and number the collected field data yield a solid basis for analysing and modelling the occurrence and properties of preferential flow in this area. Preferential flow is furthermore a transient phenomenon, which depends on the antecedent hydrologic conditions as well as event characteristics. The basic rainfall, meteorology and discharge measurements are long term measurements with a high temporal resolution. The additional measurements performed to quantify the spatial influence of preferential flow on the hydrology are strongly limited in temporal resolution. The period of measurements was therefore chosen in the fall when the main changes in hydrological conditions can be expected and most rainfall events take place.

In the following chapter the hillslope hydrological behaviour is described by thorough analysis of the measurements described above. The limited spatial resolution of the infiltration experiments is coped with by linking the parameters from the infiltration patterns to easily obtained spatial information on soil and landscape characteristics. Models are chosen which are in accordance with this conceptual behaviour. The parameterisation of the models based on the field data for the transition period from dry to wet is used to further quantify the influence of preferential flow under different conditions. The main missing information remains the spatial and temporal distribution of evapotranspiration, but can be computed from precipitation and discharge. In modelling exercises evapotranspiration will be derived as rest part of the water balance, which will be compared to values found in literature.

4 The influence of preferential flow on hillslope hydrology

Based on: Van Schaik, N.L.M.B., S. Schnabel and V.G. Jetten. 2008. The influence of preferential flow on hillslope hydrology in a semi-arid watershed (in the Spanish Dehesas). Hydrological Processes, 22, pp. 3844-3855.

4.1 Abstract

Preferential flow is known to influence hillslope hydrology in many areas around the world. Most research on preferential flow has been performed in temperate regions. Preferential infiltration has also been found in semi-arid regions, but its impact on the hydrology of these regions is poorly known. The aim of this study is to describe and quantify the influence of preferential flow on the hillslope hydrology from small scale (infiltration) to large scale (subsurface stormflow) in a semi-arid Dehesa landscape. Precipitation, soil moisture content, piezometric water level and discharge data were used to analyse the hydrological functioning of a catchment in Spain.

Variability of soil moisture content during the transition from dry to wet season (September to November) within horizontal soil layers, leads to the conclusion that there is preferential infiltration into the soils. When the rainfall intensity is high, a water level rapidly builds up in the piezometer pipes in the area, sometimes even reaching soil surface. This water level also drops back to bedrock within a few hours (under dry catchment conditions) to days (under wet catchment conditions). As the soil matrix is not necessarily wet while this water layer is built up, it is thought to be a transient water table in large connected pores, which drain partly to the matrix, partly fill up bedrock irregularities and partly drain through subsurface flow to the channels. When the soil matrix becomes wetter the loss of water from macropores to the matrix and bedrock decreases and subsurface stormflow increases.

It may be concluded that the hillslope hydrological system consists of a fine matrix domain and a macropore domain, which have their own flow characteristics, but which also interact, depending on the soil matrix and macropore moisture contents. The macropore flow can result in subsurface flow, ranging from 13% contribution to total discharge for a large event of high intensity rainfall, high discharge to 80% of total discharge for a small event with low intensity rainfall, low discharge. During large events the fraction of subsurface stormflow in the discharge is suppressed by the large amount of surface runoff.

4.2 Introduction

Most research on subsurface stormflow in hillslopes is carried out in temperate climates. In forested hillslopes in temperate climates subsurface stormflow is often found to produce a large amount of event discharge (Hendriks, 1990; Cammeraat, 1992; Beckers and Alila, 2004; Tromp-

van Meerveld and McDonnell, 2006). In semi-arid regions preferential flow and subsurface processes have traditionally been regarded as of minor importance compared to surface flows for discharge production (Maneta et al., 2008). However preferential infiltration of water has been observed in semi-arid areas (Cerdá et al., 1998 and Öhrstrom et al. 2002). Cerdá et al. (1998) found preferential infiltration of water in Spanish Dehesas, which was explained by the presence of macropores and occurrence of water repellency under the tree canopy. Soils developing under a tree canopy are richer in nutrients and organic matter, have a greater water-holding capacity and a macroporosity favorable to infiltration and redistribution of water (Joffre and Rambal, 1988). Maneta et al. (2008) concluded from their modelling analysis that high calibrated values for horizontal and vertical hydraulic conductivity suggest that fast preferential flow may play a role in the catchment scale hydrology of the semi-arid Dehesas.

The Dehesa landuse is a semi-natural landuse, which is typical for a large part of the south-western Iberian Peninsula (approximately 4 million hectares). Dehesas are openly spaced woodlands (tree densities typically are 20-40 trees per ha.), with agro-silvo-pastoral landuse, a Mediterranean, semi-arid climate and poor soils (shallow, acid, low organic matter content) (Schnabel and Ferreira, 2004). Similar landuse systems are found in other Mediterranean countries (Cerdá et al., 1998).

Hydrological research in the Dehesas in the past has focused mainly on rainfall-runoff relations (Ceballos and Schnabel, 1998; Ceballos et al., 1998) and erosion (Schnabel, 1997; Schnabel et al., 1998). When analyzing the rainfall-runoff, Ceballos and Schnabel (1998) found a strong relationship between the precipitation and evapotranspiration as well as between the precipitation and area discharge. They conclude that depending on the moisture conditions of the catchment, overland flow can be either Hortonian or saturated overland flow. The form of a hydrograph of a typical first order catchment indicates rapid surface runoff. Annual rainfall-discharge coefficients are generally low (on average 7%, varying between 1 and 15%) and comparable to those of other semi-arid watersheds. Their variability depends strongly on the distribution of precipitation throughout the year and also on the annual rainfall totals (Ceballos and Schnabel, 1998). The effect of vegetation on soil water dynamics in the Dehesas was studied (Cubera et al., 2004; Joffre and Rambal, 1993; Montero et al., 2004; Moreno et al., 2005). A grass cover exists in wintertime but dries up in summer, while the trees continue to draw water laterally from the deeper soil layers. Tree roots extend far beyond the tree canopy, which suggests they can draw water from far beyond their canopy deck (Moreno et al., 2005). Tree roots occasionally extend down into the bedrock, where they can draw some extra water from the temporary water storage in cracks or weathered bedrock. The Dehesa landscapes are threatened by erosion, soil degradation and lack of tree regrowth, in some cases caused by overgrazing and in others by land abandonment (Schnabel and Ferreira, 2004).

Macropore flow is probably the main cause for preferential flow found in the Spanish semi-arid Dehesas (Cerdá et al. 1998; Joffre and Rambal 1988). Macropore flow is flow through large pores which are significantly larger than the bulk of the soil pores (Hendrickx and Flury 2001). The water flow in macropores depends on the soil matrix infiltration capacity, interaction between macropores and matrix (Weiler, 2005) and on connectivity of macropores (Tsuboyama et al., 1994). Once the infiltration capacity of the matrix is exceeded, macropore infiltration

will start. The water which flows into the macropores will partly infiltrate into the macropore sidewalls, depending on coating of the macropores (Cammeraat, 1992), soil matrix properties and soil water content (Weiler and Naef, 2003a) and partly percolate further downwards. Macropores do not have to be filled in order to conduct water and they usually do not transport water at full capacity (Weiler, 2001). The scale at which macropores are effective depends on their connectivity, which does not mean that they are continuous, but rather that the connectivity results from a network of macropores separated by small distances of highly permeable material (Tsuboyama et al., 1994). In Luxemburg, Cammeraat (1992) found that macropores often transmit water while the surrounding soil matrix is not saturated. The amount of horizontal infiltration from macropores into the soil matrix depends on the storage time of water in the macropores. Van Beek and Van Asch (1999) conclude that the factors which influence this storage time are the total storage capacity, vertical and lateral losses from the macropores and the rate of recharge, either through a permeable topsoil or directly by runoff into the network. Flow in macropores can occur with little or no interaction with the surrounding soil-matrix. The infiltration of water from the macropores into the soil matrix can be hampered by smearing of earthworm excrements at the channel wall (Cammeraat, 1992).

Beven (2001) stated that "only a correct simulation and prediction of flow pathways lead to a correct description of the internal hydrological behaviour of a catchment". Preferential flow has been recognised as an important process in hydrological systems in many areas around the world (Beven and Germann, 1982; Doerr et al., 2000; Simunek et al.,2003; Uchida et al., 2005), with an influence on infiltration, soil moisture distribution, percolation and subsurface stormflow. In the semi-arid Dehesa landscape preferential flow may be enhanced by a large temporal variability in rainfall, resulting in periods of drought and occasionally high intensity rainfall events, shallow soils and pronounced relief.

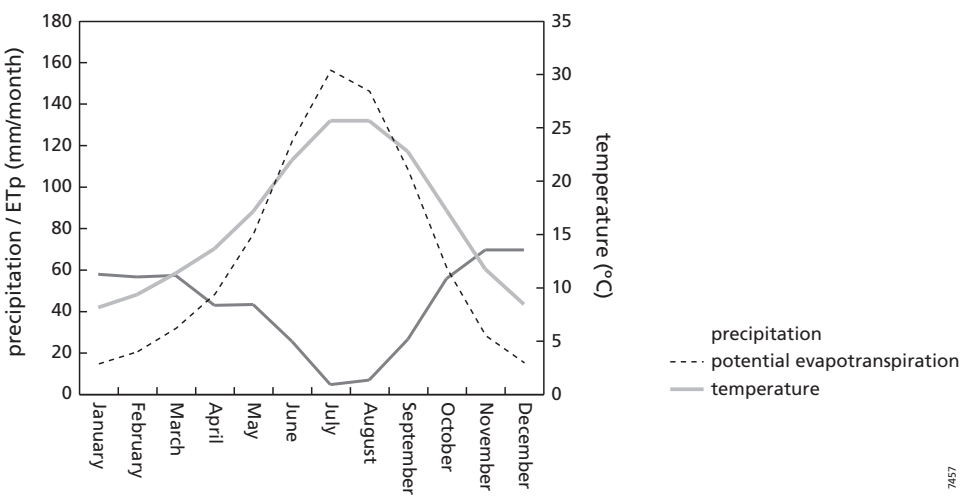

Figure 4.1: Monthly distribution of precipitation, temperature and potential evapotranspiration calculated according to Thornthwaite (1948) for the Cáceres meteorological station.

In this chapter the functioning of the hydrological system in a semi-arid Dehesa watershed with silvo-pastoral landuse in Spain is investigated, focussing on the role of preferential flow and subsurface stormflow. The scientific basis for this detailed analysis is a set of local field measurements of rainfall, soil moisture content, piezometric water level and discharge. The measured water levels in the piezometers showed rapid changes in water level from bedrock to soil surface level, while a groundwater layer was never built up during the wet season. In this chapter we explore a) whether this behaviour can be explained by preferential flow activity and b) what the contribution of subsurface stormflow to the discharge may be under different rainfall events in that case. The answers lead to a concept on the hydrological behaviour of the catchment, which will serve as a basis for future model development for the quantification of preferential flow across scales.

4.3 Study area

A detailed study area description is given in Chapter 2. Here the most important properties, needed to understand this chapter are repeated. The area chosen for the fieldwork is the Parapuños catchment near the city of Cáceres, in South-West Spain. This area is representative for the Dehesa landuse. The catchment is part of a private farm, of about 900 ha. Landuse is extensive livestock farming with sheep and Iberian pigs. The catchment is 1 km^2 in size, has average slopes of 8% and lies at an altitude of ±350 to 435 m. asl. (see Figure 4.2). It is a headwater basin, with a channel in the valley bottom, which is dry most of the year. The channel bed is very irregular and consists mostly of schist bedrock.

The region has a Mediterranean climate with Atlantic and continental influences. This results in moderate winters and hot and dry summers (June to September) (see Figure 4.1). Monthly average temperatures range from 8.1°C in January to 25.6 °C in July and August (with regular maximum temperatures above 40°C). The annual and inter-annual variability of rainfall is relatively high. The average annual precipitation is 514 mm, with a standard deviation of 155.2 mm, distributed on average over 85 rain days (based on a 90 year rainfall record, Schnabel, 1998). There is a dry season from June to September and a wet season from October to April (Meteorological station, Cáceres). The climate can be classified as semi-arid, according to the Unesco aridity index.

Thanks to the pronounced relief and the shallow soils, the spatial boundaries of the catchment can be estimated using the surface topography. Also the bottom boundary of the catchment is an almost impervious material: greywacke and schist (of Precambrian to Upper Carboniferous origin). Seepage of water into weathered cracks or root holes (which have been found to penetrate partly into the bedrock) provides extra storage capacity for water in the catchment. The permeability of this layer is probably very low, which means there may be some water storage, which can be used for evapotranspiration during the summer months, but it is not likely to contribute to significant flow in downstream direction. Furthermore the catchment dries out completely during the summer, which means a full year's water balance can be made up easily as total precipitation must equal the sum of yearly discharge and evapotranspiration (Ceballos and Schnabel, 1998).

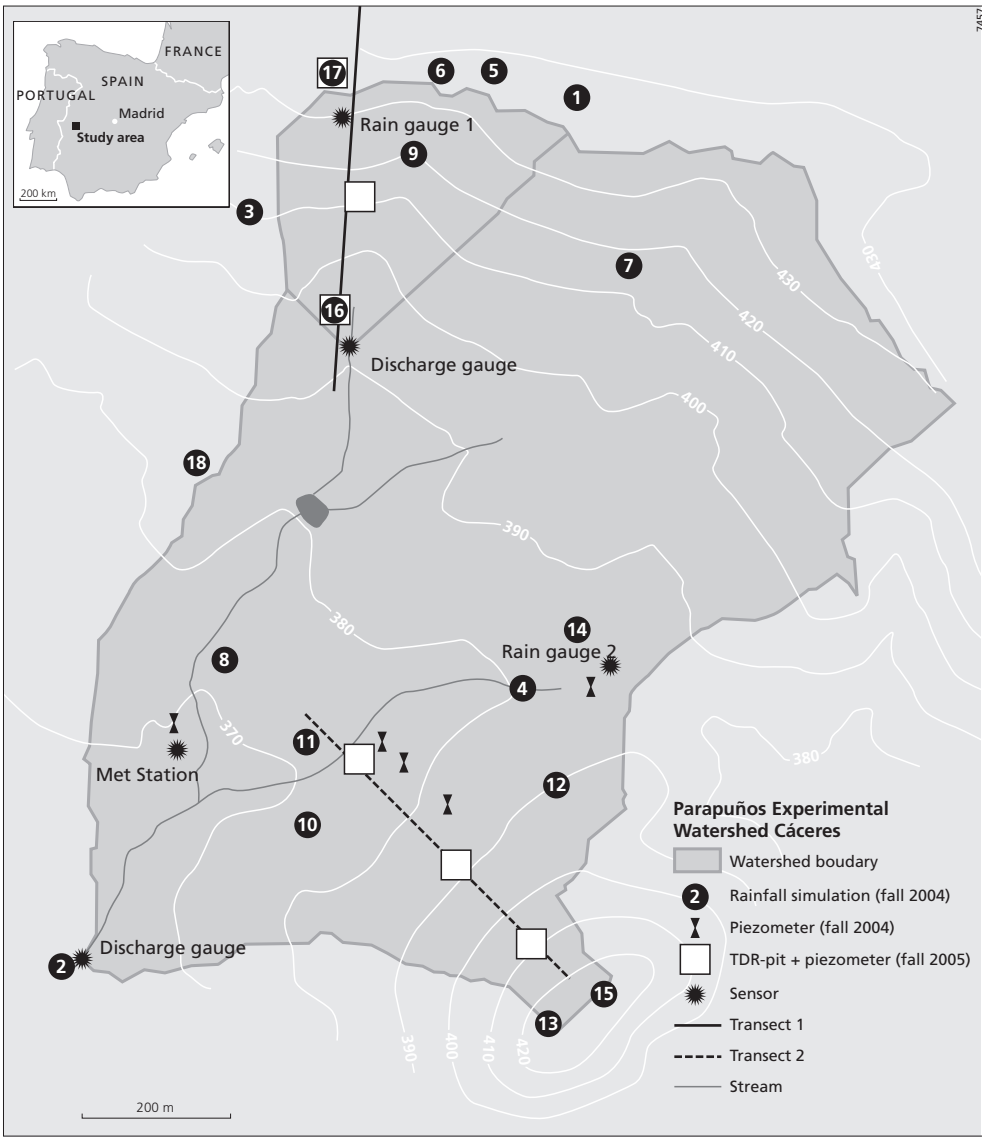

Figure 4.2: The Parapuños experimental catchment, including locations of field measurements.

The most widespread soils in the area are Cambisols and Leptosols (Schnabel, 1997), according to the FAO soil classification (FAO, 1988). Soils developed on the hilltops are developed in badly sorted sediments, deposited on top of the schists during the Pliocene-Pleistocene period. These soils have a sandy loam texture and reach depths of 80-90 cm (where slightly weathered bedrock starts). Along the hillslopes the soils are very shallow (about 20 – 40 cm). In the valley bottom a shallow alluvial fill with a maximum depth of about 90 cm is found, composed of silty loam with many large stones and occasional pebble layers. Its depth varies strongly in

Table 4.1: Texture and k-sat for hilltop, hillslope and valley bottom, measured on kopecki ring samples of 100 cm^3(average and standard deviations (number of samples)).

Location	depth (cm)	Sand	Silt	Clay	Soil type	k-sat (cm/h) average	stdev (n)
Transect 1:							
Hill top	0-5	61,4	34,7	3,9	sandy loam	15,6	14,3 (7)
	10-20	59,4	27,3	13,3	sandy loam	3,3	2,6 (8)
	>50	43,9	5,8	50,3	clay		
Hillslope	0-5	44,4	45,0	10,5	loam	1,7	0,8 (6)
	10-20	39,3	44,2	16,5	loam	1,2	1,2 (4)
	50-60	17,7	57,3	25,0	silt loam		
Valley bottom	0-5	23,5	63,6	12,9	silt loam	4,6	5,0 (6)
	20-30	14,7	51,1	34,2	silty clay loam	0,0	0,0 (6)
Transect 2:							
Hill top	0-5	75,2	19,7	5,1	loamy sand	5,0	2,5 (4)
	10-20	58,9	22,6	18,5	sandy loam		
	> 80	57,8	11,3	30,9	sandy clay loam		
Hillslope	0-5	33,4	66,6	11,8	silt loam	1,5	1,6 (6)
	10-20	32,7	51,4	15,9	silt loam	0,5	0,1 (2)
Valley bottom	0-5	35,2	56,8	8,0	silt loam	3,8	2,5 (8)
	10-20	28,4	63,2	8,5	silt loam	1,1	0,7 (8)

relation with the irregular surface of the underlying schists and frequent vertically oriented rock outcrops. Texture and k-sat for hilltop, hillslope and valley bottom (Figure 3.7b) are given in Table 4.1. Valley bottom soils are very poorly developed without a distinguishable edaphic horizon. Organic matter content in the soils is generally between 2 to 4% in the upper layer.

As mentioned in the introduction, Cerdá et al. (1998) found macroporosity and water repellency in rainfall- runoff studies in the Dehesas. Different origins of macroporosity were observed in

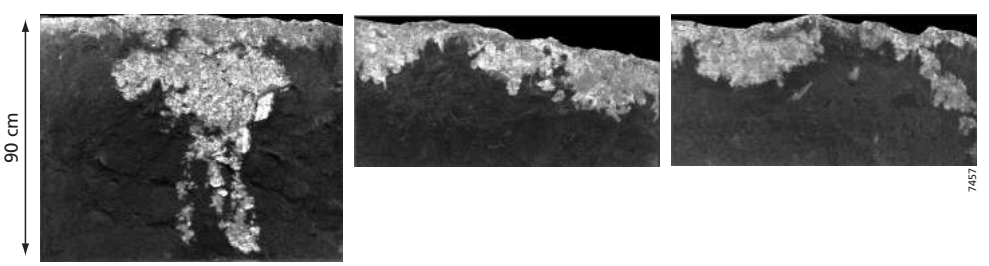

Figure 4.3: Examples of tracer infiltration profiles: a) on hilltop, b) along hillslope, c) in the valley bottom. All profile photographs have been geometrically corrected using a $1m^2$ frame, which was placed on the profiles. Light areas are coloured by infiltrating dyed water.

this study area: old root channels, ant burrows, worm burrows and even large burrows of mice were seen to cause underground rapid flow of water. Locally there were many narrow cracks visible at the soil surface in the dry period. Also the large soil heterogeneity along the upper rim and occurrence of pebble layers in the valley bottom may cause preferential flow.

Evidence of preferential flow in this study area also exists in the form of tracer infiltration profiles. These profiles were obtained from a total of 18 tracer infiltration experiments under a rainfall intensity of 44mm/h, which was continued for a full hour. Some typical examples of infiltration profiles are shown in Figure 4.3. This evidence leads us to this research on the influence of preferential flow under natural circumstances and from small to large scale.

4.4 Methods

The existing ongoing measurements include: meteorological data (temperature, humidity, net radiance, global radiance, wind speed and -direction), rainfall measurements at six locations, soil moisture content in two profiles (a total of 16 probes) and catchment discharge (all at a 5 min resolution, except for the soil moisture, which is read out manually approximately once every two weeks).

From the 1st of September 2004 to the 5th of January 2005 the piezometric head was monitored continuously at 5 locations (at a 10 min resolution) using Keller pressure transducers, which

Table 4.2: Soil profile descriptions (with Munsell colour codes), for six TDR-pits along two transects in the catchment. For locations of the pits see Figure 4.2.

Hillslope 1			**Hillslope 2**		
Hill top	Hillslope	Valley Bottom	Hill top	Hillslope	Valley Bottom
0 – 55 cm dull orange (7.5YR 6/4) sandy loam very stony	0 – 30 cm yellowish brown (10YR6/6) loamy layer with many stones	0 – 30 cm reddish brown (5YR4/8) silt loam	0-35 cm dull brown (7.5YR5/3) loamy matrix, many stones, some roots	0- 45 cm Brownish (10YR4/4) loamy matrix, many stones	0-90 cm yellow brown (10YR6/6) silt loam, some stones, some roots and some macropores
at 30 cm layer with very high stone content	30 – 35 cm clayey layer with some stones	30 – 55 cm reddish clay	35-70 cm bright reddish brown (5YR5/6) clay, occasional roots	45 cm – bedrock (schist)	fine pebble layer on top of the schist
55 – 65 Bright reddish brown (5YR5/8) clayey matrix, large stones	35 m – bedrock	55 cm – bedrock (schist)	70 cm – deeper yellow scaly material, probably weathered schist		90 cm – bedrock (schist)
65 cm – bedrock					

contain automatic dataloggers. From the 23rd of September 2005 to the 18th of May 2006 the monitoring was continued in 2 of the existing piezometer pipes and at six new locations (with a short interruption of measurements at the beginning of November). The piezometer pipes were perforated along the bottom 20 cm of the pipes and were placed down to bedrock. The measurements thus represent piezometric head, in the tubes, at bedrock level.

The fall of 2005 was used to measure the spatial and temporal soil moisture distribution in six soil profiles, located along two hillslopes in the catchment, using 67 TDR probes which were installed in soil pits and manually read out twice a day in the transition from dry to wet conditions (for all the measurement locations see Figure 4.2). The TDR probes we used were home made, consisting of two rods with a diameter of 2 mm and a length of 8.78 cm (std dev. 0.26 cm). Separation of the rods was on average 2.89 cm (std dev. 0.06 cm). Permittivity was measured manually using a 1502C Tectronix cable tester. The TDR probes were installed in horizontal layers (two to four TDR probes next to each other) at two or three different soil depths per profile. The horizontal distance was approximately 20 cm (their exact locations depending on stones in the soil profile and the profile depths or observed layering), the vertical distance depended on the depth of the profile. The measurement volume of a TDR-probe is approximately 1 dm3. Soil profile descriptions for the TDR pits are given in Table 4.2. The measurements of soil moisture content change and water level variation under natural circumstances was used to assess the influence of preferential flow on the hydrological system.

4.5 Results and discussion

The annual and inter-annual variability of rainfall is very high in the studied area, as mentioned in the description of the study area. The summers of 2004 and 2005 were dry as usual and the first significant rainfall started in October. The cumulative rainfall from September to December

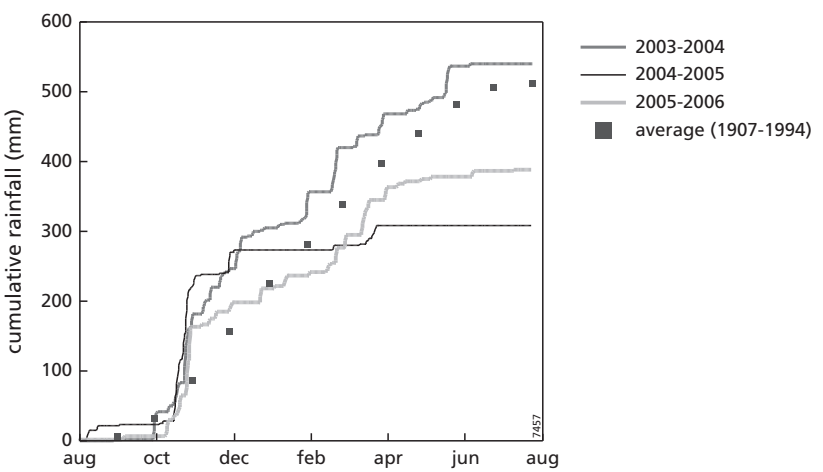

Figure 4.4: Cumulative rainfall for the years of '04-'05, '05-'06 and for the average monthly rainfall (1907-1994), also the year of '03-'04 was included as an example of a relatively wet year.

is equal to the cumulative of average rainfall, but in both years almost all this rainfall occurred in a few high intensity rain events towards the end of October (Figure 4.4). The total rainfall in October 2004 was 196.6 mm and in 2005 it was 156.2 mm, compared to a mean amount of 55.5 mm for this month (see also Figure 4.1). After October the rest of the wet season was relatively dry, with occasional rainfall events but also long periods without rain. Both years ended up to be relatively dry years.

In the following paragraphs the hydrological behaviour of the catchment is explained, based on the water level fluctuations, soil moisture content distribution and discharge data as a result of the October rainfall events, focussing on the role of preferential flow at different scales.

Water level fluctuations in piezometers

Piezometric head is measured at six locations along the two hillslopes in the area (at a few meters from the TDR-pits, see Figure 4.2). Figure 4.5 shows that piezometer reactions for the different hillslopes are slightly different. For the full measurement period the piezometers on the hilltops do not react. A strongly fluctuating water level occurs in the piezometers located at the bottom of the hillslopes and later on also in the piezometers along the slopes of the first and the second transect. The water level reactions in both transects are very rapid, both their increase and decrease. The piezometers along the first transect show a slower decrease in water level than those in the second transect, but all are empty within a week after the rainfall ends. Piezometers located within the same transect show the same behaviour. The water levels measured in the piezometer tubes are always temporary; there is no build up of a seasonal groundwater body in the course of the wet season as one might expect.

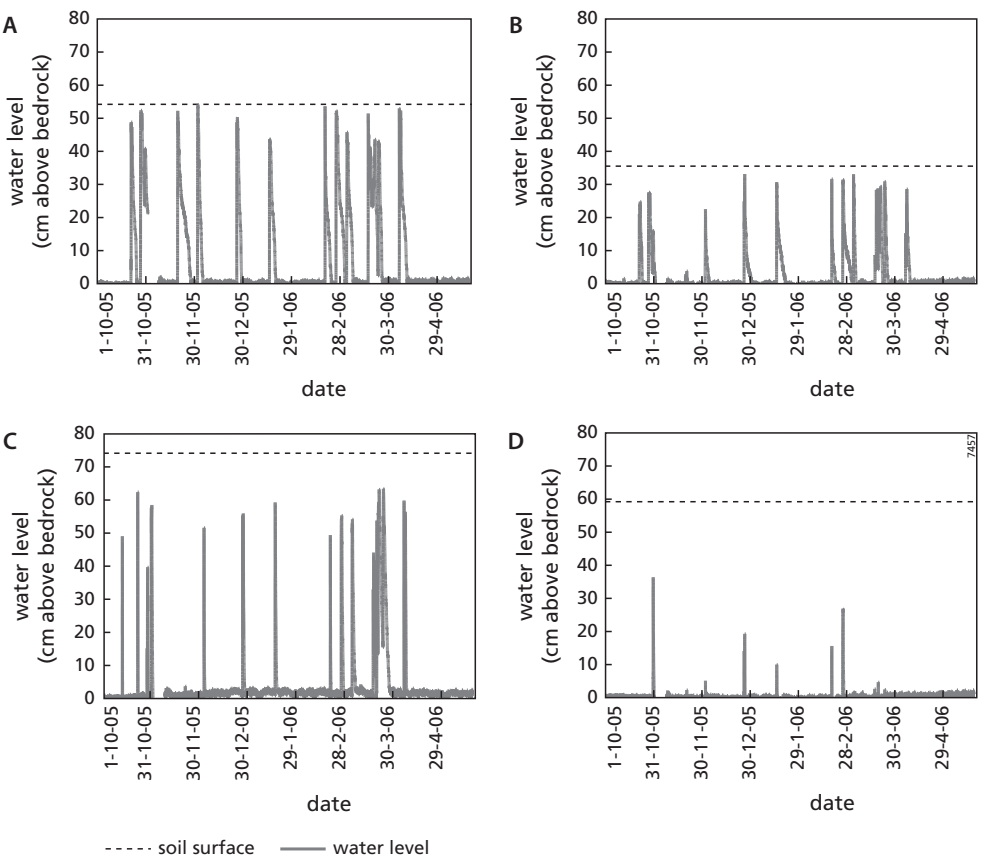

Figure 4.5: Measured water level fluctuations in the Parapuños catchment for the wet-season 2005-2006. Transect 1: a) valley bottom, b) hillslope, and transect 2: c) valley bottom, d) hillslope (for locations of the transects see Figure 4.2).

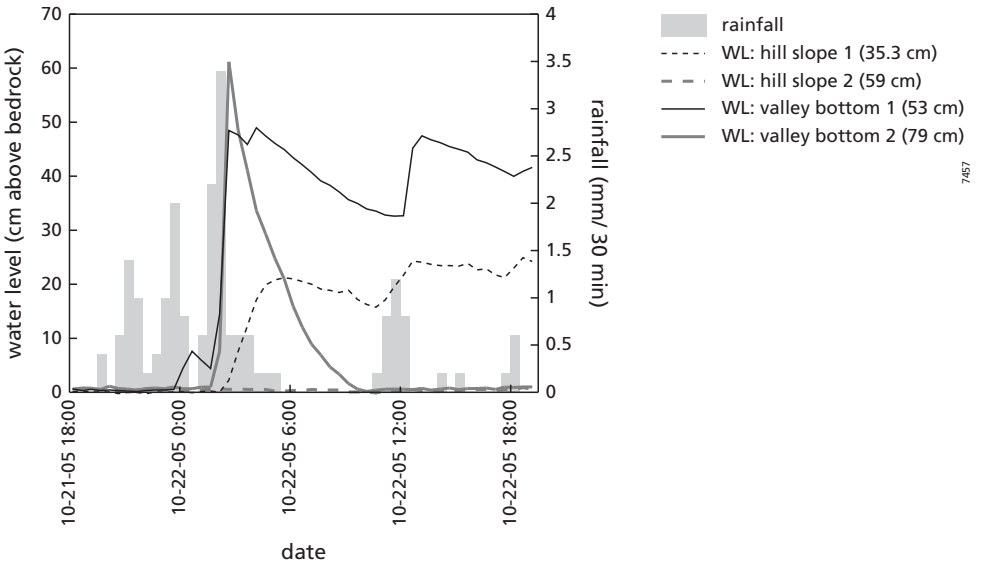

Figure 4.6: Precipitation and piezometer water level (WL) on the 22nd of October, when the soil is still relatively dry (see Figure 4.8), location and depth from soil surface to bedrock are indicated in the legend. The piezometer along the second hillslope transect (WL hill slope 2) shows no response during this event.

Focussing on a rainfall event at the beginning of the wet season, the first water level rise occurs on the 22nd of October (Figure 4.6). Before this date several small rainfall events took place, but neither of them resulted in water level rise or discharge. The water level rapidly rises to reach almost soil surface in the piezometer tubes of the valley bottom of both transects and along the hillslope of the first transect. The decrease in water level is also rapid, though much stronger along the second transect than along the first. The amount of cumulative rainfall until then is not enough to reach saturation of the soils and the soil matrix in the valley bottom is then still far from saturation, as is shown in Figure 4.8.

The rainfall events of the 28th and 30th of October are used to show the behaviour of water level rise and discharge production during rainfall events of similar magnitude (39 and 45 mm resp.), but different intensity and different antecedent moisture content. The rainfall, discharge and associated water level reactions at different locations along the two transects are shown in Figure 4.7a and 7b. The measurements show a rapid rise and a rapid fall in water level during or shortly after registering a rainfall intensity of 6.2 mmh^{-1} on the 28th of October. The short decrease in rainfall intensities in the beginning of the rainfall immediately results in a decrease in water level in the second transect. The first transect also shows a short slight decrease in water level.

By comparison of the water level measurements of two events under dry and near saturated antecedent conditions for both October 2004 and October 2005 (Table 4.3), we see that the behaviour in the different years is the same. The water level decrease is mainly large when the soil matrix is still relatively dry (8 cm h^{-1}). When the soil matrix is near saturation the water level

decrease remains quite high (approximately 3.9 cm h^{-1}) along the second transect. Along the first transect drainage under dry and wet circumstances are both much smaller than along the second transect.

There are different possible explanations for the rapid fluctuations in the piezometric head measured in the piezometers: there may be a) a pressure wave response, b) lateral flow along the hillslope in deeper layers, c) local vertical preferential flow. As the soils are very dry (± 10 vol% SMC) when the first fluctuations occur, the quick rise in piezometric head cannot be due to a pressure wave response. The possibility of lateral flow on the bedrock was checked by installing an additional piezometer at 1 m. distance of the valley bottom tube in transect 2. This piezometer was installed to a depth of 52 cm, instead of 79 cm (down to bedrock). There is more

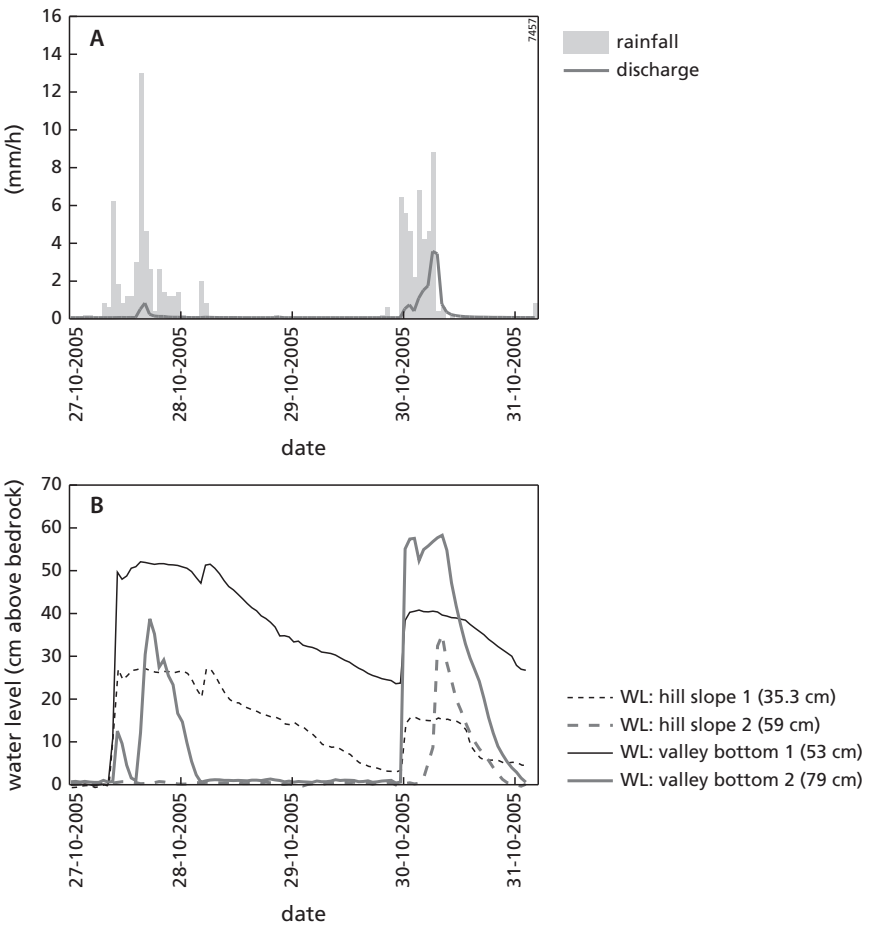

Figure 4.7: a) Rainfall-discharge for two consecutive rainfall events in the fall of 2005, b) measured water levels in piezometers along two transects in the catchment. The piezometers on the hilltops did not register any water level during the whole measurement period, so these are not included here.

than 20 cm of silty loam soil between the bottom of this piezometer and the pebble layer on the bedrock. Nevertheless the reactions of this piezometer were as fast or sometimes even faster than the neighbouring piezometer. It is therefore unlikely that the rapid reactions of the pressure head in the piezometers is due to lateral flow on the bedrock.

The third explanation of vertical preferential flow in the soils is most likely. The fact that the fluctuations are very rapid, both under very dry catchment conditions as well as under very wet conditions, lead us to the conclusion that we must be measuring the reactions of a connected macroporous network in stead of a full water layer in the soil. Under dry conditions there is not enough water to build up a full water layer and under wet conditions the decrease in water level after rainfall is so fast, that it is not likely to be caused by matrix drainage. The piezometer tubes do intersect both matrix and macropores, but the flow in macropores is much quicker than in the matrix. In case a large network of macropores with a connection to soil surface and to the bottom of the piezometer tubes fills up rapidly, this would make water level in the tubes rise freely too, while infiltration to matrix from this network is much slower (which is supported by the difference in matrix water content measurements and the piezometer behaviour).

The change in water level decrease when going from dry to wet catchment conditions supports the previous explanation of the water level as a macropore network response. Under dry conditions there is infiltration from the macropores to the matrix and also the irregular bedrock surface and the bedrock cracks and root holes can store water. Once the soil reaches saturation these stores are full and the water can only drain toward the stream, which results in a decrease of macropore drainage.

Finally the difference in drainage between the two transects can be explained partly through differences in soil texture and conductivity. The much stronger drainage in the second transect is however also thought to result from the occurrence of pebble layers in the soil. The extent of the pebble layers is not exactly known, but they were found in several pits in the south eastern part

Table 4.3: Comparison of different rainfall events from dry to wet catchment conditions for the fall of 2004 and 2005: the antecedent rainfall, event rainfall, runoff coefficient and water level decrease after rainfall stopped.

	2004 First transect		**2005 First transect**		**2005 Second transect**	
Event date (duration)	19-20 October (10 h)	27-28 October (15 h)	22 October (10 h)	30-31 October (15.5 h)	22 October (10 h)	30-31 October (15.5 h)
30 Days – Antecedent rainfall (mm)	31.4	129.5	36.2	104.8	36.2	104.8
Rainfall (mm)	17.0	41.4	16.4	45.2	16.4	45.2
Catchment runoff coefficient (%)	1.60	34.8	0.78	31.4	0.78	31.4
Water level decrease after event (cm h-1)	8.0	3.9	7.8	3.9	1.9	0.6

of the catchment (valley bottom of transect 2), and are also seen in the side profiles of the main channel. And an additional influence on the drainage velocity may come from the distance to the gully, which is smaller in the valley bottom of transect 2 than in transect 1.

There was no water table development on the hilltops of either transect. The TDR-profiles at these locations did show that the water content in the deeper layers increased more rapidly than the shallow layers. This seems to indicate that also on the hilltops there is preferential infiltration, but the infiltration capacity of the matrix on the hilltops (for k-sat values see table 4.1) may be large enough so that the macropores empty into the soil matrix instantaneously.

The impact of vertical preferential infiltration may become insignificant on a larger scale, in case lateral transport is slow. In this area lateral preferential flow is thought to be an important phenomenon in the catchment hydrology, based on the water level fluctuations both in unsaturated as well as in saturated conditions. Catchment drainage shortly after rainfall ends is thought to be mainly drainage of the macropore network.

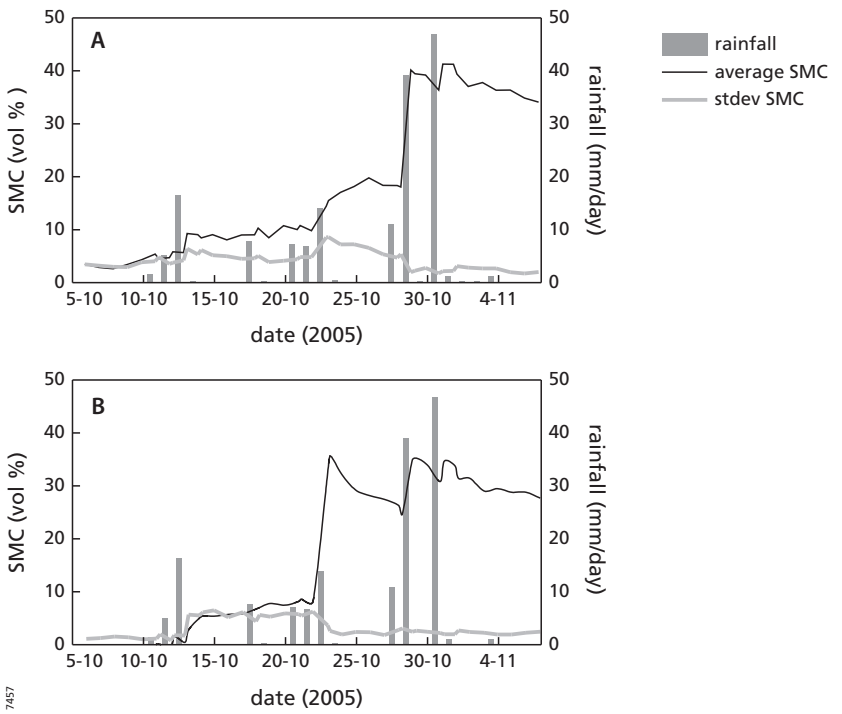

Figure 4.8: Rainfall and soil moisture content (measured twice a day) along transect 1 at the beginning of the rainy season, a) at 20-25 cm depth at the bottom of the slope (5 probes) and b) at 35 cm depth at midslope (6 probes). Presented are rainfall and average and standard deviations of SMC at each site.

Spatial and temporal soil moisture variation

If the piezometer behaviour is caused by preferential flow, a large variability in soil moisture within horizontal soil layers is to be expected. During and directly after rainfall preferential flow can cause regions of high moisture content around the preferential flow paths as opposed to relatively dry parts of the soil matrix. Between rainfall events redistribution of water can decrease the variation in soil moisture content. The fraction of matrix and preferential flow path encompassed in the measurement volume is unknown. The measured difference in water content is therefore not a direct difference between the flow regimes, but a high variability of water content within a soil layer is an indicator of preferential flow.

The soil moisture content measurements were gathered under natural conditions, during the transition from dry to wet conditions. The rainfall of October to November of 2005 is given in Figure 4.8a, together with an example of the average and standard deviation of the soil moisture content of one layer of TDR-probes. This example is a horizontal layer of 5 TDR-probes in the soil profile of the valley bottom of transect 1 installed at a depth of 20-25 cm from the surface (for the location within the catchment see Figure 4.2). Preferential flow and variation in soil moisture content is largest during and shortly after a rainstorm. As the measurements were done only twice a day at most, the moment of measurements may influence the measured variation in soil moisture content.

The TDR-measurements show for each location that the soil matrix slowly becomes wetter at the beginning of October. Then the matrix suddenly becomes saturated, as a result of two large rainfall events, and remains very wet for the remaining measurement period. There is a large variation in soil moisture content within the soil layer in the beginning of the wetting season: up to almost 8 vol%. The standard deviation of soil moisture within soil layers increases during or shortly after rainfall and then decreases slightly in between the rainfall events. On the 28th of October this soil layer becomes almost saturated and the standard deviation in water content decreases to approximately 2 vol% (this is equal to the RMSE of TDR measurements as determined in the laboratory during the soil specific calibrations of the TDR probes).

The second layer of TDR sensors in this profile lies at a depth of about 40 – 45 cm. The deeper layer is continuously at about 25 – 30 vol%, and jumps to near saturation on the 28th of October. The standard deviation in moisture content is between 2 to 3 vol% all the time. The total soil depth is about 55 cm. With the large rainfall events at the end of October apparently the whole soil profile becomes nearly saturated. The shallow TDR-profile along the hillslope of this transect (Figure 4.8b) shows a short period (from the 13th to 22nd of October) of a large variation in soil moisture content and an earlier jump to saturation: on the 22nd of October.

The increase and decrease in variation of SMC within the layers seem to indicate active preferential flow paths during the rainfall and redistribution in between rainfall events. The large standard deviation in soil moisture contents during the wetting of the soils is an indication of preferential infiltration under natural circumstances, which influences the distribution of soil moisture content. Preferential flow and variation in soil moisture content is in theory largest during and shortly after a rainstorm. As the measurements were done only twice a day at most, the moment of measurements may influence strongly the measured variation in soil moisture

content. The TDR-measurements cannot however be used to quantify the preferential flow, due to their large measurement volume and poor resolution of measurements, both spatial and temporal. The direct use of the soil moisture content measurements to characterise preferential flow may be disputable, but they can indirectly be used to support the interpretation of water level reactions of the piezometers.

Catchment discharge: surface runoff and subsurface stormflow

There are two ways in which preferential flow may influence the catchment discharge. In the first place the change in infiltration (by preferential flow) will influence the amount of surface runoff which is generated during a rainstorm. Secondly, preferential flow may lead to rapid subsurface stormflow (SSF). The amount of subsurface stormflow generated depends on the fluxes of both vertical preferential flow as well as lateral flow. In the following the influence of preferential flow at catchment scale is studied through the interpretation of the relationship between water level and catchment discharge. The rapid drainage of the macropores in the valley bottom has been described above. Figure 4.9 illustrates the relationship between water level in the piezometers and discharge at the catchment outlet, for the recession limb of five discharge events in 2005/2006. The water level information given here is from the piezometer in the valley bottom of the second transect. This piezometer is nearest to the catchment outlet and reacts fastest, so these water levels may have a large and rapid influence on the discharge. The other piezometers have a slower response time and a less strong relationship with the discharge.

The discharge generally starts half an hour to one hour after the piezometers start filling up and continues for a long time after rainfall ends. There is a clear difference between the water level – discharge relationship of the 30/31st of October rainfall and the others. Of course both the discharge and the piezometer water level depend on the rainfall amount, so a relationship between the first two is not necessarily causal. On the 30/31st of October the valley bottom is

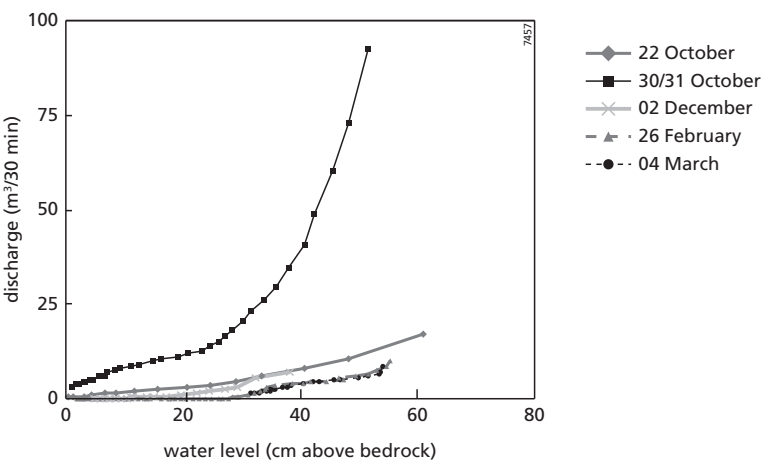

Figure 4.9: Water level (valley bottom second transect) – discharge relationship, using a time-lag of half an hour between the water level and discharge measurements, for the hydrograph recession limb of five rain events in 2005/2006, starting one hour after rainfall ended.

temporarily saturated. As concluded in the section above on water levels, the drainage of the macropores during this event is mainly subsurface flow to the streams, as the matrix is then saturated, thus the storage capacity of matrix and bedrock are then full and there may be some groundwater flow. During the other rainfall events under dryer matrix conditions the high water levels generate much lower subsurface stormflow as part of the water is lost to the matrix and bedrock storage.

Using the relationships between water level and discharge it is possible to retrieve the discharge volume which has entered the streams through subsurface discharge. As long as there is surface runoff it is not possible to determine which fraction of discharge comes from subsurface flow or surface runoff. Assuming that two hours after the end of a rainfall event surface runoff ceases

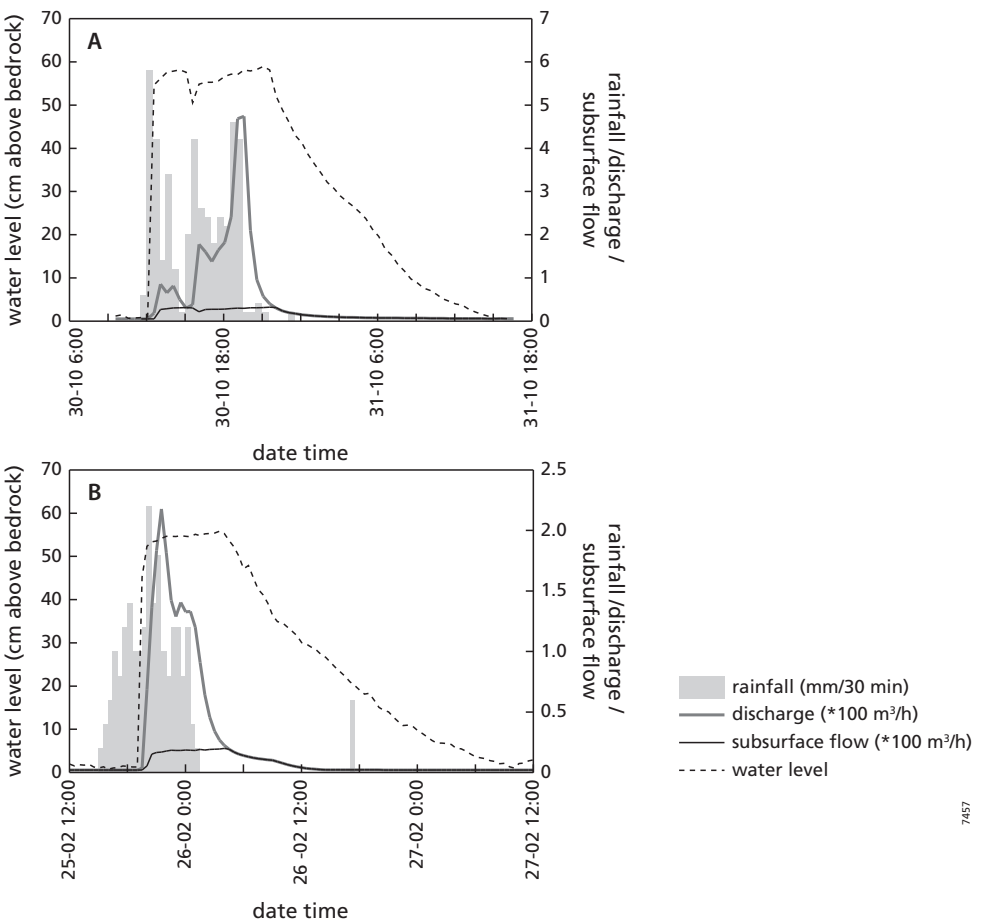

Figure 4.10: Subsurface flow (SSF) calculated for a) the 30/31st of October and b) for the 26th of February rainfall events, using the water level – discharge relationship (Figure 4.9) for the backward projection from 1 timestep after rainfall ended to 0 subsurface flow one hour after discharge and water level rise started.

Table 4.4: Rainfall-discharge amounts for five events in 2005-06, with estimations of overland flow and subsurface storm flow (SSF) fractions in the discharge (further explanation of calculations of SSF can be found in the text above).

	22 oct '05	30/31 oct '05	2 dec '05	26 feb '06	4 mar '06
Total rainfall (mm)	16.4	45.2	13.0	21.6	18.2
Max intensity (mm/30 min)	3.4	5.8	2.0	2.2	3.8
30-Day antecedent rainfall (mm)	44.5	108.6	25.6	17.5	41.0
Runoff coefficients (%)	0.8	31.4	0.2	4.5	7.4
Discharge origin (%):					
Overland flow	54.4	79.2	20.0	79.5	87.2
SSF +	54.2	20.0	92.4	20.6	12.8
SSF	45.6	20.4	80.0	20.5	12.8
SSF -	44.5	18.6	81.6	19.5	12.8
Groundwater flow	– -	0.4	– -	– -	– -

in this small catchment, we used the recession limb of the hydrograph (starting two hours after rainfall ends) to derive a relationship between the water level in the piezometers and the discharge. For this relationship a time lag of 30 min is used between the water level in soils and discharge occurrence as the time lapse between water leaving the profile and passing through the discharge gauge is expected to be small and the lapse of 30 min gives the best relationship between the two. That relationship is subsequently used to project backwards the amount of subsurface flow in the discharge, based on water levels, during the rainfall event. Then the total amount of subsurface flow can be estimated. Examples of the rainfall – discharge results are given in Figure 4.10.

This calculation assumes that all catchment discharge is generated by preferential flow. During the event of 30/31st of October there may also have been groundwater flow, as the valley bottom soils were saturated. Therefore we calculated a rough estimate of water level flow for this event. Using the average (2.4 cm $h^{-1)}$ and standard deviation (1.6 cm h^{-1}) of measured saturated conductivity for the valley bottom soils (16 samples), a slope angle of 3 degrees and the measured water level in the soils, a maximum groundwater flow was calculated. A large part of the channel length in the valley bottom (2*500 m) was taken to contribute to groundwater. The groundwater contribution amounted to 3-4 m^3 h^{-1}, with a total of 59 m^3 for the whole event. For the other events, we do not distinguish between the macropore flow and groundwater flow, as the 30-day antecedent rainfall is so low that the condition of the soil matrix is unsaturated. As the conductivity decreases strongly under unsaturated conditions, we assume that the subsurface flow is then mainly macropore flow.

In Table 4.4 the results of the subsurface flow contribution to discharge (as a percentage of total discharge) is given for five events in 2005-'06. The overland flow is taken to be the remainder of the discharge, when subsurface flow and groundwater are distracted. The fraction of discharge that is subsurface flow is largest for events with relatively small total runoff coefficients (22nd of

October and 2nd of December). For the events of the 30/31st of October, 26th of February and 4th of March discharge percentages were higher and overland flow was dominant. Nevertheless an estimated 12.8 to 20.5% of the discharge resulted from subsurface flow.

The calculations described above contain quite some assumptions, therefore it is important to keep in mind that they provide rough estimates. The assumptions which mainly produce uncertainties in the outcome are the duration of surface runoff, the backward projection of the water-level discharge relationship and the negligible matrix flow under unsaturated conditions. To start with methods such as logarithmic discharge plotting or cumulative discharge versus cumulative rainfall were used to check the duration of overland flow, but neither gave a clear argument as to when the overland flow ends. To get some idea of the influence of the assumption that overland flow ends two hours after rainfall stops, we have made the same calculations of subsurface flow as described above, taking this moment to be 30 min. earlier or 30 min later (SSF+ and SSF- resp. in Table 4.4). The uncertainty in the estimates of subsurface flow are highest for the small events, as the absolute amounts of discharge are very small. Due to hysteresis in the relationship between water level and flow the backward projection of the subsurface flow component based on this relationship may lead to an overestimation in the beginning of the event. Therefore the first hour after the discharge and water level rise start, the subsurface flow is ignored. The discharge is calculated starting one hour after the water level starts, even then we might be slightly overestimating the subsurface flow in the calculations, for the first hours of the rainfall event. Finally, as the influence of saturated flow in the matrix is so small on the total discharge (0.4% under saturated conditions of the valley bottom, table 4), the influence of unsaturated flow is highly unlikely to be significant.

Comparison with previous literature

From previous research we know that preferential flow is a phenomenon strongly related to thresholds. The first threshold in the occurrence of preferential flow is the infiltration capacity of the matrix which determines whether inflow into the macropores starts (Bronstert and Plate, 1997). The maximum flow in macropores is limited by the infiltration into the macropores as they are known never to transport at full capacity (Weiler, 2001) The horizontal and lateral connectivity of preferential flow paths is an important controlling factor for the extent of the influence of preferential flow in an area (Weiler et al, 2003). According to Jones and Connelly (2002) the subsurface flow depends also on the length of pipes. A threshold used by Beckers and Alila (2004) is a critical water table depth before rapid lateral transport starts, which is similar to the precipitation threshold found by Tromp-van Meerveld and McDonnell (2006) for lateral subsurface stormflow. This is thought to depend on the bedrock topography, which may provide storage for groundwater and form a threshold in the connectivity of the subsurface flow to the gully (Tromp-van Meerveld and McDonnell, 2006).

In this semi-arid catchment a large amount of macropores was observed and the interpretations of measurements show preferential flow through these macropores results in a large component of bypass flow to deeper layers. The fluctuations of the water level was different for the different hillslopes. Contributions of different hillslopes to the total subsurface stormflow are variable and of different duration, depending on the matrix infiltration capacity, macropore connectivity, distance to the channels and bedrock topography. Other important factors for

the lateral subsurface flow are the interaction between the macropores and the matrix, which is not necessarily saturated before lateral flow starts in the macropores and the existence of fast conducting layers in the subsoil. The rough estimation of subsurface flow amounts should therefore be treated cautiously. Nevertheless it is very likely that for this semi-arid catchment a significant fraction of discharge is subsurface flow, mainly during low intensity, low discharge events. Scherrer et al. (2007) found similar behaviour in hillslopes in the Swiss Alps, where water rapidly bypassed the (unsaturated) soil matrix, the macroporous network was rapidly filled up to soil surface and a significant part of hillslope discharge was subsurface flow.

In semi-arid environments rapid infiltration of water to deeper layers may be important for the water retention in the soils. Preferential flow increases percolation to a greater depth where the influence of evaporation is low, thus increasing water availability for trees. Drainage of a soil profile however is also important to ensure air transport to the roots and to prevent instability of sloping soil profiles. Preferential flow may be an important factor to consider in future research into the ongoing threat of degradation of Dehesas. With the large amount of data on the hillslope water balance and the acquainted knowledge on how the hydrological system works the next logical step is to use a model for quantification of fluxes in the different domains.

4.6 Conclusions

In this chapter a thorough analysis was made of the hydrological functioning and the impact of preferential flow and subsurface stormflow for a semi-arid watershed in Spain. Detailed rainfall, soil moisture content, water level and discharge were used to indicate the importance of preferential flow in the hillslope hydrological processes in this area at a range of scales. After rainfall starts there is preferential infiltration into the soils, resulting in a local variability of soil moisture content and a relatively fast percolation of part of the infiltrated water to deeper layers. Rapid fluctuations of the piezometer water levels when the soil matrix is not yet saturated indicate a macroporous domain which can fill up during high-intensity rainstorms. This macroporous domain functions separately from the soil matrix, as it can fill up and empty rapidly, while the matrix reacts more slowly. There is however, interaction between the domains depending on the degree of saturation of the different domains.

These processes influence the behaviour of the discharge in part of the season, which seems to react too slowly to consist mainly of surface runoff and is unlikely to be groundwater flow as the soil profiles are often not saturated. Rough calculations based on the relationships between the water level in the macropores and the discharge indicate that with low intensity rainfall and low discharge percentages, a large part of the discharge (up to even 80%) is subsurface stormflow. Under high intensity rainfall, high discharge events the discharge is dominated by overland flow, but still up to 20% can be subsurface flow.

5 Spatial variability of infiltration patterns related to site characteristics

Based on: Van Schaik, N.L.M.B. 2009. Spatial variability of infiltration patterns related to site characteristics in a semi-arid watershed. Catena, 78: 36–47.

5.1 Abstract

Preferential flow may strongly affect hydrology at different scales. Measurement of preferential flow however remains very difficult. Tracer infiltration profiles are often used to measure the degree of preferential flow at plot scale. These experiments are time-consuming, costly and destructive. As a result existing dye-tracer studies are often based on a limited number of profiles. The aim of this study is therefore to select a limited number of soil and landscape characteristics indicative for the occurrence and the degree of preferential flow. 18 rainfall simulations with a dye-tracer and additional site measurements such as soil type, vegetation type and soil physical parameters were performed in a 1 km^2 catchment in the Dehesa (Extremadura, Spain). A stepwise multiple regression procedure was used to select variables with a high predictive value for the degree of preferential flow.

The infiltration patterns show that preferential flow is potentially present throughout the area and is spatially variable. At first inspection the spatial variability seems to relate to the site specific variables. This is corroborated by the stepwise multiple regression results, with R^2 values of 56% to 67% for the different preferential flow parameters (uniform infiltration front, maximum infiltration depth, total stained area and preferential flow fraction of stained area). A bootstrapping procedure however indicated that the bias due to stepwise variable selection with a large number of independent input variables and a low number of cases was high. Pre-selection of a limited set of variables (vegetation, texture, slope and location) based on expert knowledge gives lower but more powerful R^2 values (50% to 66%), without the bias due to stepwise variable selection.

As a large part of the spatial variability of infiltration patterns can be explained with the selected site characteristics, the regression equations were used in combination with detailed maps of the four selected input variables to calculate maps of catchment scale spatial variability in infiltration patterns, thereby delineating sub-areas within the catchment with different infiltration patterns.

5.2 Introduction

Preferential flow is an enhanced flux of water and solute through certain channels in porous media, such that a small fraction of the soil volume participates in most of the flow. Preferential flow is therefore of importance for understanding the spatial variability in infiltration and

percolation, which affect runoff generation and groundwater recharge (Ferreira et al., 2000; Léonard et al., 2001; Weiler and Naef, 2003a). Spatial variability of preferential flow paths may strongly influence runoff production. A change in the spatial distribution or density of preferential flow may therefore have a large impact on runoff response (Zehe et al., 2005; Zehe et al., 2006), even at the meso scale (Niehoff et al., 2002) Preferential flow may also produce a lateral through flow component and result in rapid percolation to groundwater and stream flow after a rainfall event. This can affect erosion processes and transport of solutes and pollution.

Preferential flow is difficult to measure and quantify due to its high spatial and temporal variability. When using point samples, like the commonly used Kopecki ring samples of 100 cm^3 volume, for the estimation of preferential flow, a large number of samples and a well-designed sampling strategy are needed (Ritsema and Dekker, 1996). The possibility that the full variability at the plot scale is missed remains large, regardless of the sampling strategy. Therefore methods for continuous (in time and space) sampling of water and solute drainage on a larger scale are useful. These methods involve the collection of soil water drained by either gravity (e.g. gravity pan samplers, agricultural tile lines, and shallow wells) or by applying a "capillary"suction (e.g. porous cup samplers, wick-lysimeters) (Boll et al., 1992). However these methods are labour intensive and costly and the value of the results may depend on whether a good contact can be assured between the soil and the wick-lysimeter (Kohl and Carlson, 1997).

Tracer-infiltration has been used to measure the degree of preferential flow (Ghodrati and Jury, 1990; Flury et al., 1994; Forrer et al., 2000; Zehe and Flühler, 2001; Ohrstrom et al. 2002). In those cases, rainfall simulation or infiltration experiments were performed with a dye tracer after which soil pits were excavated and pictures of the soil profiles were taken. The dye-stained areas on the soil profiles indicate the infiltration pattern and the depth to which dye has infiltrated. Though the amount of infiltration or distribution of water cannot be directly derived from the stained area profiles, they can be used to quantify the degree of preferential flow (using measures that describe the frequency, depth and shape of the stains) and to compare different locations when the experiments are conducted under similar conditions.

Site specific variables such as vegetation, stoniness, slope, soil structure, texture and other soil physical properties can make a location more susceptible to preferential flow. As tracer infiltration experiments are destructive and very time-consuming, finding a relationship between the parameters describing preferential flow and site specific variables may be very rewarding. The benefit of a relationship between site specific variables and preferential flow degree would be twofold: an easier field evaluation method and a large amount of existing information can be employed in combination with specific spatial interpolation methods. The latter facilitates the production of maps of spatial distribution for risk assessment or for large scale hydrological modelling of preferential flow.

The aim of this study is therefore to select a limited number of soil and landscape characteristics with a high predictive value for the degree of preferential flow. To this purpose a stepwise multiple regression was performed on a set of preferential flow parameters and site characteristics derived from 18 dye tracer experiments in a 1 km^2 semi-arid catchment in the Dehesa (Extremadura, Spain). The results of the stepwise multiple regression were used to

map spatial distribution of preferential flow and thereby indicate areas of different degrees of preferential flow in the catchment.

5.3 Study area

The area chosen for the fieldwork is the Parapuños catchment in Spain (Figure 5.1), near the city of Cáceres, Extremadura. This area is representative for the Dehesa land-use, which is a semi-natural agro-silvo-pastoral land-use, common for Mediterranean areas. The catchment is part of a private farm, about 900 ha in area and is a first order basin with average slopes of 8%. Land-use is extensive livestock farming with sheep and Iberian pigs. The catchment is about 1 km^2 in size and lies at an altitude of ±350-435 m asl.

The climate in this region is Mediterranean with Atlantic and continental influences. This results in moderate winters and hot and dry summers (June to September). The average annual precipitation is 514 mm, distributed over an average 85 rain days. The annual and inter-annual variability of rainfall is relatively high. There is a dry period from June to September and a wet season from October to April. According to the UNESCO aridity index, the climate can be classified as semi-arid.

The most widespread soils in the area are Cambisols and Leptosols, according to the FAO soil classification (FAO, 1988). These are developed in badly sorted sediments that were deposited on top of the schists in the Pliocene-Pleistocene. Soils developed on the hilltops have a sandy loam texture and reach depths of 80-90 cm. Along the hillslopes the soils are very shallow (about 20 cm) and in the valley bottom the soil depth varies strongly in relation with the irregular surface of the underlying schists, with a maximum depth of about 90 cm and frequent vertically oriented schist rock outcrops. The texture of soils developed on the schists in the valley bottom is mainly silty loam, with many large stones and occasional pebble layers in the subsoil. Organic matter content in the upper layer of the soils is generally between 2 to 4 %. The soils are acid and poor in nutrients.

Cerdà et al. (1998) found macroporosity and water repellency in rainfall- runoff studies in the Dehesas. Different origins of macroporosity were observed in this study area: old root channels, ant burrows, worm burrows and even large burrows of mice were seen to cause underground rapid flow of water. Locally many cracks were visible at the soil surface in the dry period. Also the large soil heterogeneity along the upper rim and occurrence of pebble layers in the valley bottom may cause preferential flow.

5.4 Selection of parameters and site variables

Parameterisation of preferential flow
There are many different ways to parameterise tracer-infiltration patterns. Droogers et al. (1998) described macroporosity of 55 horizontal dye tracer profiles based on size (number of pores, total and individual area of macropores and perimeter derived parameters), several shape parameters

and spatial distribution of individual macropores. Perret et al. (1999) used the geometry and topology of macropores, hydraulic radius, tortuosity, numerical density and connectivity. Shipitalo and Butt (1999) however found that geometrical properties are unlikely to accurately predict water flow in macropores. Also Weiler (2001) found that the macropore flow capacity is not the limiting factor for infiltration or flow through macropores. So it seems more useful to search for parameters of the infiltration pattern, instead of using the macropore geometry to describe the degree of preferential flow.

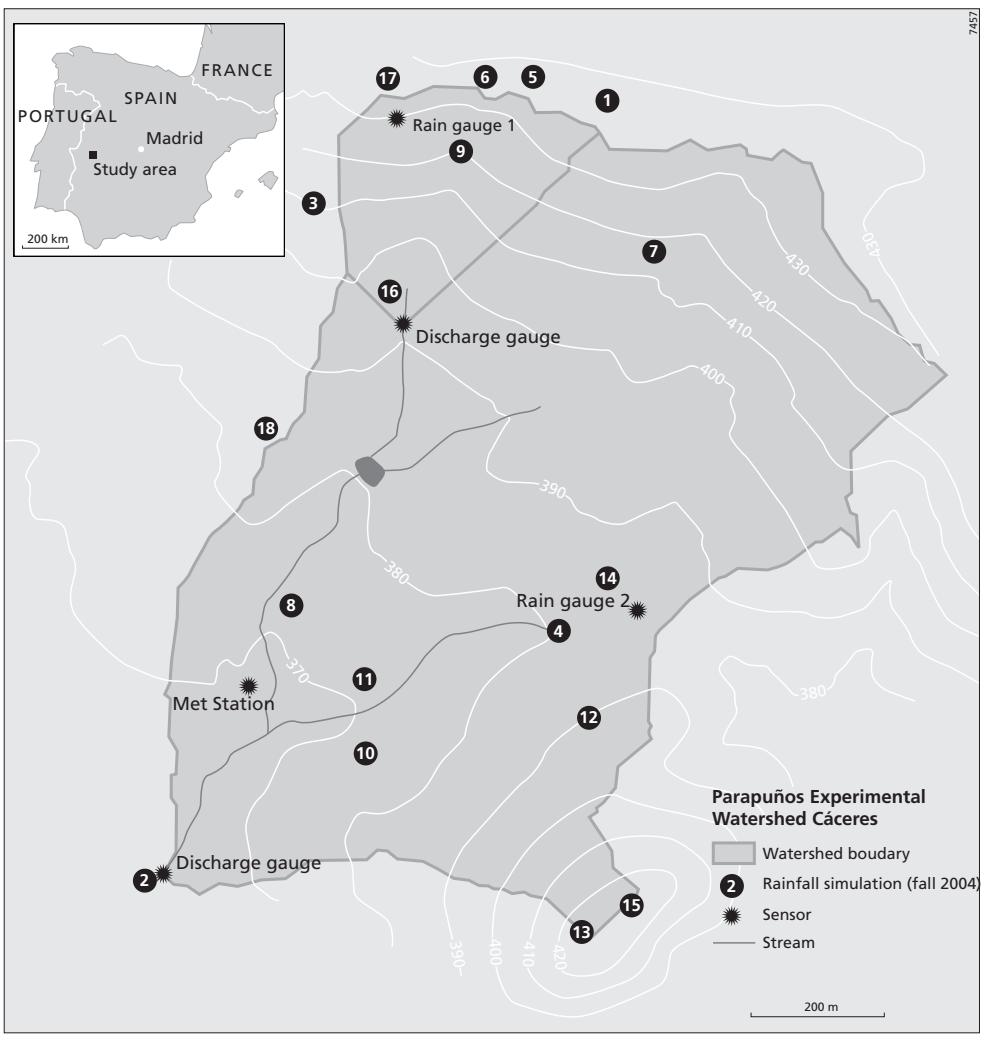

Figure 5.1 Locations of field measurements: black numbers show the 18 locations of tracer experiments and additional measurements of site characteristics. The dates of the tracer experiments can be found in Table 5.1.

Zehe and Flühler (2001) calculated the centre of mass for the individual columns in a soil profile. The average centre of mass and the standard deviation of the whole profile were subsequently used to describe the variability of infiltration into the soil. Weiler (2001) measured individual pore characteristics and macropore density but also made a classification of flow types based on the patterns of infiltration: he distinguished layers of uniform infiltration, heterogeneous infiltration and different degrees of interaction. Ohrstrom et al. (2002) used the amount of flow paths and diameter of preferential flow paths, maximum depth of stains, depth of 50% dye coverage, and horizontal semivariograms to test for random pattern of preferential flow paths.

There is no generally accepted parameter to quantify preferential flow; the previously described parameter sets all give information on the degree of preferential flow, by describing the variability of infiltration depth, flow types at different soil depths or spatial distribution and volume of macropores. However flow of water to macropores is strongly determined by the infiltration capacity of the matrix: once the infiltration capacity of the matrix is exceeded preferential flow becomes important. Therefore separation of the flow to uniform infiltration and to macropores is important. The relative influence of preferential flow for transport of water and solutes to deeper layers furthermore depends on the maximum depth of the macropores and the spatial distribution and volume. Also for the influence of preferential flow on the hydrology the maximum infiltration capacity of the soil, matrix and macropores together, is needed. It is concluded that to assess the influence of macropore flow the following information is necessary: the infiltration capacity of the soil matrix, the total infiltration capacity of the soil, the division of infiltration to matrix and macropores and the maximum depth of macropore flow.

Based on the above explanation the following parameters, which can be derived from infiltration patterns, were used:

- the uniform infiltration depth (depth at which the stained area strongly decreases; in general there is quite a clear uniform infiltration front visible): as long as the matrix infiltration capacity is not exceeded, infiltration into macropores will be low; therefore the matrix infiltration is important for initiation of macropore flow;
- maximum depth of blue stains: maximum penetration depth of water in the preferential flow paths;
- total stained area: though the total stained area is a biased estimate of the total infiltration (the distribution of the infiltrated water in the soil depends strongly on the soil physical parameters, so the increased soil moisture content is variable throughout the stained area), the total stained area is the best guess of total infiltration into the profiles: a profile with higher infiltration capacity will also have a higher conductivity and the stained area will therefore be larger;
- preferential flow fraction: the fraction of the total infiltration, which flows through the preferential flow paths. This is calculated as:

$$\text{PF-fr} = \text{PF-fr} = 1 - \frac{UniFr * 100}{TotStAr}$$

Where PF-fr is the preferential flow fraction (-), UniFr is the depth of the uniform front (cm), which is multiplied by the width of the profile (100 cm) and TotStAr is the total stained area (cm^2). The description of picture processing and analysis is described below in the methods

section. The calculation of all depth related parameters was done based on distance from the soil surface per picture column.

Site specific variables and preferential flow
In the past few years different attempts were made to link the degree of preferential flow to site specific variables: Zehe and Flühler (2001) found that the preferential flow was largest near the brook, as the main macroporosity in the area was created by earthworms, which prefer the higher water retention capacity and more stable water contents of the area near the brook. Ohrstrom et al. (2002) and Weiler and Naef (2003b) find that the higher the surface gradient, the lower the infiltration into macropores. According to Flury et al. (1994) there was no significant effect of initial soil water content on the flow pattern and maximum penetration depth. Structured soils did show a clearly deeper infiltration than unstructured soils. Devitt and Smith (2002) found that depth of moisture and tracer penetration were generally greater with higher water application rate, larger shrub size, wet antecedent conditions and uninterrupted spraying instead of several sequential events. They found that one of the main factors influencing maximum dye penetration was the presence or absence of a root system.

These results lead to a selection of the following site specific variables: soil type (indicated by texture), soil structure, vegetation, slope and position in the landscape. For the multiple regression analysis it is important that the measurements are all representative of the same scale, therefore the measurements of vegetation cover, texture, slope, stoniness, k-sat, bulk density, porosity and location (hilltop, hillslope, valley bottom) were taken at the local or plot scale. Three of these variables were nominal variables: the location in the landscape, texture class and the vegetation cover. The first were ordered from valley bottom to hill top and from coarse to fine texture. The nominal values for vegetation cover were assigned in order of increasing average values of the preferential flow parameters for the different vegetation classes.

5.5 Methods

Tracer experiments and preferential flow parameterisation
During a field campaign in the fall of 2004 rainfall simulations were performed at 18 plots with a dye tracer, to study the infiltration pattern of the water. The locations of these measurements were distributed throughout the catchment and in different soil and vegetation units (Figure 5.1). For the rainfall-tracer experiment a 1.5 by 1.5 m tent was used, with a nozzle (¼ HH SS 8W, from Spraying Systems Co) at 1.5 m height. The spatial rainfall distribution is important to prevent preferential flow occurrence due to high variation in rainfall. Tests on the spatial rainfall distribution on the soil surface showed the best results with a constant spraying pressure of 1.0 bar: this resulted in an average rainfall intensity of 44.0 mm/h and a standard deviation of 2.8 mm/h for the inner 1 m^2. This intensity is very high, but ensures the maximum infiltration to the matrix and preferential flow paths, which is needed to be able to compare potential degree of preferential flow among the locations. The intensity is comparable with the 10-minute maximum rainfall intensity with a 2-year return period, which is 48.8 mm/h (Schnabel et al., 1998).

For this study a solution of 4 g/l of the dye-tracer Brilliant Blue FCF (CI 42090, DYNEMIC PRODUCTS LTD, Ahmedabad, India) was used to visualize the infiltration pattern in the soil. Brilliant Blue FCF is often used for vadose zone hydrological studies (e.g. Ghodrati and Jury, 1990; Flury et al., 1994; Flury and Flühler, 1995; Perillo et al., 1998; Ketelsen and Meyer-Windel, 1999; German-Heins and Flury, 2000) because of the good visibility, low toxicity and weak adsorption in soils.

To obtain the infiltration profiles the method as described by Weiler (2001) was followed. One day after the tracer application three vertical soil profiles were prepared (at approximately 10-15 cm behind each other). The next day three horizontal profiles were prepared and photographed at different depths in the profile, depending on the layering in the soil and the pattern of infiltration seen on the vertical profiles. The ensemble of the soil profiles yielding an approximation of a 3D infiltration view (Figure 5.2). Of the 2.25 m^2 sprayed surface only the inner 1 m^2 was used for the preparation of the infiltration profiles, to avoid boundary effects. For the photography of the profiles a digital camera was used with a picture resolution of 2200*1700 pixels. The size of the photographed area slightly differed between the plots, but generally the full width of the photo was used for the profile width of 1 m. A frame of 1 m^2 (with a centimetre scale along two adjacent sides) was placed against the soil profiles as a reference for the geometrical correction of the photographs (which was done in Erdas Imagine 8.7). Then the stained areas were enhanced in the images by applying a colour filter (in Erdas Imagine 8.7) and classified (using both eCognition (2002) and Arcview). The three vertical infiltration profiles per location were used to calculate the stained area versus depth, an example is shown in Figure 5.3. There is in general some difference between the profile of a location, as in one profile there may be one preferential flow path, while the next may have hit on two preferential flow paths. Therefore the average stained area profiles of the three vertical profiles was used to calculate the preferential flow parameters per location. The preferential flow parameters were calculated

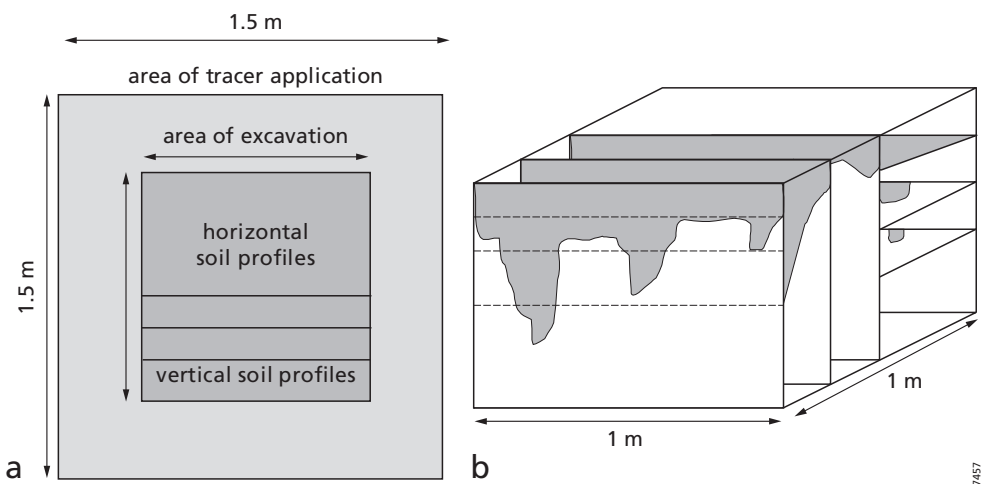

Figure 5.2 Position of the vertical and horizontal soil profiles a) within the tracer applied plot, b) relative to each other in the 3D excavated pit.

using the stained depth in relation to the soil surface per picture column. This is thought to be representative for the infiltration under 1m^2 surface area.

Site specific variables
At each of the locations of the rainfall experiments additional soil physical and landscape properties were measured. Ideally all the experiments should have been carried out under similar initial conditions. However the measurements started in September and carried on till the beginning of November. Halfway October the rain started and by the end of October there were a few large rainfall events, which completely wetted the soils. As the initial moisture content can influence the preferential flow, this was also taken into account in the multiple regression analysis, by including the initial moisture content as an independent variable for the regression.

For the multiple regression between preferentail flow parameters and site specific variables, the variables used should be representative of the same scale as the infiltration experiments. The bulk density and porosity measurements are performed on a small soil volume (Kopecki ring samples, 100cm^3) and there is a high spatial variability within the plot scale. This is why the average values of two ring samples from the surface layer (0-10 cm) were taken. The average plot scale values of these measurements however are variable at a much larger scale. The vegetation, stoniness and slope have a large variability at the plot scale, while on a larger scale the average vegetation cover and slope are more or less homogeneous for different parts of the catchement. The local slope was estimated using the average angle of the sprinkling tent with the soil surface, after the

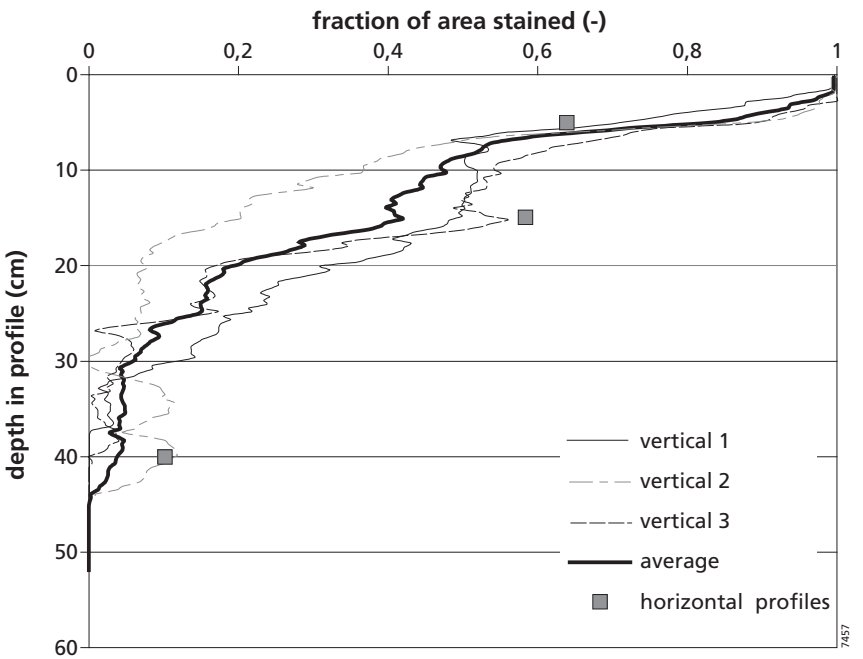

Figure 5.3 Stained area versus depth for three vertical profiles, horizontal profiles and average stained area versus depth, for location number 10.

tent was levelled for sprinkling. The surface stoniness was estimated as a fraction of soil surface coverage, using the stone counts from the soil survey, where stones were divided into different size-classes and calculating an average surface area for the stones in each class. For the multiple regression therefore the local vegetation and slope of the plot was used and not the average of the plot surroundings. The texture and location are variable at catchment scale, their variability at local scale is very low. Also the initial moisture conditions for the topsoil of the plots were measured, using gravimetric measurements, as this changed during the fieldwork period. Texture and initial moisture content were measured with Kopecki ring samples (100 cm^3).

Multiple regression analysis
All measured site characteristics potentially have an influence on preferential flow, however many are strongly correlated. This causes a multi-collinearity problem when multiple regression is used to find a relationship between a dependent and a set of independent variables. Therefore a limited number of site specific variables is chosen that can give a good prediction of the degree of preferential flow. However, due to the high correlation between the independent variables many alternative models will probably perform almost equally well. The variable selection is performed with a stepwise algorithm (using the Statistica software package (StatSoft Inc., 2004)).

The stepwise multiple regression method is well known for overestimating the strength in a relationship (e.g. Lark et al., 2007), especially when many input variables and few measurement cases are available. Therefore a bootstrap resampling procedure, with permutation and reallocation of the data (Davison and Hinkley, 1997), was used to assess the bias in the multiple regression with a small dataset and large amount of independent input variables. In other words it shows us how large R^2 could be obtained by chance from a stepwise regression procedure on a data set with the same size and distribution of variables, however randomised data. The dependent and independent variables were decoupled and each variable was randomly shuffled. The resulting dataset was completely randomised. This was repeated 60 times and the 95-percentile R^2 value of these randomised datasets was compared to the field data to get an approximate test of the 95% confidence level.

Subsequently a constrained multiple regression was performed with four pre-selected independent variables (location, vegetation, texture and slope) on each of the preferential flow parameters. These variables were chosen based on the results of the stepwise selection procedure, theoretical consideration and experimental evidence. Again the bootstrap resampling procedure was carried out to assess the power of the obtained R^2 values.

Mapping spatial distribution of preferential flow
Using the results of the multiple regression and maps of the distribution of the four fixed input variables in the study area (vegetation, texture, slope and location), a predictive map of preferential flow in the area is presented. The slope map was derived from an available DEM of the area and the location (hilltop, hillslope and valley bottom) map was based on the slope and DEM maps. The texture map was based on the textural analysis of 46 spatially distributed topsoil samples and visible changes of soil types at the soil surface, mapped during intensive field campaigns. The plot scale (1 m^2) vegetation is either tree, shrub, open space or sheep trail.

The pixels used for the catchment scale mapping are 25 m^2. Therefore the nominal value for the vegetation cover was estimated per pixel as the weighted sum of the nominal values of different vegetation types in the pixel. First of all the tree cover was derived from an aerial photograph, which was processed into a percentage of trees per pixel based on grey scale (black being full tree cover). The remaining fraction of the pixels (1-fraction of tree cover) is divided into grass, shrubs and sheep trail, based on eleven mapping units in the catchment with clearly different understory. The fraction of grass, shrubs and sheep trails were estimated for these eleven mapping units. Finally the fractions of all four vegetation covers per pixel were multiplied by the nominal value of the different vegetation classes and the sum of all four resulted in the map of average nominal value for the vegetation cover per pixel.

Table 5.1: Characteristics of the measurement locations in the field, ordered by location on the slope. For the soil physical measurements the average values of two Kopecki ring samples (100 cm^3) from the surface layer (0-10 cm) were taken.

Location (sprinkling date)	Texture	Vegetation	Initial moisture (cm^3/cm^3)	Bulk density (g/cm^3)	Porosity (m^3/m^3)	Surface Stoniness fraction (-)	Slope (%)
Hilltop							
1 (10 Sept)	loam	open space	0.02	1.56	0.33	0.04	1
5 (24 Sept)	sandy loam	tree cover	0.03	1.27	0.50	0.28	2
6 (27 Sept)	sandy loam	sheep trails	0.02	1.58	0.37	0.18	2
13 (22 Oct)	loamy sand	open space	0.25	1.31	0.48	0.41	1
15 (29 Oct)	loamy sand	tree cover	0.35	– [a]	– [a]	0.77	1
17 (5 Nov)	sandy loam	sheep trails	0.35	1.58	0.32	0.37	1
Hillslope							
3 (16 Sept)	sandy loam	shrub cover	0.05	1.49	0.40	0.03	4
7 (1 Oct)	loam	open space	0.02	1.53	0.37	0.27	7
9 (8 Oct)	loam	tree cover	0.03	1.41	0.46	0.09	8
12 (19 Oct)	silt loam	sheep trails	0.17	1.47	0.45	0.07	7
16 (1 Nov)	silt loam	shrub cover	0.36	1.63	0.40	0.02	5
18 (8 Nov)	silt loam	tree cover	0.21	1.02	0.56	0.00	2
Valley Bottom							
2 (13 Sept)	silt loam	open space	0.03	1.57	0.39	0.02	5
4 (20 Sept)	silt loam	sheep trails	0.05	1.41	0.47	0.04	1
8 (4 Oct)	silt loam	tree cover	0.05	1.06	0.59	0.01	1
10 (11 Oct)	silt loam	shrub cover	0.06	1.29	0.50	0.04	2
11 (14 Oct)	silt loam	sheep trails	0.03	1.43	0.49	0.01	1
14 (25 Oct)	silt loam	shrub cover	0.40	1.63	0.40	0.04	1

a For location 15 it was impossible to take a representative sample of the topsoil, as the soil was extremely loose and kept falling apart while taking the samples. For the regression analysis both mean substitution as well as casewise missing data deletion was applied. In both ways the bulk density and porosity appeared not to be important variables.

5.6 Results

Site characteristics and preferential flow
The measurement results of soil texture, vegetation type on the simulation plots, soil physical properties (bulk density, porosity), surface stoniness, slope and location in the landscape (hill top, slope, valley bottom) are given in Table 5.1.

The rainfall simulations with Brilliant Blue tracer resulted in three vertical infiltration profiles for each of the 18 locations. Per location one example of a vertical infiltration profile is shown in Figure 5.4. During the rainfall simulations ponding and subsequently runoff occurred at most locations. At three locations (1, 13 and 15) all the water infiltrated, these locations were all on the hilltops where the permeability of the soils is higher. At most locations preferential flow occurs. The only locations where the infiltration may be described as a uniform front are locations 1 and 7. At the other locations a clear distinction can be made between the shallow

Table 5.2: Infiltration pattern characteristics: maximum depth of stained area (MaxD), uniform infiltration depth (Uni Fr, depth of minimum 80 % stained area), total stained area (TotStA), fraction preferential flow of total stained area (PF-fr). The parameters were calculated using stained depth relative to soil surface per column of the picture.

Location number	MaxD (cm)	Uni Fr (cm)	TotStA (cm^2)	PF-fr (-)
Hill Top				
1	56.4	21.0	2874	0.27
5	76.4	6.0	2126	0.72
6	81.6	16.0	3029	0.47
13	76.4	2.4	3399	0.93
15	76.4	5.2	3833	0.86
17	66.4	2.6	2621	0.90
Hillslope				
3	40.0	4.6	1693	0.73
7	25.2	13.2	1666	0.21
9	41.2	6.5	1425	0.54
12	58.4	1.8	835	0.78
16	25.6	3.2	731	0.56
18	46.8	1.7	826	0.79
Valley Bottom				
2	40.4	3.0	1484	0.80
4	24.4	3.7	1199	0.69
8	49.2	3.0	2277	0.87
10	44.4	4.9	1296	0.62
11	18.4	2.4	597	0.60
14	38.2	8.8	1422	0.38

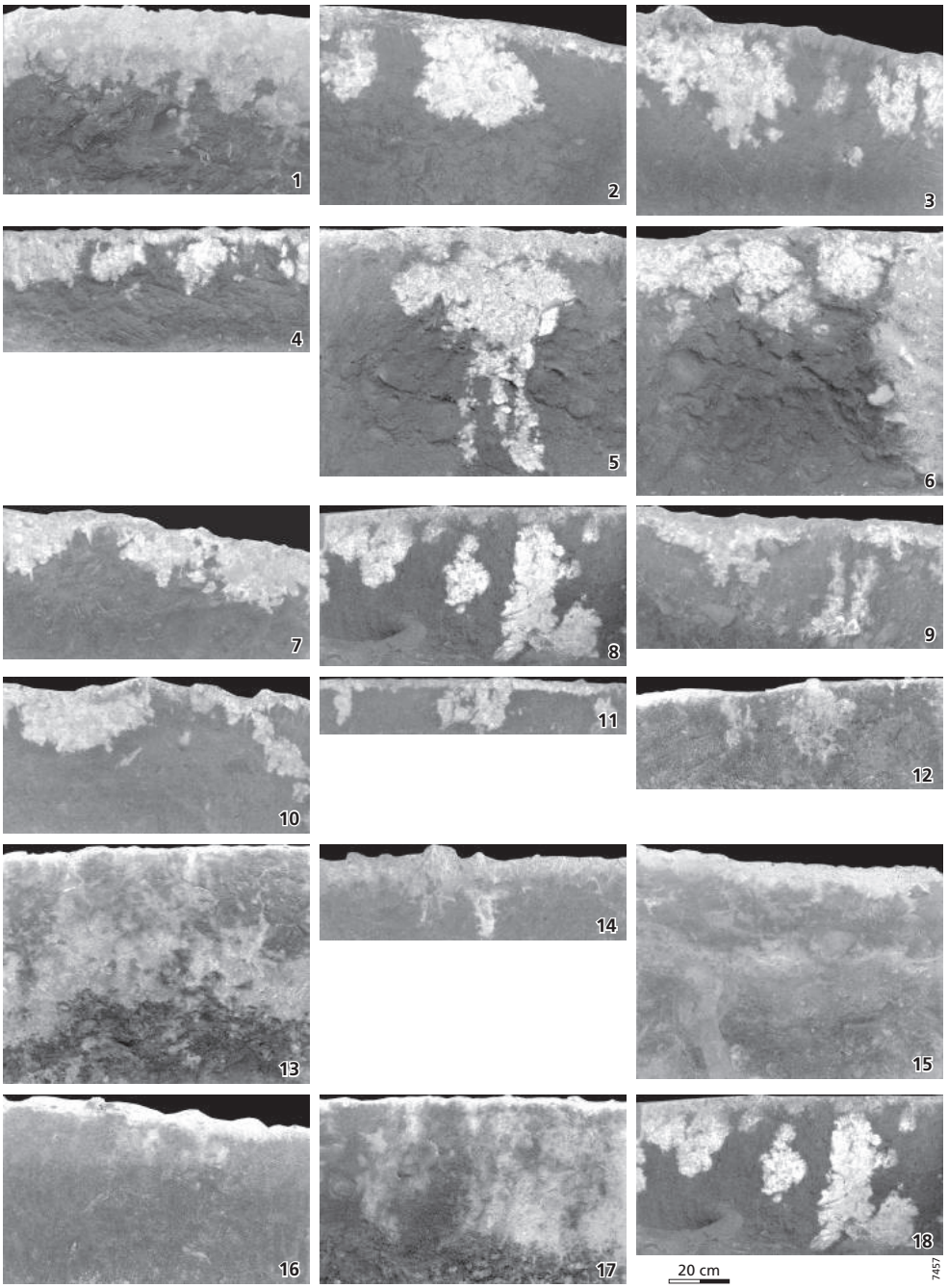
1
2
3
4
5
6
7
8
9
10
11
12
13
14
15
16
17
18
20 cm
7457

➪ *Figure* 5.4 Examples of vertical tracer infiltration profiles, one profile per rainfall simulation, for locations see Figure 5.1. All profile photographs have been geometrically corrected using a $1m^2$ frame, which was placed on the profiles. Light areas are dye stained. The preferential flow parameters were calculated using stained depth relative to soil surface per picture column.

uniform infiltration front (defined as depth of minimally 80 % stained area) and the preferential flow paths extending below this front. The maximum stained depth is generally much larger than the depth of uniform infiltration, which indicates the initiation of preferential flow (Table 5.2). In general the depth of the infiltration front and the maximum depth of the stained area are both largest on the hilltops. While the average infiltration front and maximum depths are lowest in the valley bottom, the average total stained area is higher than along the hillslope, which signifies that the width of the stained areas is lower along the hillslope. The preferential flow-fraction of the total stained area was largest on the hilltop followed by the valley bottom and smallest along the hillslopes (Table 5.2).

At locations 13 and 15 (located on the small hill in the south east of the catchment) all of the water infiltrated, but the infiltration front was thin (2.4 cm, respectively 5.2 cm). Most of the infiltration followed preferential paths (worm holes and decayed root channels) to a deeper layer, where the water stagnated on top of a clayey matrix at about 40 – 45 cm depth. Some of the water was transported through this clay layer, along macropores and was found to flow out of the vertical profiles at 75 cm depth.

At three locations (2, 11 and 16) the water was seen to flow laterally along mouse holes. The soil matrix at these locations is very fine (silty loam) and has a low saturated conductivity, possibly indicating that the supply to the mouse holes is large and infiltration from mouse holes into the matrix is low. At locations 12 and 18 the vertical profiles were dug some way down into the shallow weathered schist. Here stains and tree roots were found to penetrate at least 20 cm into the weathered schist layer.

During the rainfall simulations, stemflow along the stems of the shrub *Retama sphaerocarpa* was observed. The water reaching the base of the plant can infiltrate directly and be available to the plant, as is found on some of the profiles (location 3, 10 and 14), where the stained areas were clearly located around the base and the roots of the shrubs.

Multiple regression analysis

The results of the stepwise multiple regression analyses indicated R^2 values between 56% to 67% for the different preferential flow parameters (Table 5.3a). The location is selected as input variable with good predictive value for all the preferential flow parameters. Vegetation and texture are also important spatial variables for preferential flow prediction. The other variables with good predictive value are slope and initial moisture content for the uniform infiltration front and slope and stoniness for the total stained area. For location 15 it was impossible to take a representative sample of the topsoil, as the soil was extremely loose and kept falling apart while taking the samples. For the regression analysis both mean substitution as well as casewise missing data deletion were used. With both methods the bulk density and porosity appeared not to be important variables.

Table: 5.3a Results of the stepwise multiple regression analysis on preferential flow parameters and site characteristics (n=18 in all cases), the p-value (this is however calculated without taking into account the stepwise procedure of deleting input variables).

Dependent parameters	Input variables	Regression coefficients	Adjusted R^2 (p-value) RMSE
Uniform infiltration	Vegetation	-1.704	0.56
	Texture	-4.403	(0.009)
	Location	5.174	3.6
	Slope	-0.866	
	Initial moisture	-11.125	
		Intercept: 14,293	
Maximum depth	Vegetation	3.213	0.67
	Texture	8.672	(0.000)
	Location	12.810	11.3
		Intercept: -4.55	
Stained area	Stoniness	894.8	0.66
	Slope	56.62	(0.000)
	Location	212.2	559
		Intercept: 411.4	
PF-fr	Vegetation	0.072	0.57
	Texture	0.192	(0.002)
	Location	-0.104	0.14
		Intercept: 0.235	

Table 5.3b: Results of the stepwise multiple regression analysis on preferential flow parameters and four fixed site variables (vegetation, texture, slope, location)

Dependent parameters	Input variables	Regression coefficients	Adjusted R^2 (p-value) and RMSE
Uniform infiltration	Vegetation	-1.39	0.50
	Texture	-5.06	(0.01)
	Slope	-0.82	3.8
	Location	5.07	
		Intercept: 13.49	
Maximum depth	Vegetation	3.13	0.66
	Texture	7.73	(0.001)
	Slope	-0.63	11.6
	Location	13.15	
		Intercept: -1.05	
Stained area	Vegetation	11.85	0.53
	Texture	203.16	(0.007)
	Slope	-109.78	665
	Location	667.69	
		Intercept: 339.89	
PF-fr	Vegetation	0.074	0.56
	Texture	0.21	(0.004)
	Slope	0.015	0.14
	Location	-0.111	
		Intercept: 0.152	

The randomised datasets resulted in 95-percentile R^2 values for the uniform infiltration front and the preferential flow index which were slightly higher than the R^2 values of the field data. For the maximum depth and the stained area the 95-percentile of the randomised datasets gave significantly lower R^2 values.

The multiple regression with four pre-selected input variables (location, vegetation, texture and slope) decreases the R^2 values for the different preferential flow parameters (50% to 66%). However the decrease in R^2 values of the randomised datasets is much larger.

Spatial distribution of preferential flow parameters
The maps of the spatial distribution of vegetation, texture, slope and location are shown in Figure 5.5. These maps are used together with the linear regression models to calculate the catchment scale maps of spatial distribution of the four preferential flow parameters (see Figure 5.6).

5.7 Discussion

A first evaluation of the preferential flow parameters indicates some spatial patterns, which seem to be related to site characteristics. The statistical relationships found between the preferential flow parameters and the site characteristics are modest, which may be a result of the statistical and field methods used or the complex relationships between the variables and processes in the field. The methods are discussed first. The relationships found are thereafter explained and compared to other research results. Also the use of these results for catchment scale mapping of preferential flow is discussed.

Rainfall simulations
Multiple regression analysis between the site characteristics and the preferential flow parameters yield modest results. The vegetation, texture and location are found as important variables for the prediction of preferential flow parameters. Their treatment as nominal variables may be one of the reasons for the modest statistical relationships, as the basis for appointing the nominal values is not very strong. Vegetation and location are difficult to quantify, texture however can be replaced by the sand-, silt- and clay-content. Also the ratio's of sand: silt and silt: clay-content may be used, together they give the full information on sand, silt and clay percentages. In a preliminary study these possibilities were investigated. As they lead to additional input variables and little improvement – only the prediction of the total stained area significantly improved – they were not considered in the further study. Even though the use of nominal variables is problematic, these are pointed out as the variables with largest influence on preferential flow variability, thereby justifying their inclusion in the multiple regression. This does show that research into improvements in the discretisation or quantification of these variables may be valuable.

Andreini and Steenhuis (1990) and Perillo et al. (1998) showed that the extent of retardation of the Brilliant Blue front compared to the water front is related to the water velocity: the larger the water velocity, the smaller the retardation factor. Furthermore, sorption of Brilliant Blue FCF was found to be positively correlated with clay content and negatively correlated with organic

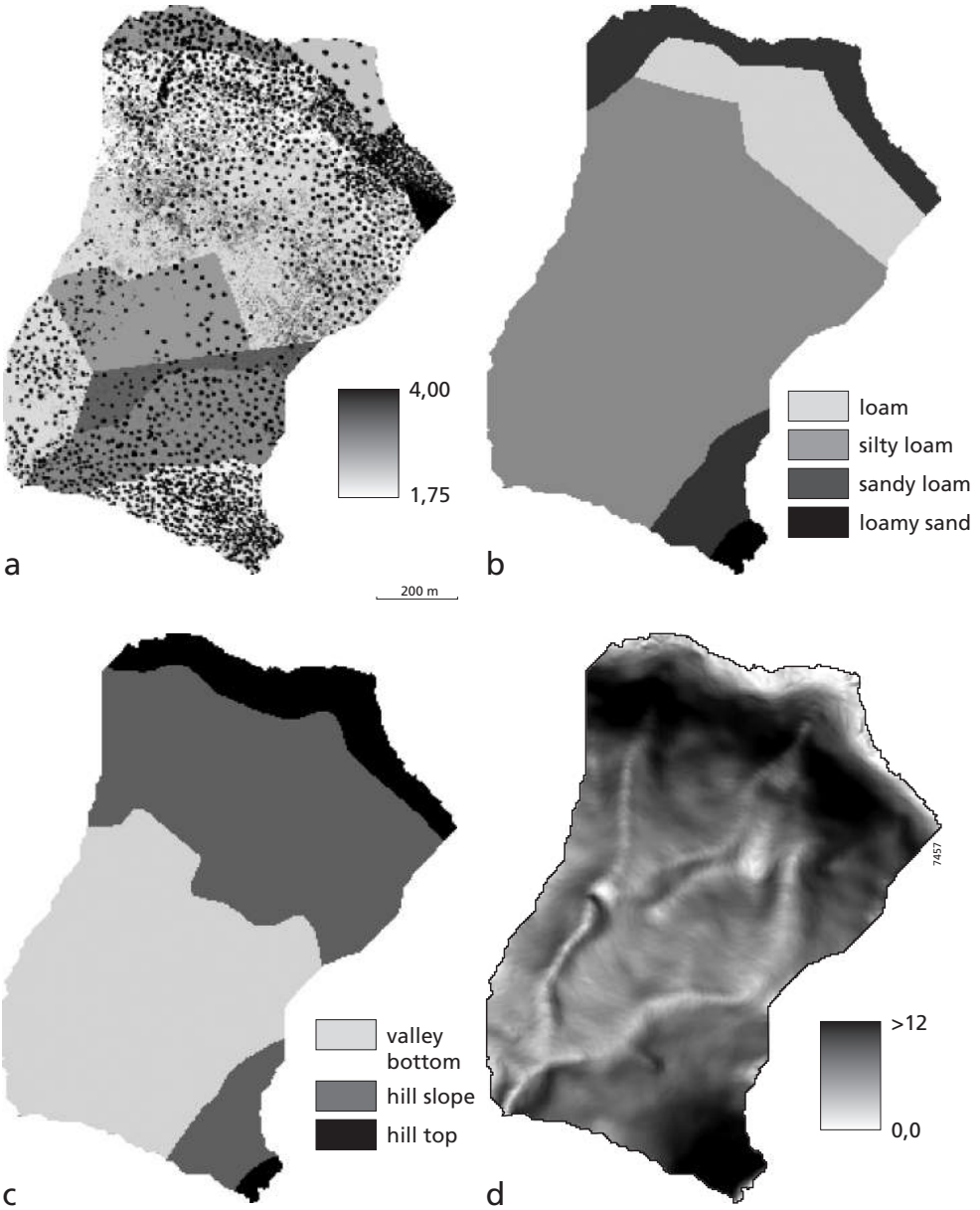

Figure 5.5: Maps of spatial distribution of site specific variables: a) vegetation, b) texture, c) location and d) slope.

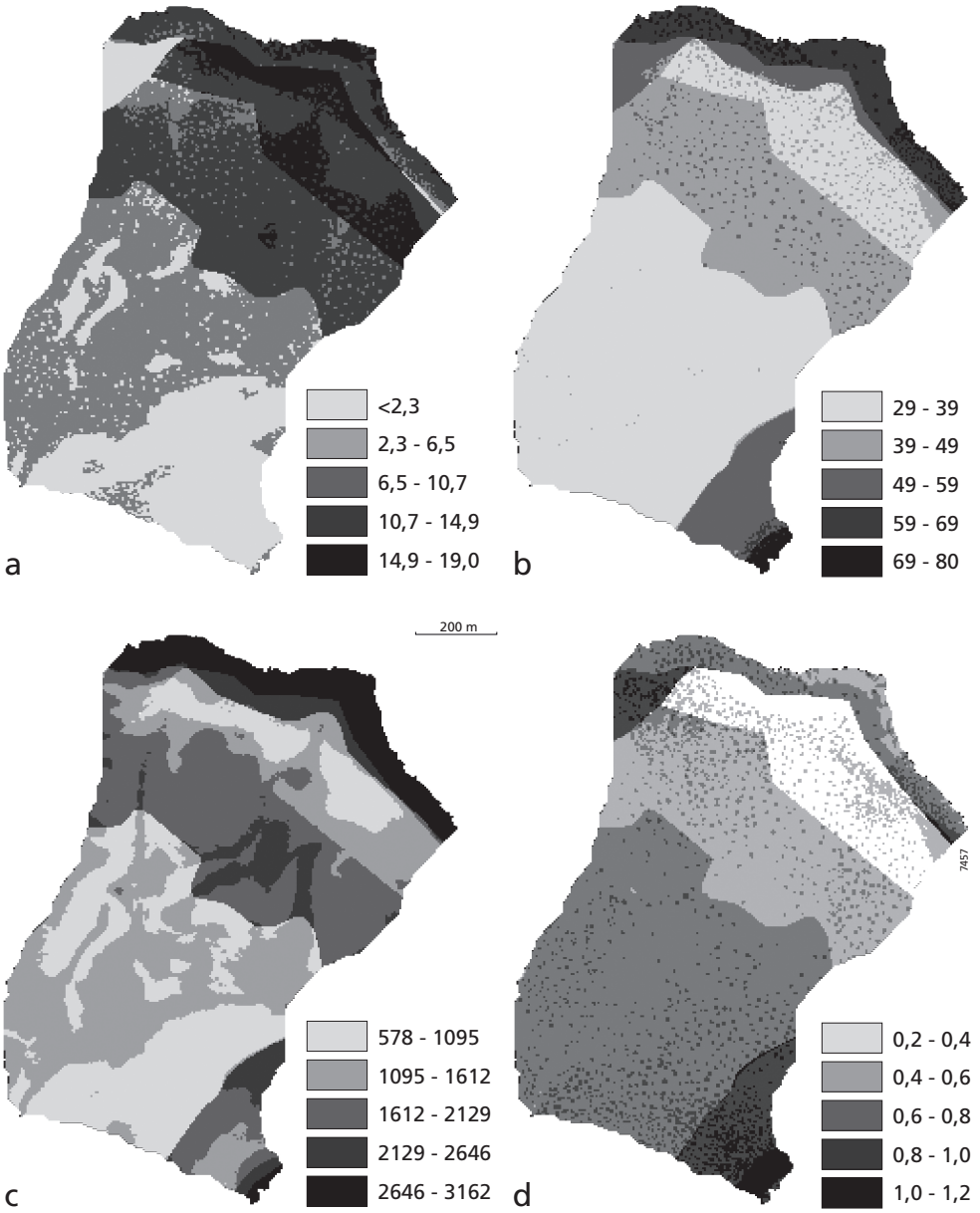

Figure 5.6 Predictive maps of spatial distribution of the four preferential flow parameters: a) uniform front (cm), b) maximum infiltration depth (cm), c) total stained area (cm^2), d) preferential flow index (-), as resulting from simple linear multiple regression results and the maps of spatial distribution of texture, vegetation, slope and location.

matter content (Ketelsen and Meyer-Windel, 1999), which reduces the eligibility of Brilliant Blue as a tracer for water flow paths. In this study area the clay and organic matter content were generally low. When excavating the soil profiles attention was paid to a possible delay in the dye-front with regard to the waterfront. The water front was occasionally seen a little further advanced than the dye-front, but this was generally in the range of a few millimetres to maximally one centimetre, which leads to the conclusion that the relative differences in infiltration pattern in the catchment are hardly influenced by dye-retardation.

Different opinions exist as to the influence of initial moisture content on the initiation of macropore flow. Beven and Germann (1982) expected that the number and size of pores in which flow would be channelled would depend on the initial soil moisture content. Flury et al. (1994) concluded from rainfall simulations under different initial conditions that initial moisture content had little or no significant influence on the type of flow. But others (e.g. Van Stiphout et al., 1987; Bouma, 1991; Trojan and Linden,1992; Feyen, 1998; Vilholth et al., 1998; Schwartz et al., 1999; Zehe and Flühler, 2001) do find an influence of initial soil moisture content on macropore flow initiation, as the initial water content influences the infiltration capacity of the soil matrix. The initial conditions of the soil changed during the fieldwork. The soil was completely dry till the ninth experiment. Thereafter a number of large rain events occurred. The profiles from location 10 onwards may be influenced by the wetter initial conditions, but this is not apparent from the results, no significant correlation was found between the initial moisture content and the preferential flow parameters. In the stepwise multiple regression analysis the initial moisture content only played a slight role in the explanation of variability in uniform infiltration front.

The results of the tracer-experiments are strongly dependent on the experimental conditions. A longer rainfall duration with a lower intensity, for instance, will result in different degrees of uniform infiltration and preferential flow. The results of the experiments may be comparable amongst each other, but direct comparison of the preferential flow parameters with other studies should not be done. The results of the multiple regression analysis, however, leading to texture, location, slope and vegetation as important variables for the indication of preferential flow are similar to results found in previous studies, as discussed in the section on selected site variables.

The stained area of the infiltration profiles is an indication of infiltrated volume, which should be interpreted as relative rather than absolute differences in infiltration amount and depth between the locations. It should not be confused with water content or dye concentrations.

Multiple regression analysis

The modest statistical results obtained may be partly due to the use of simple linear relationships. Modelling of non-linear relationships was not considered in the multiple regression analysis. Although these may be more realistic than linear relationships, with small data sets and such complex processes they are hard to infer.

A bootstrap procedure should usually be carried out with a large number of resampling replicates (say, n>1000). The limited number of replicates used here (n=60) can only provide rough initial estimates of critical (95-percentile) R^2 values that can be attributed to chance. A comparison

Table 5.4a Comparison of R2 values of stepwise multiple regressions of measurement data and randomised data sets

Dependent parameters	Adjusted R^2			
	Measurement data	Randomised datasets		
		Average	stdev	95-percentile
Uniform infiltration	0.56	0.19	0.23	0.57
Maximum depth	0.67	0.20	0.14	0.49
Stained area	0.66	0.23	0.14	0.49
PF-index	0.57	0.21	0.16	0.54

Table 5.4b Comparison of R2 values of multiple regressions with four input variables (texture, vegetation, slope, location) and randomised data sets

Dependent parameters	Adjusted R^2			
	Measurement data	Randomised datasets		
		Average	stdev	95-percentile
Uniform infiltration	0.50	0.04	0.21	0.39
Maximum depth	0.66	0.04	0.17	0.35
Stained area	0.53	0.00	0.16	0.30
PF-index	0.56	0.02	0.18	0.40

between the results of these 60 replicates and a random sample of 40 of the total amount of replicates shows almost equal results, this shows that there is not much gain in enlarging the number of replicates.

Though at first sight the R^2 values of the stepwise multiple regression seem acceptable, the bootstrap tests point out that part of the R^2 values may be attributed to chance (Table 5.4a). The multiple regression with four pre-selected site characteristics gives lower R^2 values, but the difference between R^2 values of the field data and the 95-percentile of the randomised datasets is larger (Table 5.4b). This means an increase in statistical power of the results, which is the result of eliminating the bias produced due to stepwise selection from a large number of variables compared to the limited number of cases.

In this study a comparison of the multiple regression results of stepwise selected variables with a set of pre-selected variables is performed. Lark et al. (2007) propose an alternative to the stepwise method of variable selection for multiple regression, which may be used to further improve our results in future research.

Selected site variables

The four selected site variables with the best predictive value for the preferential flow parameters are: vegetation, texture, slope and location. In the study area macroporosity is thought to be the main reason for preferential flow. The vegetation cover is an important source of macroporosity, as preferential flow can occur along fresh and decayed root channels. Also the bioactivity may

Table 5.5: Comparison between the prediction errors (difference between predictions and measurements for the eighteen measurement locations) while using the multiple regression results or inverse distance weighted spatial interpolation.

Prediction error using	**Average prediction error (st dev)**			
	Uniform infiltration	Maximum Depth	StArea	PF-fraction
Regression results	2.4 (2.3)	8.6 (4.9)	485 (297)	0.10 (0.06)
Inverse distance weighted spatial interpolation	3.4 (3.1)	13.4 (8.8)	625 (381)	0.15 (0.09)

be different underneath different soil cover types. Vegetation was also indicated as an important factor for the occurrence of preferential flow by Devitt and Smith (2002). Specifically for Dehesa landscapes Joffre and Rambal (1988) found macroporosity favourable to infiltration and redistribution of water under trees. Cerdá *et al*. (1998) shows examples of infiltration patterns around the roots of shrubs. Soil texture and location are strongly related and therefore the influence of one or the other is not easily separated, but from the multiple regressions they both appear to add significant explanatory value for the different infiltration parameters. A coarser texture increases the infiltration capacity of the matrix and also the potential influence of preferential flow is larger. Though the infiltration capacity of the matrix will not be exceeded as frequently, once this is the case the preferential flow is apparently also larger than in the finer soil texture (in the rainfall simulations extreme conditions were used to ensure full flow to both matrix as well as preferential flow paths). As described by Zehe and Flühler (2001) the location in the catchment (hill top, hillslope and valley bottom) determines the hydrological regime, which may make part of the area favourable to bio activity. In this case it was mainly the hill top which is much more favourable to preferential flow than the hillslope or valley bottom. The higher the slope, the lower the infiltration both into matrix as well as preferential flow paths, this is in accordance with the results found by Léonard et al. (1999), Weiler and Naef (2003b) and Ohrstrom et al. (2002). This can be expected as surface runoff increases with increasing slope, thereby decreasing ponding on the soil profile.

The measurements were all performed in a manner to represent the plot scale value for the site variables. The vegetation and slope represent a high local variability, while the texture and location are representative of the large scale variability. This leads to the conclusion that there is both large scale as well as local variability in the preferential flow parameters, which is covered by the use of these four input parameters. This may also be used to differentiate the local variability from the variability at the scale of the catchment.

Mapping spatial distribution of preferential flow

The maps of the spatial distribution of infiltration parameters (Figure 5.6) should be seen as a first estimate and an example for further study. These maps have now been produced on a pixel base. For distributed hydrological modelling, the user will be more interested in information on preferential flow for sub-areas in stead of pixel based, as the connectivity is very important for the impact of preferential flow at larger scale. The trees now stick out in the pixel based approach,

as trees were directly taken from the aerial photograph instead of using average tree cover per area. Still it is clearly seen in Figure 5.6 that the pixel based maps of infiltration parameters can be used to separate the catchment into a number of sub-areas with different infiltration patterns. Also for future modelling practices, information on the regression error and the subsequent prediction uncertainty should be considered in the predictive modelling. The prediction errors of the multiple regression analysis were compared to the prediction error resulting from calculations of the preferential flow parameters for each location using the measurements of surrounding locations and an inverse distance weighted spatial interpolation (Table 5.5). Both the average as well as the standard deviation of the error is smaller when the equations from the multiple regression analysis are used, which shows the multiple regression improves general prediction and the individual prediction errors are less extreme.

5.8 Conclusions

The aim of this research was to determine soil and landscape characteristics which can be used to produce indicative maps for the occurrence of preferential flow in a small catchment. The infiltration profiles of high intensity rainfall simulations show that preferential flow paths are potentially present almost everywhere in the investigated area and are spatially variable. Both theory and the infiltration tests performed for this research confirm that this variability is related to site characteristics. The deepest uniform infiltration and preferential flow paths generally occur on the hill tops (in the rather heterogeneous sandy loam soils) and the shallowest in the valley bottom (in the silty loam soils).

The stepwise multiple regression results in strongly biased R^2 values, due to the high number of input variables and few cases. A constrained multiple regression with four pre-selected input variables (texture, vegetation, slope and location) gives lower but stronger R^2 values. These four input variables are selected based on theory and multiple regression results. The use of these four input parameters explains preferential flow variability at different scales, as texture and location are representative of large scale variability while vegetation and slope are representative of local variability.

The preferential flow in this study area is caused by macroporosity. The vegetation mainly influences the bioactivity in the soil, through rooting and favourable conditions for soil fauna. The texture and location (hill top, hillslope or valley bottom) influence the hydrological regime, which may also increase or decrease bioactivity and thereby macroporosity. And finally the slope influences ponding capacity or runoff generation, which is important for the infiltration into both matrix as well as macropores. The constrained multiple regression using these four variables results in R^2 values of 50% to 66% for the different preferential flow parameters used (uniform infiltration front, maximum depth, stained area and preferential flow fraction).

The spatial maps of vegetation, texture, slope and location were used to produce some example maps of spatial distribution of preferential flow parameters for the studied catchment. These maps show that the area can be subdivided into a few units with different expected infiltration patterns.

6 Use of dye-tracer infiltration patterns for the physically based parameterization of macropore flow

Based on: Van Schaik, N.L.M.B., Hendriks, R.F.A., and van Dam, J.C., accepted. Use of dye-tracer infiltration patterns for the physically based parameterization of macropore flow. Vadose Zone Journal.

6.1 Abstract

Preferential flow is known to influence infiltration, soil moisture content distribution, groundwater response and runoff generation. Various model concepts are used to simulate preferential flow. Preferential flow parameters are often determined by indirect optimization using outflow or discharge measurements, thereby providing limited insight into model performance concerning soil moisture distribution. In this study we used a physically based macropore concept, embedded in the SWAP model, in combination with dye infiltration patterns to parameterize macropore infiltration for three locations in a catchment: hill top, hillslope and valley bottom. The model with the calibrated macropore parameters was applied and validated under natural field conditions, using detailed data of soil moisture content, rainfall and discharge.

The results show that the macropore model parameters can be optimized well to reproduce the dye-tracer infiltration patterns. The simulations of the dye patterns show much better results when macropore flow is included. However, using the tracer infiltration patterns, the optimized maximum depth of macropores depends completely on the maximum depth of stained area, while the macropores are known to extend deeper into the soil. Therefore, for long term simulations the wetting of deeper layers is too slow for both the simulations with as well as without macropores. Runoff production was better simulated with macropores. For the simulations without macropores, the soil saturated conductivity was increased; despite the resulting increased infiltration into the soil matrix, runoff generation remained far too high.

6.2 Introduction

Flow of water through the vadose zone determines the partitioning of water among various components of the hydrologic cycle: infiltration, runoff, soil moisture storage, evapotranspiration and groundwater recharge. Preferential flow is the rapid flow of water and solutes along certain pathways bypassing a large part of the porous media. Preferential flow occurring in the vadose zone directly affects these components of the hydrological cycle (Beven and Germann, 1982; Doerr et al., 2000; Sidle et al., 2001). The soil moisture distribution influences the moisture availability for different plant layers (which have different rooting depths). As preferential flow may strongly influence the flow paths and travel time of solutes through a soil, it is

generally recognized as one of the most important processes which affect solute transport and contamination (Edwards et al, 1993).

Major difficulties in modeling the impact of preferential flow are the measurement of quantitative indicators for preferential flow and conversion of measurements to input parameters for hydrological models (VanClooster et al, 2000; Herbst et al., 2005; Larsbo and Jarvis, 2005). The parameterization of preferential flow models is often performed through inverse modeling using groundwater level measurements and water or solute drainage data (Herbst et al., 2005; Christiansen et al., 2004). Even though models may contain the relevant detailed processes, model performance concerning these processes cannot be adequately tested without information on soil moisture distribution and fluxes through different soil domains. Measurement techniques for spatial flux measurements based on variable suction plates and drop counting are under development (Bloem, 2008; Mertens et al., 2008) but are not yet applicable for field studies.

Dye infiltration profiles are often used to describe and quantify preferential flow patterns (Ghodrati and Jury, 1990; Flury et al., 1994; Forrer et al., 2000; Zehe and Flühler, 2001; Ohrstrom et al. 2002). Different quantifications of the infiltration patterns are used to describe the degree of preferential flow or to describe the type of flow (Droogers et al., 1998; Perret et al. 1999; Zehe and Fluhler, 2001; Weiler, 2001; Ohrstrom et al. 2002). These quantifications use either the geometry of individual macropores or depth and shape parameters of the infiltration patterns. Tracer infiltration profiles give a lot of additional information on how water and solutes move in the soil profile. Therefore they may help in the choice of preferential flow models and in the parameterization of these models.

The occurrence of preferential flow is widely recognized to be threshold dependent (Tromp van Meerveld and McDonnell, 2006). An important threshold for macropore flow initiation is the infiltration capacity of the matrix: as long as the matrix infiltration capacity is not reached, the net precipitation will infiltrate mainly into the matrix, but as soon as the infiltration capacity is exceeded the water will start ponding and infiltration to macropores will become important (Bronstert and Plate, 1997). Therefore the separation of matrix and macropore flow is important for predicting the impact of macropore flow on hydrology and water quality and also for the determination of preferential flow parameters. The interaction between macropores and matrix determines the influence of macropore flow at larger spatial scales, as this interaction strongly determines residence time in the macropores and thus travel time and distance.

This study focuses on the use of field measurements of infiltration patterns for the parameterization of macropores in the physically based agrohydrological SWAP (Soil Water Atmosphere Plant) model (Kroes et al., 2008). Dye-tracer infiltration profiles and inverse modeling with a new macropore routine in the SWAP (Kroes et al., 2008) are used to derive the separate matrix and macropore flow properties. The aim of this modeling exercise is twofold: a) to investigate whether dye-tracer infiltration patterns are suitable for the parameterization of macropore flow and b) to evaluate the use of the resulting macropore parameter set in SWAP for a natural field situation and compare this to modeling when macropore flow is neglected. For this purpose three locations with different soil texture and initial soil moisture conditions were chosen from a semi-arid study area in the Spanish Dehesas.

6.3 Measurements and methods

The field data used for this research were gathered in the semi-arid Parapuños watershed in the Extremadura, Spain. This is a 1 km2 catchment, which has been monitored since the year 2000 by the University of Extremadura, Cáceres. The catchment is representative for the Spanish Dehesas, which is the typical agro-silvo-pastoral land use, covering a large part of the south western Iberian Peninsula (Cerdá et al., 1998) and similar land use is found in other Mediterranean countries. Due to rapid changes in management of the Dehesas during the second half of the 20th century, there is often lack of tree regrowth and many Dehesas are prone to soil erosion, soil degradation and increased runoff (Schnabel and Ferreira, 2004). Therefore in the hydrological simulations for this semi-arid area the soil moisture distribution and runoff generation are important factors. Joffre and Rambal (1988) and Cerdá et al. (1998) studied the occurrence of macroporosity in the Dehesa landscape. The main origin of preferential flow observed in the study area is macroporosity, which was caused by bio-activity. Water drop penetration time (Letey, 1969) tests were performed throughout the area, and revealed no signs of water repellency.

Thanks to the pronounced relief and the shallow soils, the spatial boundaries of the catchment can be estimated reasonably well based on the topography. The bottom boundary of the catchment is an almost impervious material: greywackes and schists (of Precambrian to Upper Carboniferous origin). Seepage of water into weathered cracks or root holes (which have been found to penetrate partly into the bedrock) is assumed to be very little and to be mainly a temporary sink, as this can be withdrawn by trees for evapotranspiration during the dry summer. The catchment dries out completely during the summer. Therefore an annual water balance can be made up easily, as total precipitation must be equal to the annual total discharge and evapotranspiration (Ceballos and Schnabel, 1998).

In the Parapuños watershed meteorological data (temperature, humidity, net radiance, global radiance, wind speed and – direction), rainfall, catchment discharge and sediment transport are measured every 5 minutes as part of an ongoing measurement campaign. Additional measurements of dye-tracer rainfall-infiltration experiments, TDR sensors and piezometers (Figure 6.1) were performed for this study.

Throughout the catchment 18 dye-tracer rainfall experiments were performed (see Chapter 3 and Chapter 5). Dye stained water (4 g/l Brilliant Blue FCF (CI 42090)) was applied on 1.5 by 1.5 m plots with a rainfall intensity of 44 mm/h, which was continued for a full hour. This extremely high rainfall intensity was used, to ensure that maximum infiltration to both matrix as well as macropores occurs at all the locations. Surface runoff was produced on all the experimental plots. The inner $1m^2$ soil under the irrigated area was then excavated to study the wetting patterns, using three vertical and three to five horizontal profiles per plot (depending on the wetting patterns and depth). Photographs were taken of each infiltration profile. These were subsequently geometrically corrected, color enhanced and classified (Figure 6.2). The $infiltration patterns were plotted as a fraction of dye stained area with depth. The average curve of the three vertical profiles per location was used as an approximation of the "3D"infiltration profile. The rainfall experiments were carried out from the beginning of September to the

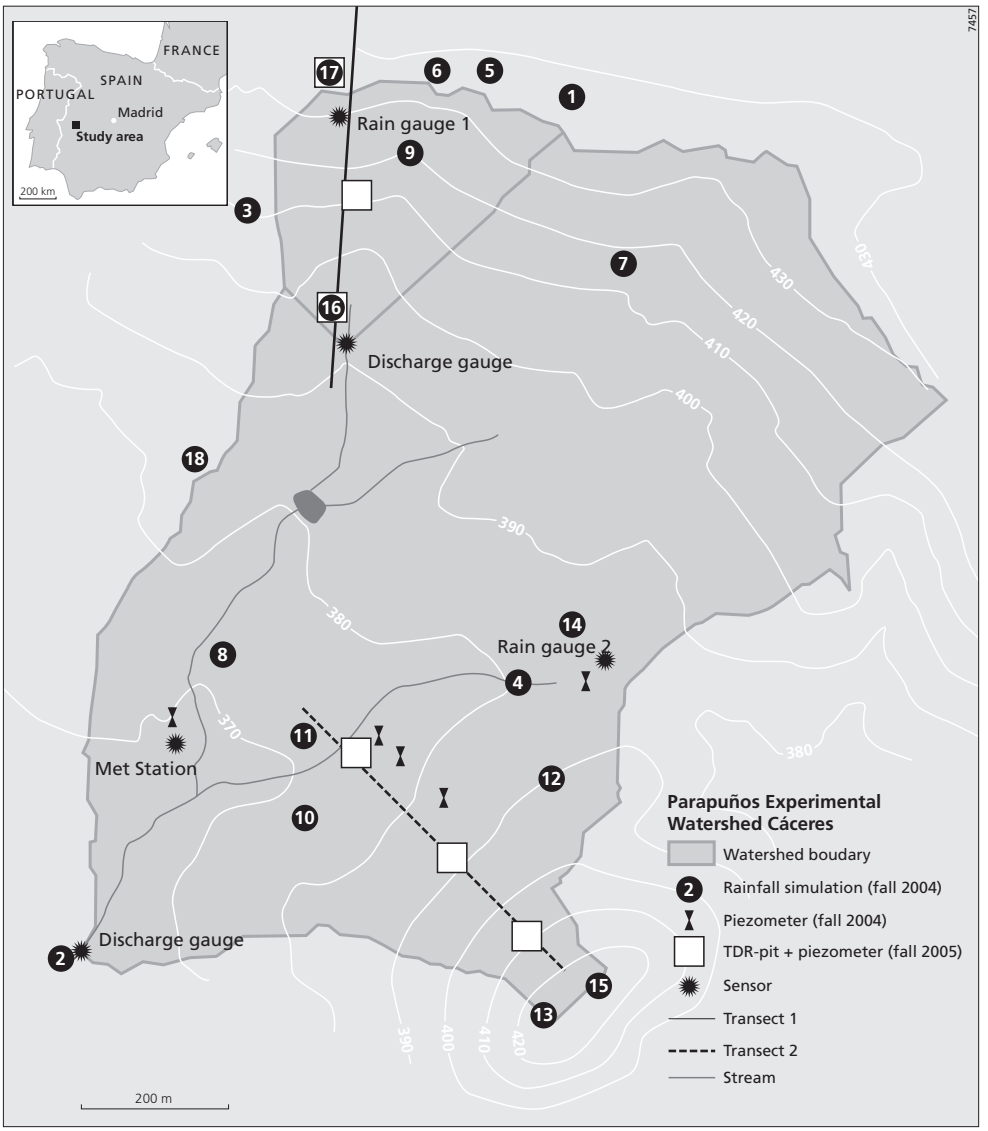

Figure 6.1: The Parapuños experimental catchment, including locations of field measurements.

beginning of November. Part of the experiments were carried out under extremely dry soil conditions. The rain started halfway into October and by the end of October there were a few large rainfall events, which completely wetted the soils. Some of the experiments were therefore performed under wet to extremely wet initial soil conditions. For this study three contrasting locations in the catchment were chosen with different texture, landscape location and initial conditions: i.e. a hill top (sandy loam, very wet initial condition), a hillslope (loam, dry initial condition) and a valley bottom (silty loam, dry initial condition) location.

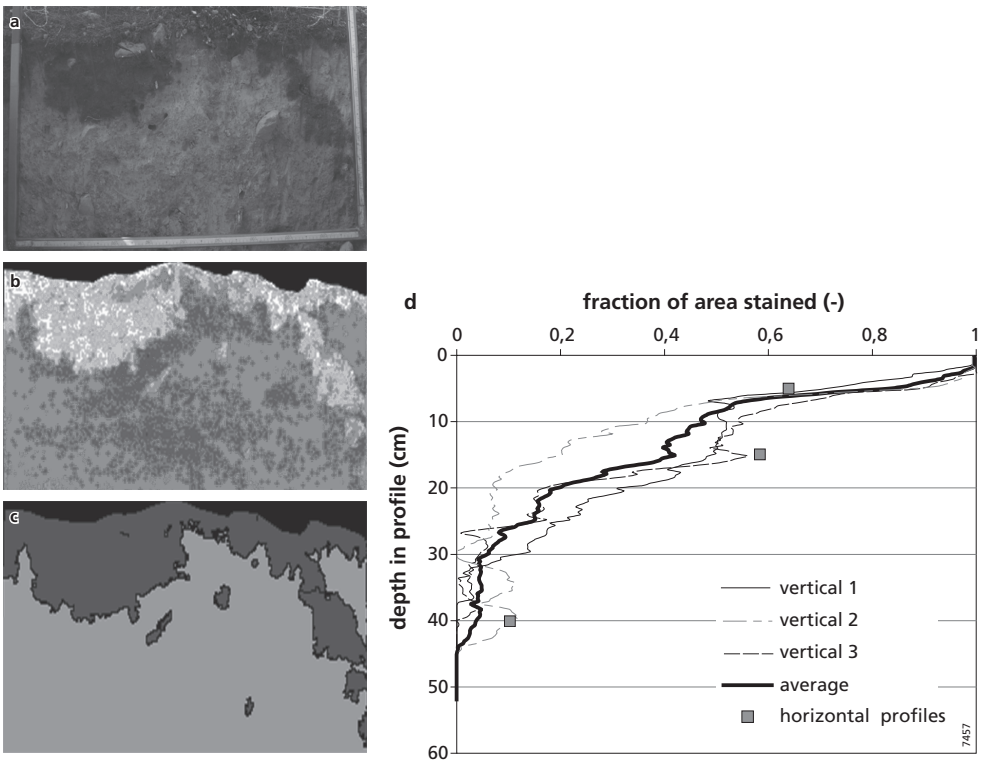

Figure 6.2: An example of the different steps in the image processing from tracer infiltration profiles to 3D infiltration approximation for one location: a) original image, b) after geometrical correction and color enhancement, c) after classification, d) fraction of stained area with depth.

At six locations in the catchment, divided along two hillslopes, the spatial and temporal distribution of soil moisture content was measured during the transition from dry to wet catchment conditions. This was accomplished with 67 handmade TDR probes distributed over six soil profiles (see Chapter 3 and Chapter 4). The TDR probes were placed in two to four horizontal layers (depending on soil depth) with two to five probes per layer.

The stained area versus depth derived form the tracer experiments was used to calibrate input parameters for the macropore concept in SWAP. Next the TDR measurements were used for validating the SWAP model and the inversely obtained macropore parameters under natural conditions. The model evaluation also involved simulations of the annual water balance.

6.4 SWAP model concept

The Soil Water Atmosphere Plant (SWAP) model simulates vertical flow of water near the soil surface under transient conditions (Kroes et al., 2008). The model includes crop growth, solute

transport and heat flow. The variably saturated water flow in the soil matrix is based on the Richards equation, including terms for root water uptake and macropore exchange:

$$\frac{\partial \theta}{\partial t} = C(h)\frac{\partial h}{\partial t} = \frac{\partial \left[K(h)\left(\frac{\partial h}{\partial z} + 1\right)\right]}{\partial z} - S_a(h) - S_m(h)$$

where θ is soil moisture content (-), t is time (T), h is soil water pressure head (L), $C(h)$ is the differential soil moisture capacity (L^{-1}), $K(h)$ is the hydraulic conductivity (LT^{-1}), z is the vertical coordinate, positive upward (L), S_a is a sink term for the root water uptake (T^{-1}) and S_m is the macropore exchange term. The soil hydraulic relationships are described according to van Genuchten (1980). Root water uptake reduction due to water and salt stress is simulated using the reduction functions as proposed by Feddes et al. (1978) and Maas and Hoffman (1977), respectively.

The top-boundary conditions are determined by precipitation, irrigation and evapotranspiration. Potential evapotranspiration is calculated with the Penman-Monteith equation (Allen et al., 1998), using daily meteorological data: total radiation, maximum and minimum temperature, humidity and wind speed. Precipitation is specified as actual amounts per time interval. There are different possibilities to describe the bottom boundary conditions in SWAP, including pressure head, soil water flux, free drainage and seepage face. The current SWAP version has a detailed concept for modeling macropore flow through cracks and/or bio-pores. In the following this macropore flow concept is briefly presented. For a more detailed description see Kroes et al. (2008).

Macropore flow concept

The predominant feature of macropore flow is that precipitation and irrigation water with solutes are routed into macropores at the soil surface, bypassing the reactive unsaturated soil. This water is transported rapidly downwards and distributed over different depths in the soil or the groundwater. In SWAP the inflow, vertical transport and distribution of water are based on the macropore geometry. Criteria for this concept were that it should be valid at field scale, functional but physically based, and require as few input parameters as possible.

The macropore geometry is described by characterizing the macropore volume according to two main properties:

- Continuity: continuous, interconnected macropores versus discontinuous, not connected macropores, ending at different depths;
- Persistency: static, permanent macropores and dynamic, temporary macropore volume depending on soil moisture status (shrinkage cracks).

Regarding continuity the macropore volume is partitioned into two classes, which are represented by two domains (Figure 6.3):

- Main Bypass flow domain (MB): main system of continuous, interconnected macropores that penetrate relatively deep into the soil. Water is transported fast and deep into the soil bypassing the soil matrix. Rapid drainage to drains can occur from this domain;

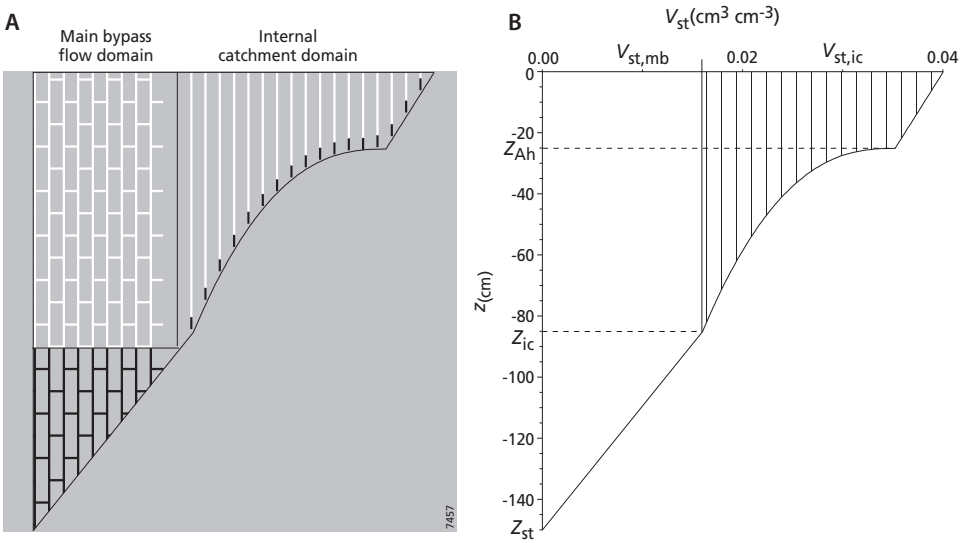

Figure 6.3: Schematic representation of the macropore volume and depth distribution a) showing the partition into two domains: Main Bypass and Internal Catchment, and b) graph of depth related static macropore volume fraction, with m, the power that mathematically describes the depth distribution of Internal Catchment macropores, = 0.5.

- Internal Catchment domain (IC): discontinuous not connected macropores, ending at different depths. Inflow is captured at the bottom of these macropores and forced to infiltrate at that depth, leading to distribution of macropore water over different depths.

The distribution of macropore volume over both domains is obtained by analytical equations with four basic input parameters: depth of A-horizon (Z_{ah}) and depth of IC domain (Z_{ic}), volumetric proportion of IC domain at the soil surface (P_{ic}) and shape-factor exponent (m) (Figure 6.4). Values of m < 1 describe shallow IC systems (Figure 6.3) and > 1 deep IC systems (Figure 6.4); value 1 results in a system with linear decline with depth of IC macropore volume. Additional shape parameters are the fraction of IC macropores that has ended at the bottom of the A-horizon (R_{zah}), and a symmetry-point that allows for S-shaped curves (S). The IC domain is divided into a number of sub-domains, which determine the vertical distribution of the bottom ends of the macropore sub-domains.

With respect to persistency, in our study the soil is rigid and does not swell and shrink. The macropore volume comprises static macropores only, originating from bio-activity. The static macropore volume is described with two parameters additional to the continuity parameters: the depth of the bottom of static macropore volume (Z_{st}), which in this case without dynamic cracks is equal to the maximum depth of the macropores, and the volume fraction of static macropores at the soil surface (V_{st})(Figure 6.4). The volume of the MB domain is constant from the soil surface to depth Z_{ic} and decreases linearly with depth to zero at depth Z_{st}.

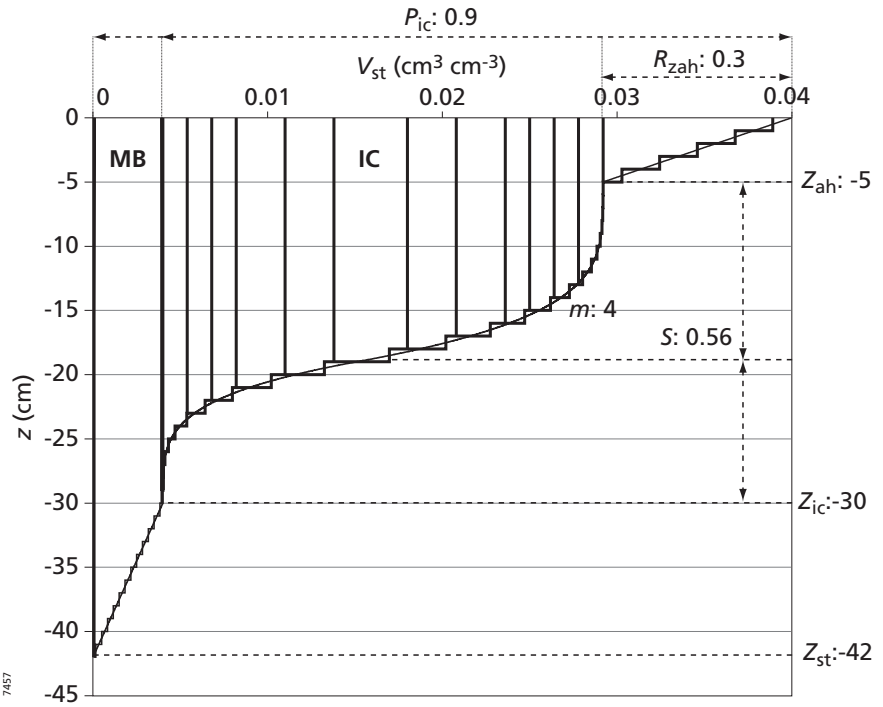

Figure 6.4: Graphical representation of the analytical description of the macropore geometry with the relevant input parameters and their values (see text for explanation of parameters). Description is based on the parameterization of the 'Valley bottom' location (Table 6.3) with some diverging parameter values for the sake of illustrational clearness.. Less than 18 sub-domains are present, because sub-domains that end in the same model compartment are functionally equal and therefore are lumped. Vertical discretization is: 1 cm thick compartments for the first 10 cm and 1.25 cm for the rest.

The horizontal distribution of macropore volume is described with an effective diameter of soil matrix polygons. This parameter controls the size of contact area between macropores and soil matrix. This vertical area of macropore wall determines the exchange of water between macropores and soil matrix. It is described as a function of depth by two input parameters (d_{mi} and d_{ma}), depending on density of macropores, with its minimum value (d_{mi}) in the top soil, where macropore density is maximal, and its maximum value (d_{ma}) at depth Z_{st}, where macropore density is minimal. The distribution of macropore depth and volume strongly influences the distribution of infiltration depth and quantity of macropore water flux. At the soil surface, the distribution of all water fluxes over macropore domains is according to the volumetric proportions of these domains.

Macropore inflow at the soil surface comprises direct precipitation into macropores and inflow of precipitation excess by runoff. As long as precipitation intensity is lower than matrix infiltration capacity, the precipitation is distributed over matrix and macropores equal to the ratio of their

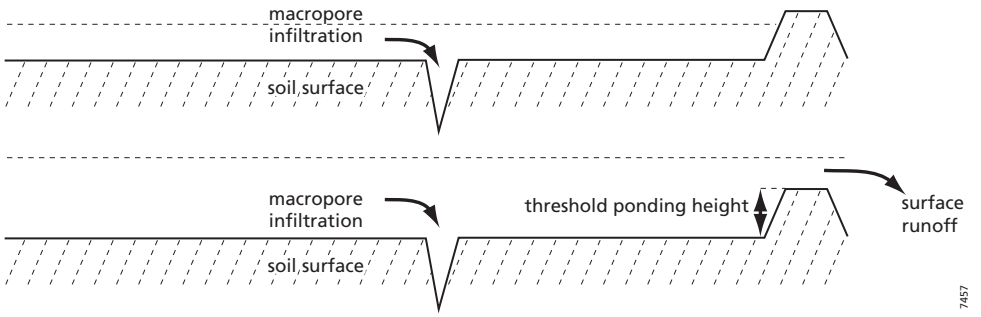

Figure 6.5: Representation of the influence of resistance and ponding height on the distribution of ponding water to macropores and to runoff.

surface areas. Once matrix infiltration capacity is exceeded the precipitation excess will flow into the macropores. A slight delay in this infiltration occurs due to the resistance to inflow, which depends on the macropore width. This resistance is very low and mostly a threshold ponding height must be exceeded before regular runoff to surface waters starts. Therefore runoff into macropores is favored over regular runoff (Figure 6.5). This implies that the latter will commonly not start before the macropore volume is filled up. The water flowing into the macropores is instantaneously added to the storage at the bottom of the macropores and infiltrates into the matrix over the depth of water storage. The infiltration flux is determined either by Philip's sorptivity (in case of dry soils) or by pressure gradient according to Darcy, depending on which flux is the largest. Infiltration along the sidewalls of macropores of water rapidly flowing down is neglected, as this is considered to be very small.

The MB domain is often connected to groundwater or drains. Therefore, from this domain rapid drainage to groundwater or drains can be generated. Flow to drains is governed by the drainage resistance and the difference in hydraulic head between macropore water and drainage level. In dry soils the macropores will mainly lose their water to the surrounding matrix, while in wetter soils rapid drainage can be triggered. Therefore a critical, user-defined soil moisture content is used to initiate drainage from macropores.

6.5 Model application

The aim of this study was on one hand to derive macropore parameters from tracer infiltration profiles and on the other hand to evaluate the performance of the SWAP model using detailed hydrological field measurements. This was performed using three different simulation rounds:

- Parameterization of the macropore parameters using the tracer infiltration profiles from the rainfall experiments;
- Comparison of simulated and measured soil moisture content profiles from dry to wet season at a high temporal resolution;
- Comparison of simulated water balance results with catchment scale measurements and literature values.

In all cases the results of the simulations with macropore flow are compared to the results of simulations neglecting macropore flow. For the simulations neglecting macropore flow high conductivity values as measured under ponded conditions on soil samples are assigned to the matrix.

SWAP input data

The simulations were run for two hydrological years ('04-'05 and '05-'06), from the 1st of September to the 31st of August. The daily meteorological data from the catchment and detailed rainfall intensity (per 15 minutes, the highest resolution for rainfall input in SWAP) were used. For the calibration of the macropore parameters on the dye-tracer infiltration profiles, the applied rainfall during the tracer experiment was added to the detailed file of the natural rainfall.

A fine numerical discretization of the profile was chosen: regardless of the profile depth, nodal distances of 4 mm were used. The bottom boundary was set as a zero flux boundary, as the soils are very shallow on top of bedrock. However there is some storage capacity in the weathered top of the bedrock, with a very low conductivity, so the subsoil was either extended a bit deeper or an extra layer with low conductivity was added beneath the soil profiles. The bottom boundary of the macropores is the maximum depth of the macropores, where the water either infiltrates to the matrix, according to the pressure head difference for wet soils or sorptivity in the case of dry soils, or is drained from the profile through rapid drainage of the macropores, once the soil profiles are very wet.

Table 6.1: Layering and Mualem van Genuchten parameters for the three simulated locations, as derived from Multi Step Outflow experiments as well as average measured k-sat from ponded soil samples.

		Average parameters from multi step outflow experiments						**Average measurement soil samples**
Soil Layer	Depth (cm)	θ_r (cm^3/cm^3)	θ_s (cm^3/cm^3)	α (1/cm)	N (-)	$k_{s,mso}$ * (cm/d)	λ (-)	$k_{s,meas}$ * (cm/d)
Hilltop (sandy loam)								
Topsoil	0-56	0.03	0.30	0.0380	1.251	12.5	-0.880	240.0
Subsoil	56-96	0.01	0.35	0.0068	1.134	0.5	1.785	143.0
Hillslope (loam)								
Topsoil	0-40	0.03	0.39	0.0144	1.117	0.7	2.0	42.0
Subsoil	40-60	0.03	0.42	0.0068	1.134	0.3	1.56	56.0
Valley Bottom (silty loam)								
Topsoil	0-8	0.03	0.35	0.0072	1.254	0.70	0.731	77.0
Subsoil1	8-56	0.03	0.38	0.0086	1.205	0.30	-0.630	33.0
Subsoil2	56-72	0.03	0.40	0.0172	1.130	1.1	0.75	1.1
Subsoil3	72-96	0.03	0.40	0.0172	1.130	0.01	0.75	0.01

* The ks,mso obtained from optimization of multi step outflow measurements is used for the matrix in the macropore simulations, the ks,meas measured on ponded kopecki soil samples is used for the simulations without macropore flow.

The hydraulic parameters of the soil matrix (Table 6.1), were derived from multi step outflow (MSO) measurements (van Dam et al., 1994) on Kopecki soil samples (100 cm^3), using five pressure steps (going from 30 to 60, 140, 250, 500 and 1000 cm). At each location of the rainfall experiments two ring samples were taken for the top soil as well as for the subsoil and occasionally a third soil layer. Of these ring samples a limited number was selected per soil type and depth for the multi step outflow experiments (with a total of 42 samples).

For each soil sample the saturated moisture content and conductivity were also measured. The saturated conductivity was measured with an imposed ponded water layer (constant head) on top of the soil samples. The measured values of saturated soil moisture content and conductivity are generally significantly higher than the fitted (MSO) values, which is attributed to the contribution of small macropores in the ring samples. Therefore the average fitted MSO saturated conductivity was used as input for the matrix characteristics in the runs with macropores, while the average measured saturated conductivity was used in the runs without macropores. As there also exists some small scale variation within a soil profile, the different samples resulted in a set of MvG parameters per soil type and depth. For the simulations the most representative of the different curves per soil type and depth was selected.

The MvG fits represent the outflow data for the range of moisture contents measured in the MSO experiment very well. However the extremely dry soil moisture contents as measured in the field in September (between 0.03 cm^3/cm^3 and 0.07 cm^3/cm^3, down to bedrock) were impossible to obtain with the fitted parameters. Most of the flow and redistribution of water takes place under these wetter circumstances and the soil dries out gradually from May to September, without much influence on the water balance for the rest of the year. Therefore we have chosen to stay with the MvG parameters as optimized with the MSO experiments. In order to allow the soils to dry out further in summer months, the original MvG curve was extended with a linear function at the dry end, starting from pF 3.0, the upper limit of the MSO measurements, to pF 4.5, the wilting point of semi-arid plants as reported in literature (≈ pF 4.5, e.g. Richards et al., 1983; Cameron, 2001; Sofo et al., 2007). For the moisture content at pF 4.5 the lowest value of soil moisture contents measured with the TDR sensors, 0.05 cm^3/cm^3, was taken.

The estimation of evapotranspiration for the different rainfall experiments is not straightforward, as it is not only related to the vegetation cover of the plots themselves. The evapotranspiration of individual Holm-oaks will come from the area under the tree canopy as well as the open grassland surrounding the trees and from deeper layers in the profile. As Moreno et al. (2005) pointed out it may be questionable whether a strict distribution of evapotranspiration below and outside the canopy is possible in an open vegetation structure as exists in the Dehesas. Therefore, two base files of the extreme situations of full grass cover and full tree cover were used for the vegetation input. For the different locations, the fraction of tree/grass cover of the area surrounding the plot was estimated and the input values of the two vegetation files were weighted accordingly. The growing season for the grass layer starts shortly after the first autumn rains and within 4-6 weeks there is a full soil cover. The grass dries out completely by the end of May.

In a detailed study of fine root distribution in Dehesas of Central Western Spain, Moreno et al. (2005) found that the root length density of herbaceous plant roots decreases exponentially with depth and their roots are mainly located in the upper 30 cm of the soil. Holm-oak root length density was found to be almost uniform with depth and distance to the tree, with 33 m maximum horizontal extension of tree roots. The root length density of trees is much smaller than that of herbaceous plants in the upper 10 cm, 2.4 km m^{-3} versus 23.7 km m^{-3}. Shrubs probably have an intermediate rooting pattern, but no information was found on their distribution. In SWAP the rooting depth is specified as a function of development stage and soil depth. The rooting depth of trees reaches down to bedrock for the full year and these roots are distributed evenly over depth. Grass roots are only present in the growing season in the upper 30 cm. To simplify the rooting pattern the maximum depth used for the simulations was invariably the bedrock and the roots were taken to decrease linearly from a relative density of 1.0 at the soil surface down to a relative density of 0.5 at maximum depth.

Mateos and Schnabel (2002) found that the interception and stemflow of Holm oaks (Quercus Ilex) amounted up to 26.8 % and 0.3% resp. of the rainfall. The canopy storage was estimated to be 2 mm. For grass, the basic SWAP grass input file is used, with throughflow of 90% and 4 mm canopy storage, which are similar to values from a study on grass interception in a Mediterranean climate: 8% interception (Corbett and Crouse, 1968).

As the SWAP macropore concept was initially based on a crack flow concept (Hendriks et al., 1999), the infiltration into macropores is strongly favored as compared to runoff and generally runoff will only become important once the macropores are entirely filled with water (Figure 6.5). In the case of cracks this seems realistic. In case of biopores, once the infiltration capacity of the matrix is exceeded, part of the water may flow into macropores, but part of the water will never encounter a macropore opening and will run off as surface runoff. To minimize this weakness in the model, the threshold ponding height for the occurrence of overland flow was set to zero in our simulations. Even then inflow resistance of macropores is much smaller than the runoff resistance, which means infiltration to macropores is still strongly favored over runoff.

Macropore parameterization
The macropore parameters were calibrated by minimizing the difference between the measured and simulated curves of infiltration with depth and the total infiltration amount into the soil profiles. As the stained area of the infiltration profiles cannot be translated to an absolute moisture content, we assume that the fraction of blue stained area at a certain depth is proportional to the increase in soil moisture content at that depth. This fraction was compared to the change in soil moisture content during the rainfall experiments at that depth simulated by SWAP. To be able to compare these curves, they are both normalized to a total area of one, resulting in curves of fraction of total infiltration per unit of depth (cm^{-1}) with depth (cm).

For the calibration of the macropore parameters, the fully stained layer at the top of the soil profiles was discarded as this was the result of the uniform infiltration front. After the rainfall experiment stopped, the moisture content of this layer decreased as the infiltration front moved to deeper layers. Consequently, for this layer the stained fraction of one was not a correct measure for the change in moisture content and, therefore, could not be used to calibrate SWAP

on moisture content changes. Thus, only the stained fractions of the area below the layer of uniform infiltration were used.

The rainfall experiments were performed with different initial soil moisture content, however, which influences the comparison with the soil moisture content increase at different depths. The dye-tracer infiltration profiles were excavated one day after the rainfall experiments. For the completely dry initial condition (hillslope and valley bottom) redistribution of antecedent water is negligible. In the SWAP simulations for these locations the change in water content between one day before and one day after the experiment was calculated. However, under wet initial conditions, redistribution of antecedent soil water can strongly influence the change in moisture content during and shortly after the dye-tracer experiment. In such conditions the change in moisture content cannot be attributed to infiltration from the soil surface. To limit the influence of this redistribution the change in soil moisture content is calculated between one hour after and one hour before the dye experiment.

Some of the macropore parameters were estimated directly from the inflection points and maximum depth of the dye infiltration patterns. These parameters are the depth of the A-horizon (Z_{ah}), depth of internal catchment (Z_{ic}) and depth of the main domain (Z_{st}) (see Figure 6.7 for an example). The minimal and maximal diameter (d_{mi} and d_{ma}) of the soil polygons was estimated based on the amount of colored spots at different depths on the excavated tracer profiles. The parameters used for the optimization are the volume fraction of macropores at the soil surface (V_{st}), proportion of internal catchment at the soil surface (P_{ic}), the shape factor exponent (m) and the symmetry point (S), which allows for S-shaped curves. The optimization was performed with PEST (Doherty, 2004), using the infiltration profiles and the cumulative infiltration into the soil together in a multi-objective optimization function. PEST uses a steepest decent searching algorithm based on Gauss-Marquardt-Levenberg. Therefore 100 PEST runs with random initial parameters were used to scan the parameter space and evaluate the shape of the error plane and in order to diminish the risk of ending in a local minimum.

Water balance data

Field and catchment scale data were collected to check the water balance. The simulated plot scale water balance cannot be directly compared to these data. To start with, the texture, slope, vegetation and soil depths of the various plots differ, which result in a spatial variation in infiltration, evapotranspiration and runoff. Furthermore, in the plot scale simulations the hillslope scale influences of runon/runoff and lateral flow are not accounted for. Though these

Table 6.2: Water balance for the hydrological years (1 Sep – 31 Aug) of '04-'05 and '05- '06 (measured precipitation and discharge and calculated evapotranspiration, using yearly closed water balance)

	October-December '04	'04-'05	October-December '05	'05-'06
Precipitation (mm)	234	336.3	196.8	368.6
Discharge (mm)	26.2	26.5	17.0	28.1
Evapotranspiration (mm)		309.8		340.5

hillslope processes do not play a role in the dye experiments which were performed locally, they do play a role in the year-round simulations.

As explained in the paragraph describing the study area, the annual water balance is closed (the catchment dries out completely in summertime), so the total annual evapotranspiration may be derived by subtracting discharge from rainfall. The mean annual rainfall is 514 mm, and mean annual discharge is 6.9 % thereof, which leaves 479 mm of calculated mean annual evapotranspiration. The rainfall, discharge coefficient and therefore the evapotranspiration show large interannual variability, as they depend strongly on the distribution of precipitation throughout the year and also on the annual rainfall totals (Ceballos and Schnabel, 1998).

Joffre and Rambal (1993) found daily transpiration values of between 1.65 and 2.04 mm for Quercus Ilex in the Dehesas slightly to the south of the research area, with monthly values of 50-60 mm in July and August. For open grass, Joffre and Rambal (1993) found daily values of 0.6 to 1.0 mm in autumn and 2.3 to 2.9 mm in spring, the period of maximum growth. Their computed mean annual evapotranspiration however is between 591 mm under tree cover to 400 mm outside tree cover, in a Dehesa area with annual rainfall between 600 and 800 mm. These values are slightly higher than the amounts found in our research area, which is probably a result of higher rainfall amounts, thus evapotranspiration is less limited by water shortage in their case. Based on the catchment scale measurements, the water balance components for the hydrological years of '04-'05 and '05- '06 were calculated (Table 6.2). These years had exceptional amounts of rainfall in the month of October, in a couple of high intensity showers, therefore these are also included. The discharge occurred mainly in October, but also for different events in December 2005 and the spring of 2006.

Table 6.3: Fixed and optimized macropore parameters, including ranges within which the parameters were optimized.

Macropore parameters	**Hill top**	**Hillslope**	**Valley bottom**	**Parameter range**
Fixed parameters				
Depth A-horizon, Z_{ah} (cm)	5.0	7.0	5.0	
Depth Internal catchment, Z_{ic} (cm)	25.0	25.0	30.0	
Depth Main domain, Z_{st} (cm)	35.0	43.0	42.0	
Minimal polygon diameter, D_{mi} (cm)	10.0	6.0	7.0	
Maximal polygon diameter, D_{ma} (cm)	40.0	50.0	50.0	
Fraction of macropores ending in A-horizon R_{zah} (-)	0.0	0.1	0.3	
Optimized parameters (with 95% uncertainty bounds)				
Volume of macropores at soil surface, V_{st} (cm^3/cm^3)	0.04 (±0.004)	0.048 (±0.001)	0.04 (±0.003)	0.01 – 0.05
Fraction of internal catchment at soil surface, P_{ic} (-)	0.90 (±0.03)	0.98 (±0.002)	0.99 (±0.001)	0.01 – 0.99
Power – m, m (-)	10.0 (±0.97)	1.69 (±0.061)	4.01 (±0.21)	0.1 – 10.0
Relative depth of S-parameter, S (-)	1.0 (±0.06)	0.37 (±0.013)	0.56 (±0.023)	0.0 – 1.0

* i.e. no s-parameter is used: results in a single convex or concave shape of macropores with depth

6.6 Results and discussion

Macropore parameterization
The parameter values for the different locations are given in Table 6.3, with the corresponding uncertainty bounds. In Figure 6.6 the root mean square error (RMSE) for the hundred different PEST optimizations of location 10 is shown against the optimized parameter values. Though PEST is occasionally either caught in local minima resulting in the sub-optimal parameter sets or the optimization criteria are too strict to reach the global minimum, the figures show a small area with the best optimizations, with almost similar parameter sets. For location 17 the optimizations of SWAP parameters with PEST were slightly problematic and uncertainty bounds could not be produced. As this location was very wet at the moment of the rainfall experiments, the infiltration to different layers mainly depended on the remaining storage capacity.

Z_{st} is the model parameter for the maximum depth of macropores. The defined value of Z_{st} is rather shallow compared to what may be expected based on the distribution of measured high conductivities in the soil profile (Table 6.1). Also in previous research on the influence of preferential flow in the area (Chapter 4), macropores are thought to reach larger depths and be well connected throughout. The Z_{st} values used here are directly inferred from the dye-stained patterns. Tsuboyama et al. (1994) and Sidle et al. (2001) describe macropore flow as flow through relatively short stretches of macropores which are connected by nodes of loose soil or organic matter. When these nodes become wet the connectivity of the macropores strongly increases. This mechanism is not included in SWAP, but it may explain the limited maximum depth of macropores deduced from the infiltration profiles, as the macropore connectivity may still be limited under the dry soil conditions of the experiments (locations 9 and 10). Furthermore the optimized value for the fraction of internal catchment macropores is generally rather high. This results in a small volume of main domain macropores, and thus a low contribution to rapid drainage in the simulations.

The infiltration patterns of the tracer experiments and the results of SWAP simulations with optimized parameters as well as matrix flow (without macropores) with the low fitted MSO k-sat and with the high measured k-sat are shown in Figure 6.7. The simulations with macropore flow are capable of reproducing the infiltration patterns very well. The matrix flow simulations with the low MSO fitted k-sat show that the depth of homogeneous infiltration into the matrix is more or less equal to the uniform infiltration depth of the dye-tracer for the hillslope and the valley bottom. For the hill top the uniform infiltration observed on the dye-infiltration profiles is even more shallow than the simulated matrix infiltration depth. For the simulations without macropore flow, the measured high matrix conductivity is used, which may be seen as the average conductivity of the joined matrix and macropore domains. The total infiltration into the soil profiles is comparable with the simulations with macropore flow for these locations. These conductivities however are extremely high and the simulated uniform infiltration front then reaches at least twice the depth of the uniform front on the stained profiles, but less than halfway the maximum depth of stained area. The use of the high measured saturated conductivity results in an elevated conductivity for unsaturated conditions too, which may have large consequences for the wetting and drying of the soil.

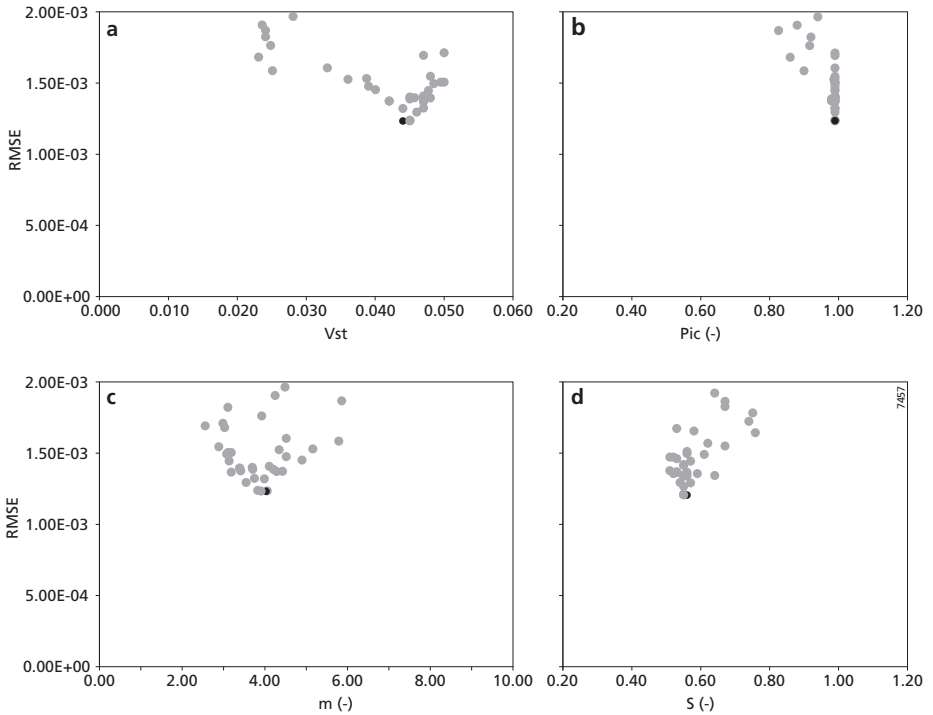

Figure 6.6: Root Mean Square Errors (RMSE) between simulated and measured fractions of total infiltration area (cm^{-1}) versus parameter values for the best optimizations from a set of 100 PEST optimizations at location 10: a) volume of macropores at soil surface (Vst), b) volumetric proportion of internal catchment domain at the soil surface (Pic), c) shape factor exponent (m), d) symmetry-point for S-shape (S). Note that the maximum value on the scale of RMSE is $2{,}00*10^{-3}$; most of the optimizations resulted in RMSE's with larger values, only the 40 best optimizations are shown within these graphs.

Soil moisture content development

The use of the macropore parameters obtained with the optimization on infiltration profiles is evaluated by comparison of simulations under natural circumstances from the 5th of October to the 6th of November 2005 with soil moisture content measurements. As SWAP is a one dimensional model the simulated soil moisture content should be seen as an average soil moisture content of a layer, this is compared with the average measured soil moisture content per layer of TDR sensors (two to five TDR sensors per soil layer). To assess the use of the macropore concept the results of simulations with and without macropores are compared, the latter with measured saturated conductivity (Figure 6.8).

The measured soil moisture contents at the beginning of the simulations are extremely low for the hillslope location (they are similar however to the gravimetric measurements performed in the field in September). Therefore the initial conditions used for the simulations were set to extremely dry. The TDR-permittivity measurements were transformed to soil moisture contents

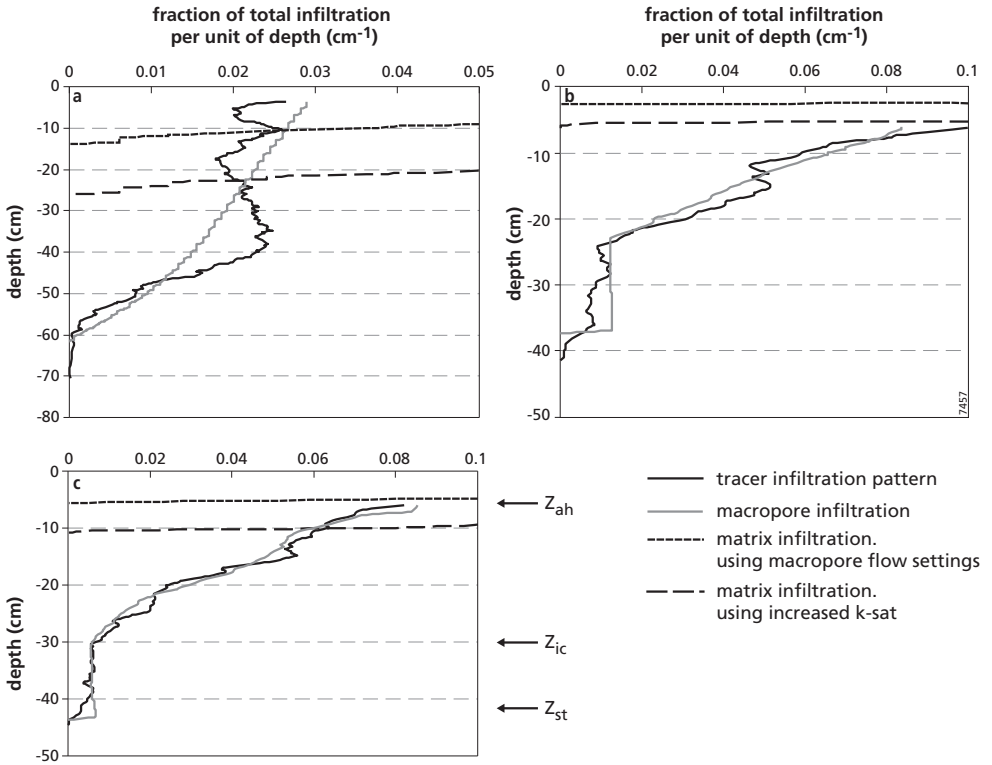

Figure 6.7: Infiltration pattern of tracer experiments and infiltration patterns derived from SWAP model simulations with optimized macropore parameters, matrix flow and adjusted matrix flow (i.e. increased k-sat values) for a) hill top, b) hillslope and c) valley bottom.

using soil specific calibration curves. This resulted in a measurement error in the order of 0.01-0.02 cm^3/cm^3 on average over the full range from dry to wet, as determined in the laboratory on soil samples from the area. The measurement error is generally slightly higher for the dry end of the soil moisture contents. Furthermore, the TDR-measurements are average values of two to five probes per soil layer.

The soil moisture contents in the topsoil are simulated slightly better for the simulations with macropores. The sudden jumps in soil moisture content after rainfall are reproduced well with both methods. In simulations without macropores, the high saturated conductivity values which are needed to ensure enough infiltration result in rapid percolation from the topsoil to deeper layers. Therefore in the simulations without macropores the top soils do not easily reach or maintain the high water contents, which according to the measurements do occur in the top soils. In the case of macropore flow the topsoils do reach high soil moisture contents more rapidly and stay at these levels longer.

In general the simulations both with and without the macropores do not produce enough rapid water flow to deeper layers. Conducting the rainfall experiments under dry initial soil

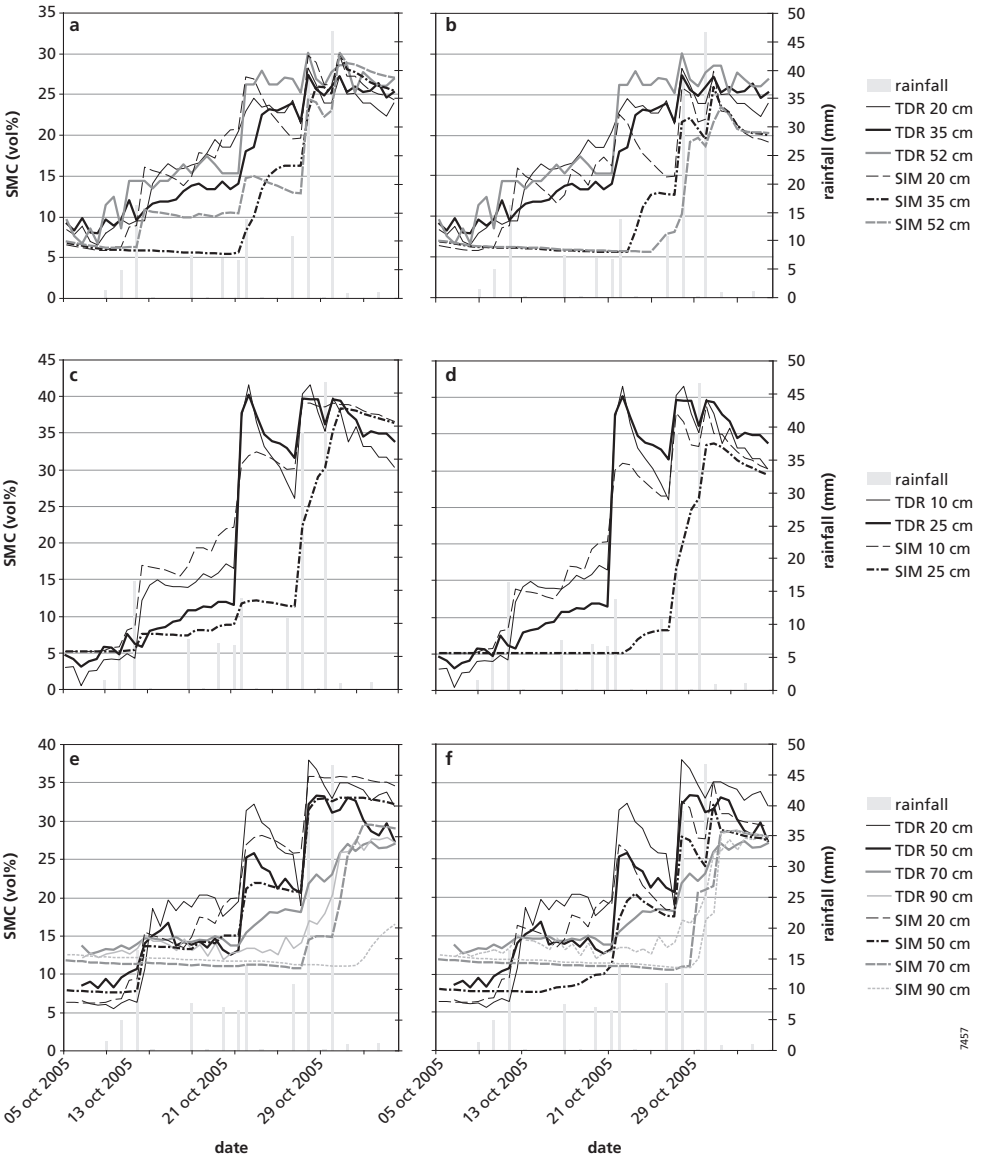

Figure 6.8: Soil moisture content development for the fall of 2005: a comparison between TDR-measurements and results of simulations with macropores and without macropores, but with measured k-sat: a) hill top (macropores), b) hill top (without macropores), c) hillslope (macropores), d) hillslope (without macropores), e) valley bottom (macropores), f) valley bottom (without macropores).

conditions possibly leads to an underestimation of the macropore depths as the connectivity of the macropores may not yet be optimal during the dye experiments. Though this explanation would apply for the valley bottom, where the dye experiment was carried out under dry soil conditions in the beginning of October, it is less likely for the hill top, with a very wet initial soil condition (this rainfall experiment was carried out in the beginning of November). Part of this underestimation of the rapid wetting of the subsoil in the SWAP simulations may also be due to the fact that the model is one dimensional and therefore the simulated moisture content is a laterally uniformly distributed moisture content. In reality, the soil around the macropores will remain wetter, showing a lateral gradient that is not present in the modeled one-dimensional vertical soil column, and therefore have a higher conductivity than the surrounding soil during the wetting process. Rapid percolation to deeper layers through the macropores and surrounding relatively wet soil may therefore be underestimated due to the use of uniformly distributed moisture contents for the model compartments. The soil moisture contents used for comparison with simulation results are average values of the TDR-sensors within a layer. The measurement results however show that the variability of soil moisture contents within a layer is generally high under unsaturated conditions and increases after high rainfall events (Chapter 4). The large variability in soil moisture contents within a soil layer in the lateral direction can cause high flow variability, with high conductivities along the preferential flow paths, while the surrounding soil is still relatively dry. As in SWAP the uniformly distributed moisture content is used, the matching conductivity will be lower than the actual average conductivity of matrix and preferential flow paths.

Water balance

The results for both hydrological years which were simulated are similar and the year of '05-'06 is shown here as an example (Figure 6.9). The main differences between the simulations with and without macropores are that the actual evapotranspiration in the simulations with macropores is generally higher and the runoff is lower (except for the hill top location).

For the year-round simulations of the water balance the temporal distribution of evapotranspiration is evaluated and compared to literature results. There is some slight variation in the temporal distribution of simulated total evapotranspiration (composed of interception and actual evaporation and transpiration) between the different locations and the simulations with and without macropores, but the pattern is similar. From October to January the average simulated evapotranspiration is about 1 mm/d. Then for February, March and April the simulated evapotranspiration is high, between 1.0 and 2.6 mm/d on average. The simulated evapotranspiration in May is already decreasing (1.4 mm/d on average) due to water shortage and by June evapotranspiration is strongly limited by the low soil moisture availability. These results seem realistic, compared to the literature results as discussed earlier (Joffre and Rambal, 1993).

Most of the measured discharge occurs in October and there are a few discharge events in the Spring. In the simulations discharge (runoff plus drainage) also occurs mainly in October. The simulations with macropore flow predict the total discharge amounts very well (0.0%, 7.8% and 7.4% of the precipitation respectively for hill top, hillslope and valley bottom) as compared to the total discharge at catchment scale (7.6% of the precipitation). The spatial distribution of this runoff generation, no runoff on the hill tops and most is generated along the hill slopes,

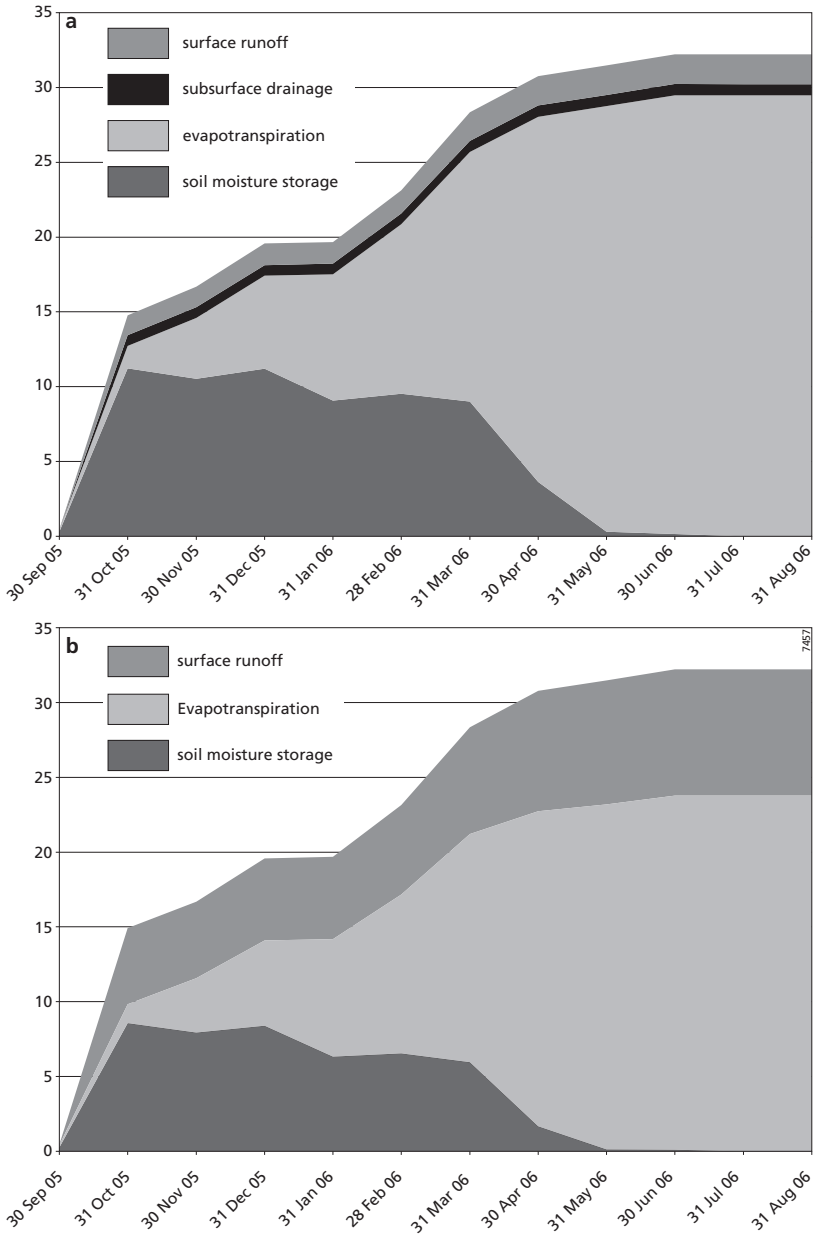

Figure 6.9: Yearly cumulative waterbalance (cm) for the hillslope location: distribution of rainfall to soil moisture storage, evapotranspiration, surface runoff and subsurface drainage for simulations with macropores (a) and without macropores (b).

is realistic. However there are a few more runoff events (in December and in June) in the simulations than in the measurements.
The subsurface lateral drainage in the simulations is limited to October, but should be more, both in amount as well as in frequency. This is due to the calibrated very large fraction of internal catchment macropores which limited the volume of macropores that contributed to rapid lateral drainage.

The total runoff for the simulations without macropores seems to be slightly underestimated for the valley bottom, but strongly overestimated for the hill top, where no runoff is expected at all, and the hillslope (1.8%, 24.0% and 5.0% of the precipitation respectively. for hill top, hillslope and valley bottom). Though the high saturated conductivity results in correct infiltration amounts during the rainfall experiments and quick percolation of the water to deeper layers, it results in too few runoff moments for the valley bottom. In the semi-arid areas correct runoff simulations are important as runoff is strongly related to erosion problems and water availability. Thus the overestimation of runoff along the hillslope is not acceptable.

6.7 Conclusions

The aim of this study was a) to use dye-tracer infiltration patterns for the parameterization of macropore flow in the SWAP agrohydrological model and b) to evaluate the use of the SWAP model with the optimized macropore parameter set for a natural field situation and compare this to modeling without macropore flow.

The parameterization of macropore flow using the infiltration profiles and total amount of infiltration from the rainfall experiments, yields a unique set of four optimized macropore parameters, with small uncertainty bounds, for all three distinguished locations. When we assume that the depth of uniform infiltration as obtained from the dye patterns is representative for the matrix infiltration depth, this uniform infiltration depth is simulated well in the macropore simulations, which use the fitted Mualem van Genuchten parameters from the Multi Step Outflow experiments for the matrix parameterization. In order to simulate soil moisture contents and water balances without macropores, the measured average saturated conductivity was used, which was much higher than the fitted value. Though with these very high values the total infiltration amount may be matched, the maximum depth of infiltration in the simulations without macropore flow is far from the maximum depth seen on the infiltration profiles. Thus the simulation of separate matrix and macropore flow with model parameters based on soil physical measurements and the infiltration patterns results in a much better prediction of measured distribution of infiltration with depth as compared to simulations without macropore flow.

Furthermore, for both soil moisture content as well as water balance, the simulations with macropores show better results the than simulations without macropores. The soil moisture content simulations of the topsoil yield better results using the macropore model. Wetting of the deeper layers is too slow for both the simulations with and without macropores. This indicates that there is more preferential flow to the deeper layers than is calculated using the

parameterization based on the dye-tracer infiltration profiles. Runoff amounts are simulated well with macropores, but strongly overestimated in the simulations without macropores, even though these simulations were performed with the very high, measured saturated conductivity values.

7 Modeling macropore flow at catchment scale with Hillflow 3D

7.1 Introduction

Subsurface stormflow is often thought mainly to occur in humid environments with steep terrains and conductive soils. In drier climates and in lowlands it is thought only to occur under extreme conditions and high antecedent soil moisture contents (Weiler et al., 2005). However in Chapter 4 of this thesis the hydrological behaviour of the Parapuños catchment is described and subsurface stormflow is found to play a large role in the catchment drainage. Hydrological modelling of the Parapuños experimental catchment by Maneta et al. (2008) showed that the discharge has a faster component attributed to runoff and a slower base flow component, but simulating this proved to be difficult. The simulated runoff had to be slowed down with extremely high Manning's n values, while the simulated groundwater release to the channel was too slow compared to measured fluctuations in piezometers. They concluded that this is probably mainly a result of compensation in the calibration procedure for the lack of correct subsurface flow in the model. Also from the plot scale simulations for this catchment in SWAP (Chapter 6) modelling with a macropore flow concept shows better results than without a macropore concept, while in the latter case high (measured) saturated conductivities are used to ensure high infiltration into the soil.

Due to changes in management and climate change many semi-arid areas are prone to increased runoff, soil erosion and landscape degradation (Nearing et al., 2005). Decreasing soil moisture availability can have a negative influence on vegetation cover, which in turn decreases the macroporosity and infiltration capacity of soils. For these areas the distribution of rainfall to surface or subsurface flow is therefore an important issue and correct prediction is necessary.

The analysis of the soil moisture content, water level, rainfall and discharge measurements in Chapter 4 pointed out that a significant part of the catchment discharge may be produced by subsurface macropore flow, instead of surface runoff. A large connected macropore network is thought to exist, which can transport water laterally regardless of the soil moisture content of the matrix. Under dry conditions the macropores loose a lot of water to the matrix, but can also transport water as rapid subsurface stormflow. Under near saturated conditions there is little infiltration to the matrix and most of the water will become subsurface stormflow. Therefore the main criteria for the model were that it should: a) treat matrix and preferential flow separately; b) allow lateral preferential flow when the soil matrix is still unsaturated and c) include interaction between macropores and matrix as function of soil moisture content. Therefore Hillflow 3D (Bronstert, 1995) was chosen. Under extremely dry circumstances the infiltration into the matrix was strongly limited by the matrix conductivities and therefore the simulated infiltration

remained too low. In order to apply this model to the semi-arid catchment infiltration based on sorptivity was included in the model.

Models are always a simplification of reality. For more complex models, more parameters are needed and more degrees of freedom arise. This is mainly a problem when it is not possible to make physically based estimates of the parameter values. When the parameters are calibrated a model may give the right results for a wrong reason and subsequently running scenarios with the model may result in erroneous predictions (Beven and Freer, 2001). It is important to find a model which is as simple as possible, but does include the most important processes and to use measurements or physically based values for the parameterisation as much as possible. Therefore the aim of this research is to study the rainfall- discharge production of a semi-arid area using a macropore flow model which is in agreement with the conceptual behaviour of the catchment. If results are beter than modelling with a classical runoff-groundwater concept, this implies that a preferential flow concept is better concept for the behaviour of such a catchment. The catchment scale runoff is simulated with a slightly adapted version of the physically based Hillflow 3D model (Bronstert, 1995). Subsequently rainfall-discharge behaviour under extreme conditions is assessed using scenarios of 30 minute high intensity rainfall events with a return period of 2, 10 and 50 years, for both dry and wet catchment conditions. The results are compared to simulations without macropores, but with high saturated conductivities.

7.2 Hillflow application

Model concept
Hillflow 3D (Bronstert, 1995) simulates all relevant processes at catchment scale: interception, evapotranspiration, soil water flow through matrix and macropores, surface runoff and channel flow. Hillflow 3D is a dual porosity model; it treats the macropores as a separate domain, which can rapidly transport water both vertically as well as laterally. Infiltration to macropores starts when the matrix infiltration capacity is exceeded, thereby increasing total infiltration into the soil. Surface runoff starts only after the macropore volume is full. Interaction between macropores and matrix is controlled by the pressure gradient and the conductivity of the matrix as a function of actual moisture content. Lateral subsurface flow starts when the macropore infiltration is larger than the flux from macropores to matrix (Figure 7.1). Channels are explicitly taken into account, with a given width, depth and roughness coefficient for each channel element. The slope is calculated using the surface slope and the channel depth.

Macroporosity like all other input variables can be given either as spatially constant or distributed. In the case of spatially variable input the model runs can become very slow. The macropore volume is equally distributed over depth and flow in macropores is assumed to be parallel to soil surface. Soil water flow is simulated three dimensionally and the surface and subsurface runoff is simulated using the surface slope in two dimensions. Surface runoff is calculated using the Manning-Strickler equation:

$$v_0 = \sqrt{S_0}\, k_{st}\, h_0^{5/3}$$

v_0: surface runoff velocity (L^2T^{-1})

S_0: surface slope (LL^{-1})
k_{st}: Strickler coefficient ($L^{1/3}T^{-1}$)
h_0: flow depth (L)

And macropore flow is calculated using a function of slope and a so-called "interflow conductance"(according to Eagleson 1970, in Bronstert, 1995):

$v_z = S_0 \cdot k_z$
v_z: macropore flow velocity (LT^{-1})
k_z: interflow conductance (LT^{-1})

Model adaptation
The infiltration from macropores to matrix in Hillflow 3D is limited under very dry conditions as it depends on the unsaturated conductivity of the matrix. Therefore this infiltration was adapted in order to apply the model under the extremely dry circumstances of the semi-arid research catchment: sorptivity was included in the model according to the method used in SWAP (Kroes et al., 2008). Under dry circumstances the sorptivity was used to calculate infiltration in stead of the Darcian flux.

$$S_0 = S_{\max}\left(1-\frac{\theta_0-\theta_r}{\theta_s-\theta_r}\right)^{\alpha}$$

S_0: sorptivity at the beginning of infiltration to macropores ($LT^{-1/2}$)
S_{max}: maximum sorptivity of the soil ($LT^{-1/2}$)
θ_0: soil moisture content at the beginning of infiltration to macropores ($L^3\ L^{-3}$)
θ_r: residual soil moisture content ($L^3\ L^{-3}$)
θ_s: saturated soil moisture content ($L^3\ L^{-3}$)

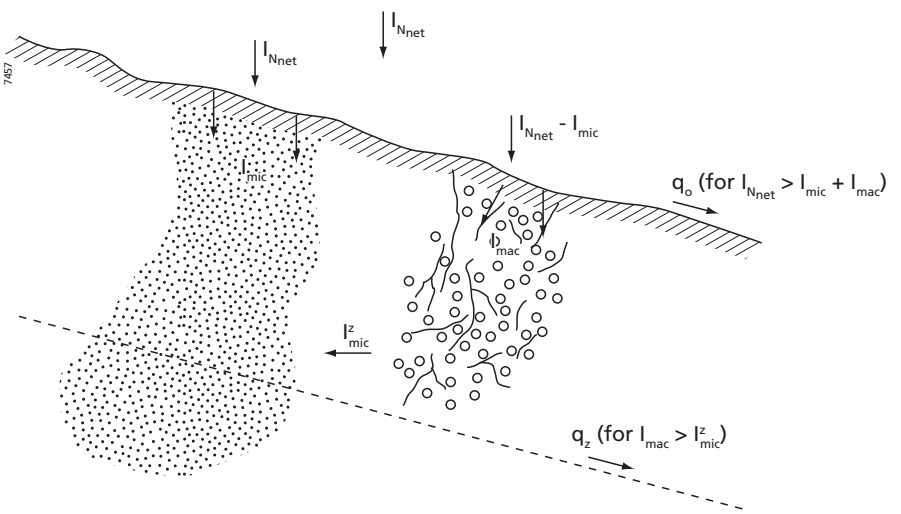

Figure 7.1: Distribution of net rainfall to macropore, matrix and surface and subsurface runoff (Bronstert, 1995). I_{Nnet} is net rainfall, i.e. precipitation minus interception, I_{mic} is matrix infiltration, I_{mac} is macropore infiltration, I^z_{mic} is infiltration from macropores to matrix in depth, q_o is surface runoff, q_z is subsurface stormflow.

α: sorptivity decrease factor

The actual sorptivity is dependent on the relative moisture content of the soil. The cumulative infiltration due to sorptivity is then calculated using Philip's (1957) infiltration formula:

$I(t)I_{cum}(t) = S_0 * \sqrt{t}$

I_{cum}: cumulative infiltration (mm) due to sorptivity at time t (T) after the beginning of infiltration to the macropores. The infiltration due to sorptivity *I(t)* is then calculated using the cumulative infiltration starting from the moment infiltration to macropores starts, minus the cumulative infiltration of the previous time:

$I(t) = I_{cum}(t) - I_{cum}(t-\Delta t)$

In case of a wet soil the infiltration due to sorptivity will be negligible. Depending on the soil moisture content either the sorptivity (capillary forces are dominant) or gravity driven flow is dominant. Therefore both fluxes are calculated per time step and the infiltration is set equal to the largest of the two.

Parameterization

The aim of this study is to model the catchment scale rainfall – discharge response with a physically based model, which is consistent with the hydrological behaviour, using measurement values. The grid size is set to 15 by 15 m. Spatial maps of vegetation and texture are used for the modeling. The rainfall resolution used for the model is 30 min and the daily actual evapotranspiration is according to Penman Monteith (Allen et al., 1998). In Hillflow it is not possible to vary soil depth or depth of macropores in the soil over the catchment area. The soil depth therefore is 1.0 m for the whole area (consisting of seven layers: 5, 5, 5, 10, 15, 20 and 40 cm respectively). The deepest layer is made unpermeable for the shallow hillslope soils. The macropore volume only exists in the top five layers (to 40 cm depth). For the soil physical parameterization of the matrix, the Mualem van Genuchten parameters obtained with MSO experiments (Chapter 3, Table 3.4) were used. For the simulations with macropore flow concept the fitted saturated conductivities of the MSO experiments were used and for the simulations without macropore flow the measured saturated conductivities were used (as explained in Chapter 6 for the SWAP simulations).

At the catchment scale the connectivity of macropores is thought to be more important than the spatial pattern of macropore volumes and depths. In chapter 4 the water table fluctuations were observed to differ between the two hillslopes, but within the hillslopes similar water table increase and decrease was observed. These differences may be (partly) due to the different soil textures and the distances to the discharge gully, which complicates the determination of the parameters for the different hillslopes. As there is not enough basis for rationally determining the variability of parameters from one hillslope to the other, spatially and temporally constant values were used for all the surface and subsurface parameters. These parameters were estimated from literature based values (Table 7.1). The surface runoff coefficient is based on the expected surface roughness value for a dense grass cover (which by the end of October covers the area) with slightly rough soil surface. The interflow conductance is set to 1.5 ms^{-1}, as the subsurface stormflow is seen to be very rapid too (Chapter 4). Note that this value is much higher than Brontert's (1995) interflow conductance in the examples in the Hillflow manual, which is 0.15 ms^{-1}. A representative sorptivity value for a fine silty loam soil is used.

Table 7.1: Catchment scale parameters for surface and subsurface runoff

	Parameter values set 1	Parameter values set 2
Strickler surface runoff coefficient ($m^{1/3}s^{-1}$)	4.0	4.0
Interflow conductance (ms^{-1})	1.5	0.15
Volume % macropores	0.1	1.5
Sorptivity max ($mms^{-1/2}$)	0.6	0.6
Alpha (-)	0.5	0.5

Table 7.2: Maximum rainfall intensity for rainfall events of 30 minute duration, with different return periods (Xn) for the city of Cáceres using the Gumbel method (Schnabel et al, 1998)

Xn	Maximum 30 min rainfall (mm)
X2	13.3
X10	20.9
X50	27.8

The Hillflow3D model concept does fit the concept of the hydrological behavior in the research catchment, as lateral subsurface flow is possible under unsaturated conditions of the matrix. There are however some limitations in Hillflow3D:

- the macropores have to be completely filled before surface runoff starts. In reality surface runoff starts well before the macropores are filled and both infiltration to macropores as well as surface runoff will increase simultaneously. Once the macropore infiltration capacity is reached the increase in surface runoff will become very large;
- the soil depth and the interflow depth are both homogeneous for the whole catchment and though the macropore volume can be varied spatially, the distribution with depth is homogeneous.

To ensure surface runoff production under the high intensity rainfall events, macropore infiltration has to be exceeded; therefore the macropore volume was necessarily set to a low value of 0.1 volume percent.

The value of 0.1 volume percent of macropores is extremely low, which is an artefact of the distribution of water to macropores and surface runoff. A second simulation is therefore performed with a realistic estimation of the macropore porosity and therefore an adapted interflow conductance (Table 7.1). In this case the runoff coefficient used by Bronstert in his examples (1995) is used. The influence of this parameterisation on the discharge is discussed. The model is also run without sorptivity, to assess the use of this addition to the model.

Rainfall – discharge scenarios

As the climate change for semi-arid regions is generally predicted to result in less events, but with high intensity rainfall the influence of a few high intensity events on the catchment scale discharge under dry and under wet catchment circumstances is studied. For these high intensity rainfall-discharge scenarios the maximum 30 min rainfall intensities with return periods of two, ten and fifty years were used (Table 7.2 (Schnabel et al. 1998))

Finally the model results are compared to simulations with the same model but without macropores, in the latter case using a raised saturated conductivity (effective conductivity of matrix and macropores) to induce high infiltration at the soil surface.

7.3 Results and discussion

Model performance
In this research the model choice was based mainly on the ability to simulate lateral subsurface runoff under unsaturated matrix conditions. The model parameter values were estimated based on literature and measurements. The only parameter, which was adapted to ensure a good result in the modeling, was the macropore volume. The macropore volume is constant with depth and all macropores have to fill up before surface runoff starts. Therefore a small macropore volume is necessary to ensure both surface as well as subsurface runoff, for comparison also a parameter set with a more realistic macropore volume was used.

Using the spatially and temporally constant parameter values (Table 7.1) for the adapted Hillflow 3D model the rainfall – discharge behavior of the catchment for the October 2005 period was simulated (Figure 7.2). The peak discharge values for both of the rainfall events were well reproduced. Under the dry catchment conditions the infiltration from the macropores into the soil was high, resulting in a sharp falling limb of the hydrograph after the rainfall event of October the 28th. The tail of the hydrograph, which is thought mainly to result from subsurface stormflow, was not reproduced. Also the first smaller peaks of the rainfall event under very wet catchment conditions (end of October) were not reproduced. The high intensity rainfall in the beginning of this event does not yet produce surface runoff, as the runoff can only start once the macropores are full. During this rainfall event the soils become saturated. Under the wet catchment conditions, reached by the end of the event, the tail of the hydrograph was better simulated as the infiltration from macropores to matrix is then reduced. The total discharge for the October month is however overestimated in the simulations, 21.5 mm, versus 16.9 mm of measured discharge for the simulated period.

As the macropore volume is very low, the results are compared to a simulation with a more realistic macropore volume of 1.5 vol%. This leads to a slower increase in discharge at the beginning of the rainfall event and a lower peak for the first event as all the water enters the macropores. Also the discharge continues for longer and the decrease in discharge after the rainfall ends is slower. There is no surface runoff for the first event and only during the second event the macropores are filled up and surface runoff is produced, then the peak discharge is reproduced. This shows that to get the rapid and high peaks and also the slower tails of the hydrographs a combination of rapid surface runoff and a slower subsurface discharge component is needed. Thus the model should be adjusted to allow for a more realistic macropore volume as well as surface runoff production.

Results of the simulation without sorptivity show that the infiltration without the sorptivity component is too low for the dry period as the unsaturated conductivity of the matrix, determining the infiltration is then extremely low. This leads to extreme discharge production

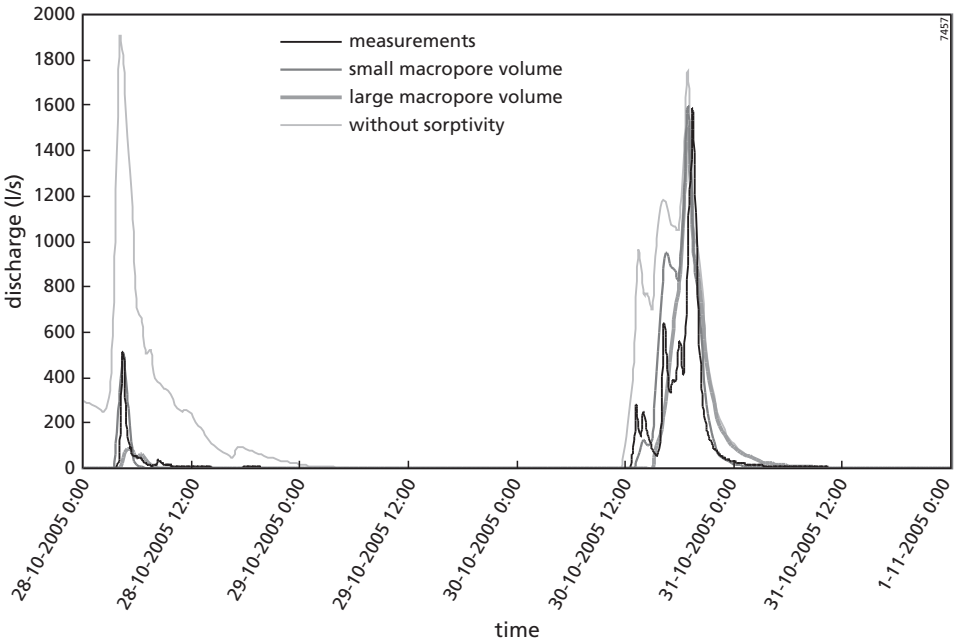

Figure 7.2: Rainfall – discharge production, measured versus simulated discharge with sorptivity, using small and realistic macropore volumes, and without sorptivity.

for the first events and only for the last event end of October, when the soil becomes wet, the discharge production becomes better. Note that due to the low infiltration in the course of the first events, the soil only starts to become wet during the 30th/31st of October, while in reality the soil is already near saturation at that time. When sorptivity is included, the simulations do result in near saturated soils by the 30th/31st of October.

Rainfall – discharge scenarios

Scenarios of rainfall discharge production for 30 minute high intensity rainfall events, with a return period of 2, 10 and 50 years respectively, show that the produced total runoff and the peak flow increase exponentially with an increase in rainfall intensity (Table 7.3). This can be expected, as the soil matrix conductivity is very low. The macropores allow for a high infiltration into the soil, but once the macropore network fills up completely, the bulk infiltration capacity of the soil will decrease rapidly and surface runoff will increase exponentially. As in this modelling exercise the parameter value for the macropore volume is very small the influence of higher rainfall intensity on the discharge is exaggerated. Nevertheless this sudden strong increase of runoff when the infiltration to macropores reaches its maximum capacity is an important feature, which can be expected to occur in the presence of macropores. These runoff coefficients may seem high, but the results of the 2 year return period compared well to what was observed in October 2005, with runoff coefficients of 0.78% and 31.4% for natural high intensity rainfall events, under dry and wet catchment conditions respectively.

Table 7.3: Rainfall – discharge behaviour for high intensity rainfall events under dry and wet catchment conditions, with macropore flow simulations.

	Rainfall intensity (return period)		
	13.3 (2y)	20.9 (10y)	27.8 (50y)
Dry antecedent conditions, small macropore volume			
Total discharge (mm)	0.07	1.47	12.20
Peak discharge (l/s)	16	821	2400
Runoff coefficient (%)	0.5	7.0	43.9
Wet antecedent conditions, small macropore volume			
Total discharge (mm)	5.07	11.79	17.75
Peak discharge (l/s)	674	1642	2898
Runoff coefficient (%)	38.1	56.4	63.8
Wet antecedent conditions, realistic macropore volume			
Total discharge (mm)	0.001	0.035	0.84
Peak discharge (l/s)	0.04	5.06	140
Runoff coefficient (%)	0.01	0.17	3.02

Using the larger macropore volume there is too little discharge production. For the dry catchment conditions there is no discharge at all, for any of the rainfall intensities. The macropore network is then large enough to let all the water infiltrate via the macropores into the dry soil. Under wet circumstances there is some discharge production, but even then this is too little and not realistic. The use of the larger, more realistic, macropore volume leads to too much infiltration into the soil, as the surface runoff only starts after the macropores are full.

Simulations without macropore flow

The model results are now compared to the results of modelling without macropores, but with high saturated conductivities. The hydrograph (Figure 7.3) shows that for the relatively dry situation on the 28th of October the peak discharge is reasonably simulated, but the subsequent discharge continues too high for too long. For the rainfall event of the 30th/31st of October the peak discharge is too low though the first few peaks of the event are well simulated. The tail of the hydrograph is reasonably well simulated, though the decline in discharge is a bit too fast. The total discharge for this simulation, 25.6 mm, overestimates the measured discharge of 16.9 mm. Of course the simulations may be improved through model calibration, but in this case the model results using purely measured and literature data for the model parameters were compared. The model with macropore flow shows better results.

The rainfall – discharge scenarios show that the runoff for the high intensity rainfall events is less than in the case of macropore flow simulations. The peak discharge under dry catchment conditions grows exponentially with increasing rainfall intensities, under the wet antecedent conditions the increase in discharge is less dramatic. The rainfall intensity with a 50 year return period shows almost the same peak discharge for the dry and wet antecedent conditions. Even though the total discharge for the October month of 2005 is overestimated with these simulations, the scenario's run without macropores produce much less discharge and with a lower

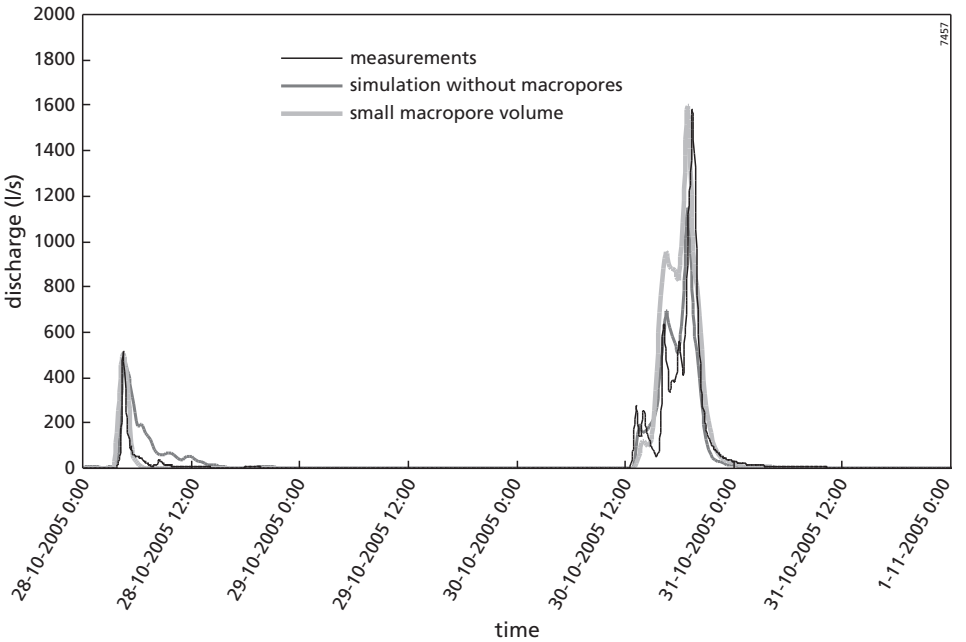

Figure 7.3: Rainfall – discharge production, measured versus simulated discharge, with and without macropores (the latter with high saturated conductivities).

peak discharge. Compared to the October 2005 discharge of 0.78 and 31.4% discharge under high intensity rainfall events for dry and wet catchment conditions, these simulated discharge amounts are rather low (Table 7.4).

Model concept evaluation

In this model some processes are simplified or neglected which according to different studies are important to include in subsurface stormflow modeling, such as soil depth variability,

Table 7.4: Rainfall – discharge behaviour for high intensity rainfall events under dry and wet catchment conditions, without macropore flow, using high saturated conductivities.

	Rainfall intensity (return period)		
	13.3 (2y)	20.9 (10y)	27.8 (50y)
Dry antecedent conditions			
Total discharge (mm)	0.03	0.88	4.82
Peak discharge (l/s)	7	151	1087
Runoff coefficient (%)	0.2	4.2	17.3
Wet antecedent conditions			
Total discharge (mm)	0.3	3.7	9.3
Peak discharge (l/s)	75	774	1926
Runoff coefficient (%)	2.3	17.7	33.5

bedrock storage and seepage. The bedrock irregularity and resulting storage capacity in bedrock depressions as well as the seepage into cracks in the bedrock (Nijland et al., 2009) provide storage which has to be overcome before the lateral subsurface flow becomes important. Also the connectivity of the macropores has to grow before the lateral subsurface flow paths will conduct significant amounts of water to the stream. Tromp van Meerveld and Mcdonnell (2006) call this the fill and spill mechanism. Though the bedrock can provide extra water storage and delay of the lateral flow component, the question remains whether this should be modeled explicitly. In the experimental catchment all the water, which is stored, whether in the soil matrix or in the bedrock is thought to leave the catchment during the dry summer months as evapotranspiration. Under dry circumstances the infiltration from macropores to matrix in the model results in less lateral preferential flow, and the infiltration to the matrix is stored there and all used for evapotranspiration through the year. In other words the question is then whether it is important to specify the storage location of the water: in the matrix or in the bedrock.

As for the connectivity of the macropores, when the soils get wet the nodes between macropores are activated and the preferential flow network grows (Tsuboyama, 1994). This is a complex relationship. Using the sorptivity, infiltration from macropores to the matrix is enhanced under dry catchment conditions, which results in an extra delay in lateral flow under dry catchment conditions. Though this is not the same as the concept of growing flow path connectivity, the resulting delay in lateral subsurface flow is similar.

Summarised the model does fit the concept of subsurface stormflow regardless of the soil saturation and the interaction with matrix depending on the matrix moisture content. The most important limitation is the fact that the surface runoff only starts after the macropores infiltration is exceeded. This influences the parameterisation (the macropore volume is forced to be small in the model) and may therefore make the model scenarios less reliable. In reality surface runoff starts almost simultaneously with the infiltration to macropores and both increase with increasing rainfall intensity and duration.

7.4 Conclusions and recommendations

In previous research macropore flow was found to play an important role in the catchment scale hydrology of the semi-arid Parapuños catchment. In this research therefore the catchment scale behaviour was simulated using a macropore flow model, which was consistent with the conceptual behaviour of the catchment. The macropore flow model was able to reproduce the rainfall- discharge behaviour very well, though the total discharge was slightly overestimated. The model without macropores but with high saturated conductivity results in a larger difference between measured and simulated hydrograph and the total surface runoff is too high in that case.

Rainfall – discharge scenarios showed that high intensity rainfall can lead to extreme discharge (both peak flows as well as total discharge) once the infiltration capacity to the macropore volume is exceeded. The extreme reactions of the discharge to higher rainfall intensities were much stronger in the model that included macropore flow than in the model without. This is

partly a model artefact, due to the small macropore volume. However this rainfall – discharge behaviour is likely, though maybe slightly weaker.
The present day situation may be simulated reasonably well without including macropores, but the results of model scenarios are very different. Therefore it seems best to use a model that fits the concept of hydrological functioning of the modelled area. Though the Hillflow 3D model shows good results, the inability to let surface runoff start before the macropores are full is considered to be a strong limitation. Adapting the distribution of the rainfall excess to macropore infiltration as well as to surface runoff and simultaneously increasing both is recommended to improve the model.

Results of a simulation run without including sorptivity show an infiltration under dry circumstances which is much too low, so this process should certainly be used when modeling dry areas.

8 Synthesis

In view of worldwide problems of landscape degradation, flooding and solute transport it is important to correctly describe the main hydrological processes playing a role at different scales. Preferential flow is lately recognized to influence moisture distribution and hydrological fluxes at different scales. In this thesis the role of preferential flow from plot to catchment scale is investigated based on the analysis of a large amount of field measurements and hydrological modeling, of which the most important results are recalled here. Then an overall discussion follows of these results. This is completed by some recommendations for future research.

8.1 Main results of this study

In a small (approximately 1 km^2), clearly delimited semi-arid experimental catchment "Parapuños"in the Extremadura (Spain) the role of preferential flow was intensively studied and measured:

- at eighteen sites small scale tracer infiltration experiments were performed with at each sites additional measurements of initial moisture content, texture, porosity, bulk density, hydraulic conductivity, vegetation cover, slope and stoniness;
- at six sites, three per hillslope, soil pits were filled with TDR sensors and were monitored to follow the moisture distribution in the soil profiles going from dry to wet period. In the vicinity of the soil pits piezometer tubes were also installed and continuously monitored;
- the results of all measurements were analysed in combination with the rainfall, meteorology and discharge measurements of the study area.

The analysis of spatial soil moisture contents, piezometer water tables, rainfall and discharge measurements shows how the research catchment behaves in a hydrological sense (Chapter 4). A large system of connected macropores is found to rapidly fill up under high intensity rainfall events. When the catchment conditions are dry, the macropores drain mainly to the matrix and a portion of the infiltration water can reach the catchment gully as subsurface flow. Under very wet circumstances there is less infiltration from macropores to the matrix and most of the macropore water flows as subsurface flow towards the gully. The subsurface contribution to the discharge ranges between 13% for a large event of high intensity rainfall, with high discharge and 80% of total discharge for a small event with low intensity rainfall and low discharge. This percentage depends depends mainly on the surface runoff production, which suppresses the fraction of subsurface stormflow in the discharge during high intensity rainfall.

In Chapter 5 it was shown that preferential infiltration at plot scale occurs throughout the catchment. The degree of preferential flow was characterized using four parameters derived from dye-tracer infiltration patterns: depth of the uniform infiltration front, maximum infiltration

depth, total stained area and preferential flow fraction of stained area. Using multiple regression 50 to 66% of the spatial variability of these preferential flow parameters could be predicted using the local variables vegetation, texture, slope and location.

The plot scale preferential flow is simulated in Chapter 6 using SWAP (Kroes et al., 2008). The parameterization of macropores is derived by inverse modeling on dye-tracer infiltration patterns. The obtained preferential flow parameters are shown to perform well for the simulations of year round water balance. A comparison of these results to simulations without macropores, with high saturated conductivity values, shows that the macropore model performs better, mainly for topsoil moisture contents and runoff production. The wetting of the deeper layers is too slow for both the macropore model as well as the model without macropores.

Results of the catchment scale model Hilllow 3D (Bronstert, 1995), presented in Chapter 7, show that using a macropore flow model results in a good simulation of the high peaks and a slow hydrograph decline. The macropore volume used in the catchment scale modeling is however set to a very low value to ensure that the macropores are filled up under high intensity rainfall and thus surface runoff is generated. A comparison of some rainfall-discharge event simulations shows that the model with macropores gives very different results from the model without macropores, although both perform reasonably well on the basic simulations. It seems preferable to use a model that incorporates all important hydrological processes, like the macropore model does.

8.2 Preferential flow from plot scale to catchment scale

Macropore volume estimation from plot to catchment scale
Shipitalo and Butt (1999) and Weiler (2001) found that macropore geometry or volume and therefore flow capacity is usually not the limiting factor for infiltration or flow through macropores. Therefore it is interesting to compare the estimates of effective macropore volume at different scales using the results from this research. A first rough estimation of macroporosity can be obtained by subtracting the fitted saturated water content of the Multi Step Outflow experiments from the measured saturated water content (Table 3.6). This leads to an absolute volume of macropores of 0.01 to 0.06 cm^3/cm^3.

Using the relationship found in Chapter 4 (Figure 4.9) between subsurface stormflow production and the water level decrease in the piezometers a rough calculation can be made of the macropore volume (Table 8.1). This calculation is based on the macroporosity needed to generate the subsurface stormflow for the very wet catchment conditions, when we can assume that losses to bedrock storage and matrix are minimal. Herefore we roughly assume that only 10% of the whole catchment, i.e. the valley bottom nearest to the streams, would contribute to the rapid drainage shortly after rainfall stops. The contributing area of course does change in time, but for this rough calculation this is not taken into account. This macroporosity is based purely on the direct relationship between the streamflow and piezometer water level in the valley bottom. Areas further from the stream do also contribute to the streamflow, though slower and less direct, so this macroporosity is possibly overestimated. Nevertheless the values for

Table 8.1: Estimated effective macroporosity for different depths in the soil profile, inferred from the water table-discharge relationship.

Depth from soil surface (cm)	Macroporosity needed to generate streamflow (cm^3/cm^3)
30	0.025
40	0.013
50	0.011
60	0.007
70	0.005

macroporosity seem plausible. These values represent effective, i.e. connected macroporosity and are slightly lower than the absolute values of absolute macroporosity described above.

Comparing the estimated effective values of macroporosity from Table 8.1 with the SWAP model parameters for the plot scale, obtained by inverse modeling show a similar order of magnitude of macropore volumes (0.04 cm^3/cm^3 at soil surface in SWAP versus 0.025 cm^3/cm^3 at 30 cm depth, inferred from the water table – discharge relationship). Also there is a strong decrease of macroporosity with depth in both estimates. The total macropore depths obtained by the inverse modeling on dye-tracer infiltration profiles, are however underestimated. As can be seen in Table 8.1 the macroporosity probably extends much deeper than the maximum of 42 cm under soil surface which was found for the valley bottom profile. These macropore parameters were derived using field infiltration patterns and they do improve model results when compared to modeling with raised (effective) k-sat values. Nevertheless the method should still be improved as the macropore depth is slightly underestimated and resulting flow to deeper layers is still too slow in the simulations.

In the catchment scale modeling in Hillflow 3D, the macroporosity can not be varied with depth and the runoff starts only after macropores are full. Therefore, an average effective macroporosity has to be used for the full throughflow depth and the macropore volume has to be set to a very low value to ensure surface runoff. This macropore volume is required to run the model as it is, but does not represent the true distribution in the field.

The macropore models at plot scale and catchment scale need different levels of simplification. The macropore volume description with depth used in SWAP is detailed, while the macropore volume in Hillflow cannot be varied with depth. Also the manner of distributing infiltration excess to macropore infiltration and surface runoff affects the macropore parameterisation. Therefore even though the different models are physically based, the parameter values can differ and are not easily compared between models nor obtained directly from measurement values.

Preferential flow influence on water balance

Preferential flow influences all parts of the water balance: from infiltration and soil moisture content variability to subsurface stormflow and discharge. The plot scale total infiltration is enhanced by preferential flow. Preferential flow also influences the distribution of water in the soil profile. Through preferential infiltration a large volume of water is directly transported to deeper layers, bypassing the topsoil and entering the root zone of the deeper rooting plants. This

distribution therefore influences the water availablility for evapotranspiration. Also as seen in the SWAP modeling exercises the matrix conductivities for simulations with macropores are much lower than for simulations without macropores (the latter use effective average conductivities). Therefore drainage of the matrix is slower and thus water retention in the case of explicit preferential flow modeling is higher than in models without explicit preferential flow.

The infiltration patterns vary spatially. At a larger scale, the local preferential flow and its spatial distribution mainly influence the surface runoff production. In my opinion, in view of the decrease in effective macropore volume with increasing spatial scale, subsurface stormflow production probably depends more on the connectivity of preferential flow paths at hillslope scale than on the distribution of the local infiltration patterns and on the infiltration from macropores to matrix. The hilltop profiles for example show the deepest macropore infiltration patterns, but the piezometer pipes on the hilltop never showed any water layer occurrence, so there is probably never any lateral flow in the large porous network.

Water versus solute transport

This study focused on the influence of preferential flow on water transport. Preferential flow is shown to influence the water fluxes to the different hydrological components, from plot scale to catchment scale and from dry to wet catchment conditions. The extra parameters needed to include preferential flow in physically based models are however difficult to deduce from measurements. This can be a reason not to use these detailed models with a high amount of parameters but rather a much simplified model, with fast and slow reservoirs. However, as was shown in Chapters 6 and 7, the models including preferential flow generally perform better than the models without. When the preferential flow process is not explicitly included, the model should be calibrated to represent the measurements, but running scenarios might lead to large errors, as the processes are not well represented. It is often recognized that taking preferential flow into account for solute transport studies is even more important than for the water balance.

As mentioned in the first chapter of this thesis the chemical signature of discharge water is often used to perform a hydrograph separation and deduct the origin or flowpaths of the discharge water. The idea of using tracers to deduct flow pathways was often proposed in the course of this PhD. In my opinion however, the use of tracers may not be such a trivial method. As the preferential flow is expected to be even more important for solute transport than for water transport (Nielsen et al., 1986; Simunek et al., 2003; Christiansen et al., 2004), I would like to elaborate on my ideas of what to expect hypothetically when studying tracers in the discharge.

Under low soil moisture contents there may be a considerable amount of macropore flow which travels through the soil and contributes up to even 80 % of the discharge. The main movement of water is expected to find place from macropore to the dry matrix. In this case the mixing of macropore and matrix water due to dispersion and diffusion along the sides of the macropores will probably be negligible. Thus the water flowing through the macropores is likely to keep the rainfall signature when the soil matrix is completely dry. As the soils get wetter, there is less infiltration from macropores to matrix. The discharge thus increases. In the mean time the interaction (diffusion and dispersion) along the sides of the macropores also increases. This may lead to an increasingly old signature of the discharge water with increasing soil wetness. Thus

the signature of the discharge might depend not only on the mixing of surface and subsurface water, but also on the soil moisture conditions. Without the clear evidence provided in this thesis on the occurrence of rapid subsurface stormflow in macropores, the previously explained hypothetical discharge signatures may be wrongly interpreted. Under dry circumstances all discharge may be explained as surface runoff when it has the rainfall signature, while under wet circumstances the obtained soil water signature due to mixing along macropore sidewalls cannot rule out the theoretical explanation of a pressure wave which ensures a rapid release of riparian zone water to the stream. This shows how carefull one should be to deduct flowpaths purely based on chemical signature of the discharge water. It is in my opinion very important first to understand the hydrological system and then to use the chemical signature as extra proof.

Origin and function of preferential flow
This research focuses on the influence or result of preferential flow on the hydrology from plot scale to catchment scale, thereby mainly trying to discern the matrix flow from preferential flow. It is shown that for hydrological modeling the process of preferential flow should be taken into account explicitly for its influence on the flow pathways and on the water balance. In this synthesis I would like to take the opportunity to philosophise about the role/importance of the preferential flow process for the ecosystem. I explain how in my opinion the existence of preferential flow is of vital importance for the ecosystem.

Macropores are large pores in a soil originating from bioactivity and resulting in preferential flow pathways which allow for enhanced water and solute transport and a deep aeration of a soil profile. In enhancing the total infiltration into a soil profile preferential flow decreases the surface runoff and thereby decreases the erosion problems, which are important in semi-arid areas such as the study catchment. In the meanwhile distribution of water to deeper layers ensures moisture availability in the rootzones of the different vegetation layers: the grasses, shrubs and the trees. In case the water would infiltrate uniformly with an average effective conductivity, evapotranspiration in the toplayer could be much larger, decreasing moisture availability for the deeper rooting plants, especially trees. Also the occurrence of preferential flow paths enhancing infiltration and distributing the water over a larger soil depth, thereby allow the soil matrix conductivity to be low, without causing problems of flooding or severely limited infiltration, i.e. water availability. In the mean while the large pores can drain the soil preventing long term saturation, while the matrix with the slower conductivity can also retain its soil moisture for longer. Thus the coexistence of a rapid and a slow system can be very beneficious for the moisture and air conditions in the soil as opposed to one domain with average characteristics.

In summary the coexistence of a rapid macropore system and a slow matrix system is necessary to ensure a good water management and aeration in the soil profiles. In my opinion it is an important process not just for the hydrological balance and sustainability of a hillslope but also for the ecosystem. It is therefore important to include preferential flow in the prediction of future reactions to system disturbance in hydrological but also vegetation and ecological research.

8.3 Recommendations

In this research preferential flow is measured and parameterized from plot scale to catchment scale. The field measurements are used for the parameterisation of preferential flow models. Some rough estimates of the preferential flow can be made based on the field measurements. The most important conclusion based on the measurement analysis is that the lateral subsurface stormflow component due to preferential flow is seen to produce a large contribution to the catchment scale discharge even under completely unsaturated soil matrix conditions.

Though models including preferential flow perform better than models without, using field measurements for the parameterisation of such models remains an important challenge to improve in the future. Determination of the effective macropore volume at different scales is not trivial.

Also in view of hydrological scenario modelling, for landscape degradation, flood risk predictions, pollution modelling or agricultural practices it is important to see that the use of a preferential flow model as opposed to effective bulk hydraulic conductivity makes a large difference in predictions of water flow paths and fluxes, even when simulations of present day situations perform similarly well.

Finally though preferential flow occurrence is often seen as a problem, which results in rapid loss of nutrients or transport of solutes towards groundwater, its positive influence on soil moisture availability and aeration should not be forgotten. Therefore the focus should not be on how to change the flow paths or influence the preferential flow process, but rather how to cope with the results.

Abstract

Desertification and landscape degradation is a worldwide problem, which is expected to grow in time due to unsustainable land use and climate change. In view of these problems, knowledge of the interaction between vegetation, soil moisture and surface runoff, with subsequent erosion risk is essential. This requires mapping of the spatial and temporal variability of infiltration and runoff production. The influence of preferential flow thereupon is nowadays widely recognized. Therefore in this thesis the role of preferential flow from plot scale to catchment scale on the hydrology is investigated, using field measurements and model applications.

To start with a literature summary of the state of the art on preferential flow is given, including process descriptions, measurement methods and modeling concepts. In the next chapters the research catchment "Parapuños"(approximately 1 km^2) in the Extremadura (Spain) is described and an overview of the used measurement methods is given.

The measurement results show that preferential flow occurs throughout the catchment and at different scales. An elaborate analysis of the soil moisture content development, piezometer water-levels and rainfall – discharge relationships, leads to the conclusion that a large network of connected macropores exists. Rapid vertical as well as lateral flow through this network occurs, regardless of the matrix soil moisture conditions. This subsurface flow can contribute from 13% (under wet catchment conditions) up to 80% (under dry catchment conditions) of total discharge.

The spatial variability in preferential flow at the plot scale is deduced from dye-tracer infiltration experiments at 18 locations throughout the research catchment. Four characteristics of the stained infiltration patterns are described: the uniform infiltration depth, the maximum depth, the total stained area and the fraction of preferential infiltration. Per plot a large set of additional measurements were performed: porosity, bulk density, saturated conductivity, texture, vegetation, slope, stoniness, and geographical location. Using multiple regression, four of these site variables were found to explain most (50 – 66%) of the spatial variability in preferential flow: texture, vegetation, slope and geographical location. These site variables were used to generate a catchment map with preferential flow characteristics.

For local scale infiltration and runoff simulation, we used the ecohydrological model SWAP. Three of the infiltration plots were used to determine SWAP macropore parameters using inverse modeling. The infiltration patters can generally not be reproduced in the simulations without the macropore concept. Also for water balance modeling under natural circumstances, the macropore model leads to slightly better results for infiltration and surface runoff behavior, than the model with an "effective"measured average saturated conductivity.

For catchment scale modeling, the 3D macropore model Hillflow is used, which fits the conceptual behavior of the catchment. The results of this model are as good as the results of modeling without a macropore concept, but scenario runs with both models show large differences in rainfall- discharge relationships. This is a strong argument for the use of the model which better fits the real hydrological processes in the research area.

Samenvatting

De rol van macroporien stroming van punt schaal tot stroomgebiedsschaal
Een studie in een semi-aride gebied

Wereldwijd is verdroging en landschapsdegradatie een groot probleem, dat zich naar verwachting steeds verder uitbreidt door verkeerd landgebruik en door klimaatsverandering. Gezien deze problemen is kennis over de wisselwerkingen tussen vegetatie, bodemvochtverdeling en ook oppervlakte afstroming met daardoor veroorzaakte erosie risico essentieel. Daarom is het van groot belang de ruimtelijke en temporele variatie in infiltratie en oppervlakte afstroming goed in kaart te brengen. De invloed van preferente stroming daarop wordt steeds vaker erkend. Daarom wordt in dit proefschrift de rol van preferente stroming op de hydrologie van plot schaal tot stroomgebiedschaal onderzocht, aan de hand van veldmetingen en model toepassingen.

Om te beginnen wordt een literatuur overzicht gegeven van de huidige kennis van preferente stroming, van basis proces kennis tot meetmethoden en modelleren. In de volgende hoofdstukken wordt het onderzoeksgebied "Parapuños"(ongeveer 1km^2) in de Extremadura (Spanje) beschreven en een overzicht van de meetmethoden gegeven.

De meetresultaten laten zien dat preferente stroming in het hele stroomgebied voorkomt, op verschillende schalen. Een uitgebreide analyse van bodemvochtveranderingen, piezometerstanden- en neerslag-afvoer relaties, leidt vervolgens tot de conclusie dat er een groot aaneengeschakeld netwerk van macroporiën bestaat. Zowel verticale alsook laterale stroming door dit preferente netwerk treedt op ongeacht de matrix bodemvochttoestand en kan tussen de 13% (onder natte omstandigheden) tot 80% (onder droge omstandigheden) aan de totale gebiedsafvoer bijdragen.

De ruimtelijke variatie in preferente stroming op de plot schaal is afgeleid van gekleurde tracer-infiltratie profielen op 18 plots verdeeld door het gebied. Van de blauwgekleurde infiltratie patronen zijn vier karakteristieken beschreven: de uniforme infiltratie diepte, maximale diepte, totale gekleurde oppervlak en fractie preferente stroming. Per plot zijn ook een grote set locale variabelen gemeten: porositeit, bulk dichtheid, verzadigde doorlatendheid, textuur, vegetatie, helling, geografische locatie, stenigheid en helling. Met behulp van multipele regressie is vervolgens aangetoond dat de preferente stroming vooral beïnvloed wordt door de textuur, geografische locatie, helling en vegetatie, die samen 50 – 66% van de ruimtelijke variatie kunnen verklaren. Deze locale variabelen zijn vervolgens gebruikt om stroomgebiedkaarten te maken van de preferente stroming karakteristieken.

Voor de simulaties van locale infiltratie en oppervlakte afstroming is het ecohydrologische model SWAP gebruikt. Drie van de infiltratie patronen zijn gebruikt om door middel van inverse modelleren de macropore parameters van SWAP te vinden. Deze infiltratie is zonder macropore concept niet goed te simuleren en ook voor simulaties van de waterbalans onder natuurlijke omstandigheden geeft het gebruik van het macroporiën concept lichtelijk betere resultaten

voor de infiltratie en oppervlakte afstroming dan het gebruik van “effectieve”ofwel gemeten gemiddelde verzadigde doorlatendheden.

Voor de stroomgebiedmodellering is het 3D macropore model Hillflow gebruikt dat conceptueel past bij het hydrologisch functioneren van het proefgebied. De resultaten van dit model zijn even goed als de resultaten van het stroomgebiedmodelleren zonder macroporiën, maar scenario runs van een aantal extreme buien geven voor de conceptueel verschillende modellen zeer verschillende resultaten in neerslag-afvoer relaties. Dit is een sterk argument voor het gebruik van het model dat beter past bij de werkelijke hydrologische processen in het onderzoeksgebied.

References

Allen, R.G., Pereira, L.S., Raes, D. and Smith, M., 1998. Crop evapotranspiration. Guidelines for computing crop water requirements. Irrigation and Drainage Paper 56, FAO, Rome, Italy.

Amin, M.H.G., Chorley, R.J., Richards, K.S., Hall, L.D., Carpenter, T.A., Cislerova, M. and Vogel, T., 1997. Study of infiltration into a heterogeneous soil using magnetic resonance imaging. Hydrological Processes, 11: 471-483.

Andreini, M.S. and Steenhuis, T.S., 1990. Preferential paths of flow under conventional and conservation tillage. Geoderma, 46: 85-102.

Angulo-Jaramillo, R., Gaudet, J.-P., Thony, J.-L. and Vauclin, M., 1996. Measurement of hydraulic properties and mobile water content of a field soil. Soil Science Society of America Journal, 60 (3): 710-715.

Bauters, T.W.J., DiCarlo, D.A., Steenhuis, T.S. and Parlange, J.-Y., 1998. Preferential Flow in Water Repellent Sands. Soil Sci. Soc.Am. J. 62: 1185-1190.

Bauters, T.W.J., Steenhuis, T.S., DiCarlo, D.A., Nieber, J.L., Dekker, L.W., Ritsema, C.J., Parlange, J.-Y. and Haverkamp, R., 2000. Physics of Water Repellent Soils. J. Hydrol. 231-232: 233-243.

Beckers, J. and Alila, Y., 2004. A model of rapid preferential hillslope runoff contributions to peak flow generation in a temperate rainforest watershed. Water Resources Research 40. DOI:10.1029/2003WR002582.

Bell, J.P., Dean, T.J. and Baty, A.J.B., 1987. Soil moisture measurement by an improved capacitance technique, Part II. Field techniques, evaluation and calibration. J. of Hydrology. 93:79-90.

Beven, K., 2001. Rainfall-runoff modelling: the Primer. John Wiley & Sons Ltd.

Beven, K. and Freer, J., 2001. Equifinality, data assimilation, and uncertainty estimation in mechanistic modelling of complex environmental systems using the GLUE methodology, Journal of Hydrology, 249(1-4): 11-29.

Beven, K. and Germann, P., 1982. Macropores and water flow in soils. Water Resources Research, 18(5): 1311-1325.

Bishop, K., Seibert, J., Köhler, S. and Laudon, H., 2004. Resolving the Double Paradox of rapidly mobilized old water with highly variable responses in runoff chemistry. Hydrological Processes, 18: 185-189.

Bloem, E. 2008. Variation in space and time of water flow and solute transport in heterogeneous soils and aquifers: a new multi-compartment percolation sampler and a new parameterization of the spatio-temporal solute distribution. PhD thesis. Wageningen University and Research Centre, Wageningen, The Netherlands.

Boll, J., Steenhuis, T.S. and Selker, J.S., 1992. Fiberglass wicks for sampling of water and solutes in the vadose zone. Soil Science Society of America Journal, 56: 701-707.

Booltink, H.W.G. and Bouma, J., 1991. Physical and morphological characterization of bypass flow in a well-structured clay soil. Soil Science Society of America Journal, 55:1249 – 1254.

Booltink, H.W.G., Hatano, R. and Bouma, J., 1993. Measurement and simulation of bypass flow in a structured clay soil: a physiomorphological approach. J. Hydrol. 148: 149 – 168.

Bouma, J., 1991. Influence of soil macroporosity on environmental quality. Advances in Agronomy, 46: 1-37.

Bronstert, A., 1995. User manual for the HILLFLOW-3D Catchment Modelling System. Potsdam Institute for Climate Impact Research. Potsdam, Germany.

Bronstert, A., 1999. Capabilities and limitations of detailed hillslope hydrological modelling. Hydrological Processes 13: 21 – 48.

Bronstert, A. and Plate, E.J., 1997. Modelling runoff generation and soil moisture dynamics for hillslopes and micro-catchments. Journal of Hydrology, 198:177-195.

Brooks, E.S., 2003. Distributed hydrologic modeling of the eastern Palouse, Ph.D. dissertation, Univ. of Idaho, Moscow.

Burch, G.J., Moore, I.D. and Burns, J., 1989. Soil hydrophobic effects on infiltration and catchment runoff. Hydrological processes, 3: 211-222.

Buttle, J.M., 1994. Isotope hydrograph separations and rapid delivery of pre-event water from drainage basins. Progress in Physical Geography 18: 16 – 41.

Cameira, M.R., Ahuja, L., Fernando, R.M. and Pereira, L.S., 2000. Evaluating field measured soil hydraulic properties in water transport simulations using the RZWQM. Journal of Hydrology, 236(1-2): 78-90.

Cameron, D., 2001. The extent of desiccation near trees in a semi-arid environment. Geotechnical and Geological Engineering, 19: 357-370.

Cammeraat, L.H., 1992. Hydro-geomorfologic processes in a small forested sub-catchment: preferred flow-paths of water, Universiteit van Amsterdam, Amsterdam, 146 pp.

Cammeraat, L.H., 2004. Scale dependent thresholds in hydrological and erosion response of a semi-arid catchment in southeast Spain. Agriculture, Ecosystems & Environment, 104 (2): 317-332.

Cammeraat, L.H. and Imeson, A.C., 1999. The evolution and significance of soil-vegetation patterns following land abandonment and fire in Spain. CATENA, 37 (1-2): 107-127.

Ceballos, A. and Schnabel, S., 1998. Hydrological behaviour of a small catchment in the Dehesa landuse system (Extremadura, SW Spain). Journal of Hydrology, 210: 146-160.

Ceballos, A., Schnabel, S., Gomez-Amelia, D. and Cerdá, A., 1998. Relación entre la escala espacial y escorrentía superficial en una pequeña cuenca hidrográfica semiárida ante condiciones contrastadas de humedad del suelo (Extremadura, suroeste de España). Cuaternario y Geomorfología, 12(1-2): 63-75.

Cerdà, A., Schnabel, S., Ceballos A. and Gomez-Amelia, D., 1998. Soil hydrological response under simulated rainfall in the Dehesa land system (Extremadura, SW Spain) under drought conditions. Earth Surface Processes and Landforms, 23: 195-209.

Christiansen, J.S., Thorsen, M., Clausen, T., Hansen, S. and Refsgaard, J.C., 2004. Modelling of macropore flow and transport processes at catchment scale. Journal of Hydrology, 299(1-2): 136-158.

Corbett, E.S. and Crouse, R.P., 1968. Rainfall interception by annual grass and chaparral losses compared. US Forest Serv. Res. Paper PSW-48. Berkeley, California.

Cubera, E., Montero, M.J. and Moreno G., 2004. Effect of land use on soil water dynamics in Dehesas of Central-Western Spain. In: Sustainability of agrosilvopastoral systems – Dehesas, Montados – Advances in Geoecology, volume 37, Schnabel S, Ferreira A (eds). Catena Verlag, Reiskirchen.

Davison, A.C. and Hinkley, D.V., 1997. Bootstrap methods and their application. Cambridge Series in Statistical and Probabilistic Mathematics. Cambridge University Press, Cambridge, United Kingdom.

De Rooij, G.H., 1996. Preferential flow in water-repellent sandy soils- model development and lysimeter experiments., Wageningen University, Wageningen.

De Rooij, G.H., 2000. Modeling fingered flow of water in soils owing to wetting front instability: a review. Journal of Hydrology, 231-232: 277-294.

De Rooij, G.H. and F. Stagnitti. 2002. Spatial and temporal distribution of solute leaching in heterogeneous soils: analysis and application to multisampler lysimeter data. J. Contam. Hydrol., 54:329-346.

DeBano, L.F., 2000. Water repellency in soils: a historical overview. Journal of Hydrology, 231-232: 4-32.

Dekker, L.W. and Ritsema, C.J., 1994. How water moves in a water repellent sandy soil 1. Potential and actual water repellency. Water Resources Research, 30(9): 2507-2517.

Devesa Alcaraz, J.A., 1995. Vegetación y flora de Extremadura. Universitas, Badajoz, España.

Devitt, D.A. and Smith, S.D., 2002. Root channel macropores enhance downward movement of water in a Mojave Desert ecosystem. Journal of Arid Environments, 50: 99-108.

Diffenbaugh, Noah S., 2005. Sensitivity of extreme climate events to CO2-induced biophysical atmosphere-vegetation feedbacks in the western United States, Geophysical Research Letters, 32, L07702, doi:10.1029/2004GL022184.

Doerr, S.H., 1998. On standardising the water drop penetration time and the molarity of an ethanol droplet techniques to classify soil water repellency: a case study using medium textured soils. Earth surface processes and Landforms, 23: 663-668.

Doerr, S.H., Ferreira, A.J.D., Walsh, R.P.D., Shakesby, R.A., Leighton-Boyce, G. and Coelho, C.O.A., 2003. Soil water repellency as a potential parameter in rainfall-runoff modelling: experimental evidence at point to catchment scales from Portugal. Hydrological processes, 17(2): 363-377.

Doerr, S.H., Shakesby, R.A. and Walsh, R.P.D., 1996. Soil water repellency variations with depth and particle size fraction in burned and unburned Eucalyptus globulus and Pinus pinaster forest terrain in the Agueda basin, Portugal. Catena, 27(1): 25-47.

Doerr, S.H., Shakesby, R.A. and Walsh, R.P.D., 2000. Soil water repellency: its causes, characteristics and hydro-geomorphological significance. Earth Science Reviews 51: 33-65.

Doherty, J., 2004. PEST-Model-independent parameter estimation user's manual. 5th ed. Watermark Numerical Computing, Brisbane, Australia

Droogers, P., Stein, A., Bouma, J. and de Boer, G., 1998. Parameters for describing soil macroporosity derived from staining patterns. Geoderma, 83: 293 – 308.

eCognition, 2002. eCognition, User Guide. Definiens Imaging GmbH, eCognition, Munich.

Edwards, W.M., Shipitalo, M.J. and Owens, L.B., 1993. Gas, water and solute transport in soils containing macropores: a review of methodology. Geoderma 57: 31- 44.

Elsenbeer, H., Lack, A. and Cassel K., 1995. Chemical fingerprints of hydrological compartments and flow paths at La Cuenca, western Amazonia. Water Resources Research 31: 3051 – 3058.

Fannin, R.J., Jaakkola, J., Wilkinson, J.M.T. and Hetherington, E.D., 2000. Hydrologic response of soils to precipitation at Carnation Creek, British Columbia, Canada. Water Resources Research, 36(6): 1481-1494.

FAO, 1988. FAO-UNESCO Soil Map of the World. Technical report 60, FAO, Rome.

Ferreira, A.J.D., Coelho, C.O.A., Walsh, R.P.D., Shakesby, R.A., Ceballos, A. and Doerr, S.H., 2000. Hydrological implications of soil water-repellency in Eucalyptus globulus forests, north-central Portugal. Journal of Hydrology, 231-232: 165-177.

Feyen, H., 1998. Identification of runoff processes in catchments with a small scale topography. PhD thesis, ETHZ, Swiss federal institute of technology, Zurich.

Flühler, H., Durner, W. and Flury, M., 1996. Lateral solute mixing processes – A key for understanding field-scale transport of water and solutes. Geoderma, 70 (2-4): 165-183.

Flury, M. and Flühler, H., 1995. Tracer characteristics of Brilliant Blue FCF. Soil Science Society of America Journal, 59: 22-27.

Flury, M., Fluhler, H., Jury, W.A. and Leuenberger, J., 1994. Susceptibility of soils to preferential flow of water: a field study. Water Resources Research, 30(7): 1945-1954.

Forrer, I. N., Papritz, A., Kasteel, R., Flühler, H. and Luca, D., 2000. Quantifying dye tracer in soil profiles by image processing. European Journal of Soil Science, 51: 313-322.

García Navarro, A. and López Piñeiro, A., 2002. Mapa de suelos de la provincia de Cáceres. Escala 1:300,000, 119th Edition. Universidad de Extremadura, Cáceres.

German-Heins, J. and Flury, M., 2000. Sorption of Brilliant Blue FCF in soils as affected by pH and ionic strength. Geoderma, 97: 87-101.

Ghodrati, M. and Jury, W. A., 1990. A field study using dyes to characterise preferential flow of water. Soil Science Society of America Journal, 54: 1558-1563.

Hendrickx, J.M.H. and Flury, M., 2001. Uniform and preferential flow mechanisms in the vadose zone. In: Conceptual Models of Flow and Transport in the Fractured Vadose Zone, edited by National Research Council, National Academy Press, Washington DC, p. 149-187.

Hendriks, M.R., 1990. Regionalisation of hydrological data, effects on lithology and landuse on storm runoff in east Luxembourg, PhD-thesis, Vrije Universiteit, Amsterdam, 168 pp.

Hendriks, R.F.A., Oostindie, K. and Hamminga, P., 1999. Simulation of bromide tracer and nitrogen transport in cracked clay soil with the FLOCR/ANIMO model combination. J. Hydrol. 215: 94-115.

Herbst, M. and Diekkruger, B., 2003. Modelling the spatial variability of soil moisture in a micro-scale catchment and comparison with field data using geostatistics. Physics and Chemistry of the Earth, Parts A/B/C, 28(6-7): 239-245.

Herbst, M., Fialkiewicz, W., Chen, T., Pütz, T., Thiéry, D., Mouvet, C., Vachaud, G., and Vereecken, H., 2005. Intercomparison of flow and transport models applied to vertical drainage in cropped lysimeters. Vadose Zone Journal, 4:240-254.

Hillel, D. and Baker, R.S., 1988. A descriptive theory of fingering during infiltration into layered soils. Soil Science, 146:51-56.

Huisman, J.A., Hubbard, S.S., Redman, J.D. and Annan, A.P., 2003a, Measuring soil water content with Ground Penetrating Radar: a review. Vadose Zone Journal 2: 476-491.

Huisman, J.A., Snepvangers, J.J.J.C., Bouten, W. and Heuveling, G.B.M., 2003b, Monitoring temporal development of spatial soil water content variation:: comparison of ground-penetrating radar and time domain reflectometry. Vadose Zone Journal 2: 519-529.

IGME, 1987. Mapa geológico de españa, serie magna. hoja 679, Aldea de Trujillo.

Intergovernmental Panel on Climate Change, 2007. Climate change 2007. The physical Science Basis-summary for policy makers, Geneva Switserland.

Jaramillo, D.F., Dekker, L.W., Ritsema, C.J. and Hendrickx, J.M.H., 2000. Occurrence of soil water repellency in arid and humid climates. Journal of Hydrology, 231-232: 105-111.

Jarvis, N.J., 1998. Modeling the impact of preferential flow on nonpoint source pollution. In: Selim, H.M., Ma, L. (Eds.), Physical Nonequilibrium in Soils: Modeling and Application, Ann Arbor Press, Chelsea, MI, pp. 195 – 221.

Joffre, R. and Rambal, S., 1988. Soil water improvement by trees in the rangelands of southern Spain. Oecology Plantarum, 9: 405-422.

Joffre, R. and Rambal, S., 1993. How tree cover influences the water balance of Mediterranean rangelands. Ecology 74(2): 570-582.

Jones, J. P., Sudicky, E.A. and McLaren, R.G., 2008. Application of a fully-integrated surface-subsurface flow model at the watershed-scale: A case study, Water Resour. Res., 44, W03407, doi:10.1029/2006WR005603.

Jones, J.A.A., 1997. Pipe flow contributing areas and runoff response. Hydrological Processes, 11: 35 – 41.

Jones, J.A.A. and Connelly, L.J., 2002. A semi-distributed simulation model for natural pipeflow. Journal of Hydrology 262: 28-49.

Jones, S.B., Wraith, J.M. and Or, D., 2002. Time domain reflectometry measurement principles and applications. Hydrological Processes, 16(1): 141-153.

Ju, S.H. and Kung, K.J.S., 1997a. Impact of Funnel Flow on Contaminant Transport in Sandy Soils: Numerical Simulation.. Soil Science Society America Journal, 61: 409 – 415.

Ju, S.H. and Kung, K.J.S., 1997b. Steady-State Funnel Flow: Its Characteristics and Impact on Modeling. Soil Science Society America Journal, 61: 416 – 427.

Kelleners, T.J., Seyfried, M.S., Blonquist, J.M., Bilskie, J. and Chandler, D.G., 2005. Improved interpretation of water content reflectometer measurements in soils. Soil Science Society Of America Journal, 69(6): 1684-1690.

Ketelsen, H. and Meyer-Windel S., 1999. Adsorption of brilliant blue FCF by soils. Geoderma, 90: 131-145.

Kirchner, J.W., 2003. A double paradox in catchment hydrology and geochemistry. Hydrol. Process. 17, 871 – 874.

Kitahara, H., Shimizu, A. and Mashima, Y., 1988. Characteristics of pipe flow in a subsurface soil layer of a gentle hillside. J. Japan. For. Soc. 70, 318-323.

Kohl, R.A. and Carlson, C.G., 1997. Volumetric sampling of soil water flow using wicks. Transactions of the ASAE, 40 (5): 1373-1376.

Koorevaar, P., Menelik, G. and Dirksen, C., 1983. Elements of soil physics: Developments in Soil Science, 13. Elsevier, Amsterdam/Oxford/New York/Tokyo, 228 pp.

Kroes, J.G., Van Dam, J.C., Groenendijk, P., Hendriks, R.F.A. and Jacobs, C.M.J., 2008. SWAP version 3.2. Theory description and user manual. Alterra Report 1649. Alterra. Wageningen, Netherlands.

Kung, K.-J.S., Hanke, M., Helling, C.S., Kladivko, E.J., Gish, T.J., Steenhuis, T.S. and Jaynes, D.B., 2005. Quantifying Pore-Size Spectrum of Macropore-Type Preferential Pathways. Soil Sci. Soc. Am. J. 69: 1196 – 1208.

Kung, K-J.S., 1990. Preferential flow in a sandy vadose zone: 1. field observation & 2. mechanism and implications. Geoderma 46: 51-71.

Kung, K-J.S., 1993. Laboratory observation of the funnel flow mechanism and its influence on solute transport. J. Environ. Qual. 22:91-102.

Lark, R.M., Bishop, T.F.A. and Webster, R., 2007. Using expert knowledge with control of false discovery rate to select regressors for prediction of soil properties. Geoderma, 138 (1-2): 65-78.

Larsbo, M. and Jarvis, N., 2005. Simulating solute transport in a structured field soil: uncertainty in parameter identification and predictions. Journal of Environmental Quality, 34:621-634.

Larsbo, M. and Jarvis, N., 2003. Macro 5.0. A model of water flow and solute transport in macroporous soil. Technical description. Studies in the Biogeophysical Environment, Emergo 2003: 6, 48p.

Léonard, J., Esteves, M., Perrier, E. and de Marsily, G., 1999. A spatialized overland flow approach for the modelling of large macropores influence on water infiltration. International Workshop of EurAgEng's Field of Interest on Soil and Water, Leuven, 313-322.

Léonard, J., Perrier, E. and De Marsily, G., 2001. A model for simulating the influence of a spatial distribution of large circular macropores on surface runoff. Water Resources Research, 37: 3217 – 3225.

Letey, J. 1969. Measurements of contact angle, water drop penetration time and critical surface tensions. p. 43 – 47. *In* Proc. Symp. Water Rep. Soils, 6 – 10 May 1968. University of California Riverside, CA.

Llorens, P. and Domingo, F., 2007. Rainfall partitioning by vegetation under Mediterranean conditions. A review of studies in Europe. Journal of Hydrology 335: 37-54.

Logsdon, S.D., 1995. Flow mechanisms through continuous and buried macropores. Soil Science, 160, 237 – 242.

Logsdon, S.D., 2002. Determination of Preferential Flow Model Parameters. Soil Science Society of America Journal, 66: 1095-1103.

Ludwig, R., Gerke, H.H. and Wendroth, O., 1999. Describing water flow in macroporous field soils using the modified macro model. Journal of Hydrology, 215(1-4): 135-152.

Ma, L. and Selim, H.M., 1997. Physical nonequilibrium modeling approaches to solute transport in soils. Advances in Agronomy, 58: 95-150.

Malicki, M.A., Plagge, R. and Roth, C.H., 1996. Improving the calibration of dielectric TDR soil moisture determination taking into account the solid soil. European Journal of Soil Science, 47: 357 – 366.

Mallants, D., Jacques, D., Tseng, P.H., Van Genuchten, Th. and Feyen, J., 1997a. Comparison of three hydraulic property measurement methods. Journal of Hydrology, 199: 295-318.

Mallants, D., Mohanty, B.P., Vervoort, A. and Feyen, J., 1997b. Spatial analysis of saturated hydraulic conductivity in a soil with macropores. Soil Technology, 10: 115-131.

Maneta, M.P., 2006. Modeling of the hydrologic processes in a small semi-arid catchment. Geografia y ordenacion del territorio, Caceres, University of Extremadura, Spain.

Maneta, M.P., Schnabel, S. and Jetten, V.G., 2008. Continuous spatially distributed simulation of surface and subsurface hydrological processes in a small semi-arid catchment. Hydrological Processes, 22(13): 2196-2214.

Marañón, T., 1985. Diversidad florística y heterogeneidad ambiental en una dehesa de Sierra Morena. Anales de Edafología y Agrobiología 44: 1183 – 1197.

Martín Vicente, A. and Fernández Alés, R., 2006. Long term persistence of dehesas. Evidences from history. Agroforestry systems. 67: 19-28.

Mateos, B. and Schnabel, S., 2002. Rainfall interception by holm oaks in mediterranean open woodland. In: Environmental change and Water Sustainability, García-Ruiz, J.M., Jones, J.A.A. and Arnáez, J. (eds). Instituto Pirenaico de Ecología. Zaragoza, Spain.

Mertens, J., Tuts, V., Diels, J., Vanderborght, J., Feyen, J. and Merckx, R., 2008. Design and testing of a drop counter for use in Vadose zone water samplers. Vadose Zone J. 7:434-438.

Molz, F. J., Rajaram, H. and Lu, S., 2004. Stochastic fractal-based models of heterogeneity in subsurface hydrology: Origins, applications, limitations, and future research questions, Rev. Geophys., 42, RG1002, doi:10.1029/2003RG000126.

Montero, M.J., Obrador, J.J., Cubera, E. and Moreno, G., 2004. The role of Dehesa landuse on water status in Central-Western Spain. In: Sustainability of Agrosilvopastoral systems – Dehesas, Montados -Schnabel S, Ferreira A (eds),. Advances in Geoecology. Catena Verlag GMBH, Reiskirchen.

Moreno, G., Obrador, J.J., Cubera, E. and Dupraz, C., 2005. Fine root distribution in Dehesas of Central-Western Spain. Plant and Soil 277(1 – 2): 153 – 162.

Mualem, Y., 1974. A conceptual model of hysteresis. Water Resources Research, 10: 514-520.

Nearing, M. A., Jetten, V., Baffaut, C., Cerdan, O., Couturier, A., Hernandez, M., Le Bissonnais, Y., Nichols, M.H., Nunes, J.P., Renschler, C.S., Souchere, V. and van Oost, K., 2005. Modeling response of soil erosion and runoff to changes in precipitation and cover. Catena, 61(2-3): 131-154.

Negishi, J.N., Sidle, R.C., Ziegler, A.D., Noguchi, S. and Abdul Rahim, N., 2008. Contribution of intercepted subsurface flow to road runoff and sediment transport in a logging-disturbed tropical catchment. Earth Surface Processes and Landforms, 33:8, pp. 1174-1191.

Nguyen, H.V., Nieber, J.L., Ritsema, C.J., Dekker, L.W. and Steenhuis, T.S., 1999. Modeling gravity driven unstable flow in a water repellent soil. Journal of Hydrology, 215(1-4): 202-214.

Nieber, J.L., 1996. Modeling finger development and persistence in initially dry porous media. Geoderma, 70(2-4): 207-229.

Nieber, J.L., Bauters, T.W.J., Steenhuis, T.S. and Parlange, J.-Y., 2000. Numerical simulation of experimental gravity-driven unstable flow in water repellent sand. Journal of Hydrology, 231-232: 295-307.

Niehoff, D., Fritsch, U. and Bronstert, A., 2002. Land-use impacts on storm-runoff generation: Scenarios of land-use change and simulation of hydrological response in a meso-scale catchment in SW-Germany. Journal of Hydrology, 267(1-2): 80-93.

Nielsen, D.R., van Genuchten, M.Th. and Biggar, J.W., 1986. Water flow and solute transport processes in the unsaturated zone. Water Resources Research, 22 (9): 89 – 108.

Nijland, W., Van der Meijde, M., Addink, E.A., De Jong, S.M. and Van der Meer, F.D., 2009. Detecting soil water use by Mediterranean vegetation on rocky soils using electrical resistivity tomography. Geophysical Research Abstracts, Vol. 11, EGU2009-7067.

Öhrstrom, P., Persson, M., Albergel, J., Zante, P., Nasri, S., Berndtsson, R. and Olsson, J., 2002. Field-scale variation of preferential flow as indicated from dye coverage. Journal of Hydrology, 257: 164-173.

Overmeeren, R.A. van, Sariowan, S.V. and Gehrels, J.C., 1997, Ground penetrating radar for determining volumetric soil water content; results of comparative measurements at two test sites. Journal of Hydrology, 197: 316-338.

Paola, C., Foufoula-Georgiou, E., Dietrich, W.E., Hondzo, M., Mohrig, D., Parker, G., Power, M. E., Rodriguez-Iturbe, I., Voller, V. and Wilcock, P., 2006. Toward a unified science of the Earth's surface: opportunities for synthesis among hydrology, geomorfology, geochemistry and ecology. Water Resources Research, 42.

Perillo, C., Gupta, S., Nater, E. and Moncrief, J., 1998. Flow velocity effects on the retardation of FD&C blue no. 1 food dye in soil. Soil Science Society of America Journal, 62(1): 39-45.

Perillo, C.A., Gupta, S.C., Nater, E.A. and Moncrief, J.F., 1999. Prevalence and initiation of preferential flow paths in a sandy loam with argillic horizon. Geoderma, 89: 307-331.

Perret, J., Prasher, S. O., Kantzas, A. and Langford, C., 1999. Three-dimensional quantification of macropore networks in undisturbed soil cores. Soil Science Society of America Journal, 63: 1530-1543.

Philip, J.R., 1957. The theory of infiltration: 4. Sorptivity and algebraic infiltration equations. Soil Science 84, 264-275.

Plieninger, T. and Wilbrand, C., 2001. Land use, biodiversity conservation and rural development in the dehesas of Cuatro Lugares, Spain. Agroforestry Systems, 51: 23 – 34.

Raats, P.A.C. 1973. Unstable wetting fronts in uniform and non-uniform soils. Soil Science Society America Proceedings, 37:681-685.

Richards, B.G., Petev, P. and Emerson, W.W., 1983. The effects of vegetation on the swelling and shrinking of soils in Australia. Geotechnique, 33(2): 127-139.

Ringrose-Voase, A.J., 1996. Measurement of soil macropore geometry by image analysis of sections through impregnated soil. Plant andSoil, 183: 27-47.

Ritsema, C.J. and Dekker, L.W., 1994. How water moves in a water repellent sandy soil 2. dynamics of fingered flow. Water Resources Research, 30(9): 2519-2531.

Ritsema, C.J. and Dekker, L.W., 1996. Influence of sampling strategy on detecting preferential flow paths in water-repellent sand. Journal of Hydrology, 177(1-2): 33-45.

Ritsema, C.J. and Dekker, L.W., 2000. Preface. Journal of Hydrology, 231-232.

Ritsema, C.J., Dekker, L.W., Nieber, J.L. and Steenhuis, T.S., 1998. Modeling and field evidence of finger formation and finger recurrence in a water repellent sandy soil. Water Resources Research, 34(4): 555-567.

Robinson, D.A., Campbell, C.S., Hopmans, J.W., Hornbuckle, B.K., Jones, S.B., Knight, R., Ogden, F., Selker, J. and Wendroth, O., 2008. Soil Moisture Measurement for Ecological and Hydrological Watershed-Scale Observatories: A Review. Vadose Zone J., 7: 358-389.

Robinson, D.A., Jones, S.B., Wraith, J.M., Or, D. and Friedman, S.P., 2003. A review of advances in dielectric and electrical conductivity measurement in soils using time domain reflectometry. Vadose Zone Journal, 2: 444-475.

Roth, C.H., Malicki, M.A. and Plagge, R., 1992. Empirical evaluation of the relationship between soil dielectric constant and volumetric water content and the basis for calibrating soil moisture measurements by TDR. Journal of Soil Science, 43: 1 – 13.

Roulier, S. and Jarvis, N., 2003. Analysis of inverse procedures for estimating parameters controlling macropore flow and solute transport in the dual-permeability model MACRO. Vadose Zone Journal. 2:349-357.

Roulier, S. and Schulin, R., 2008. Guest Editor´s preface to special issue on preferential flow. European Journal of Soil Science, 59 (1).

Scherrer, S., Naef, F., Faeh, A.O. and Cordery, I., 2007. Formation of runoff at the hillslope scale during intense precipitation. Hydrology and Earth System Sciences 11: 907-922.

Schnabel, S. and Ferreira, A.J.D., (Editors) 2004. Sustainability of Agrosilvopastoral systems -Dehesas, Montados-. Advances in Geoecology, 37. Catena Verlag GMBH, Reiskirchen, Germany.

Schnabel, S., 1997. Soil erosion and runoff production in a small watershed under silvo-pastoral landuse (Dehesas) in Extremadura, Spain, PhD-thesis, Geoforma Ediciones, Logroño, Spain.

Schnabel, S., 1998. La precipitaci´on como factor en los procesos hidrol´ogicos y erosivos. In: Schnabel, S., G´omez-Amelia, D., Ceballos, A. (Eds.), Norba. Revista de Geografía. Vol. 10. Universidad de Extremadura, Cáceres.

Schnabel, S., Gómez, D. and Ceballos, A., 1998. Extreme events and gully erosion, Commission on land degradation and desertification. Proceedings of "Land degradation and desertification", Spain-Portugal.

Schwartz, R.C., McInnes, K.J., Juo, A.S.R. and Cervantes, C.E., 1999. The vertical distribution of a dye tracer in a layered soil. Soil Science, 164: 561-573.

Selker, J.S., Steenhuis, T.S. and Parlange, J.-Y., 1996. An engineering approach to fingered vadose pollutant transport. Geoderma, 70(2-4): 197-206.

Shipitalo, M.J. and Butt, K.R., 1999. Occupancy and geometrical properties of Lumbricus terrestris L. burrows affecting infiltration. Pedobiologia, 43: 782-794.

Sidle, R.C., Noguchi, S., Tsuboyama, Y. and Laursen, K., 2001. A conceptual model of preferential flow systems in forested hillslopes: evidence of self organization. Hydrological Processes, 15: 1675-1692.

Simunek, J., Jarvis, N.J., van Genuchten, M.T. and Gardenas, A., 2003. Review and comparison of models for describing non-equilibrium and preferential flow and transport in the vadose zone. Journal of Hydrology, 272(1-4): 14-35.

Sofo, A., Manfreda,S., Dichio, B., Fiorentino, M. and Xilyannis, C., 2008. The Olive tree: a paradigm for drought tolerance in Mediterranean climates. HESS, 12: 293-301.

Sonneveld, M.P.W., Backx, M.A.H.M. and Bouma, J., 2003. Simulation of soil water regimes including pedotransfer functions and land-use related preferential flow. Geoderma, 112(1-2): 97-110.

StatSoft Inc. 2004. Statistica. http://www.statsoft.com/textbook/stathome.html.

Steenhuis, T.S, Ritsema, C.J. and Dekker, L.W., 1996. Introduction. Geoderma, 70 (2-4).

Steenhuis, T.S., Boll, J., Shalit, G., Selker, J.S. and Merwin, I.A., 1994. A simple equation for predicting preferential flow solute concentrations. Journal of environmental quality, 23: 1058 – 1064.

Topp, G.C., Davis, J.L. and Annan, A.P., 1980. Electromagnetic Determination of Soil Water Content: Measurements in Coaxial Transmission Lines. Water Resources Research, 16(3): 574-582.

Trojan, M. and Linden, D., 1992. Micro relief and rainfall effects on water and solute movement in earthworm burrows. Soil Science Society of America Journal, 56: 727-733.

Tromp-van Meerveld H.J. and McDonnell, J.J., 2006. Threshold relations in subsurface stormflow: 2. the fill and spill hypothesis. Water Resources Research, 42. DOI: 10.1029/2004WR003778.

Tromp-van Meerveld H.J. and Weiler, M., 2008. Hillslope dynamics modeled with increasing complexity. Journal of Hydrology, 361: 24-40.

Tsuboyama, Y., Sidle, R.C., Noguchi, S. and Hosada, I. 1994. Flow and transport through the soil matrix and macropores of a hillslope segment. Water Resources Research., 30(4): 879-890.

Uchida, T., 2004. Clarifying the role of pipe flow on shallow landslide initiation. Hydrological Processes, 18(2): 375-378.

Uchida, T., Tromp-van Meerveld, H.J. and McDonnell, J.J., 2005. The role of lateral pipe flow in hillslope runoff response: an intercomparison of non-linear hillslope response. Journal of Hydrology, 311: 117-133.

Van Beek, L.P.H. and Van Asch, T.W.J., 1999. A combined conceptual model for the effect of fissure -Induced infiltration on slope stability. In: Process Modelling and Landform Evolution, Hergarten, S., Neugebauer, H., (eds), Springer-Verlag: New York; 147-169.

Van Dam, J.C., 2000. Field-scale water flow and solute transport. SWAP model concepts, parameter estimation, and case studies. PhD-thesis Thesis, Wageningen University, Wageningen, 167 pp.

Van Dam, J.C., de Rooij, G.H. and Heinen, M. 2004. Concepts and dimensionality in modeling unsaturated water flow and solute transport. In: Unsaturated-zone modeling± progress, challenges and applications. Feddes,, R.A., de Rooij,, G.H., and van Dam, J.C.. Wageningen UR Fontis series (vol. 6), Kluwer Academic Publishers, Dordrecht.

Van Dam, J.C., Stricker, J.N.M. and Droogers, P., 1994. Inverse method to determine soil hydraulic functions from Multistep Outflow Experiments. Soil Science Society of America Journal, 58 (3): 647-652.

Van Genuchten, M.Th., 1980. A Closed-form Equation for Predicting the Hydraulic Conductivity of Unsaturated Soils. Soil Science Society of America Journal, 44: 892-898.

Van Stiphout, T.P.J., van Lanen, H.A.J., Boersma, O.H. and Bouma, J., 1987. The effect of bypass flow and internal catchment of rain on the water regime in a clay loam grassland soil. Journal of Hydrology, 95: 1-11.

Vanclooster, M., Boesten, J.J.T.I., Trevisan, M., Brown, C.D., Capri, E., Eklo, O.M., Gottesburen, B., Gouy, V. and van der Linden, A.M.A., 2000. A European test of pesticide-leaching models: methodology and major recommendations. Agricultural Water Management 44(1-3):1-19.

Vilholth, K., Jensen, K. and Frederica, J., 1998. Flow and transport processes in a macroporous subsurface drained glacial till soil: 1. field investigation. Journal of Hydrology, 207: 98-120.

Walter, M.T., Kim, J.-S., Steenhuis, T.S., Parlange, J.-Y., Heilig, A., Braddock, R.D., Selker, J.S. and Boll, J., 2000. Funneled flow mechanisms in a sloping layered soil: Laboratory investigation. Water Resources Research, 36 (4): 841-849.

Watson, C.L. and J. Letey. 1970. Indices for characterizing soil-water repellency based upon contact angle-surface tension relationships. Soil Sci. Soc. Am. Proc. 34:841 – 844.

Weiler, M. 2001. Mechanisms controlling macropore flow during infiltration, dye tracer experiments and simulations. PhD-thesis, ETHZ, Swiss federal institute of technology, Zurich.

Weiler, M., 2005. An infiltration model based on flow variability in macropores: development, sensitivity analysis and applications. Journal of Hydrology 310: 294-315.

Weiler, M. and McDonnell, J.J., 2007. Conceptualizing lateral preferential flow and flow networks and simulating the effects on gauged and ungauged hillslopes, Water Resour. Res., 43, W03403, doi:10.1029/2006WR004867.

Weiler, M. and Naef, F., 2003a. An experimental tracer study of the role of macropores in infiltration in grassland soils. Hydrological Processes, 17: 477-493.

Weiler, M. and Naef, F., 2003b. Simulating surface and subsurface initiation of macropore flow. Journal of Hydrology, 273: 139-154.

Weiler, M., McDonnell, J.J., Tromp-van Meerveld, I. and Uchida, T., 2005. Subsurface stormflow. Encyclopedia of Hydrological Sciences.

Weiler, M., Uchida, T. and McDonnell, J.J., 2003. Connectivity due to preferential flow controls water flow and solute transport at the hillslope scale. In: Proceedings of MODSIM 2003, Townsville, Australia.

Zehe, E. and Flühler, H., 2001. Slope scale variation of flow patterns in soil profiles. Journal of Hydrology, 247: 116-132.

Zehe, E., Maurer, T., Ihringer, J. and Plate, E., 2001. Modeling Water Flow and Mass Transport in a Loess Catchment. Phys. Chem. Earth (B), 26 (7-8): 487-507.

Zehe, E., Becker, R., Bardossy, A. and Plate, E., 2005. Uncertainty of simulated catchment sale runoff response in the presence of threshold processes: role of initial soil moisture and precipitation. Journal of Hydrology, 315 (1-4):183-202.

Zehe, E., Lee, H. and Sivapalan, M., 2006. Dynamical process upscaling for deriving catchment scale state measures and constitutive relations for meso-scale process models. Hydrol. & Earth Syst. Sci. 10, 981 – 996

Zhang, G. P., Savenije, H. H. G., Fenicia, F. and Pfister, L., 2006. Modelling subsurface storm flow with the Representative Elementary Watershed (REW) approach: application to the Alzette River Basin, Hydrol. Earth Syst. Sci., 10: 937-955.

Zurmuhl, T. and Durner, W., 1996. Modeling transient water and solute transport in a biporous soil. Water Resources Research, 32(4): 819-829.

Curriculum Vitae

Loes van Schaik was born on the 9th of June 1976 in Chitokoloki, Zambia. After moving several times (a few years in Malawi and a few in Tanzania), the van Schaik family settled in Wageningen, in the Netherlands, in the summer of 1987. From 1988-1994 Loes attended the Marnix College (Grammar School) in Ede. She spent one year in Paris as an "au pair"for a family of four children. Then it was back to Wageningen to study "Soil, Water and Atmosphere", and specialise in Hydrology. After the Bachelor she took a year off to work on a small scale development project in La Joya, Mexico. For the Masters degree she enjoyed the opportunity to explore different branches in Hydrology doing one internship at Alterra on agrohydrological modelling, another internship at the University of Cordoba in Spain on modelling gully erosion, a master thesis on ecohydrology and water management and finally the main thesis on Soil Physics, which she graduated on in June 2002. After one year of searching for the perfect job she started off on this PhD research in the Department of Physical Geography in Utrecht, in June 2003. From the 1st of June 2009 she is working on a postdoc position in the department of Geoecology at the University of Potsdam, within the Biopore project.

Scientific presentations

Scientific articles:

Van Schaik, N.L.M.B., S. Schnabel and V.G. Jetten. 2008. The influence of preferential flow on hillslope hydrology in a semi-arid watershed (in the Spanish Dehesas). Hydrological Processes, 22: 3844-3855.

Van Schaik, N.L.M.B.. 2009. Spatial variability of infiltration patterns related to site characteristics in a semi-arid watershed. Catena, 78: 36-47.

Van Schaik, N.L.M.B., Hendriks, R.F.A., and van Dam, J.C., *accepted*. Use of dye-tracer infiltration patterns for the macropore parameterization of a physically based model (SWAP). Vadose Zone Journal.

Van Schaik, N.L.M.B., *in preparation*. Catchment scale modelling of macropore flow, using field data and an adapted version of the physically based Hillflow 3D model.

Other articles/reports:

Van Schaik, N.L.M.B., 2006. De invloed van preferente stroming in onverzadigde zone op de waterbalans- van processchaal naar stroomgebiedsschaal. Stromingen, 12 (3): 47-54.

Van Schaik, N.L.M.B., 2002. Exploratory analysis of temporal and spatial drainage distribution data. MSc thesis, Wageningen University.

Van Schaik, N.L.M.B., 2001. Nutriëntenhuishouding van het Merkske, onderzoek ter ondersteuning van natuurontwikkelingsplannen in een bijzonder beekdallandschap. MSc thesis. TNO-rapport NITG 01-018-A. NITG-TNO, Utrecht, Nederland.

Van Schaik, N.L.M.B., 2000. Simulatie van bodemvocht en maïsopbrengst in verdichte zandbodem bij Westerhoven. Verkennende berekeningen. Internship report. Wageningen

Van Schaik, N.L.M.B., 2000. Modelleren van geulenvorming op proefboerderij Fuente Asnera, provincie Córdoba, Spanje. Internship report. Wageningen

Oral Presentations and Posters:

Van Schaik, N.L.M.B. (2009). Preferential flow from plot scale to cacthment scale in a semi-arid catchment. Oral presentation, abstract in: *Geophysical Research Abstracts*. Vienna, Austria: European Geosciences Union (EGU).

Van Schaik, N.L.M.B., J.C. van Dam, and R.F.A Hendriks (2009). Use of dye-tracer infiltration patterns for the macropore parameterization of a physically based model (SWAP). Poster presentation, abstract in: *Geophysical Research Abstracts*. Vienna, Austria: European Geosciences Union (EGU).

Van Schaik, N.L.M.B. (2009). Runoff simulations using a physically based hydrological model for a semi-arid catchment in the Spanish Dehesas. Poster presentation, abstract in: *Geophysical Research Abstracts*. Vienna, Austria: European Geosciences Union (EGU).

Van Schaik, N.L.M.B. (2008). Preferential Flow from plot scale to catchment scale: a case study. Invited lecture, Delft, The Netherlands.

Van Schaik, N.L.M.B. (2008). Preferential Flow from plot scale to catchment scale: a case study. Guest lecture, Wageningen, The Netherlands.

Van Schaik, N.L.M.B., Hendriks, R.F.A. & Van Dam, J.C. van (2007). Determination of matrix and macropore flow characteristics (using infiltration profiles and inverse modelling in SWAP). Oral presentation, abstract in: *Geophysical Research Abstracts*. Vienna, Austria: European Geosciences Union (EGU).

Van Schaik, N.L.M.B. (2006). Spatial variability of preferential flow related to site characteristics in a DEHESA catchment. Oral presentation. Monte Veritá, Switzerland, 4-9 November 2006.

Van Schaik, N.L.M.B., Jetten, V.G., De Jong, S.M, Ritsema, C., and Van Dam, J.C. (2005). The influence of Preferential Flow at Catchment Scale. Poster presentation, abstract in: *Geophysical Research Abstracts.* Vienna-Austria: European Geosciences Union (EGU).

De Jong, S.M., Jetten, V.G., Van Asch, Th.W.J., Ritsema, C., Van Dam, J.C., and Van Schaik, N.L.M.B. (2004). Assessment of the influence of preferential flow on the water balance at catchment scale. Poster presentation, abstract in: *Geophysical Research Abstracts*. Nice – France: European Geosciences Union (EGU).

NEDERLANDSE GEOGRAFISCHE STUDIES / NETHERLANDS GEOGRAPHICAL STUDIES

355 W BORREN Carbon exchange in Western Siberian watershed mires and implication for the greenhouse effect; A spatial temporal modeling approach -- Utrecht 2007: Knag/Faculteit Geowetenschappen Universiteit Utrecht. 125 pp, 36 figs, 17 tabs. ISBN: 978-90-6809-396-4, Euro 13,00

356 S O NEGRO Dynamics of technological innovation systems; The case of biomass energy -- Utrecht 2007: Knag/Copernicus Institute. 166 pp, 24 figs, 17 tabs. ISBN: 978-90-6809-397-1, Euro 18,00

357 R NAHUIS The politics of innovation in public transport; Issues, settings and displacements -- Utrecht 2007: Knag/Copernicus Institute. 184 pp, 9 figs, 40 tabs, 4 box. ISBN 978-90-6809-398-8, Euro 20,00

358 M STRAATSMA Hydrodynamic roughnesses of floodplain vegetation; Airborne parameterization and field validation -- Utrecht 2007: Knag/Faculteit Geowetenschappen Universiteit Utrecht. 180 pp, 55 figs, 28 tabs. ISBN: 978-90-6809-399-5, Euro 23,00

359 H KRUIZE On environmental equity; Exploring the distribution of environment quality among socio-economic categories in the Netherlands -- Utrecht 2007: Knag/Copernicus Institute. 219 pp, 76 figs, 25 tabs. ISBN: 978-90-6809-401-5, Euro 25,00

360 T VAN DER VALK Technology dynamics, network dynamics and partnering; The case of Dutch dedicated life sciences firms -- Utrecht 2007: Knag/Copernicus Institute. 143 pp, 23 figs, 25 tabs. ISBN: 978-90-6809-402-2, Euro 15,00

361 M A SCHOUTEN Patterns in biodiversity; Spatial organisation of biodiversity in the Netherlands -- Utrecht 2007: Knag/Copernicus Institute. 152 pp, 16 figs, 20 tabs. ISBN: 978-90-6809-403-9, Euro 20,00

362 M H J W VAN AMSTEL – VAN SAANE Twilight on self-regulation; A socio-legal evaluation of conservation and sustainable use of agrobiodiversity by industry self-regulation -- Utrecht 2007: Knag/Copernicus Institute. 167 pp, 15 figs, 13 tabs, 5 box. ISBN: 978-90-6809-404-6, Euro 20,00

363 S MUHAMMAD Future urbanization patterns in the Netherlands, under the influence of information and communication technologies -- Utrecht 2007: Knag/Faculteit Geowetenschappen Universiteit Utrecht. 187 pp, 82 figs, 20 tabs. ISBN: 978-90-6809-405-3, Euro 20,00

364 M GOUW Alluvial architecture of the Holocene Rhine-Meuse delta (The Netherlands) and the Lower Mississippi Valley (U.S.A.) -- Utrecht 2007: Knag/Faculteit Geowetenschappen Universiteit Utrecht. 192 pp, 55 figs, 14 tabs. ISBN: 978-90-6809-406-0**,** Euro 22,00

365 E HEERE & M STORMS Ormeling's cartography; Presented to Ferjan Ormeling on the occasion of his 65th birthday and his retirement as Professor of Cartography -- Utrecht 2007: Knag/Faculteit Geowetenschappen Universiteit Utrecht. ISBN: 978-90-6809-407-7, Euro 20,00

366 S QUARTEL Beachwatch; The effect of daily morphodynamics on seasonal beach evolution -- Utrecht 2007: Knag/Faculteit Geowetenschappen Universiteit Utrecht. 125 pp, 39 figs, 7 tabs. ISBN: 978-90-6809-408-4, Euro 12,50

367 R O VAN MERKERK Intervening in emerging nanotechnologies; A CTA of Lab-on-a-chip technology regulation -- Utrecht 2007: Knag/Copernicus Institute. 206 pp, 19 box, 35 figs, 12 tabs. ISBN: 978-90-6809-409-1, Euro 20,00

368 R M FRINGS From gravel to sand; Downstream fining of bed sediments in the lower river Rhine -- Utrecht 2007: Knag/Faculteit Geowetenschappen Universiteit Utrecht. ISBN: 978-90-6809-410-7**,** Euro 25,00

369 W IMMERZEEL Spatial modelling of the hydrological cycle, climate change and agriculture in mountainous basins -- Utrecht 2008: Knag/Faculteit Geowetenschappen Universiteit Utrecht. 147 pp, 54 figs, 12 tabs. ISBN: 978-90-6809-411-4, Euro 25,00

370 D S J MOURAD Patterns of nutrient transfer in lowland catchments; A case study from northeastern Europe -- Utrecht 2008: Knag/Faculteit Geowetenschappen Universiteit Utrecht. 176 pp, 44 figs, 19tabs. ISBN: 978-90-6809-412-1**,** Euro 20,00

371 M M H CHAPPIN Opening the black box of environmental innovation; Governmental policy and learning in the Dutch paper and board industry -- Utrecht 2008: Knag/Copernicus Institute. 202 pp, 41 figs, 30 tabs. ISBN: 978-90-6809-413-8, Euro 22,50

372 R P ODDENS & M VAN EGMOND Ormelings atlassen; Catalogus van atlassen geschonken aan de Universiteit Utrecht door de hoogleraren F.J. Ormeling sr. en jr. – Utrecht 2008: Knag/Faculteit Geowetenschappen Universiteit Utrechts. ISBN: 978-90-6809-415-2, Euro 15,00

373 R VAN MELIK Changing public space; The recent redevelopment of Dutch city squares – Utrecht 2008: Knag/Faculteit Geowetenschappen Universiteit Utrecht. 323 pp, 47 figs, 32 tabs. ISBN: 978-90-6809-416-9, Euro 20,00

374 E ANDRIESSE Institutions and regional development in Southeast Asia; A comparative analysis of Satun (Thailand) and Perlis (Malaysia) -- Utrecht 2008: Knag/Faculteit Geowetenschappen Universiteit Utrecht. 250 pp, 42 figs, 43 tabs, 18 box. ISBN: 978-90-6809-417-6, Euro 25,00

375 E HEERE GIS voor historisch landschapsonderzoek; Opzet en gebruik van een historisch GIS voor prekadastrale kaarten -- Utrecht 2008: Knag/Faculteit Geowetenschappen Universiteit Utrecht. 231 pp, 73 figs, 13 tabs. ISBN: 978-90-6809-418-3, Euro 30,00

376 V D MAMADOUH, S M DE JONG, J F C M THISSEN & J A VAN DER SCHEE Dutch windows on the Mediterranean; Dutch Geography 2004-2008 -- Utrecht 2008: Knag/International Geographical Union Section The Netherlands. 104 pp + cd-rom, 38 figs, 9 tabs. ISBN: 978-90-6809-419-0, Euro 10,00

377 E VAN MARISSING Buurten bij beleidsmakers; Stedelijke beleidsprocessen, bewonersparticipatie en sociale cohesie in vroeg-naoorlogse stadswijken in Nederland -- Utrecht 2008: Knag/Faculteit Geowetenschappen Universiteit Utrecht. 230 pp, 6 figs, 31 tabs. ISBN: 978-90-6809-420-6, Euro 25,00

378 M DE BEER, R C L BUITING, D J VAN DRUNEN & A J T GOORTS (Eds.) Water Wegen; Op zoek naar de balans in de ruimtelijke ordening -- Utrecht 2008: Knag/VUGS/Faculteit Geowetenschappen Universiteit Utrecht. 91 pp, 18 figs, 1 tab. ISBN: 978-90-6809-421-3, Euro 10,00

379 J M SCHUURMANS Hydrological now- and forecasting; Integration of operationally available remotely sensed and forecasted hydrometeorological variables into distributed hydrological models -- Utrecht 2008: Knag/Faculteit Geowetenschappen Universiteit Utrecht. 154 pp, 65 figs, 12 tabs. ISBN 978-90-6809-422-0, Euro 15,00

380 M VAN DEN BROECKE Ortelius' *Theatrum Orbis Terrarum* (1570-1641); Characteristics and development of a sample of *on verso* map texts -- Utrecht 2009: Knag/Faculteit Geowetenschappen Universiteit Utrecht. 304 pp + cd-rom, 9 figs, 65 tabs. ISBN 978-90-6809-423-7, Euro 30,00

381 J VAN DER KWAST Quantification of top soil moisture patterns; Evaluation of field methods, process-based modelling, remote sensing and an integrated approach -- Utrecht 2009: Knag/Faculteit Geowetenschappen Universiteit Utrecht. 313 pp, 108 figs, 47 tabs. ISBN 978-90-6809-424-4, Euro 30,00

382 T J ZANEN 'Actie, actie, actie…'; De vakbeweging in regio Noord-Nederland, 1960-1992 -- Utrecht/ Groningen 2009: Knag/Faculteit Ruimtelijke Wetenschappen Rijksuniversiteit Groningen. ISBN 978-90-6809-425-1, Euro 30,00

383 M PERMENTIER Reputation, neighbourhoods and behaviour -- Utrecht 2009: Knag/Faculteit Geowetenschappen Universiteit Utrecht. 146 pp, 10 figs, 19 tabs. ISBN 978-90-6809-426-8, Euro 15,00

384 A VISSER Trends in groundwater quality in relation to groundwater age -- Utrecht 2009: Knag/Faculteit Geowetenschappen Universiteit Utrecht. 188 pp, 47 figs, 24 tabs. ISBN 978-90-6809-427-5, Euro, 20,00

385 B A FURTADO Modeling social heterogeneity, neighborhoods and local influences on urban real estate prices; Spatial dynamic analyses in the Belo Horizonte metropolitan area, Brazil -- Utrecht 2009: Knag/Faculteit Geowetenschappen Universiteit Utrecht. 236 pp, 50 figs, 48 tabs. ISBN 978-90-6809-428-2, Euro 25,00

386 T DE NIJS Modelling land use change; Improving the prediction of future land use patterns -- Utrecht 2009: Knag/Faculteit Geowetenschappen Universiteit Utrecht. 206 pp, 59 figs, 32 tabs. ISBN 978-90-6809-429-9, Euro 25,00

387 I J VISSEREN-HAMAKERS Partnerships in biodiversity governance; An assessment of their contributions to halting biodiversity loss -- Utrecht 2009: Knag/Copernicus Institute. 177 pp, 4 figs, 4 tabs. ISBN 978-90-6809-430-5, Euro 20,00

388 G ERKENS Sediment dynamics in the Rhine catchment; Quantification of fluvial response to climate change and human impact -- Utrecht 2009: Knag/Faculteit Geowetenschappen Universiteit Utrecht. ISBN 978-90-6809-431-2, Euro 30,00

389 M HIJMA From river valley to estuary; The early-mid Holocene transgression of the Rhine-Meuse valley, The Netherlands -- Utrecht 2009: Knag/Faculteit Geowetenschappen Universiteit Utrecht. ISBN 978-90-6809-432-9, Euro 25,00

390 N L M B VAN SCHAIK The role of Macropore Flow from PLOT to catchment scale; A study in a semi-arid area -- Utrecht 2010: Knag/Faculteit Geowetenschappen Universiteit Utrecht. ISBN 978-90-6809-433-6, Euro 20,00

For a complete list of NGS titles please visit www.knag.nl. Publications of this series can be ordered from KNAG / NETHERLANDS GEOGRAPHICAL STUDIES, P.O. Box 80123, 3508 TC Utrecht, The Netherlands (E-mail info@knag.nl; Fax +31 30 253 5523). Prices include packing and postage by surface mail. Orders should be prepaid, with cheques made payable to "Netherlands Geographical Studies". Please ensure that all banking charges are prepaid. Alternatively, American Express, Eurocard, Access, MasterCard, BankAmericard and Visa credit cards are accepted (please specify card number, name as on card, and expiration date with your signed order).